# The Causality between Electroencephalogram (EEG) and Central Neuropathic Pain (CNP), and the Effectiveness of Neuromodulation Strategies on Cortical Excitability and CNP in Patients with Spinal Cord Injury

**Mohammed Sabah Jarjees**

SUBMITTED IN FULFILMENT OF THE REQUIRMENTS FOR THE DEGREE OF
Doctor of Philosophy (PhD)

**Department of Biomedical Engineering**

College of Science and Engineering
University of Glasgow

February 2017

# Abstract

Spinal Cord Injury has primary consequences visible immediately upon injury and secondary consequence which develop some time after injury. One of the primary consequences of SCI is loss or impairment of sensory and motor functions. Related secondary consequences of the injury are Central Neuropathic Pain (CNP) and spasticity. Several studies have found that CNP can affect the cortical activity of the patient and long term CNP causes anatomical cortical changes. Therefore, early prediction and treatment of CNP could potentially prevent these changes and hopefully increase responsiveness to the treatment. Neurofeedback (NF) technique, which is a sub-category of biofeedback that uses brain waves as physiological parameters to be modulated, can be used to alter this change in cortical activity and treat CNP. The sensory motor cortex is the area of the brain responsible for voluntary control of movement and for cortical modulation of reflexes. NF provided from the sensory-motor area can therefore affect both CNP and voluntary and reflex movements.

The aim of this PhD project was to explore the influence of neuromodulation strategies over the central cortex on the H reflex and CNP following SCI. It also aimed to investigate the causal relationship between the change in EEG activity and the transitional period from early symptoms of CNP to the chronic phase of CNP following SCI.

The first study of this project was performed on able-bodied volunteers to explore the effect of the short-term neuromodulation strategies: NF, motor imagery (MI) and mental math (MM) of the sensory-motor rhythm (SMR) on the soleus H reflex. Results of the study showed that it is possible to achieve short-term modulation of the H reflex through short-term modulation of the SMR. Various mental tasks dominantly facilitate the H reflex irrespective of the direction of SMR modulation. The results of this study can be used to explain the effect of NF therapy on spasticity in SCI patient, for example.

The second study analysed predictors of CNP in sub-acute SCI patients who have not yet developed physical symptoms of pain. It compared EEG signal between patients who did and did not develop pain within the first six months after EEG recording as well as patients with CNP and able bodied volunteers. This study demonstrated that changes in spontaneous and induced EEG can be both predictors and consequences of CNP following SCI.

The third study explores the effectiveness of Neurofeedback (NF) on treatment of CNP in subacute SCI patients with CNP. The results of this study demonstrate that the NF treatment has a positive effect on the reduction of pain, at least over the period of the study. However, numerous factors, and in particular patients' low prioritization of pain, indicate that early NF of CNP in SCI patients might not be a practical solution.

The fourth study utilizes advanced methods of source analysis to define dynamic signatures of long standing CNP by using Measure Projection Analysis (MPA) for movement related cortical potential (MRCP). To separate the effect of long-term paralysis from the effect of long-term CNP, brain activity has been compared between three groups: able bodied volunteers, patients with chronic paraplegia (paralysis of lower limbs) with no pain and patients with chronic paraplegia and long standing CNP. This study showed that the movement related potential is dominantly influenced by paralysis while both CNP and paralysis affect the reafferentation component of the MRCP. Additionally, CNP influences cognitive processes in a manner that depends on the functional area of the cortex.

# Table of Contents

# List of Tables

# List of Figures

# Acknowledgments

***"Read and your Lord is the most generous (3) Who has taught (the writing) by the pen (4) He has taught man that which he knew not (5)" (Al-Alaq,96:3-5)***

First and foremost, I thank Allah, the almighty, for helping me and giving me the knowledge and strength to successfully complete this PhD project.

I wish to express my sincere gratitude and appreciation to my principal supervisor Dr Aleksandra Vučković for her support, guidance, encouragement, and insightful comments which led to progression of this project and raised its quality. Similarly, I offer gratitude to my co-supervisor Professor Jonathan Cooper for his help in several aspects of this project.

My sincere gratitude and appreciation go to my sponsor, the higher committee for education and development in Iraq (HCED), for their administrative and financial support and to my college, Northern Technical University/ Technical College/ Mosul for giving me this opportunity to develop in my career path and eventually serve my beloved country (IRAQ).

I would like to express my deepest gratitude and thanks to my parents for all their moral support and prayers. I would not have gotten this far without their love and encouragement. In addition I am sincerely grateful to my mother-in-law for her prayers and patience during the years of parting with her daughter.

No words can express my gratitude and thanks to my wife for caring for our family while I was busy with my study, and for her patience and endless support. I appreciate all her sacrifices. I would also like to acknowledge my two lovely children, Abdullah and Nawara, who are the pride and joy of my life. I appreciate all your patience and support throughout Dad's PhD study. Thank you for being the most supportive family in the world and helping me accomplish my PhD dream.

I would also like to thank Dr Henrik Gollee for the help he offered me – especially in regards to the technical aspects and programing.

My gratitude and thanks extend to Mr Matthew Fraser, Dr Mariel Purcell and Dr Alan McLean at the Queen Elizabeth National Spinal Injuries Unit, Queen Elizabeth University Hospital for their help with patient recruitment. I also appreciate all the help I received from the therapists and nurses at the hospital, especially Jon Hasler. Thank you!

I would like to thank all patients and able bodied volunteers for their time and contribution to my PhD project.

I would like to express my appreciation to the administration at the College of Science and Engineering, especially Heather Lambie and Elaine McNamara for their unlimited support when I was desperately in need of it.

The only way to overcome the difficulties and stressful moments of the PhD study was to share it with my sincere colleagues. My special thanks go to Muhammad Abul Hasan, Bethel Osuagwu, Margaret Armentano, Manaf Kadum Hussein Al-taleb, Salim Mohammed Hussein Al-wasity, Aso Fatih Muhamed, Jose Alberto Alvarez Martin, Sarah Comincioli, Anna Zulauf-Czaja, Anna Sosnowska, Ruslinda Binti Ruslee, Finda Putri, Jennifer Miller and Nina Petric-Gray. I could not have made it without you all! Thank you!

There are also many more people whom I would like to thank, but the time and space force me to stop here.

Thank you all!

# Author's Declaration

I, Mohammed Sabah Jarjees, hereby declare that except where explicitly reference is made to the contribution of others, this thesis is the result of the work of the named and has not been submitted for any other degree at the University of Glasgow or any other institution.

December 2016

# Abbreviations

| | |
|---|---|
| **AB** | Able Bodied |
| **ACC** | Anterior Cingulate Cortex |
| **ADHD** | Attention Deficit Hyperactivity Disorder |
| **AIC** | Anterior Insular Cortex |
| **ANOVA** | Analysis of Variance |
| **ANS** | Autonomic Nervous Systems |
| **ASIA** | American Spinal Cord Injury Association |
| **BA** | Brodmann Area |
| **bNP** | below Level Neuropathic Pain |
| **BOLD** | Blood Oxygen Level Dependent |
| **CNP** | Central Neuropathic Pain |
| **CNS** | Central Nervous System |
| **CNV** | Contingency Negative Variation |
| **DBS** | Deep Brain Stimulation |
| **DFT** | Discrete Fourier Transform |
| **EC** | Eyes Closed |
| **ECG** | Electrocardiogram |
| **EEG** | Electroencephalogram |
| **EMG** | Electromyogram |
| **EO** | Eyes Opened |
| **ERD** | Event Related Desynchronization |
| **ERP** | Event Related Potential |
| **ERS** | Event Related Synchronization |
| **ERSP** | Event Related Spectral Perturbation |
| **F** | Feet |
| **FDR** | False Discovery Rate |
| **fMRI** | functional Magnetic Resonance Image |
| **GUI** | Graphical User Interface |
| **H Reflex** | Hoffmann's Reflex |
| **HEG** | Hemoencephalography |
| **IASP** | International Association for the Study of Pain |
| **ICA** | Independent Component Analysis |
| **IIR** | Infinite Impulse Response |
| **ISNCSCI** | International Standards for Neurological Classification of Spinal Cord Injury |
| **KVIQ** | Kinaesthetic and Visual Imagery Questionnaire |
| **LA** | Left Arm |
| **LANSS** | Leeds Assessment of Neuropathic Symptoms and Signs |
| **LORETA** | Low Resolution Brain Electromagnetic Tomography |
| **M Wave** | Muscle Response Wave |
| **M1** | Primary Motor Cortex |
| **MCS** | Motor Cortex Stimulation |
| **MEG** | Magnetoencephalography |

| | |
|---|---|
| **MEP** | Motor-Evoked Potential |
| **MI** | Motor Imagery |
| **MM** | Mental Math |
| **MNI** | Montreal Neurological Institute |
| **MPA** | Measure Projection Analysis |
| **MPT** | Measure Projection Toolbox |
| **MRCP** | Movement Related Cortical Potential |
| **MRI** | Magnetic Resonance Imaging |
| **MRP** | Motor Related Potential |
| **NF** | Neurofeedback |
| **NP** | Neuropathic Pain |
| **NPQ** | Neuropathic Pain Questionnaire |
| **NPSI** | Neuropathic Pain Symptom Inventory |
| **NRS** | Numeric Rating Scale |
| **PCC** | Posterior Cingulate Cortex |
| **PdP** | Patient Developed Central Neuropathic Pain |
| **PET** | Positron Emission Topography |
| **PMC** | Premotor Cortex |
| **PNP** | Peripheral Neuropathic Pain |
| **PnP** | Patient with no Central Neuropathic Pain |
| **PNS** | Peripheral Nervous System |
| **PSD** | Power Spectral Density |
| **PT** | Perceptual Threshold |
| **PwP** | Patient with Central Neuropathic Pain |
| **PwP_C** | Patient with Central Neuropathic Pain Control Group |
| **PwP_NF** | Patient with Central Neuropathic Pain Treatment Group |
| **RA** | Right Arm |
| **RMS** | Root Mean Square |
| **rTMS** | Repetitive Transcranial Magnetic Stimulation |
| **S1** | Primary Somatosensory Cortex |
| **S2** | Secondary Sensory Cortex |
| **SCI** | Spinal Cord Injury |
| **SCS** | Spinal Cord Stimulation |
| **sLORETA** | standardized Low Resolution Brain Electromagnetic Tomography |
| **SMC** | Supplementary Motor Cortex |
| **SMR** | Sensory-Motor Rhythm |
| **STFT** | Short Time Fourier Transform |
| **STT** | Spinothalamic Tract |
| **tDCS** | Transcranial Direct Current Stimulation |
| **TENS** | Transcutaneous Electrical Nerve Stimulation |
| **V3** | Visual Association Area |
| **VAR** | Variance |
| **VAS** | Visual Analogy Scales |

# Publications

## Journal Paper

M. Jarjees, A. Vučković, (2016) "***The effect of voluntary modulation of the sensory-motor rhythm during different mental tasks on H reflex***". International Journal of Psychophysiology, 106, 65-76.

## Conferences and Proceeding

Mohammed Jarjees, Aleksandra Vuckovic' "***Effect of Voluntary Modulation of Alpha Rhythm over the Primary Motor Cortex on the Hoffmann Reflex***", Glasgow Neuroscience Day 2015, Glasgow, UK, 16th January 2015,

Mohammed Jarjees, Aleksandra Vuckovic' "***Effect of Voluntary Modulation of Alpha Rhythm over The Primary Motor Cortex on The Hoffmann Reflex***" , The First HCED Scholars Conference 2015, London, UK, 29th May 2015

Mohammed Jarjees, Aleksandra Vuckovic' "***Modulation of H Reflex Amplitude during Mental Tasks in Able Bodied Volunteers***", The 25th Congress of the international Society of Biomechanics ISB 2015, Glasgow, UK, 12th July 2015.

Mohammed Jarjees, Aleksandra Vuckovic, "***Neurofeedback Treatment of Central Neuropathic Pain (CNP) in Sub-acute Patients with Spinal Cord Injury (SCI)***", The 9th IEEE EMBS UK & Republic of Ireland Postgraduate Conference on Biomedical Engineering and Medical Physics, Liverpool, UK, 14th – 16th July 2015.

Mohammed Jarjees, Matthew Fraser, Margaret Purcell, Aleksandra Vuckovic,"***Cortical Predictors of Central Neuropathic Pain (CNP) in Sub-acute Patients with Spinal Cord Injury (SCI)***", Scottish Pain Research Community (SPaRC), Sixth Annual Scientific Meeting, Dundee, UK, 18th March 2016.

Mohammed Jarjees, Matthew Fraser, Margaret Purcell, Aleksandra Vuckovic, "***Cortical Predictors of Central Neuropathic Pain (CNP) in Sub-acute Patients with Spinal Cord Injury (SCI)***", British Pain Society, Annual Scientific Meeting 2016, Harrogate, UK, 10th –12th May 2016.

# 1
# Background

# Chapter 1 Background

This chapter provides an overview of the anatomy and physiology of the Central Nervous System (CNS), Spinal Cord Injury (SCI) and its consequences, such as Neuropathic Pain (NP) and spasticity. It also includes an introduction to biosignals, specifically Electroencephalogram (EEG) and Electromyogram (EMG). A Neurofeedback (NF) technique and its applications are also discussed. Furthermore, signal processing used to process EEG and EMG signals are described. Therefore, this chapter has been divided into six sections: anatomy and physiology of CNS, SCI and its consequences, Biosignals, NF technique and its applications, analysis methods of EEG and EMG signals, and thesis aims and objectives.

## 1.1 Anatomy and Physiology of the Central Nerve System

The nervous system is divided into two parts: CNS, consists of the brain and the spinal cord and the Peripheral Nervous System (PNS)[1]. The PNS includes somatic (voluntary) and autonomic (involuntary) nervous systems (ANS). The ANS has two sections: sympathetic and parasympathetic[1].

### 1.1.1 Brain

The brain is a part of the CNS and is located in the skull which protects it from injury and gives structure to the head. In addition to the skull, the brain is protected by cranial meninges and cerebrospinal fluid. It has four main parts: cerebrum, cerebellum, brainstem and diencephalon[1,2].

The cerebrum is the main and largest brain structure. It covers the upper part of the cranial cavity and is divided into two cerebral hemispheres, left and right[1,2]. Although the left and right hemispheres are almost identical in shape and structure, they have different functions. The left hemisphere is responsible for controlling the right side movement of the

body, while the right hemisphere controls the left side movement of the body[1]. The left hemisphere is involved in speech, language, mathematical calculation and logical activities[2]. The right hemisphere is involved in analyzing emotional context, creativity, face recognition, understanding three dimensional relationships, and estimation calculation.

Both hemispheres of the cerebellum, which receives sensory information from the spinal cord and motor information from the cerebral cortex, control the balance of the body. The brainstem regulates the autonomic functions of the body and it relays information to or from the spinal cord to the cerebrum and cerebellum[2].

The cerebral hemispheres and the brain stem are linked structurally and functionally by the diencephalon[3]. The wall of the diencephalon is composed of the thalamus, which acts as the final relaying point for most of the ascending sensory information and conveys them to the sensory and motor regions in the brain[1,3]. It is divided into anterior, medial, and lateral thalamic nuclei groups. These groups can be subdivided into anterior, posterior, dorsal, and ventral.

The floor of the diencephalon is composed of the hypothalamus[1]. This structure contains the control and integrative centers for pain, pleasure, and sexual function as well as regulation of body temperature, heart rate, and blood pressure. Additionally, it plays a role in the functions associated with the limbic system.

The cerebrum is covered by a thin layer of gray matter which comprises the cortex and the deeper cerebrum structure (subcortex). The cerebral cortex and the subcortex were categorized to 47 patterns according to the cytoarchitecture of the tissue by Korbinian Brodmann in 1909[4]. Therefore, each cortex can be represented by Brodmann Areas (BA) derived from the above mentioned patterns.

Anatomically, the cerebral cortex consists of four lobes: frontal, parietal, occipital and temporal. Functionally, it includes: motor cortical areas, sensory cortical areas, association

areas, visual cortical areas, auditory cortical areas, and insula cortical area[2]. Figure 1.1 shows the lobes and cortical areas of the brain. The brain cortical areas which are more relevant of this PhD will be discussed.

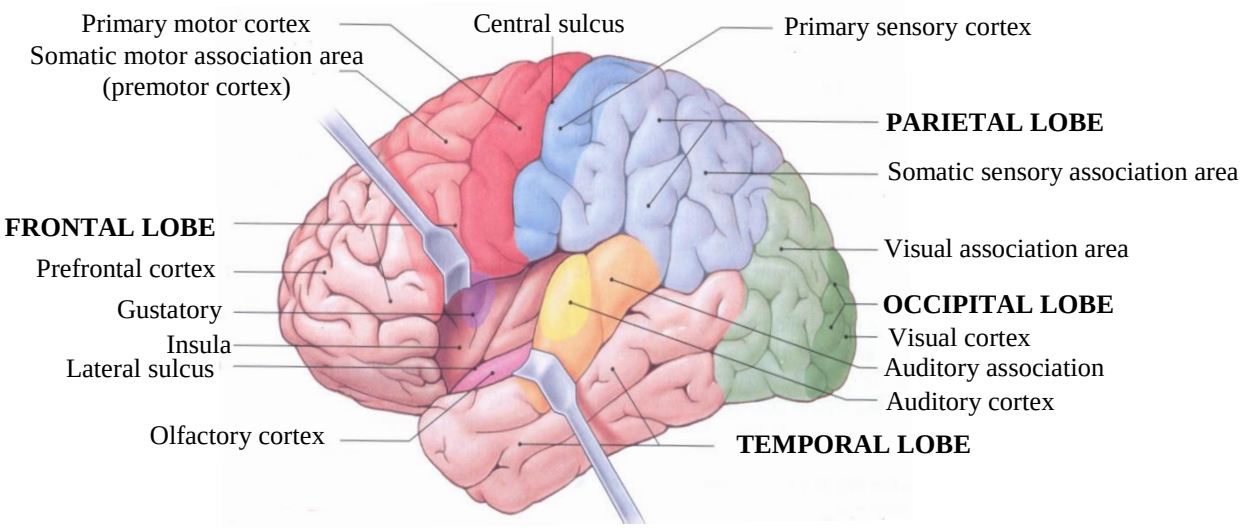


**Figure 1.1**: Lobes and cortical areas of the brain[2]

The motor cortical area is responsible for planning, controlling and executing the motor functions[1,2]. It is located in frontal lobe and it includes the primary motor cortex (M1), somatic motor association area (premotor cortex (PMC)) and Supplementary Motor Cortex (SMC)[2].

- The M1 is located on the surface of the precentral gyrus of the frontal lobe[1,2] and is represented by BA 4[4]. It controls somatic motor neurons in the brain stem and spinal cord leading to direct control of voluntary movement[1,2].

- The PMC is located in front of the M1. It is responsible for the preparation and coordination of learned movement. The PMC relays the instructions to M1 when performing a voluntary movement. It can be represented by BA 6[4].

- The SMC is represented by BA 8[4] and is involved in coordinating movements of both sides of the body[1,2].

The sensory cortical area receives and controls the somatic sensory information such as pressure, temperature, pain, touch, and taste[1,2]. It is located in parietal lobe and it includes primary somatosensory cortex (S1) and somatic sensory association area (secondary sensory cortex (S2)).

- S1 is located on the surface of the postcentral gyrus of the parietal lobe, and is represented by BA 1, 2, and 3[4]. It receives the somatic sensory information relayed by the thalamus[1,2].

- S2 is located laterally to S1, in the parietal lobe. It is responsible for monitoring activities in S1 and can be presented by BA 40 and 43[4].

The location on the body of somatosensory input to S1 and the motor control output from M1 of each part of the body can be topically represented by the homunculus (Figure 1.2)[3].

The visual cortical area is located in the occipital lobe[1,2]. It includes the visual cortex (BA 17 and 18[4]) and visual association area (BA 19). It is responsible for receiving visual information. The insula cortical area is a deep brain structure involved in consciousness, perception, cognitive function, motor control, and regulating body homeostatic. It can be represented by BA 13, 14 and 16[4].

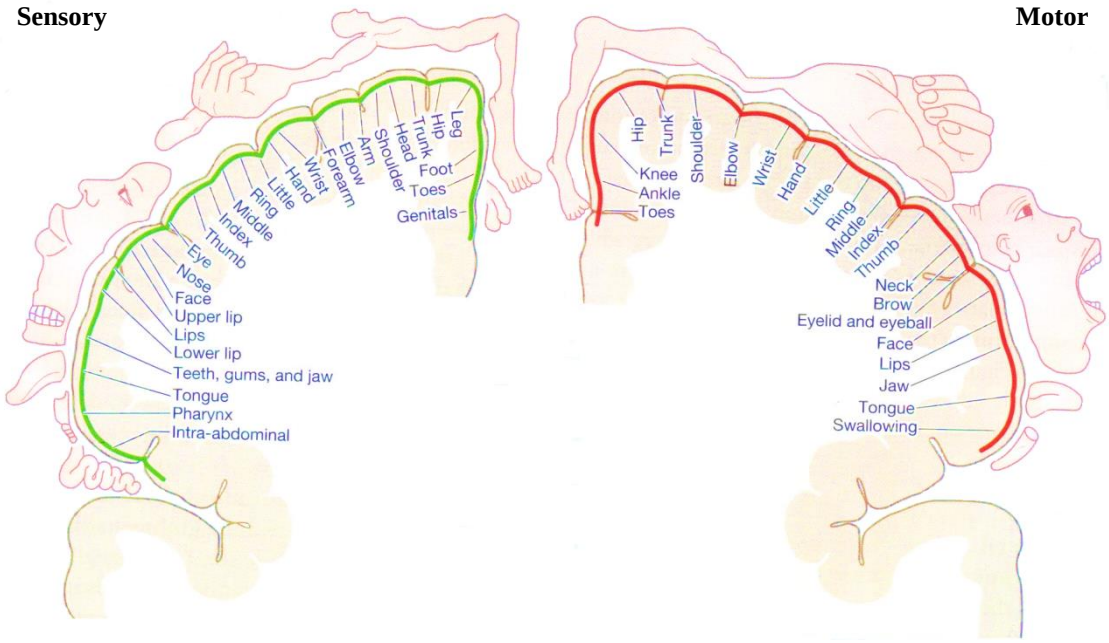


**Figure 1.2**: Somatotopic cortical representation of primary sensory and motor cortices[3]

## 1.1.2 Spinal Cord

The spinal cord is a bundle of nerves that conveys sensory information to the brain and motor information from the brain to the other parts of the body[2]. It also contains motor neurons which are responsible for reflex responses. Figure 1.3 shows the gross anatomy and the cross sectional structures of the spinal cord[1].

Spinal cord is divided into 31 segments which are named according to vertebral segments of the spine. They are: the cervical (C1-C8), thoracic (T1-T12), lumbar (L1-L5), sacral (S1-S5) and one coccygeal, as seen in Figure 1.3a. Each spinal segment contains a pair of dorsal root ganglia which contain cell bodies of sensory neurons, shown in Figure 1.3b. The dorsal roots contain the axons of the sensory neurons which carry sensory information into the spinal cord. The spinal cord sends motor information through the axons of the motor neurons which are located in the ventral root. The spinal nerves, which are a type of mixed nerves, contain both sensory (afferent) and motor (efferent) fibers. Each group of the spinal nerves is responsible for conveying the sensory and motor information from/to spinal cord to/from different parts of the body (Figure 1.4)[2]. It also

contains the interneurons which are responsible for relaying information between sensory and motor neurons.

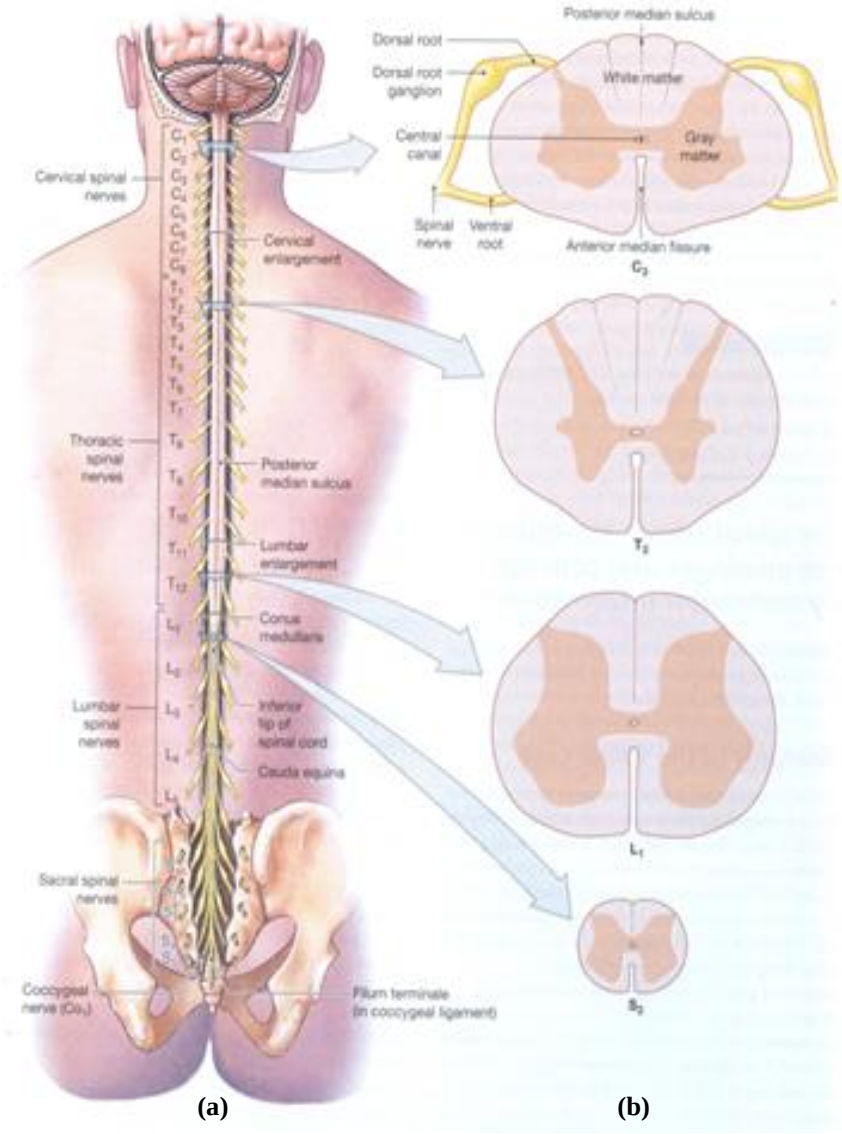


**Figure 1.3**: The gross anatomy and the cross sectional structures of the spinal cord, a: the gross anatomy structure of the adult spinal cord, b: the cross section structure of the spinal cord for 4 different segments[1].

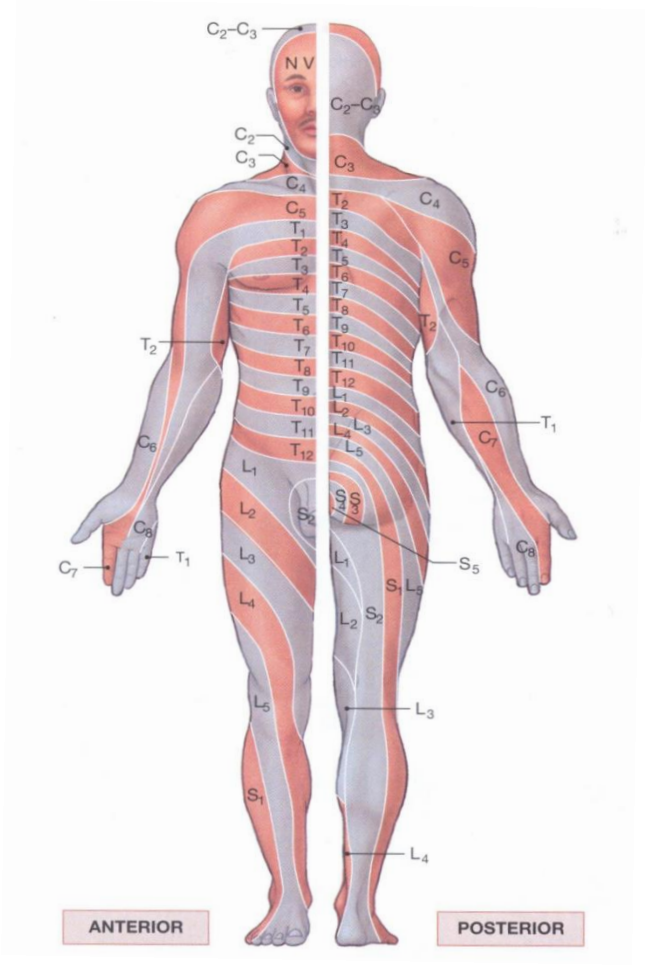


**Figure 1.4**: The anterior and posterior dermatomes. The NV means fifth cranial nerve[2].

### *1.1.2.1 White matter of spinal cord*

The outer layer of the spinal cord is called white matter. The white matter is made of spinal tracts (bundles of neuron axons) which share specific functional and structural properties[2]. There are two types of spinal tracts: ascending (sensory) tracts and descending (motor) tracts[1–3].

The ascending tracts include: posterior (dorsal) column, spinothalamic tract (STT) and spinocerebellar tracts[3] (Figure 1.5). The posterior column carries the sensation of touch, vibration, and proprioception. The sensory information from the first order neurons ascend in the ipsilateral posterior column and synapse with second order neurons; then second

order neurons ascend through the contralateral region of the brain stem to synapse with third order neurons in the ventral posterior lateral nucleus of the thalamus. The neurons that arise in the thalamus ascend to the related areas in S1 and S2.

STT carries the sensation of pain, temperature and itching[3,5]. Sensory information first ascends in the contralateral spinothalamic tract, then in the lateral region of the spinal cord and brain stem to synapse in the ventral posterior lateral nucleus of the thalamus. Finally the neurons that arise in the thalamus ascend to the related areas in S1 and S2.

The spinocerebellar tract sends proprioceptive information directly to the cerebellum[3,5]. All ascending tracts carry sensory information from different parts of the body towards the brain.

The descending or motor tracts of the spinal cord convey motor commands from M1 cortical area to other parts of the body[2,3,5]. The most important descending tract in the spinal cord is the corticospinal tract. The neurons (upper motor neurons) in the M1 carry motor information through the pons in the brain stem down to the contralateral corticospinal tract of the spinal cord. The lateral corticospinal tract of the spinal cord synapses with motor neurons in the spinal cord. The lower motor neurons in the spinal cord exit through the ventral roots to peripheral nerves and neuro-motor junctions of the skeletal muscles associated with the spinal nerve.

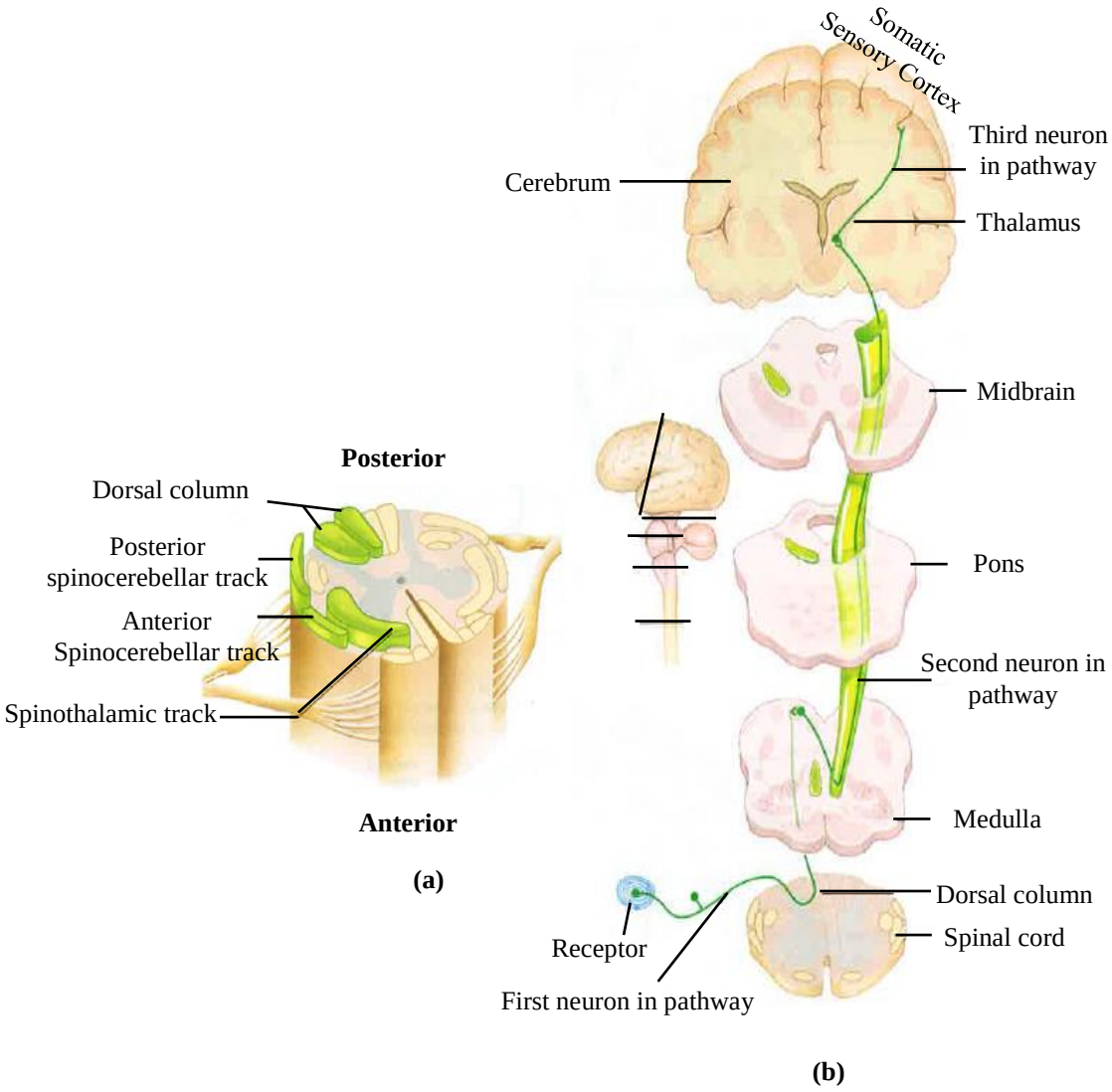


**Figure 1.5**: Ascending tracts of spinal cord[6].

### *1.1.2.2 Grey matter of spinal cord*

The inner layer of the spinal cord is called gray matter[2]. The gray matter of the spinal cord contains the cell bodies of neurons organized in groups according to their functions. These functional groups, called nuclei, exist in two types: sensory nuclei, which are responsible for receiving and relying sensory information from the periphery, and motor nuclei, which are responsible for sending motor commands to the periphery.

The grey matter is divided into dorsal (posterior) and ventral (anterior) horns[2,3]. The dorsal horns contain sensory nuclei, while the ventral horns contain motor nuclei. The

visceral motor nuclei are located in lateral horns which can only be found in the thoracic (T1-T12) and lumbar (L1-L5) segments of the spinal cord.

## 1.2 Pain

According to the International Association for the Study of Pain (IASP), "pain is an unpleasant sensory and emotional experience associated with actual or potential tissue damage, or described in terms of such damage"[7]. This definition shows that pain includes both pain perception and nociception[8]. Perception relates to subjective experience of pain, while nociception relates to neural mechanism of pain.

Pain has been classified as nociceptive or neuropathic. Nociceptive pain can be defined as pain arising from actual damage to the tissue[9,10]. Neuropathic pain (NP) has been defined by IASP as a pain that is caused by injuries or diseases to the somatosensory system[11]. Both types of pain can either be acute, that is lasting less than 6 moths, or chronic, lasting more than 6 months[8,12].

### 1.2.1 Pain Pathway

Peripheral sensory fibers, such as myelinated A-delta (Aδ) and non-myelinated C fibers, carry the nociceptive information of pain from the periphery to the lateral division of the dorsal horn of the spinal cord[2,13]. Aδ fibers carry the information of rapid (sharp) pain, while the C fibers carry the slow (dull) pain.

The STT ascends the nociceptive information to the ventral posterior lateral nucleus of the thalamus, where it synapses with third order neurons[13]. Then the third order neurons terminate in specific areas of S1 and S2. S1 and S2 are important for localization, intensity, and quality of pain. The spinoreticular tact ascends the nociceptive information to the brainstem reticular formation, and then the reticular formation sends impulses to the

thalamus, hypothalamus, and limbic system. The hypothalamus and limbic system have an important role in reflex and emotional components of pain[13].

Several imaging studies have demonstrated that the perception of pain is not only processed at level of S1 and S2 cortices but also in other regions of the brain[14–16]. These regions are anterior cingulate cortex, anterior insular cortex, frontal cortex, supplementary motor area, and motor cortex. Anterior cingulate cortex and anterior insular cortex are connected to the limbic system which is involved in emotional components of pain. These cortices are called the '**pain matrix**'.

## 1.3 Spinal Cord Injury (SCI)

Spinal cord injury is caused by a lesion on the spinal cord, which can be a result of an accident, called traumatic SCI, or by a disease, called non-traumatic SCI[17]. The patient with SCI may suffer various impairments to the physiological and neurological system. The type and degree of these impairments depend on several factors, such as the level of lesion and severity of the injury.

### 1.3.1 Level of SCI

According to the International Standard for Neurological Classification of SCI, the neurological level of SCI is defined as "the most caudal segment of the spinal cord with normal sensory and antigravity motor function on both sides of the body"[18].

SCI can be divided into two types according to the level of injury. (i) Injury that occurs within the cervical segments may lead to Tetraplegia, an impairment of both upper and lower limbs functions[18]. (ii) Injury to the thoracic, lumbar, or sacral segments may result in paralysis of lower limbs, called Paraplegia. The injury within thoracic segments also affects different groups of abdominal muscles (Figure 1.4).

## 1.3.2 Completeness of SCI

According to American Spinal Cord Injury Association (ASIA), SCI can be classified into five groups based on the degree of retained sensory and motor function[18]. If there is no sensory or motor function preserved in the lowest sacral segment (S4-S5), the SCI will be classed as ASIA A (complete SCI). If there is partial sensation and/or motor function below the level of an injury, the SCI will be defined as an incomplete SCI.

There are several ASIA subdivisions for incomplete SCI. Class ASIA B refers to the complete loss of motor function and partially preserved sensory information below the level of injury. Class ASIA C refers to the incomplete preservation of sensory and motor function below the level of injury, with more than half of the key muscles below the level of injury having muscle function grade < 3 (Table 1.1). Class ASIA D means that motor function is preserved below the level of injury with at least half of the key muscles below the level of injury having muscle function grade ≥ 3. Class ASIA E is used when sensory and motor functions are normal.

To determine the level of sensation, the sensitivity to pin prick and to light touch is tested in all dermatomes. The light touch test is used to evaluate the integrity of the dorsal column pathway[19,20] and the pin prick test is used to evaluate the integrity of STT pathway[21]. Three point scale (0 to 2) is used to describe the sensation (0 for absent, 1 for impaired and 2 for normal)[22].

**Table 1.1 :** Muscle function grading[23]

| Grades | Description |
|---|---|
| **0** | Total paralysis |
| **1** | Visible contraction |
| **2** | Active movement with gravity eliminated |
| **3** | Active movement against gravity |
| **4** | Active movement against gravity and moderate resistance in a muscle specific position |
| **5** | Normal movement |
| **NT** | Not testable patient (immobilization, severe pain) |

## 1.3.3 Consequences of SCI

The consequences of the SCI can be divided into primary and secondary consequences. Primary consequences are presented immediately after injury while secondary consequences are not caused directly to the injury but are related consequences of SCI. This PhD is focused in two secondary consequences: neuropathic pain and spasticity days or even years after the injury.

### *1.3.3.1 Neuropathic Pain (NP)*

NP occurs as the result of damage to the nerve pathways at any point between the nociceptor (peripheral) and the brain (cortical)[22]. NP could be central (CNP), peripheral (PNP) or mixed[23].

PNP is a consequence of a lesion to or damage to the peripheral nerve, plexus, dorsal root ganglion, or root[22]. There are several conditions that can cause PNP, such as diabetic neuropathy, post-herpetic neuralgia, and post-surgical NP. CNP can arise from a lesion or dysfunction affecting the CNS, which is the brain or the spinal cord. The conditions that can cause CNP are: multiple sclerosis, stroke, limb amputation, or SCI[24]. In SCI patients, the CNP can be at or below the level of SCI[17].

"At level NP" can be due to damage of nerve roots or spinal cord which is located within the 3 dermatomes below the SCI, one dermatome above the SCI, or both[25]. It, therefore, can be mixed between PNP and CNP. "Below level NP" (bNP) is perceived in three or more dermatomes below SCI and it is caused by damage to the spinal cord. It is believed that the below level NP has a central origin, and it is therefore also referred as CNP. Approximately 41% of SCI patients experience bNP within the first six months following SCI[26].

#### 1.3.3.1.1 Mechanism of NP following SCI

The NP associated with SCI is one of the most complex pain syndromes[11,17,27]. It can be developed by multiple mechanisms due to structural and biochemical changes caused by SCI[28]. The mechanisms supposed to contribute to development of NP after SCI include central sensitization, central disinhibition, and central imbalance[17].

Central sensitization is caused by a decrease of the activation threshold of spinothalamic neurons due to excessive glutamate release following SCI[28]. It can also result in the hyperexcitability to mechanical, thermal, and nociceptive stimuli[12,17,29]. The hyperexcitability can be also caused by a reduction in gamma-aminobutyric acid, increase in N-methyl-D-aspartate receptors, and change in sodium and calcium channel expression[30,31]. The hyperexcitability can also be induced by reduced central inhibition.

The central disinhibition is caused by a decrease in the interneuron inhibitory function of the spinal cord[17]. The change in thalamic integrative circuitry can generate and amplify aberrant nociceptive impulses, which cause an inappropriate interpretation by the brain and hence the development of NP[31].

The central imbalance occurs when some of the spinal tracts pathways are more damaged than the others, which leads to an imbalanced the integration between the

spinothalamic tracts and the dorsal column tract activities. This imbalance may amplify the nociceptive activity and cause the development of NP[17,29].

#### 1.3.3.1.2 Assessment of NP

There are several assessment methods for NP, which can be divided into: **questionnaires** and **clinical examination**[22]. **Questionnaires** are a verbal report of various items, such as symptoms and signs of the pain, and related symptoms, such as mood, sleep and activity of daily life. These questionnaires include Neuropathic Pain Symptom Inventory (NPSI)[32], Brief Pain Inventory[33], the Leeds Assessment of Neuropathic Symptoms and Signs (LANSS)[34], the Neuropathic Pain Questionnaire (NPQ)[35], and McGill Pain Questionnaire[36]. Visual Analogy Scales (VAS) or Numeric Rating Scale (NRS) can also be used to subjectively measure the intensity of pain[20,23].

**Clinical examination** is used to test the sensory response. According to IASP, there are several clinical examinations tools[22], such as a piece of cotton wool or a soft brush for touch sensation, tuning fork (64 or 128 Hz) for vibration, wooden cocktail sticks for pinprick and sharp pain, cold object (20˚C) for cold sensation, and warm object (40˚C) for warmth sensation. Allodynia (painful sensation to a normally non-painful stimulus) and hyperalgesia (increased sensitivity to pain) are also evaluated by testing the perceptual threshold using monofilaments[20]. Perceptual threshold can be defined as the lowest stimulus intensity to which an individual reports pain[37].

#### 1.3.3.1.3 Management of NP

The management of the NP can be divided into pharmacological and non-pharmacological treatments. The pharmacological treatments include several types of medications, such as tricyclic antidepressants, anticonvulsants, analgesics, and opioids[38]. However, these treatments of NP can have side-effects, such as dizziness, sedation,

drowsiness, and constipation[39]. Additionally, only 40-60 % of the patients with NP report a relief from pain with the aid of such pharmacological treatments[40].

Non-pharmacological treatments of NP include transcranial direct current stimulation[41], repetitive transcranial magnetic stimulation[42], invasive motor cortex stimulation[43], deep brain stimulation, and Neurofeedback (NF)[44]. All these techniques are used to directly alter activity of the pain related areas of the brain. There are also treatments which change person's attitude toward pain, such as hypnosis, mindfulness[45].

#### *1.3.3.2 Spasticity*

Patients with spinal cord injury may suffer from spasticity and spasms after a period of spinal shock which is also related to the altered activity of STT[46]. At the first year following SCI, about 60% to 80% of SCI patients report symptoms of spasticity[17]. Spasticity after SCI is the exaggerated reflex below the level of injury. It occurs as a consequence of the disrupted nerve pathways between the brain and spinal cord[47]. Central control of spinal reflexes can be lost as a consequence of the damage which occurs to the upper motor neurons or their descending pathways[17]. Figure 1.6 shows that spinal reflexes are affected by descending inputs from the brain to the Ia synapse and the motoneuron[48]. Therefore, the brain can adjust these reflexes by modifying the control signals to Ia synapse and the motoneurons to adapt different actions.

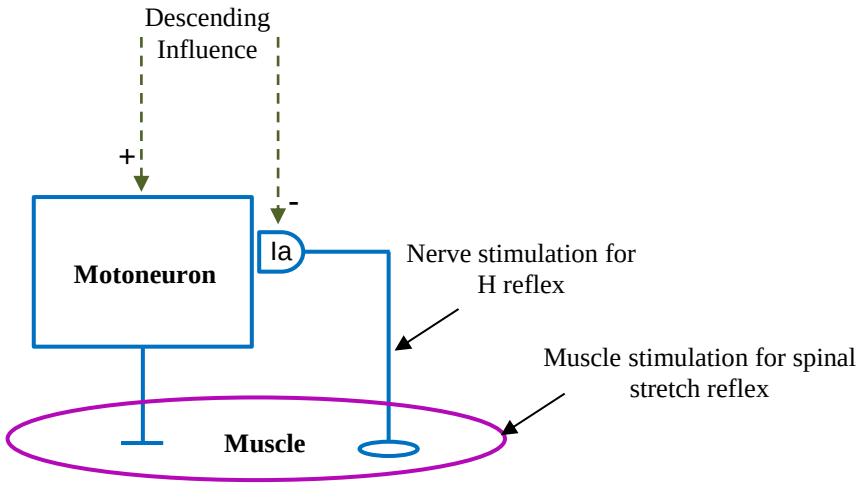


**Figure 1.6**: The main pathway of the H reflex and spinal stretch reflex[48]

The absence of this modulation signal results in the spinal reflex being more responsive to the sensory signal- this causes muscle spasms[47]. In able-bodied people, the brain modifies the reflex of the affected muscle by sending an inhibitory signal to the spinal cord to control the intensity of the reflex response[17]. The damage may occur at several descending spinal tracts pathways, and it may differ between pathways leading to altered type and strength of the input signal to the spinal cord[17]. This may cause a decrease in the discharge rate of the motoneuron, leading to a decrease of the voluntary drive (inhibition), or to an increase in the discharge rate of motoneuron (exaggerated reflex). Patients with SCI have a disrupted connection between the brain and the spinal cord due to injury. Therefore, the brain is unable to regulate a muscle reflex; a relatively small sensory stimulus causes a large reflex response resulting in spasticity.

A spinal reflex is also altered due to the change of the input signal to the interneurons, which regulate the activity of the motoneuron[17]. All these changes affect the excitability of the spinal reflex and the transmission of the spinal pathways. The Hoffmann reflex (H reflex), which is the electrical equivalent of the stretch (mechanical) reflex, has been used to measure the change in Ia afferent fiber transmission to the motoneuron[17]. Percutaneous

electrical stimulation activates a group of Ia afferent fibers. The sensory volley at that point proceeds to the spinal cord prompting a monosynaptic excitation of the objective motoneurons and leading to activate the muscle fibers[49].

#### 1.3.3.2.1 Assessments of Spasticity

The assessment methods of spasticity can be divided into: clinical examination, rating scales, biomechanical examination, and electrophysiological tests. Clinical examination uses a tapping technique to examine the strength and the reflex of the muscles[50]. Rating scale, such as the Ashworth Scale, can also be used to assess the spasticity and to determine the response to treatment[51]. Similarly, biomechanical examination, for example the pendulum test, can be used as an assessment method of spasticity[52]. In terms of the electrophysiological test, H reflex can be used as an indirect measure of spasticity by testing the integrity of spinal pathways[49,53].

#### 1.3.3.2.2 Management of Spasticity

There are several treatment methods that have been used to manage spasticity including physical rehabilitation, pharmacologic interventions, and surgery[46]. Physical rehabilitation uses several physical procedures in order to improve voluntary movements[17]. Pharmacological interventions include antispastic drugs, such as, Baclofen, Diazepam, Dantrolene and Tizanidine. Finally, intrathecal baclofen can be used to manage the spasticity particularly in patients with SCI[46].

## 1.4 Biosignals

Biosignals can be defined as signals extracted from a biological system, including the human body. Bio-electrical signals are generated as the result of the electrical potentials of nerve or motor cells[54]. There are several types of bio-electrical signals which arise from different tissues. For example, electrocardiogram (ECG) represents the electrical activity of

the heart muscles, electromyogram (EMG) represents the electrical activity of a muscles, and electroencephalogram (EEG) is a measure of brain related electrical potential. This PhD focuses on EMG and EEG.

## 1.5 Neurofeedback

Biofeedback is a method in which individuals train to voluntarily modulate their body functions, such as heart rate and breathing[55]. Neurofeedback (NF) is a as a sub-category of biofeedback that uses brain activity as a physiological parameter to be modulated at will[56]. By implementing NF technique, individuals can learn to voluntarily control or modify their brain activity[56,57]. The principal purpose of EEG based NF training is to provide subjects with feedback information regarding their instantaneous brain activity[57,58].

Similar to most training and learning modalities, NF requires training two to three times a week and for several weeks in order to learn the NF strategy[57]. The number of NF sessions may vary from 15 to 60 sessions depending on its application, type of NF, and the individual's learning ability[57].

### 1.5.1 Types and History of NF

There are several types of NF: ***Hemoencephalography (HEG)***, ***functional Magnetic Resonance Image (fMRI)***, ***Low Resolution Brain Electromagnetic Tomography*** (***LORETA***), ***Magnetoencephalography*** (***MEG)*** and ***EEG NF***.

In ***HEG based NF***, subjects train to voluntarily control their cerebral blood flow and the oxygenation density at a selected scalp site[57]. There are two types of HEG based NF near and passive infrared HEG[59]. It uses red and infrared light to detect and control cerebral blood flow and oxygen levels at small frontal regions of the brain (orbital gyrus, ventral medial cortex, or ventral lateral prefrontal lobes (Fp1, Fp2, Fpz, F7 or F8))[57].

The passive infrared HEG (pirHEG) uses non-contact infrared detector to detect changes in a brain thermal activity as the result of changes in a cerebral blood flow in large skull areas[59]. Although both nirHEG and pirHEG NF training may require less learning and shorter training session, have more immediate effect, and are less affected by artifacts than EEG NF, they are not suitable for all scalp locations due to interference from hair, and have lower temporal resolution than EEG NF[57].

Real time fMRI is based on blood oxygen level-dependent (BOLD) response in the brain[60]. In ***fMRI based NF***, subjects train to voluntarily regulate their BOLD response by using real time fMRI[61]. This BOLD response is related to the neuronal activity of the brain. fMRI has a high spatial resolution, therefore, it allows subjects to voluntarily regulate their brain activity within deep cortical structures. However, real time fMRI has a low temporal resolution due to a physiological time delay of BOLD in response to neural activity as well as due to the time delay associated with data recording and analysis[62,63]. The combined time delay of these two factors is approximately 6s to 8s[62,63].

***MEG*** was first measured by David Cohen in 1986[64]. It is a non-invasive recording technique that is used to record magnetic fields created by the brain by using very sensitive magnetometers[65]. This magnetic field is used for mapping brain activity. In MEG NF subjects train to voluntarily regulate their neuro-magnetic fields. Although, ***MEG NF*** provides a high spatial resolution and millisecond-scale temporal resolution, it is expensive and non-portable[65].

In ***EEG based NF*** subjects train to voluntarily regulate the electrical brain activity based on visual or auditory real time feedback of specific EEG features[66]. It was first used by Joseph Kamiya in 1963[57], who trained subjects to voluntarily regulate their alpha band (8-12 Hz). Then, in 1968 Barry Sterman used EEG NF to train cats to increase their SMR (which unlike human is 12-15 Hz); regularly in NF terminology 12-15 Hz is called SMR

instead of BCI terminology when SMR refers to 8-12 Hz. Training using EEG based NF is often designed to modulate the activity of a chosen EEG frequency band[57].

NF training protocol includes the choice of NF parameters, such as EEG recording montages, EEG electrode locations, EEG frequency bands, methods of providing the feedback (visual or audio feedback), and the type of NF modulation (reinforced or suppressed)[57]. NF parameters, which are the EEG features to be used as feedback, include the absolute or relative power of specific EEG frequency bands, power ratio of two different EEG frequency bands, coherence between two EEG electrodes or power ratio and Z score- derived measure based on many electrodes. The trainee may be asked to increase (reinforced) or decrease (suppressed) the activity of a frequency band depending on the NF application. One can also learn to modulate a ratio of two frequencies (alpha/theta)[67] or ratio between power in two electrode locations, typically located over two hemispheres.

***LORETA based NF*** is one of the modality of EEG NF in which subjects train to voluntarily regulate their intracranial current density at the brain region of interest[68]. It is based on the LORETA algorithm[69] and it requires a minimum of 19 EEG electrodes placed according to the 10–20 system[68]. It utilizes LORETA source localization which is widely used for off-line EEG analysis.

The reward threshold value of the NF training electrode can be set either by 10-20% above or under the mean absolute/relative power value or root mean square (RMS) value of the EEG calculated from pre-baseline spontaneous EEG (eyes opened or eyes closed state)[70], or the NF training parameter exceeds the threshold about 50-80% of time[71,72]. Threshold can also be set so that the amplitude is larger/smaller than threshold for 70% of time. This 70% baseline corresponds to RMS EEG. The time of updating the NF training parameter should be less than 0.5s[73].

### 1.5.2 EEG based NF Application

Various NF protocols have been designed to treat different types of disorders or to enhance the performance of healthy individuals. For example, the NF protocol for the reinforced SMR (12-15 Hz) and suppressed theta and beta band power over frontal, central, and parietal regions, with visual or audio feedback has been used for potential treatment of attention deficit hyperactivity disorder (ADHD)[57,72,74,75]. A NF protocol that reinforces (12-15 Hz) over the sensory-motor cortex has also been used for treatment of sleep disorders[76,77]. Additionally, (12-15 Hz) reinforced over the central and frontal cortex has been used for treatment of epilepsy in humans[78–80].

The alpha band asymmetry NF protocol over the frontal cortex has been used for the treatment of depression and anxiety[81,82]. The alpha-theta NF protocol over the occipital cortex has been used for treatment of post-traumatic stress disorder[83]. Connectivity based NF protocol has been used for the treatment of autism spectrum disorder[84]. The reinforced alpha band over the occipital cortex during eyes closed state has been used to increase the pain threshold and to reduce headaches after a head injury[85]. The reinforced SMR and suppressed theta and high beta bands have been used to reduce pain in patients with fibromyalgia syndrome[86,87]. The reinforced alpha combined with suppressed theta and high beta bands protocol has been used for the treatment of chronic pain in patients with SCI[44,88].

## 1.6 Biomedical Signals Processing

Biomedical signal processing can be used to extract and classify features from biomedical signals to be used for diagnosis and treatment of a medical condition. In this section, the methods of pre-processing and analysis of EEG and EMG used in this thesis will be discussed.

## 1.6.1 Event Related Potential (ERP)

An event related potential (ERP) can be defined as a change in the electrical activity of the brain generated in time domain by specific event or stimuli[89,90]. It is usually recorded by EEG. ERP can be generated as a response to an external event stimulus or psychological influence of an induced activity[89]. It can be used to assess the brain activity as a response to a particular external or internal stimulus. ERP analysis is problematic because of the low signal to noise ratio of the EEG[90,91], however, this can be solved by averaging in time the ERP activities for the multiple repetitive trails of the same task.

ERP includes various stimulus dependent waveform components (peaks)[89] which can be described by their polarity and latencies. For instance, N200 is a negative peak that occurs at 200ms, and P300 represents a positive peak that occurs at 300ms following an external stimulus. ERP components can be divided into sensory (exogenous) and cognitive (endogenous) components. The exogenous components occur early- that is within the 100-200ms window after a stimulus, as response to the physical characteristic of the stimulus. The endogenous components occur late - as a response to psychological influence of the stimulus[89,91]. Exogenous ERP are classified as visual, auditory, somatosensory and pain/thermal.

Movement related cortical potential (MRCP) is a type of ERP. It represents the change in the electrical activity of the brain generated during execution of overt or covert movement[92–94]. MRCP comprises of several components: readiness potential[95], premotor positivity[96], motor potential[97] and reafferent potential[98]. Readiness potential appears during the preparation of movement (before movement execution), while premotor positivity, motor potential, and reafferent potential appear after movement execution. The impairment of the sensory motor system can affect these MRCP components. Different experimental paradigms (cue based, self-paced, and multiple choice cue based) affect the morphology of

MRCP[92]. Studies show that patients with spinal cord injury have abnormal pattern of MRCP compared to able-bodied individuals[92–94].

## 1.6.2 Event Related Spectral Perturbation (ERSP)

An event related spectral perturbation (ERSP) is an example of time-frequency analysis of event related phenomenon. ERSP can be estimated by using wavelet analysis or short time Fourier transform (STFT) Equation 1.2[99]. It is one of the approaches to describe the change of the EEG spectral power evoked by stimulus in both time and frequency domain[100]. A negative value of ERSP is known as an event related de-synchronization (ERD) and a positive value of ERSP is known as event related synchronization (ERS)[101]. The ERD/ERS represents decreased/increased power in a chosen frequency band during task related state compared to the baseline (resting) state. A strong activation in the brain is represented by large ERD. The reason for the apparent reduction of the amplitude is desynchronized firing of neurons which when summed up because they do not fire at same time create smaller average amplitude. In the resting state, neurons fire simultaneously (synchronized) therefore the resulted amplitude looks higher. ERS/ERD can be calculated by Equation 1.1.

$$ERS/ERD = \frac{Power_{task} - Power_{baseline}}{Power_{baseline}} \quad \textbf{1.1}$$

$$ERSP(f,t) = \frac{1}{n}\sum_{k=1}^{n} |F\_k\ (f,t)|^2 \quad \textbf{1.2}$$

Where
n = the number of trials.
Fk(f,t) = the spectral estimation of trial k at frequency f and time t.

ERSP represents the average dynamic changes of the signal in both time and frequency domain[102]. It is more suitable to provide comprehensive descriptions of non-stationary

signals such as EEG, in which it is possible to simultaneously have ERD on one frequency and ERS on the other.

STFT can be computed by applying Discrete Fourier Transform (DFT) to a subset of the data. The number of the data points in the subset (M) can be equal or less than the total number of data points in the whole data (N). When the M = N, the STFT is same as DTF. The STFT is given by Equation 1.3.

$$X(k) = \frac{1}{Fs \times N} \sum_{n=0}^{N-1} x(n)w(n)e^{-j\omega_k n} \qquad k = 0, 1, 2, \ldots, N-1 \qquad \textbf{1.3}$$

Where:
x(n) = a discrete time signal n=1,2,3…. N
X(k) = a frequency representation of x(n)
w(n) = a windows function to select a subset of x(n) signal
N = the length of the x(n) signal
Fs = sampling frequency

In terms of wavelet analysis, a non-stationary signal, such as EEG, is decomposed into wavelets rather than trigonometric functions which are used in STFT[103]. The wavelet function φ(t), which is given by Equation 1.4[103], can be shifted by $\boldsymbol{a}$ and rescaled by $\boldsymbol{b}$ in order to match the original signal to be analyzed; where $\boldsymbol{a}$ and $\boldsymbol{b}$ are real numbers.

$$\varphi_{a,b}(t) = a^{-0.5} \times \varphi\left(\frac{t-b}{a}\right) \qquad \textbf{1.4}$$

The advantage of the wavelet analysis over the STFT is that the STFT uses the same window length in time domain for all frequencies in the signal, while wavelet uses larger window length for lower frequency and smaller window for higher frequencies. These properties of the wavelet analysis can provide smaller time resolution for higher frequencies and larger time resolution for lower frequencies. It is particular suited for EEG (higher frequencies have smaller energy). In ERD analysis, for example, it is more suitable to use larger frequency band on higher frequencies than lower frequencies. Additionally,

transient phenomenon can be better noticed with shorter time windows. There are several wavelets families, such as morlet[104], meyer[105] and daubechies. The morlet wavelet is one of the common biologically inspired wavelet[104,106]. It has been used to model biological signals such as EEG. Morlet wavelet comprises of several sinusoidal wave cycles windowed by Gaussian function (envelope function). The morlet wavelet, which is implemented in EEGLAB software (http://sccn.ucsd.edu/ eeglab/), has been used in this PhD thesis.

### 1.6.3 Frequency Domain Analysis

The raw EEG and EMG signals are the function of time (time domain). The signal in frequency domain contains information about the distribution of the amplitude and phase[107.] In order to transfer these signals to the frequency domain, spectral estimation techniques are required. There are several types of spectral estimation techniques, for instance the continuous or discrete Fourier transform. These techniques can be used to convert the time domain signal to its representation in the frequency domain. Equation 1.5 represents the continuous Fourier transform, where **x(t)** is a continuous time signal, **X(f)** is a frequency representation of x(t), and **ω** is 2πf.

$$X(f) = \int_{-\infty}^{\infty} x(t) e^{-j\omega t}\ dt \qquad \textbf{1.5}$$

Equation 1.6 represents the discrete Fourier transform (DFT), where **x(n)** is a discrete time signal, **X(k)** is a frequency representation of **x(n)**, and **ω** is 2πk/N where N is the total number of samples[108].

$$X(k) = \sum_{n=0}^{N-1} x(n) e^{-j\omega_k n} \qquad k = 0, 1, 2, \dots\dots\dots, N-1 \qquad \textbf{1.6}$$

## 1.6.4 Power Spectral Analysis

The power spectrum represents the power distribution of the signal in frequency domain of a signal of a finite duration[107,109]. It can be estimated by squaring the amplitude of signal in frequency domain as shown in Equation 1.7, where **P(f)** is the power spectral and **F(f)** is a signal in frequency domain[109]. The power spectral for a finite frequency interval between $\mathbf{f_1}$ and $\mathbf{f_2}$ can be calculated by Equation 1.8. The power of the signal can be absolute as calculated by Equations 1.7 and 1.8 or relative $\mathbf{P_{relative}(F)}$ at specific frequency (**F**) which can be calculated by Equation 1.9.

$$P(f) = |F(f)|^2 \quad \textbf{1.7}$$

$$P_{finte\ interval}(f) = \sum_{f=f_1}^{f_2} P(f) \quad \textbf{1.8}$$

$$P_{relative}(F) = \frac{P(F)}{P_{finte\ interval}(f)} \quad \textbf{1.9}$$

## 1.6.5 Independent Component Analysis (ICA)

Independent Component Analysis (ICA) is a linear decomposition method that can be applied to a multivariate signal such as EEG. In order to decompose it into maximally temporal independent components a spatial filter is created with relative fixed projections to the recording electrodes and maximally independent time courses of the data[110–112]. ICA is a method used to determine a linear representation of non-Gaussian signal in which the components are statistically independent[113]. It can be described by Equation1.10 [113]. Three assumptions have been made in order to estimate the unknown mixing matrix $\boldsymbol{a_{jn}}$: (i) the components $\boldsymbol{s_n}$ are statistically independent, (ii) $\boldsymbol{s_n}$ have non-Gaussian distribution and (iii) $\boldsymbol{a_{jn}}$ matrix is square[113].

$$x_j = a_{j1}s_1 + a_{j2}s_2 + \cdots + a_{jn}s_n \quad \text{for all j} \qquad \textbf{1.10}$$

Where:
$x_j$ = a random variable measured at $j^{th}$ site
$s_n$ = $n^{th}$ independent component (IC) which is also random variable
$a_{jn}$ = weighted sum of $n^{th}$ IC activity measured at $j^{th}$ site

EEG is a type of multivariate signal recoded over the scalp; hence it is composed of signals generated from different dipole sources located at different cortical or sub-cortical regions of the brain. It is also affected by several types of artifacts, such as eye movements, eye blinks, muscle activity, and line noise[110,114]. Equation1.10 can be rewritten as equation1.11 to represent EEG signal, where ***EEG*** is the EEG channel matrix (scalp channels (n) by time points (m)), ***S*** is the source matrix (no. of sources (n) by time points (m)) generated by artifacts, deep cortical and/or sub cortical activities, and ***A*** is the mixing square matrix (scalp channels (n) by no. of sources (n)). ICs can be obtained by multiplying the inverse of ***A*** matrix (***W=A$^{-1}$***) with ***EEG***, as shown in Equation1.12. The back projection of the ICs to the EEG data after removing artifacts and noisy ICs can be obtained by Equation 1.13.

$$EEG_{m,n} = A_{n,n}.S_{m,n} \qquad \textbf{1.11}$$

$$S_{m,n} = W_{n,n}.EEG_{m,n} \qquad \textbf{1.12}$$

$$EEG_{m,n} = W^{-1}{}_{n,n}.S_{m,n} \qquad \textbf{1.13}$$

## 1.7 Aim and Objectives

This thesis aims, firstly, to investigate the effectiveness of neuromodulation of alpha (8-12 Hz) EEG band on excitability of corticospinal tract, as measured by the H reflex. Secondly, to understand the causal relation between the brain activity measured by EEG and CNP early after SCI. Thirdly, to test the effectiveness of NF treatment on CNP early after SCI. Finally, to explore differences in MCRP activity between able bodied volunteers

and SCI patients with and without CNP, within functionally connected areas in the brain including deeper cortical structures which cannot be directly assayed by EEG.

The primary objectives are:

- To explore the possibility of short-term modulation of the soleus H reflex during different neuromodulation strategies (NF, motor imagery, and mental math) of the EEG alpha band (8-12 Hz) in abled bodied volunteers. (**Chapter 3**)
- To define causal relation between EEG and first symptoms of CNP by comparing both spontaneous and induced EEG activity of three sub-acute SCI patients groups: a group of patients with pain, a group of patients with no pain, and a group of patients who developed pain within six months after EEG recording, as well as a control group of able bodied volunteers. (**Chapter 4**)
- To test the efficiency of NF for treatment of CNP by comparing two groups: a group with CNP receiving NF treatment (Treatment group), and a group with CNP not receiving NF treatment (monitoring group). (**Chapter 5**)
- To define how the presence of long standing CNP affects two main EEG phenomena which characterize a motor action, ERS/ERD and MPCP, in order to find the relation between the activation of the motor cortex and the CNP. This is achieved by comparing EEG during imagined movement task between three groups of participants (a group of chronic SCI patients with CNP, a group of chronic SCI patients with no pain, and a control group of able bodied volunteers) using measure projection analysis (MPA) method. (**Chapter 6**)

The secondary objective is:

- To investigate long term changes in the brain activity as a result of NF training, used for treatment of CNP.

# 2
# Literature Review

# Chapter 2 Literature Review

This chapter presents an overview of the current state of the art in the area of neural plasticity following SCI and its influences on SCI patients. Studies which have been conducted to investigate brain plasticity following SCI and following CNP will be reviewed. Furthermore, studies which have explored spinal cord plasticity following SCI will be discussed. A number of possible non-pharmacological therapies of CNP and spasticity following SCI will also be described. Moreover, several prediction studies for CNP following SCI will be explored.

## 2.1 Neural Plasticity following SCI

Neural plasticity is the reorganization of activation patterns at various levels of the CNS in response to acquiring new skills, development and neuro-rehabilitation following injury to the CNS[115]. It can be functional and/or structural plasticity. Functional plasticity occurs due to modification of the strength of existing neural connections, while structural plasticity occurs due to development of new neural networks. There is considerable evidence that neural plasticity occurs after SCI as a consequence of disruption of afferent and/or efferent pathways between the brain and the spinal cord[116–119]. Neural plasticity after SCI may occur in cortical structures[116,119], such as the somatosensory area, and in subcortical structures such as the thalamus[119,120] and spinal cord[121,122].

### 2.1.1 Brain Plasticity following SCI

Brain plasticity is the ability of the brain to adjust its functions and structure in response to changes in the body or its environment. Brain imaging studies, such as fMRI, positron emission topography (PET) and EEG, revealed that cortical and sub-cortical reorganization occurs after SCI[115,119].

fMRI studies comparing brain activity between chronic complete paraplegic patients and healthy controls demonstrated that SCI patients have a larger activation over the primary motor cortex (M1)[123–127], supplementary motor area (SMA)[124,125], primary sensory cortex (S1)[123,124], prefrontal cortex[123,128] and thalamus[124,128] during both imagined[123–125,128] and attempted[124,125] movement of the paralysed limb and executed movement of non-paralysed limbs[126,127], thus indicating that paralysis causes wide spread changes which also affect brain areas of the non-paralysed parts of the body. Additionally, tetraplegic patients exhibited smaller, task-related activity, in M1 early post-SCI in comparison to healthy controls during right wrist extension movement and this activation increased over time during the recovery period[129].

A PET study comparing brain activation between chronic complete SCI patients and healthy controls during wrist extension of the right hand reported that paraplegic SCI patients and healthy controls had increased activation over the sensorimotor cortex (SMC) and thalamus, while tetraplegic patients only had a significant increase in activity over SMA[130]. This study also demonstrated that the activation of the contralateral SMC was correlated with the function of the hand in tetraplegic patients. Bruehlmeier et al.[131] reported that SCI patients showed higher activation over SMA, SMC, thalamus and cerebellum during repetitive joystick movements of the right hand and these activations were stronger in paraplegic patients in comparison to tetraplegic patients.

EEG studies comparing the MRCP of chronic SCI patients with healthy controls reported that large negativity in MRCP amplitude was noticed in SCI patients during imagined movements of paralyzed lower limbs[92,132]. Green et al. demonstrated that the shifting of MRCP location from posterior to anterior regions occurs in SCI patients in response to improved motor function[133]. Gourab and Schmit reported that chronic SCI patients exhibit stronger 13-35 Hz ERD and lower 13-35 Hz ERS during toe plantar-flexion attempted movement of the right lower limb as compared to able-bodied

controls[134]. A longitudinal EEG study on sub-acute tetraplegic patients reported that patients had strong ERD 7-13 Hz and 14 -30 Hz EEG oscillations during attempted movement of the right hand and this activity was negatively correlated with functional improvements of the patients[135].

To summarise these findings, SCI patients showed increased[123–128,130,131] activation over somatosensory and motor area in the brain, shifting in cortical representation (somatotopic reorganization)[133], stronger ERD[134,135] and larger negativity of MRCP amplitude[92,132] during actual[125–127,130,131,133,134], attempt[129,135] or imagery[92,123–125,128,132,135] movement tasks. The majority of these studies assumed that the main reason for brain or cortical plasticity after SCI is the deafferentation of the CNS[116,119,123,131,132,135].

### 2.1.2 Brain Plasticity following CNP

The relation between brain reorganization and CNP following SCI have been reported by many neuroimaging studies[16,136–138]. Neuroimaging studies also demonstrated that the degree of brain reorganization is associated with the intensity of CNP[136,138].

EEG studies comparing spontaneous (resting state) EEGs of chronic paraplegic SCI patients with and without CNP with EEGs of healthy controls reported that, during eyes closed relaxed state, patients with CNP exhibited reduction and shifting of dominant alpha frequency towards the lower frequency compared with the other two groups[24,138–140]. Jensen et al. reported that higher frontal alpha band activity was associated with higher intensity of CNP[138].

An EEG study by our research group reported that power spectral density (PSD) of alpha band (8 to12 Hz) increased over most of the EEG electrode locations in patients with CNP and a larger PSD of theta band (4 to 8) was noticed in patients with CNP over the frontal and occipital cortical areas as compared with patients with no pain during eyes open

relaxed state[140]. Moreover, patients with CNP had increased ERD during imagined movement of both unaffected upper and affected lower limbs over Cz[140].

A fMRI study by Gustin et al. comparing SCI patient with CNP to healthy controls revealed that SCI patients with CNP showed increased activation in left M1 and the right superior cerebellar cortex while imagining movement of right ankle plantar flexion and dorsiflexion[141]. Gustin et al. also reported that increased activity in the right dorsolateral prefrontal cortex, anterior cingulate cortex, SMA and right premotor cortex were significantly correlated to the severity of CNP during the same motor imagery task[141]. Another fMRI study by Wrigley et al. on chronic SCI patients with CNP noticed a shift in cortical representation of the little finger in S1 towards leg (painful limb) cortical representation during light brushing of the fingers[136]. Furthermore, this reorganization in S1 was correlated with the intensity of CNP[136].

Yoon et al. revealed using structural MRI that SCI patients had a significant decrease of grey matter volume in the left middle frontal gyrus, bilateral anterior insula, and right subgenual anterior cingulate cortex compared with healthy controls[142]. Yoon et al. additionally reported that mean diffusivity values in some of the deep and superficial white matter areas were diminished in SCI patients with CNP. Hypometabolism of brain glucose, which was measured by fludeoxyglucose positron emission tomography (FDG-PET), was also noticed in the left middle frontal gyrus and right medial frontal gyrus in SCI patients with CNP compared with healthy controls[142].

In summary, SCI patients with CNP showed reduction in power and shifting in dominant alpha frequency[24,138–140] and increased in theta (4 to 8 Hz) frequency band[140] during relaxation. Moreover, increased ERD over sensorimotor cortex during motor imagery was noticed[140]. Over activation[141], shifting[136] and volume loss[142] were also noticed in SCI patients with CNP in both cortical and subcortical structures. Although differences in outcomes among studies are more likely due to the differences in

experimental tasks and neuroimaging techniques, the reorganization and over-activation of the sensorimotor cortex has been consistently reported, and can be considered as the cortical signature of CNP[140,141].

### 2.1.3 Spinal Cord Plasticity following SCI

Spinal cord plasticity after SCI can be in response to structural, functional and/or molecular changes in the spinal cord[115,143]. Structural plasticity includes atrophy, demyelination and degeneration of spinal neurons[144,145]. Molecular or neurochemical plasticity may present as a change in amino acids, cytokines, ions and microglial activation[146]. Changes in spinal reflexes can also occur after SCI, resulting in a functional plasticity[115,147,148].

MRI studies on chronic SCI patients revealed that they had a reduced cross-sectional spinal cervical cord area in comparison to healthy controls[144,145,149]. A significant reduction was noticed in the anterior-posterior width of the spinal cord area while there was no significant reduction in the left-right width. SCI patients with tetraplegia show greater reduction in spinal cord area than SCI patients with paraplegia[144]. Moreover, the smaller cord area in SCI patients was associated with the presence of below-level CNP[144] and impaired upper limb function[145].

Another MRI study by Lundell et al. also found that chronic SCI patients exhibited a decrease in spinal cord area in both anterior-posterior width and left-right width[149]. Additionally, the international standards for neurological classification of SCI scores of sensory and motor functions were positively correlated to the anterior-posterior width and the left-right width of the spinal cord, respectively[149]. A fast decline in the cross-sectional area of the spinal cord was noticed over 12 months post SCI[150]. The decrease of the white matter volume of the corticospinal tract was also noticed in SCI patients, over the first year after SCI, compared to healthy controls[150].

An animal experimental study by Gwak et al. testing neurochemical plasticity of SCI demonstrated that rats with SCI exhibited loss in spinal GABAergic cells function as measured by behavioural and electrophysiological procedures using a von Frey filament (VFF, 24.5 mN) and extracellular single-unit recordings of wide dynamic range (WDR) dorsal horn neurons, respectively[151]. Gwak et al. also reported that the hypo-function of GABA results in dorsal horn neuronal hyperexcitability which contributes to development of CNP[151]. Hains et al. demonstrated that SCI induces the up-regulation of Nav 1.3 sodium channel expression, resulting in dorsal horn neuronal hyperexcitability associated with CNP following SCI[152]. Gao et al. also demonstrated that an injury to the spinal cord may result in the down regulation of GABA receptor expression, causing spasticity as a secondary consequence of SCI[153].

A study by Hiersemenzel et al. tested the excitability of spinal neuronal circuits measured by electrophysiological procedures. They revealed that SCI patients during spinal shock had small F-waves and an absence of flexor reflexes associated with a loss in muscle tone and a loss of tendon reflexes in the affected leg[147]. According to Hiersemenzel et al., the reappearance of F-waves and flexor reflexes occurred a month after injury and was associated with the recovery of muscle tone and tendon reflexes[147]. No change in H reflex amplitude was found. However, paraplegic chronic patients showed a decrease in M wave and flexor reflex amplitudes, which are associated with the clinical signs of spasticity[147]. This study suggested that spasticity is a result of impairment/degeneration of motoneurons due to long standing SCI[147].

A study by Leis et al. comparing acute and chronic SCI patients noticed that the loss of F-waves was presented in acute but not in chronic patients[154]. Leis et al. reported that in acute SCI patients, H reflex amplitude was very small within the first 24 hours after injury and returned back to its normal amplitude within a few days after injury, as patients were in a state of spinal shock[154]. However, the loss of F-waves continued within the several

weeks after SCI. The authors of this study suggested that the loss of H reflexes and F waves at the early stage (within 24 hours following an injury) were caused by the hyperpolarization of spinal motoneurons, which can remain for more than 3 weeks following the injury[154]. They also suggested that restoration of the H reflex amplitude 24 hours after injury was due to changes in the synaptic function of Ia motoneurons.

Involuntary muscle contraction (spasticity) in SCI patients has also been attributed to increased motoneuron excitability within the spinal cord[155,156]. The alteration of spinal reflex activity can also occur as a result of changes in spinal pathways[157,158]. A study by Barthélemy et al., on chronic incomplete SCI patients, tested the relation between the impairment of the corticospinal tract and the degree of foot drop (inability to dorsiflex the ankle) during rest and walking[159]. In this study, the activity of the corticospinal tract was measured by motor-evoked potentials (MEPs) over tibialis anterior muscle elicited by transcranial magnetic stimulation. It was demonstrated that a weaker ankle dorsiflexion during walking (larger foot drop) correlated with smaller MEPs which are associated with impairment of the corticospinal[159].

In summary, spinal cord plasticity can happen after SCI as a result of structural, functional and molecular changes. After SCI, changes in motoneurons excitability, modification of spinal reflexes and activation of spinal tracts can contribute to several locomotion problems such as involuntary muscle contraction and increased muscle tone. Structural, functional and molecular plasticity after SCI can contribute to developing both spasticity and CNP.

## 2.2 Non-pharmacological Treatments of CNP

Non-pharmacological interventions can be used to directly alter the cortical and subcortical activity following CNP which can result in reduction of intensity of CNP. These interventions include motor cortex stimulation (***MCS***)[160–162], deep brain stimulation

(***DBS***)[163,164], transcranial direct current stimulation (***tDCS***)[165–174], repetitive transcranial magnetic stimulation (***rTMS***)[166,173–177] and neurofeedback (***NF***)[44,56,87,88,178–182]. There are also non-pharmacological treatments which can be used to change a patient's behaviour and attitude toward the pain, such as ***hypnosis***[183–188] and ***mindfulness***[45,188–190]. A Cochrane study by Bold et al. identified tDCS, rTMS, and hypnosis but not MCS, DBS, NF, and mindfulness as non-pharmacological treatments for chronic pain following SCI[173]. This may be because there were no many studies of them investigating this area.

***MCS*** and ***DBS*** are invasive cortical stimulation methods which use electrical stimulation to activate deep brain structures[160]. They require the implantation of stimulation electrodes which involves surgical procedures[160]. DBS studies revealed that stimulation of periventricular/periaqueductal grey matter (PVG/PAG) in addition to the sensory thalamus and internal capsule was more effective in reducing neuropathic pain than stimulation of the sensory thalamus alone[163,164]. Nguyen et al noticed that MCS can reduce trigeminal neuropathic pain in 75% of patients[161]. However, Im et al. reported that only 50% of SCI patients with CNP showed 50% of short-term pain relief compared with 80% and 100% of patients with post-stroke central pain and peripheral neuropathy, respectively[162]. Im et al. also reported that MCS resulted in a larger long-term pain relief on central pain associated with stroke and peripheral neuropathic pain than on CNP following SCI[162].

***tDCS*** is a non-invasive cortical stimulator that has been used to modulate cortical excitability by applying low amplitude direct current (≥ 2mA) through electrodes attached to the specific area of the skull above the neural tissue that has to be excited[165,166]. tDCS can increase cortical excitability by applying surface positive (anodal) electrode stimulation which causes depolarization of neuronal membranes and an increase in the spontaneous firing rate[165,167]. It can also be used to decrease cortical activity by applying

negative (cathodal) electrode stimulation, causing neuronal hyperpolarization and a decrease in neuronal firing rate[165,167].

Results of tDCS studies using anodal tDCS stimulation (2 mA current during 20 min) to stimulate the M1 cortex in chronic SCI patients (complete and incomplete) with CNP demonstrated a significant reduction in CNP compared to sham stimulation[168–170,172]. On the contrary, a tDCS study on complete chronic SCI patients with CNP did not report a reduction in CNP after anodal tDCS stimulation (2 mA current during 20 min)[171]. Furthermore, a study by Zaghi et al. reported that the perception and thresholds of pain can be increased by anodal tDCS over M1[166].

***rTMS*** is another type of non-invasive neuromodulation technique. In rTMS, a varying magnetic field is used to induce electrical current in the neurones of a specific area of the cerebral cortex by applying magnetic stimulation coils to the scalp[175]. It has been documented that rTMS may not only stimulate the cortical area below the site of stimulation but also the distant cortical areas through the lateral neuronal pathways[191,192]. Depending on the stimulation frequency, it can cause a decrease or an increase in cortical excitability[166]. For example, rTMS stimulation frequency in the range of 1 Hz can decrease cortical excitability, while stimulation frequency in the range of 20 Hz can increase cortical excitability[166]. High frequency (≥ 5 Hz) rTMS stimulation leads to increased neuronal firing by reducing the neuronal firing threshold and causing an increase in cortical excitability[193]. In contrast, low frequency (≤1 Hz) rTMS stimulation leads to decreased neuronal firing by raising the neuronal firing threshold and inhibiting cortical excitability[193].

rTMS studies on chronic paraplegic patients with CNP showed similar significant reductions in CNP intensity immediately after each treatment session in both the treatment and sham group[176,177]. However, 2 to 6 weeks after the rTMS therapy, the treatment group showed more reduction in CNP than the sham group[176,177]. rTMS parameters for these

studies were 500 trains at 5 Hz over a period of 10s[176] and 30 trains at 10 Hz over a period of 5s[177] applied over lower limbs (painful limbs) presentation of the motor cortex. rTMS showed a beneficial long-term but not short-term reduction effect on CNP when it was applied over M1 in patients with chronic SCI[174,176,177].

***NF*** in a non-invasive treatment that is used to voluntary modulate brain activity[56]. It is believed that NF can improve synaptic strength and modulate brain connectivity within and between brain structures which can result in neuroplasticity[178]. NF has been used to treat several types of chronic pain, such as complex regional pain syndrome, migraines and fibromyalgia syndrome[87,179–182]. However, the mechanisms and the protocols of NF treatment of CNP are still a matter of debate[88]. Most NF studies of chronic pain adopt up-regulation of alpha or lower beta band activity and down-regulation of theta and higher beta band activity over the central or temporal cortex as part of their protocol[87,88,179,182]. Studies chose this protocol based on previous studies which linked the presence of CNP with more theta and beta activity and less alpha [138,140,194].

A NF study by Jensen et al. on SCI patients with chronic pain tested three different NF protocols and failed to show any significant difference on short-term pain intensity between these protocols[88]. Jensen et al. also reported that only 2 out of 10 SCI patients achieved a clinically significant reduction in pain intensity (>30%) when treated with a NF protocol in which (10 -15 Hz) was up-regulated and both beta (13-21 Hz) and theta (4 -7.5 Hz) band relative power were supressed over central and parietal cortices[88]. This study suggested that the small number of NF treatment sessions (12 sessions, 4 for each NF protocol) is the reason for inconclusive results.

A pilot study by our research group tested several NF protocols for treatment of chronic CNP in patients with paraplegia. It noticed that down-regulating theta (4-8 Hz) and higher beta (20-30 Hz) and up-regulating alpha (9-12 Hz) relative power over M1 (C3/C4 EEG electrode location) had a beneficial short-term and long-term effect on CNP[44].

Additionally, SCI patients who received ≥ 20 NF treatment sessions had clinically and statistically significant reduction of CNP with effects lasting at least one month after therapy[44]. NF therapy had a neurological effect not only on the cortical but also on deeper cortical structures involved in the pain matrix. Assessment of cortical activity during imagined movement of both painful and non-painful parts of the body demonstrated a reduction of excessive cortical activity, in particular in the theta band. It has been reported that NF not only activates areas directly influenced by training but also other distant functionally related areas[44].

It has been reported that ***hypnosis*** therapy has an effect on chronic pain in general[183–185]. A case study by Stoelb et al. reported that a hypnotic therapy was able to reduce the experience of chronic pain after SCI[186]. Another study on SCI with chronic pain by Jensen et al. reported that SCI patients showed a significant reduction in average pain intensity during hypnosis therapy[187]. The same study also reported that the SCI patients who received hypnosis therapy had a significant reduction in long-term pain intensity (3 months follow-up period) compared with SCI patients who received EMG biofeedback relaxation therapy[187]. A hypnosis study on SCI patients with chronic nociceptive and/or neuropathic pain revealed that a significant reduction in pain intensity was associated with changes in EEG activity: an increase in theta activity over frontal and posterior areas, an increase in alpha activity spread over a whole area and a decrease in gamma activity over central areas was noticed[188].

Studies showed that ***mindfulness*** therapy can also be used to reduce the intensity of chronic pain[46,188,189]. It has been demonstrated that a single mindfulness session can produce a significant reduction in chronic pain following SCI, associated with significant increases in alpha and beta bands EEG activities over left parietal areas[188]. Zeidan et al. noticed using mindfulness and fMRI that healthy participants exhibited significant reductions in pain intensity generated by noxious thermal stimulus[45]. This was associated

with the reduced activation of contralateral S1 cortex, thalamic deactivation and increased activity in anterior cingulate cortex (ACC) and anterior insular cortex (AIC)[45].

In summary, several neuromodulation treatments seem to be at least partially effective in the treatment of CNP in SCI patients. A review study by Jensen et al. suggested that NF, rTMS and tDCS have preliminary promising results in short-term effects of CNP relief[193]. Boldt et al also suggested that tDCS has short and mid-term effects in reducing CNP[173]. The majority of these techniques target the sensory-motor cortex. Moreover, the reduction of CNP intensity was associated with modulation of the brain activity in pain related areas as measured by fMRI or EEG. According to Boldt et al, however, there was insufficient evidence to suggest that rTMS and hypnosis interventions are influential in decreasing CNP following SCI due to the weakness in the methodology[173].

## 2.3 Non-pharmacological Treatments of Spasticity Following SCI

Spinal cord plasticity following SCI can cause spasticity through mechanisms described in section 2.1.3. There are several non-pharmacological treatment methods that can be used to reduce spasticity. These methods include: physiotherapy treatments[195,196], transcutaneous electrical nerve stimulation (TENS)[197–199], spinal cord stimulation (SCS)[195,200–202] and repetitive transcranial magnetic stimulation (rTMS)[153,201].

Elbasiouny et al. reported that an increase in muscle tone can cause spasticity as well as affect the mobility of joints and the range of motion in individuals with SCI[195]. Therefore, stretching the spastic muscle every day may reduce muscle tone and enhance the range of motion and the mobility of the joint[195]. Another study on chronic SCI with spasticity by Onushko and Schmit reported that the sensory information of contralateral hip afferents plays an important role in the modulation of the excitability of the reflex response in the ipsilateral leg[196]. Onushko and Schmit also reported that sensory information from the

contralateral hip crossed the spinal cord and modulated the excitability of the reflex response in the ipsilateral leg. Therefore, it was suggested that manipulation of the hip position may reduce the effect of spastic reflex during locomotion[196].

Ping et al. revealed using TENS on SCI patients with lower limb spasticity that one hour of TENS session (stimulation parameters 0.25 ms pulse duration, 100 Hz frequency, 15 mA current intensity) over the common peroneal nerve resulted in significant and immediate decreases in lower limb spasticity of patients with SCI in comparison to the placebo TENS group[197]. Oo et al. also reported using TENS on sub-acute SCI with lower limb(s) spasticity that one hour TENS (0.2 ms pulse duration, 100 Hz frequency, 15 mA current intensity) session over the common peroneal nerve followed by 30 minutes physical therapy had significant reduction on lower limb(s) spasticity of patients with SCI compared with the control group with just 30 minutes physical therapy[198]. In both studies, the level of spasticity was measured by a composite spasticity score[197,198]. TENS aims to alter the abnormality of spinal inhibitory circuits, interneuron activities[199] and alpha motor neuron activity[198] in the spinal cord.

Spinal Cord Stimulation was also used as a minimally invasive technique to treat spasticity. Chronic SCI patients with lower limb spasticity exhibited reduction on spasticity using Spinal Cord Stimulation (SCS) over the posterior epidural space at vertebral levels T11 to L1; the effectiveness of SCS depended on SCS electrode location and stimulation parameters[200]. Hofstoetter et al. reported that transcutaneous SCS, in patients with chronic SCI and lower limb spasticity, for a 30 minute duration (2ms, 50Hz, 20V) over the T11/T12 vertebral level, led to reduced spasticity[201]. However, Midha et al. demonstrated that SCS had a short-term but not long-term effect on reducing spasticity in chronic SCI patients[202]. It was suggested that SCS increases the level of presynaptic inhibition and increases the activities of inhibitory networks in the spinal cord[195,200].

rTMS study by Kumru et al. on chronic incomplete SCI patients with lower limb spasticity demonstrated that 20 Hz rTMS over the primary motor cortex of the leg caused a reduction in lower limb spasticity in patients receiving treatment as compared with the control group of patients who received a sham rTMS stimulation[203]. In this study the Modified Ashworth Scale was used to assess the spasticity. On animals with complete SCI, a rTMS study by Gao et al. revealed that 10 Hz rTMS causes a decrease in spasticity and enhances motor recovery[153]. rTMS treatment aims to increase corticospinal inhibitory input and reduce segmental spinal excitability by increasing the excitability of M1[203].

In summary, several non-pharmacological treatment methods can be used to treat spasticity following SCI. These methods aim to alleviate one or more of the spinal plasticity processes that cause spasticity. Physiotherapy targets biomechanical components of the spasticity[195]. TENS regulates the abnormality of spinal inhibitory circuits, interneuron activities[199] and alpha motor neuron activity[198] in the spinal cord. SCS increases the level of presynaptic inhibition and increases the activities of inhibitory networks in the spinal cord[195,200]. The corticospinal and segmental spinal excitabilities are targeted during rTMS treatment[203].

## 2.4 Prediction of CNP following SCI

Studies have investigated the sensory profile and the cortical activation of SCI patients in early post-injury and in a later follow-up period, in order to find a predictor of CNP. A clinical or cortical predictor of CNP may lead to the development of a preventive therapy to minimize the risk of CNP in SCI patients[20,204].

A study by Levitan et al. on acute SCI using the sensory components of the international standards for neurological classification of spinal cord injury (ISNCSCI) to predict CNP after SCI demonstrated that patients who developed CNP within the first year

after injury showed a lower pinprick score than SCI patients who did not develop CNP[204]. Additionally, patient who developed CNP showed a higher light touch than pinprick score. Levitan et al. suggested that the sensory components of ISNCSCI, which is a routine examination of all SCI patients, can be used to predict the CNP[204].

Zeilig et al. reported that incomplete acute SCI patients who developed CNP within the first 6 months after injury, had higher thermal thresholds than patients who did not develop CNP[20]. Moreover, the thermal threshold of SCI patients who developed CNP gradually increased over time. Zeilig et al. also reported that SCI patients, who developed CNP showed dynamic allodynia within the first 2 months after injury. Therefore, it was suggested that a loss of the spinothalamic tract function and enhancement of the dorsal column function over time lead to the development of CNP[20].

A prospective study by Finnerup et al. demonstrated that the present of sensory hypersensitivity (dysesthesia) in patients within the first month after SCI can be used as predictor for a later development of CNP[205]. They suggested that sensory hypersensitivity after SCI can be result from neural hyperexcitability preceding the development of CNP. Zeilig et al. also suggested that neural hyperexcitability preceding the development of CNP after SCI and it can be consequent to damage to spinothalamic tracts[20]. Finnerup et al. reported that the present of sensory hypersensitivity not only can be used as a predictor but also can be used to distinguish between at or below the level of injury CNP[205].

Wasner et al. examined the function of STT of chronic complete SCI patients with and without CNP using quantitative sensory testing[206]. They noticed that 8 out of 12 patients with CNP perceived the sensation of the thermal stimuli combined with topical capsaicin as painful stimuli. In contrast, no sensations were induced in patients without pain. Wasner et al. suggested that the deficits in STT function can lead to the development of CNP below the level of injury[206]. Cruz-Almeida et al. used a quantitive sensory test to assess the function of STT in chronic complete SCI patients with and without CNP and reported that

the greater severity of CNP below the level of injury was associated with greater sensitivity to thermal stimuli[207]. They suggested that residual STT function leads to severe CNP following SCI. Cruz-Almeida et al. also demonstrated that the deficits in STT function may be necessary for the development of CNP[207].

An fMRI study by Lee et al. tested the relation between cortical activities during passive movement of the toe and the development of CNP after SCI. They revealed that SCI patients with a higher incidence of CNP showed a significant change in the blood oxygenation level dependent (BOLD) response in the ipsilateral frontal lobe[208]. It was suggested that CNP after SCI is more likely to develop when changes in the BOLD response in the ipsilateral frontal lobe are detected during proprioceptive stimulation[208].

In summary, a clinical or cortical predictor for CNP following SCI has been investigated by several studies. Abnormality in the sensory profile below the level of injury of SCI patients and the sparing of the STT can be utilized to predict CNP. Moreover, changes in the BOLD response to the proprioceptive stimulation of the ipsilateral frontal lobe in SCI patients can lead to expected CNP. Early prediction of CNP following SCI can be used to initiate a preventive therapy to reduce its development.

## 2.5 Summary

The plasticity of the brain and spinal cord following SCI have been invistgated by various neuroimaging studies. Most of the brain imaging studies reported over-activation of the somatosensory and motor areas of the brain following SCI, while other studies reported shifting somatotopic reorganization and associated changes of MRCP with SCI. The plasticity of the brain after CNP has also been reported by brain imaging studies. They demonstrated that reduction in power, shifting in dominant frequency and an increase in ERD over the sensorimotor cortex, were associated with CNP following SCI. Over-activation, shifting and volume loss in both cortical and subcortical structures of the brain

were also noticed in SCI patients with CNP. However, none of these studies provide information about the dynamic changes in the activity of deep cortical structures of the brain.

The structural, functional and molecular changes of the spinal cord following SCI were also investigated by neuroimaging studies. They reported that changes in motoneuron excitability, modification of spinal reflexes and activation of spinal tracts associated with SCI can contribute to developing both spasticity and CNP. Neuromodulation treatments seem to be at least partially effective in the treatment of CNP following SCI and the reduction of CNP intensity was associated with modulation of the brain activity in pain related areas as measured by fMRI or EEG. Although neuromodulation treatments have been found to have an effect in reducing CNP following SCI, the samples used were in the chronic phase of SCI. Therefore, it will be beneficial to treat SCI patients for CNP in the early stage of injury. Moreover, a cortical predictor of CNP following SCI in early post injury may lead to the development of a preventive therapy to minimize the risk of CNP in SCI patients.

## 2.6 Contribution to the Literature

This thesis provides several contributions to the literature, in the area of real time modulation of brain activity and in the area of CNP

This is the first study showing the modulation of the H reflex during NF and it is also the first study demonstrating the relationship between the modulation in EEG activity and the H reflex amplitude during various neuromodulation strategies. This study provides a novel, important first step towards understanding the effect of voluntary modulation of SMR on the H reflex amplitude, as an integral part of the neurorehabilitation of movement. This study should inform development of future motor rehabilitation brain-computer

interface, which often assume that the modulation of SMR is a sufficient cortical representative of motor imagination.

Clinical predictors of CNP following SCI have been investigated in several studies showing that patients at risk of developing CNP have altered sensations to mechanical and thermal stimuli. These tests are less applicable to patients with complete injury. EEG is a biological signal that can be reliably measured in all patients independent of the level or completeness of injury. This thesis demonstrates for the first time EEG predictors of CNP in patients with SCI, even before signs of allodynia to a mechanical stimulus. This study provides multiple evidence that gradual changes in cortical activity do not exclusively occur as a consequence of long standing pain but that they also precede pain, possibly contributing to its chronification. It also shows that following the onset of pain, cortical activity undergoes further changes, which are very similar to changes previously observed in chronic SCI patients with long standing pain. This provides the evidence that the presence of pain affects cortical activity on a much shorter timescale than previously believed.

NF treatments have been found to have an effect in reducing CNP following SCI. However, patient populations were in the chronic phase of SCI. The contribution of this thesis is in exploring the effectiveness of NF training on CNP in subacute SCI patients and providing evidence that NF treatment of the recently developed CNP has the same effect as NF of long-standing CNP.

Electroencephalography signatures of CNP in patients with chronic SCI have been defined by several studies. The effects of CNP on dynamic EEG signatures on wider cortical structures have been explored only by researchers in our laboratory, but these were defined for time-frequency features only. A related analysis of movement related cortical potentials was inconclusive and limited to only several electrodes located over the central cortex. There is no published literature that investigates the effect of CNP on the event

related potential of wider cortical structures. This study utilised the recently developed Measurement Projection Analysis method to define functionally related cortical areas with specific morphology of evoked potentials during a cue based motor imagery task. It shows that in contrast to event-related synchronisation/desynchronisation, MRCP is not affected by CNP during preparation of movement, but that the main effect is noticeable on the sensory, reafferentation component of MRCP. It also provides evidence that a neurological condition which affects the activity of the sensory-motor cortex may affect post-synaptic responses of main pyramidal neurons (i.e. ERP including MRCP) and oscillations in the neuronal networks (i.e. ERS/ERD) in a very different way.

# 3

# The Effect of Voluntary Modulation of the Sensory-Motor Rhythm during Different Mental Tasks on H Reflex

# Chapter 3 The Effect of Voluntary Modulation of the Sensory-Motor Rhythm during Different Mental Tasks on H Reflex

## 3.1 Abstract

***Objective:*** Exploring the possibility of the short-term modulation of the soleus H reflex through self-induced modulation of the sensory-motor rhythm (SMR) as measured by electroencephalography (EEG) at Cz.

***Methods***: Sixteen healthy participants took part in one session of neuromodulation. Motor imagery and mental math were strategies for decreasing SMR, while neurofeedback was used to increase SMR. H reflex of the soleus muscle was elicited by stimulating tibial nerve when SMR reached a pre-defined threshold and was averaged over 5 trials.

***Results:*** Neurofeedback and mental math both resulted in the statistically significant increase of H reflex ($p = 1.04 \cdot 10^{-6}$ and $p = 5.47 \cdot 10^{-5}$ respectively) while motor imagery produced an inconsistent direction of H reflex modulation ($p = 0.57$). The average relative increase of H reflex amplitude was for neurofeedback 19.0 ± 5.4%, mental math 11.1 ± 3.6% and motor imagery 2.6 ± 1.0%. A significant negative correlation existed between SMR amplitude and H reflex for all tasks at Cz and C4.

***Conclusion:*** It is possible to achieve a short-term modulation of H reflex through short-term modulation of SMR. Various mental tasks dominantly facilitate H reflex irrespective of direction of SMR modulation. Significance: Improving understanding of the influence of sensory-motor cortex on the monosynaptic reflex through the self-induced modulation of cortical activity.

## 3.2 Introduction

The H reflex has been regarded as a valuable tool for investigating the excitability of the spinal reflex pathways[49,53]. It is believed that the H reflex can be conditioned through spinal and supraspinal sites[209,210]. At the supraspinal level, the sensory-motor cortex has been identified as the main cortical center for H reflex conditioning. It has been shown that the H reflex amplitude is modulated during overt and covert motor tasks[211–214]. In general, the H reflex amplitude is increased during Motor Imagery (MI)[212–214] during which similar neural mechanisms are activated and rules followed as for overt movement[215]. However, the direction of H reflex change may be affected by the amount of MI practice. For example, in elite speed skaters, who perform mental simulation of voluntary motor actions as a part of athletic training, the soleus H reflex amplitude is reduced during mental movement simulation (i.e., vividly imagining skating movement)[216,217].

The H reflex can also be modulated during a mental task such as Mental Math (MM). MM reduces the alpha rhythm in the posterior and occipital region[218]. Oishi and Maeshima observed a significant increase in the H reflex amplitude during MM in non-elite athletes but not in elite athletes[217]. It appears that the mental tasks of MI and MM have differing effects on spinal reflex excitability depending on the athletic training background of the subjects. On the cortical level, both MI and MM decrease the power of 8-12 Hz band measured by electroencephalography (EEG)[219]. However, while MI directly modulates localized sensory-motor rhythm (SMR), MM modulates a wide spread 8-12 Hz activity as well as activity in the delta band[220]. To date, EEG activity and the H reflex have not been measured concurrently during MM or MI tasks.

While both MM and MI result in reduction of SMR, it is an open question how an increase of SMR would affect the H reflex amplitude. Apart from relaxation, which results in an increase of wide-spread alpha rhythm (8-12 Hz), it is hard to define a verbalised

mental strategy that would result in SMR increase. Nevertheless, people can be trained to voluntarily modulate their brain activity if visual or auditory feedback is provided in real time. This technique is called 'neurofeedback' (NF) and has been used for treatment of a range of neurological and psychiatric conditions, such as ADHD, epilepsy, depression, and pain[44,59]. Because NF relies on non-verbalised rules, it typically requires training over several daily sessions. For example, in a research study by our group, we trained chronic paraplegic patients with CNP to increase SMR over the primary motor cortex of the right hand to reduce sensation of pain[44]. They successfully learned the strategy over 3-4 daily sessions. Power in 8-12 Hz band increased predominantly over central areas of the cortex, indicating that patients modulated sensory-motor mu rhythm rather than a wide-spread alpha rhythm. Recently there have been several controlled randomised studies involving patients which demonstrated that people can successfully learn to increase power in the upper alpha (10-12 Hz) frequency band, resulting in improved memory performance[221,222]. A person can also be trained to decrease SMR using NF. This strategy has been used in brain computer interface studies, where visual feedback increases the degree of event-related desynchronisation during MI tasks, hence decreasing the power of the SMR[223]. However, training to modulate SMR in both directions using non-verbalised strategies would require an even greater number of training sessions. Occasionally people may be able to verbalise their mental NF strategies (relaxation, imagination, singing, praying, and focussing), but strategies vary among people for the same task. It should be mentioned however, that while there is no published literature on modulation of H reflex using NF, other biofeedback strategies, not directly exploiting the activity of brain, have been successfully applied to modulate the amplitude of the H reflex in a desired direction in humans and animals[209,224].

The purpose of this study was (i) to explore the possibility of a short term modulation of the soleus H reflex through a self-induced modulation of the SMR rhythm, (ii) to assess

whether the direction of H reflex modulation is correlated with the direction of SMR modulation (i.e. increase or decrease in EEG power), and (iii) to assess whether different mental tasks, which modulate SMR in the same direction (i.e. MM and MI) affect the amplitude of the H reflex in a similar way across different cortical locations. We used NF to train subjects to increase SMR, and used both MI and MM to reduce the SMR. Defining the relationship between the self-induced modulation of SMR and the amplitude of H reflex is important for understanding the mechanism through which the sensory motor cortex contributes to the conditioning of the H reflex.

## 3.3 Methods

### 3.3.1 Participants

Sixteen able-bodied volunteers (10 male and 6 female, age 27.9 ± 4.1 years) participated in the study. The exclusion criteria were any known history of neurological disorder or an ongoing injury to the upper or lower limbs. One of the participants was excluded from the study due to the inability to detect H reflex. All participants provided informed consent for the study, which was reviewed and approved by the College of Science and Engineering ethics committee, University of Glasgow. All methods used in the experiment comply with the Declaration of Helsinki.

### 3.3.2 Experimental Setup

Throughout the experiment participants' posture and head position were maintained to be unchanged. Participants were seated at a desk, with both legs flexed at the hip ($90^o$), knee ($90^o$), and ankle ($0^o$). During the experiment they were facing a computer screen (15" size) at an approximate distance of 120cm. Participants kept hands on their thighs. They were instructed to stay still and relaxed throughout the experiment. Figure 3.1 shows the experimental setup.

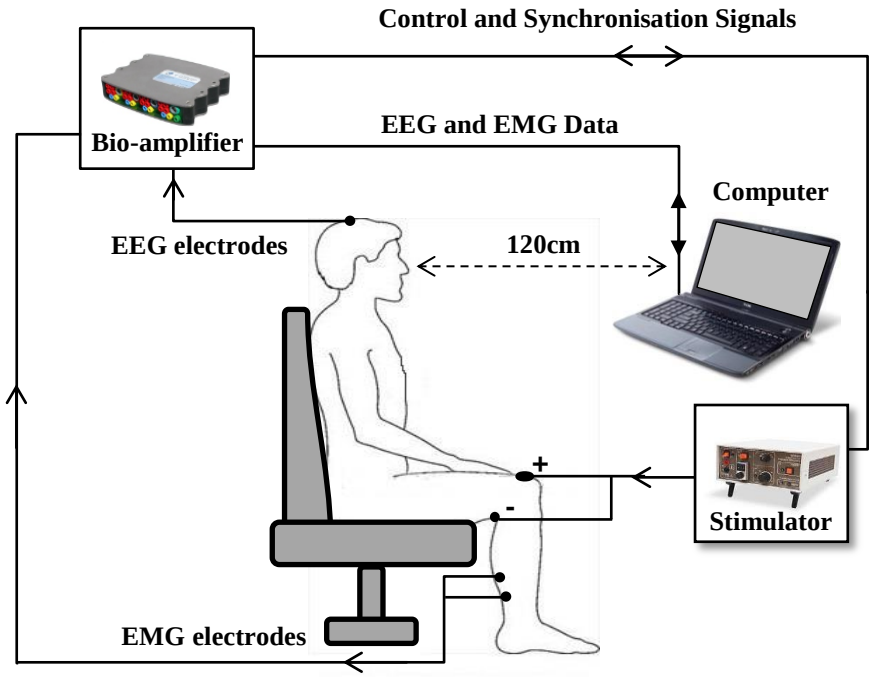


**Figure 3.1** The experimental setup diagram. Participants sit straight looking towards the computer screen. Visual feedback was provided during NF task only. During each of the tasks, computer calculated power of SMR recorded by EEG device and based on its value activated the stimulator to elicit H reflex

A 16 channel biosignal amplifier (g.USBamp, Guger Technologies, Austria) was used to record EEG and electromyogram (EMG). The amplifier consisted of 4 subunits with 4 channels each, which can have separate or common reference and ground. EEG and EMG were recoded with separate reference and ground. EEG sampling frequency was 2400Hz, and was band-pass filtered between 2 and 60Hz (and notch filtered at 50Hz) using 5th order infinite impulse response (IIR) digital Butterworth filter within the g.USBamp device. The reference electrode was attached to the left earlobe, while the ground electrode to the right earlobe. Impedance was kept under 5kΩ. EEG was recorded from the central, parietal and occipital cortical areas, C3, Cz, C4, P3, P4 and Oz, according to the international 10-20 system[225]. For 5 participants, additional EEG recordings were acquired using electrodes C3, Cz, C4, P3, P4, Oz, C1, C2, CPz and FPz. EMG sampling frequency was 2400 Hz and was band pass filtered between 5Hz and 500Hz using 5$^{th}$ order IIR digital Butterworth filter within the g.USBamp device.

For EMG recording, skin was prepared with alcohol swabs and abrasive gel and shaved if necessary. EMG of the soleus muscle was recorded using bipolar surface pre-gelled electrodes with Ag/AgCl sensors (Meditrace,USA, 133, 3cm diameter), placed over the muscle belly with center to center distance of 2cm. The ground electrode was placed at the medial malleolus and reference electrode at the lateral malleolus.

For EEG, the skin was prepared with a combined abrasive-conductive gel (Abralyt 2000) and EEG was recorded with Ag/AgCl electrodes. The SMR (8-12 Hz) was measured from electrode Cz (corresponding to the primary motor cortex location for legs), or, for EEG recordings with additional electrode sites, using the Laplacian derivative[226] as described in Equation 3.1. The calculation was performed on-line in Simulink, Matlab (Mathworks, USA).

$$Cz_{LAPLACE} = C_z - \left( \frac{C_1 + C_2 + FC_z + CP_z}{4} \right) \qquad \textbf{3.1}$$

Monopolar recording is known to record mixed activity of both local and distant sources, thus possibly recording both alpha and SMR activity. The Laplacian derivative is a spatial filter which preserves only the activity of the local sources, thus possibly reducing the influence of wide spread alpha rhythm[226]. The reason for two different EEG montages was to compare the effect of modulation of local and distant EEG sources on H reflex. SMR (8-12Hz) rhythm is an oscillatory activity primarily reflecting sensory-motor processing in the fronto-parietal networks[227]. An internal event (e.g. imagination of movement) or an external stimulus causes asynchronous firing of the underlying neuronal substrate, i.e. desynchronisation, which manifest itself as reduced amplitude of the SMR. Pfurtscheller and Lopes da Silva describe evoked or induced reduction of central (8-12Hz) rhythm (here referred to as SMR) as Event Related Desynchronisation (ERD), which presents an active state[228]. The increase in the amplitude of this rhythm is a result of synchronous firing of neuronal substrate and is called Event Related Synchronization

(ERS). This is considered as an 'idling' state[228,229] in which a system is not involved in processing sensory input or preparing motor output. The 'occipital alpha' rhythm is an EEG correlate of relaxed wakefulness, best observed with the eyes closed. It is usually found in the occipital, parietal, and temporal regions[230]. Increased (synchronized) occipital alpha rhythm can be considered as an `idling rhythm' of the visual area. Both SMR and alpha rhythms contribute to EEG recorded at central regions of the brain, with the occipital alpha thought to be due to the volume-conduction effect; therefore it could be reduced by Laplacian derivation. In this chapter, EEG signal in 8-12 Hz range recorded with both montages will be referred to as SMR.

### 3.3.3 Measurement of H Reflex

Participants' H reflex was evoked with self-adhesive electrodes (Anode: 9 × 4cm, Cathode: 3cm diameter, Pals platinum, Nidd Vally Medical Ltd, UK). The cathode was placed over the tibial nerve in the popliteal fosse and the anode was placed on the patella. Bipolar electrical stimulator Digitimer (Stimulator Model DS7, England) was used to deliver the 1ms long rectangular pulses. Current intensity was increased in increments of 2mA to obtain a maximal muscle response (M wave). The exact location of the cathode was determined by hand held bar stimulation electrode (9 mm diameter, AD instruments). The normalized H reflex was chosen on the rising part of the recruitment curve so that the M wave amplitude was approximately equal to 20% of the maximum M wave. Minimum time between two stimuli was 15s to avoid habituation.

### 3.3.4 Study Procedure

Prior to the experiment which modulated H reflex, all participants took part in 3 daily NF training sessions, because this technique requires previous training. The NF training sessions will be explained later in the text, in Section 3.3.6. On the fourth day all participants took part in Experiment 1 (as described in Section 3.3.70), following

procedures shown in Figure 3.2. Five participants took part in the subsequent Experiment 2 (as described in Section 3.3.8) on the same day, in which Laplacian EEG derivation was applied following the same experimental protocol (Figure 3.2).

As a part of Experiment 1 and Experiment 2, the H reflex was measured in five conditions: a relaxed state before neuromodulation tasks (PreRelax), during each of three mental tasks in the following order: MM, NF and MI, and in a relaxed state following the three mental tasks (PostRelax). The H reflex was evoked when SMR reached a predefined threshold for at least 0.5s. For the NF task, threshold was set to 60% above the baseline relative SMR power, and for MM and MI task it was set to 80% under the baseline relative SMR power (details on baseline recording provided in Section 3.3.7). For each experimental condition, the H reflex was evoked 5 times and mean ± standard deviation (SD) values presented in the results. Minimum time between two H stimulus was 15s to avoid habituation. The stimulation parameters were kept constant throughout the experiment.

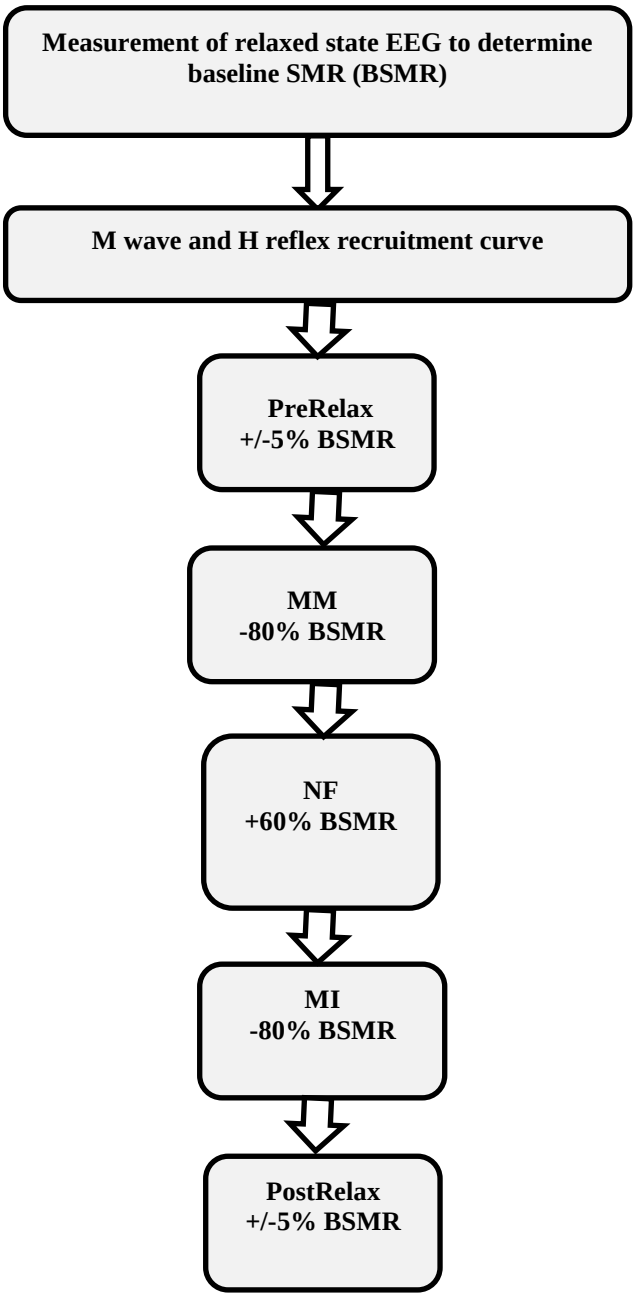


**Figure 3.2** Experimental protocol for Experiments 1 and 2. Sensory-motor rhythm (SMR) refers to the normalized power in the 8-12 Hz band measured from Cz in either monopolar (Experiment 1) or Laplacian derivation (Experiment 2). Threshold SMR of each condition was measured with respect to a corresponding baseline SMR (BSMR). An H reflex was evoked when SMR reached a threshold for 0.5s. Numbers in boxes describing conditions present corresponding threshold values to evoke H reflex

### 3.3.5 Real-Time Data Acquisition and Analysis

Real time data acquisition and processing were performed with g.RTanalyzer (Guger technologies, Austria) in Simulink. A graphical user interface was developed in LabView (National Instruments, USA). Real time data acquisition software, from the same

manufacturer as the EEG device, contains a block in Simulink representing the EEG device that can be used to select recording electrode sampling frequency, common ground, and other recording parameters.

The EEG device sends signal in batches, the size of batch depending on the sampling frequency. For 2400 samples/s it is 128. Then, EEG data was down-sampled to 300 samples/s using 'Downsample' block in Simulink (down sample factor, K = 8). To calculate the relative EEG power in 8-12Hz bands, down sampled EEG recorded at Cz (or Laplacian derivation calculated in Simulink) was bandpass filtered ($5^{th}$ order IIR Butterworth) in 8-12Hz and 2-30Hz bands using two independent filter blocks in Simulink. Filtered EEG in both bands was then squared and smoothed/averaged over a half second sliding window (150 samples), updated after each sample (1/300s), to obtain the band power features. However, because of receiving signals in batches, the sliding window was effectively updated after every 8 samples. Following this, a relative power was calculated by dividing power in 8-12Hz band with the power in 2-30Hz band. This value was compared with a reference value for a given task, which was previously calculated based on 2min EEG recording in the relaxed eyes opened (EO) state, using a graphical user interface developed in LabView. For different tasks, conditions to activate electrical stimulator to elicit H reflex were met when relative power calculated over one sliding window of 150 samples reached the threshold.

### 3.3.6 NF Pre-Training

Neurofeedback strategy requires several training sessions in which participants explore the non-verbalised mental strategy that results in a desired outcome (operant conditioning). Prior to Experiment 1, participants were trained to increase SMR amplitude during 3 training sessions organized over three separate days. Throughout SMR training for all participants, the Laplacian derivation was not used. Each session was divided into 6 sub-

sessions lasting 5min each (30min in total). At the beginning of each NF practice session, monopolar EEG was recorded in EO relaxed state for 2min. During EO EEG recording, participants were asked to stay still and to concentrate on a small cross in the middle of a computer screen to avoid eyes movement. This EEG was used as the baseline EEG for a subsequent NF training. During NF training, participants were instructed to control a graphical object (bar) on the computer screen using their EEG. A graphical user interface was developed in LabView. Real time data acquisition and processing was performed with g.RTanalyzer in Simulink.

The height of the bar was proportional to the power of the SMR and changed color from red to green when the power increased above the threshold, set at 20% above the baseline value (Figure 3.3). This threshold was lower than during NF experiment, because a threshold set too high in the initial training would result in poor performance and might cause frustration. Electrical stimulation was not applied during NF pre-training sessions.

### 3.3.7 Experiment 1

EEG baseline activity in EO state was measured. Participants sat still looking in front of them at a cross at the computer screen for 2min. EEG was visually inspected and portions of EEG exceeding 100μV were removed before calculating the power of the SMR. Following this, an H reflex recruitment curve was created and stimulation amplitude of H reflex was determined as previously described. Next, participants were asked to perform a maximum isometric dorsiflexion of both feet for 10s, as a reference for defining 60% of maximum voluntary contraction for a subsequent MI task. The raw EMG was observed on the computer screen, its amplitude measured during maximum contraction, and approximate amplitude for 60% of maximum contraction calculated. The participants were verbally informed when their contraction reached that level. Participants performed several

real muscle contractions at about 60% of maximum voluntary contraction which facilitated subsequent kinaesthetic imagination (KI) of movement (described in Section 3.3.7.3).

In Experiment 1, H reflexes were measured in five experimental conditions: PreRelax, NF, MI, MM and PostRelax. Participants were allowed to rest 5 min between each of the conditions.

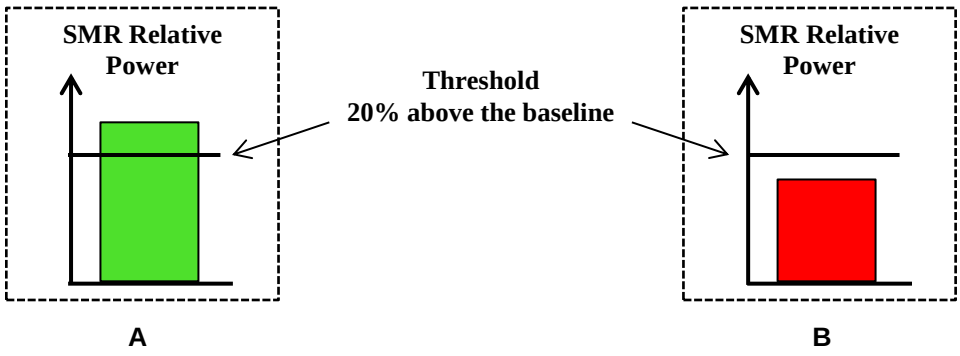


**Figure 3.3** Visual feedback during neurofeedback, bars represent normalized power of SMR averaged over 0.5s sliding window. When SMR was above the threshold (20% above the baseline for pre-training, 60% for Experiments 1 and 2), the color of the bar was green, otherwise it was red

### *3.3.7.1 Measuring H Reflex Amplitude in a Relaxed State*

The same procedure was adopted for measuring H reflex amplitude in PreRelax and PostRelax condition. Participants sat still and relaxed in front of a computer screen looking at a cross in the middle of the screen (to minimize saccadic eye movement). Their SMR was monitored, and H reflex was evoked when SMR was within 5% of the baseline SMR measured at the beginning of the experiment for at least 0.5s. At least 15s was allowed between two H reflex evocations to avoid habituation.

### *3.3.7.2 Neurofeedback Task*

During NF training, participants were instructed to control a graphical object (bar) on the computer screen using their EEG. During the NF condition, participants were asked to increase the SMR amplitude. The size of the bar was proportional to the power of the SMR rhythm and changed the color from red to green when it increased above the threshold

(Figure 3.3), set at 60% above the baseline value. H reflex was automatically evoked when the power of SMR rhythm was 60% above the baseline for at least 0.5s. The H reflex was elicited five times with a minimum inter-stimulus interval of 15s.

#### *3.3.7.3 Motor Imagery Task*

Following a visual cue on a computer screen, participants were instructed to imagine repetitive ankle dorsiflexion at 60% of the maximum voluntary contraction of the soleus muscle at their preferred pace. They were instructed to imagine feeling muscles in their legs (kinaesthetic imagery) rather than a simple visual imagery because of their distinctive activation of the sensory-motor cortex[230]. After each cue, 5s were given to participants to concentrate on the tasks prior to SMR measurement. Visual feedback was not provided for this task. H reflex was evoked when SMR was 80% under the baseline value for at least 0.5s. An H reflex was evoked following each cue. The H reflex was evoked five items with a minimum inter-stimulus interval of 15s.

#### *3.3.7.4 Mental Mathematics Tasks*

During MM, participants were instructed to subtract numbers in intervals of 7 starting from a random large number. H reflex was evoked if SMR was 80% under the baseline value for at least 0.5s. Visual feedback was not provided for this task. The H reflex was evoked five times with a minimum inter-stimulus interval of 15s.

In order to examine whether there is any short term carry-over effect, following the three experimental conditions (MM, NF and MI), participants were asked to relax and sit still while 5 H reflexes were elicited at rest (PostRelax).

### 3.3.8 Experiment 2

Five participants took part in Experiment 2. They were given a 10min rest between Experiments 1 and 2. The same experimental procedure was adopted as in Experiment 1;

except SMR was calculated at Laplacian-derived Cz. Current amplitude to evoke the H reflex was kept the same as in Experiment 1. A baseline SMR from $Cz_{LAPLACE}$ was calculated (see Equation 3.1) from EEG measurement at the very beginning of the experiment, prior to Experiment 1, when it was also recorded from Cz monopolar montage.

### 3.3.9 Kinaesthetic and Visual Imagery Questionnaire (KVIQ)

Following Experiments 1 and 2, on a separate day, participants' level of visual and kinaesthetic imagery were tested by using Kinaesthetic and Visual Imagery Questionnaire (KVIQ)[231]. KVIQ is divided into two imagery tests: kinaesthetic and visual imagery. Each test comprises 17 questions. Participants were asked to perform a specific movement of a limb or a trunk, which was presented verbally. Then, they were asked to imagine performing the same movement and to rate it on a 5 grades scale, which describes the imagination clarity. For kinaesthetic imagery, 0 means no sensation, and 5 means as intense a sensation as if executing the action.

### 3.3.10 Off line Signal Processing

Offline analysis was performed using Matlab. Normalized power, with respect to power in 2-30Hz band was calculated for theta (4-8Hz), SMR (8-12Hz) beta 1 (12-15Hz), and beta 2 (16-24Hz) band. The Pearson correlation test was performed to examine a possible correlation between the H reflex amplitude, normalized with respect to the maximum amplitude for each participant, and the power in all frequency bands for the initial baseline period and all three tasks.

To exclude the influence of background EMG on H reflex, the stability of the background EMG was examined post hoc by calculating the root mean square (RMS) value of the EMG for both 100ms and 2s pre stimulus intervals in all five conditions. The short 100ms period was based on the requirements of studies looking into the modulation of H reflex during MI[213]. A choice of the 2s period was based on results of biofeedback

studies[224] which recommended that background EMG should be stable (i.e. within a predetermined range) for at least 2s before stimulation in order to ensure no effect of EMG backgorund on the H reflex. The relative amplitude of the H and M waves during MM, NF, MI and PostRelax tasks was expressed with respect to the H and M waves during the initial relaxed period (PreRelax) – see Equation 3.2 and Equation 3.3 respectively.

$$H(\%) = \frac{H_{TASK} - H_{PRERELAX}}{H_{PRERELAX}} \quad \textbf{3.2}$$

$$M(\%) = \frac{M_{TASK} - M_{PRERELAX}}{M_{PRERELAX}} \cdot 100 \quad \textbf{3.3}$$

Normalized H reflex amplitude was presented as the percentage of maximum H reflex amplitude for that person. While relative H reflex amplitude presents the H reflex of a task with respect to the H reflex in a relaxed condition, normalized H reflex characterizes a certain task, independent of the baseline value, and can therefore be also calculated for PreRelax period. The former is convenient measure to assess the effect of a mental task on the H reflex, while the latter is more appropriate measure to find a correlation between the amplitude of different brain rhythms and the amplitude of the H reflex.

### 3.3.11 Statistical Analysis

A non-parametric test (paired sign rank sum, p=0.05) was used to check whether there was a statistically significant difference between any pair of tasks. A linear correlation between two independent variables was measured using the Pearson correlation test. A correction for multiple comparisons was performed using Holm-Bonferroni correction[232]. To test whether there existed a statistically significant difference in mean values between more than two variables across repeated measures, a non-parametric Friedman test (non-parametric, repeated measure ANOVA) was used. In cases of several factors e.g. one factor montage and other factor task, Friedman test had to be applied to each factor separately, because it does not allow analysis of interaction between factors. All

calculations were performed in Matlab. H reflex was considered stable (no habituation or carry-over effect) if the absolute difference between PreRelax and PostRelax was less than ± 5%.

## 3.4 Results

In this section we first present the results of modulation of H reflex and M wave amplitude during all three mental tasks for both monopolar and Laplacian montage. This is followed by the analysis of correlation between the H reflex and EEG power in different frequency bands during MM, NF and MI tasks during Experiments 1 and 2. We subsequently present modulation of power in different frequency bands over the central, parietal and occipital cortex during different mental tasks. Finally, we show results of a correlation between the H reflex and vividness of KI.

### 3.4.1 The Variation of Relative H Reflex and M Wave during Neuromodulation Tasks

The average relative H reflex and M wave amplitudes during different conditions are presented in Figure 3.4 and Figure 3.5 respectively. The average relative amplitude increase of H reflex (with respect to PreRelax) was largest during NF (19.0 ± 5.4%, mean ± median) followed by MM (11.1 ± 3.6%) and MI (2.6 ± 1.0). During MM, NF, and MI, 12 out of 15 participants achieved modulation of H reflex amplitude larger than 5% in at least one task. During NF the amplitude of H reflex significantly increased as compared to the PreRelax ($p = 1.04 \cdot 10^{-6}$), and similarly during MM as compared to the PreRelax ($p=5.47 \cdot 10^{-5}$). Low values for the relative H reflex amplitude during MI are due to a fact that in about half participants with significant (> 5%) modulation, the amplitude of the H reflex increased and in the other half it decreased. This resulted in overall non-significant difference compared to PreRelax (p=0.57). There was a statistically significant difference

in relative H reflex amplitude between the tasks (MM vs NF p=0.037, MM vs MI p=0.0064 and NF vs MI $p=1.93 \cdot 10^{-5}$).

There was no statistically significant difference in H reflex amplitude between PreRelax and PostRelax state (p=0.69). In all participants, the H reflex amplitudes PostRelax remained stable (variation less than ± 5%) as compared to the amplitude during PreRelax. This indicates that there was no modulation of H reflex due to habituation.

On a group level, there was no statistically significant difference in M wave amplitude between the baseline level PreRelax and all three tasks together (p=0.0723). There was also no statistically significant difference in M wave amplitude between neuromodulatory tasks (MM vs NF p=0.0818, MI vs NF p=0.9305 and MM vs MI p=0.1765). The M wave for all participants remained stable during all tasks (variation less than ± 5%) compared to the amplitude before the experiment (PreRelax). This indicates the stability of direct efferent muscle response throughout the whole experiment.

Figure 3.6 shows the H reflex and M waves during PreRelax, all three neuromodulation tasks, and PostRelax for three representative participants. Figure 3.6.A shows an example in which H reflex increased in all neuromodulatory tasks, in particular during NF, and returned to the baseline value during PostRelax task (P8, in Figure 3.4 and Figure 3.5). Figure 3.6.B shows an example in which H reflex decreased during MI and slightly increased during NF (P4, in Figure 3.4 and Figure 3.5). Finally, Figure 3.6.C shows an example with no changes in H reflex during neuromodulatory tasks (P3, in Figure 3.4 and Figure 3.5). Note that in all participants and in all 5 conditions the M wave remained stable.

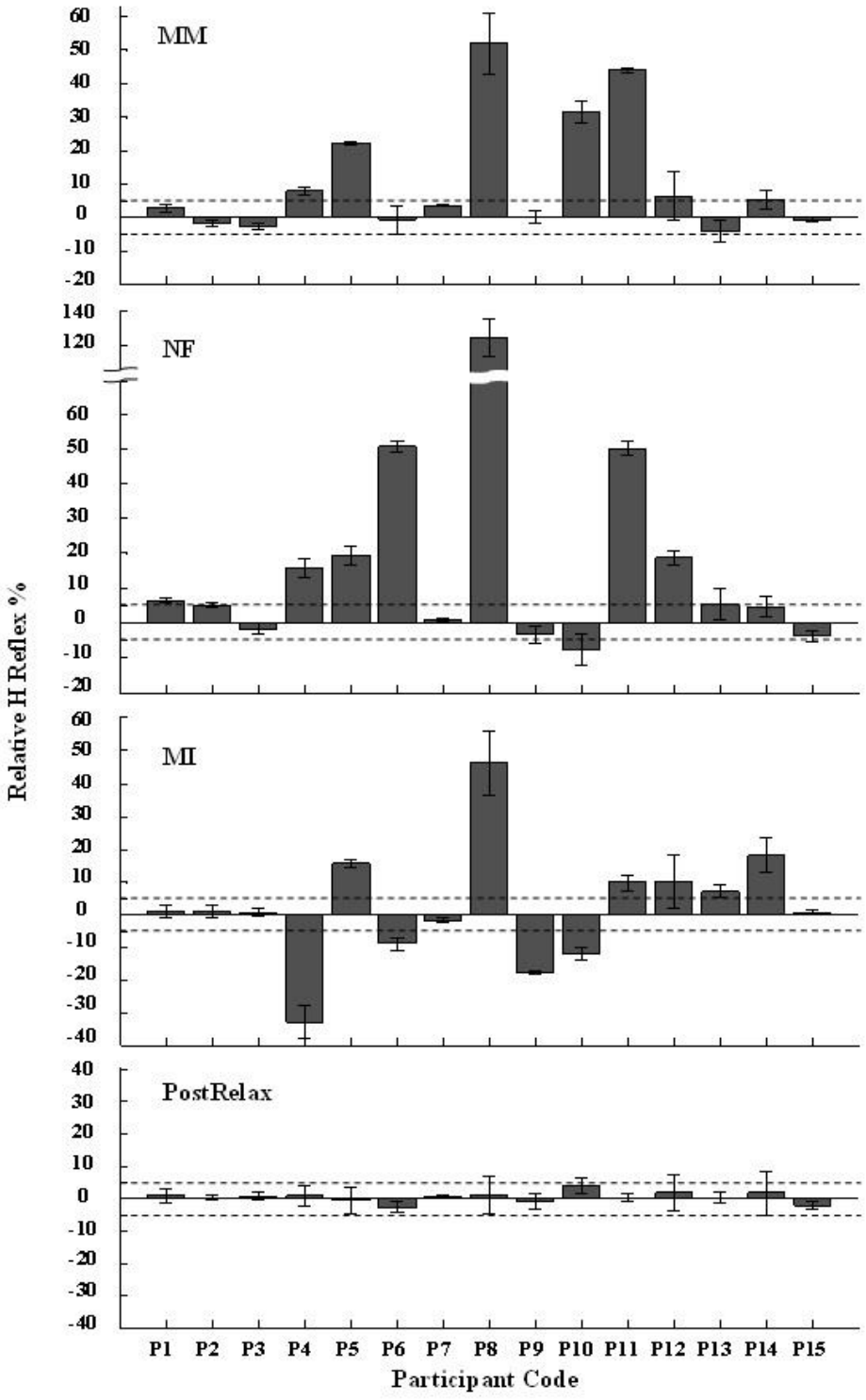


**Figure 3.4** Relative H wave amplitude with respect to the values in relaxed state before the neuromodulatory tasks (PreRelax). The horizontal dashed lines mark ± 5 % change of the H reflex amplitude compared to the PreRelax; MM: mental mathematics; NF: neurofeedback; MI: motor imagery; PostRelax: relaxed state following all neuromodulatory tasks. Error bars present a standard error.

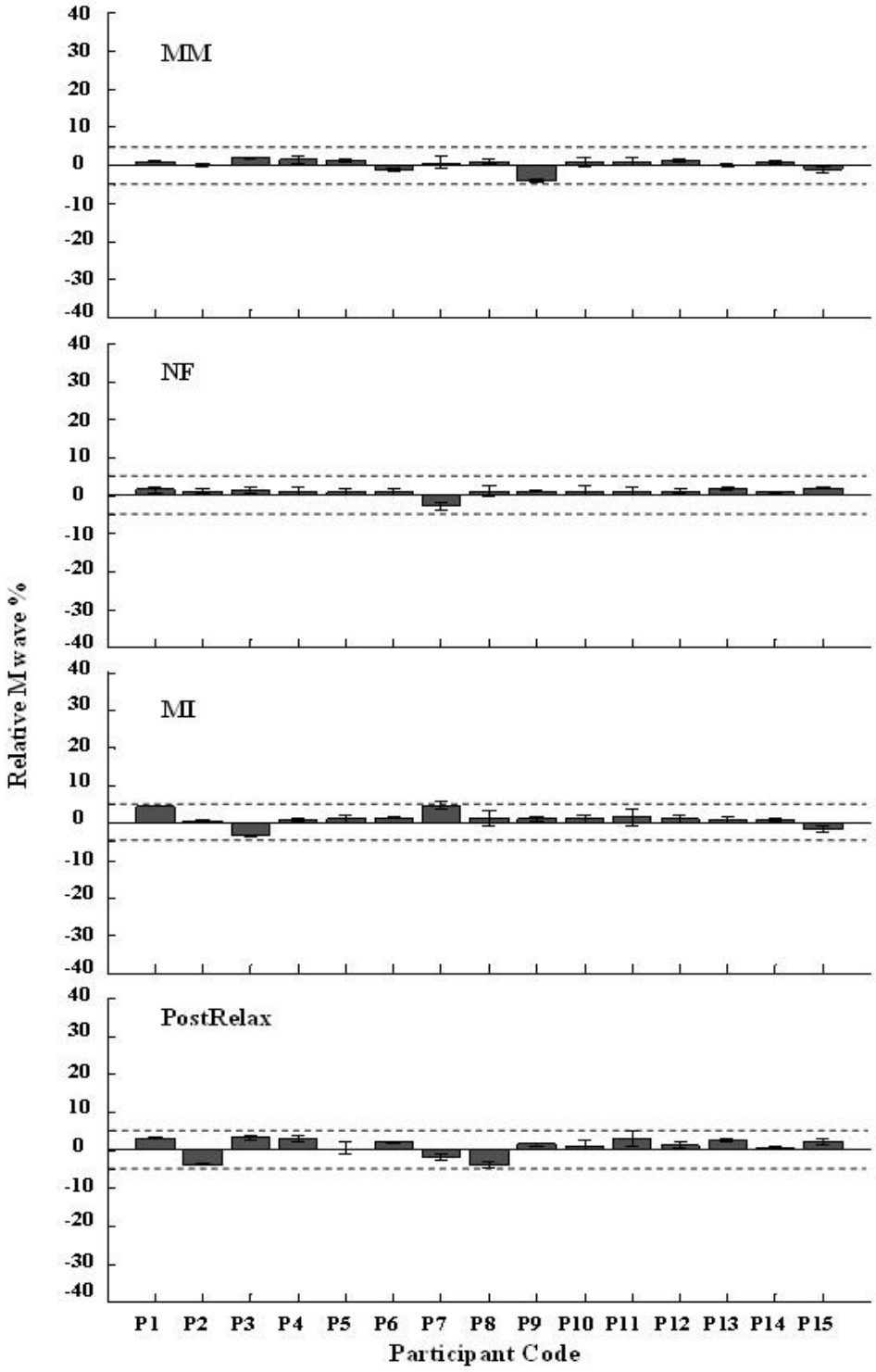


**Figure 3.5** Relative M wave amplitude with respect to the values in relaxed state before the neuromodulatory tasks (PreRelax). The horizontal dashed lines mark ± 5 % change of the H reflex amplitude compared to the PreRelax; MM: mental mathematics; NF: neurofeedback; MI: motor imagery; PostRelax: relaxed state following all neuromodulatory tasks. Error bars present a standard error.

### 3.4.2 Correlation between H Reflex and EEG Power for Different Frequency Bands, Tasks and Electrode Locations

For each participant all responses to all 5 stimuli for each task were normalized with respect to the maximum H amplitude. Power of theta, SMR, beta1 and beta 2 for each stimulus were expressed as power normalized with respect to 2-30Hz band. Beta 1 (12-15Hz) is called SMR in neurofeedback literature and is used for different neurofeedback protocols[233], and beta 2 (16-24Hz) is in the frequency range of beta SMR related to the control of movements[228]. Midline-frontal theta rhythm (4-8Hz) is influenced by increased level of concentration and might be involved in all active tasks[234].

For electrodes at the central, parietal, and occipital cortex, a linear regression was calculated between the H reflex amplitude of all participants (5*15=75) and the normalized power of a single frequency band. Figure 3.7 shows a linear regression between SMR and H reflex for all three mental tasks at Cz. The largest negative correlation was found between the H reflex amplitude and SMR at C4 and Cz (Table 3.1). A statistically significant correlation existed between H reflex and SMR power for all three tasks and PreRelax. A statistically significant negative correlation was also found between H reflex and SMR for MM at all examined electrode locations. In other frequency bands, a statistically significant correlation was found only between H reflex amplitude and the beta 2 band for NF at Oz ($p=0.0016$ and $R=-0.3578$). A general conclusion was made that there exists a negative correlation between the H reflex amplitude and the SMR power. Note that larger SMR power characterises synchronised neuronal activity (ERS), which describes the 'idle' state[228], so there is effectively a positive correlation between the active SMR (ERD) and the H reflex amplitude.

The analysis of the contribution of individual participants reveals that in most cases for both MM and MI the same participants had low or high H reflex amplitude (e.g. P2 and P5 had low H reflex amplitude, and P11, P12, and P14 had high H reflex amplitude). In

addition, the same participant P15 had a very high SMR power for low H amplitude, and removing this single 'outlier' participant would result in nonsignificant correlation between SMR power and H reflex amplitude for MM task (p=0.0958 and R=-0.2006) while for MI this correlation would still have remained statistically significant (p=-0.0363 and R=-0.2507). In case of NF there is less similarity than between MM and MI cases. For example, P6, who for MM and MI had high H reflex amplitude for low SMR power, during NF had low H reflex amplitude for low SMR power. Participant's P15 results do not appear to be outliers as they overlap with results of P1 and P7.

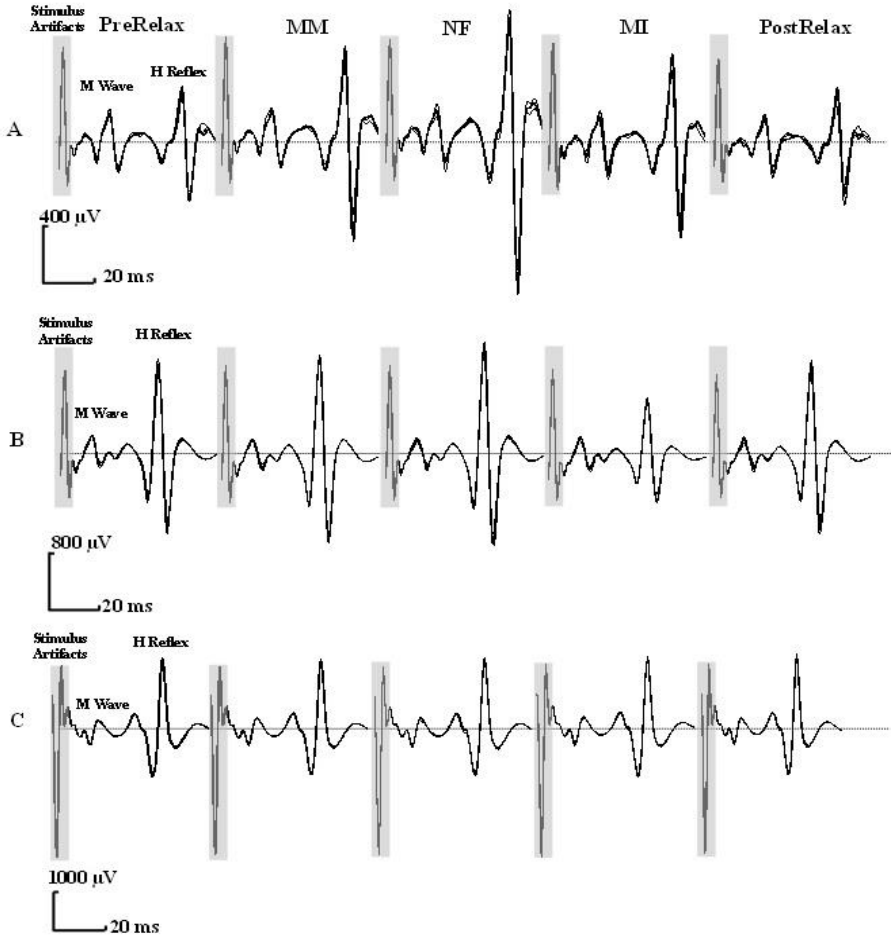


**Figure 3.6** The H and M waves for two baseline periods before (PreRelax) and after (PostRelax) neuromodulation tasks and during neuromodulation tasks (MM, NF and MI) for three representative participants (A: highest increase in H reflex, B: highest decrease in H reflex and C: no change in H reflex). The black thin line represents the M and H reflex for each stimuli and the black thick line represents their average.

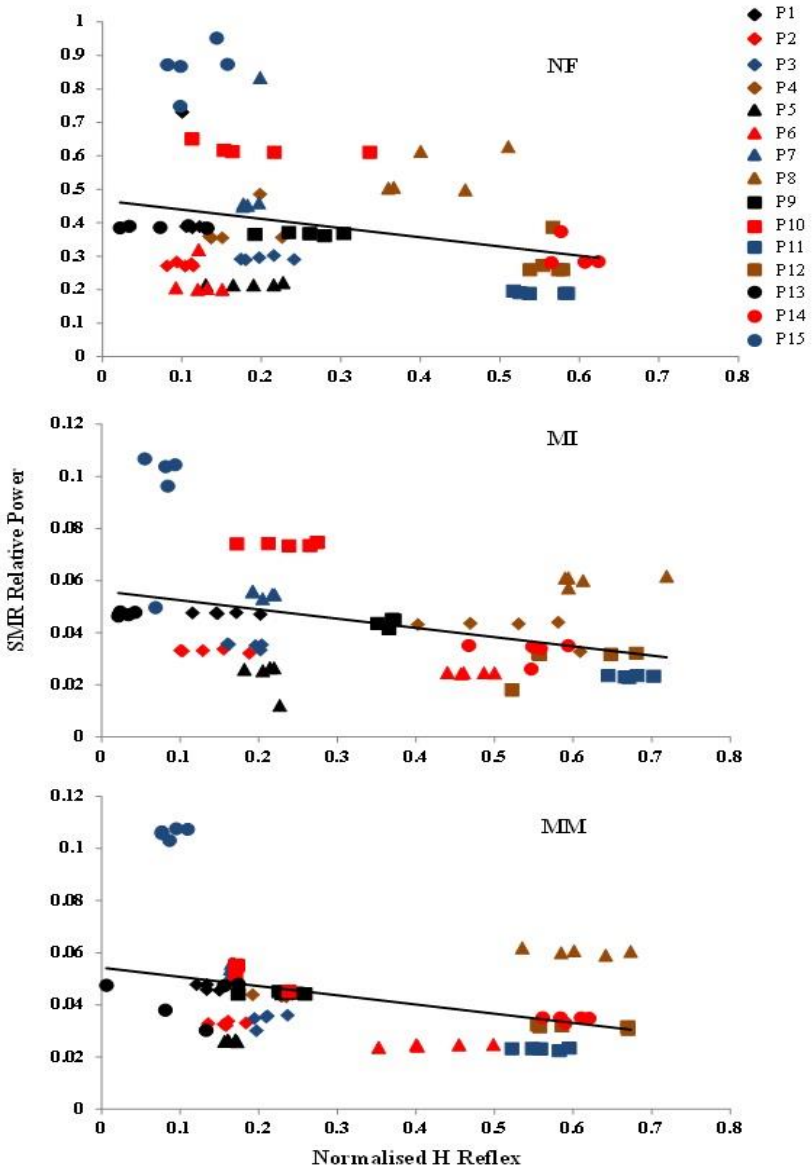


**Figure 3.7** Linear correlation between SMR measured and normalised H reflex amplitude for different mental tasks. NF (p=0.0325, R=-0.2472), MI ($p=9.6\cdot10^{-4}$, R=-0.3734) and MM (p=2.4·10-4, R=-0.412). The combination of different symbols and colours presents contribution of a single participant.

**Table 3.1** Linear correlation (p and R values) between normilised H reflex amplitude and SMR power across different conditions and different electrode locations. PreBL: baseline before the experiment, NF: neurofeedback, MM: mental math, MI: motor imagery. Bold marks statistically significant values

| | PreRelax | | MM | | NF | | MI | |
|---|---|---|---|---|---|---|---|---|
| | p | R | p | R | p | R | p | R |
| C3 | 0.0793 | -0.2039 | **$6.95 \cdot 10^{-6}$** | **-0.4932** | 0.1447 | -0.17 | 0.0903 | -0.197 |
| Cz | **$6.42 \cdot 10^{-4}$** | **-0.3853** | **$2.40 \cdot 10^{-4}$** | **-0.412** | **0.0325** | **-0.2472** | **$9.67 \cdot 10^{-4}$** | **-0.3734** |
| C4 | **0.0108** | **-0.2928** | **0.0031** | **-0.3376** | **0.0337** | **-0.2456** | **0.0336** | **-0.2458** |
| P3 | 0.2711 | -0.1287 | **0.005** | **-0.3212** | 0.0755 | -0.2065 | 0.2526 | -0.1337 |
| P4 | 0.1849 | -0.1548 | **$2.43 \cdot 10^{-6}$** | **-0.5138** | 0.0854 | -0.2 | 0.4196 | -0.0946 |
| Oz | 0.9749 | $3.7*10^{-3}$ | **0.0054** | **-0.3181** | 0.555 | -0.0692 | 0.4437 | -0.0898 |

### 3.4.3 H Reflex during Monopolar and Laplacian EEG Derivation

To assess the influence of neuromodulation based on EEG measurement of local and wide spread sources, five participants were asked to repeat the same five tasks (PreRelax, MM, MI, NF and PostRelax) while EEG was recorded from an additional 4 electrodes (see methods). For all five tasks, SMR was calculated from Laplacian-derived Cz. The relative amplitude of the H reflex during monopolar and Laplacian EEG derivations are presented in Figure 3.8, showing a similar trend except for MI task in P11, and NF tasks in P15. A two way repeated measures Friedman test was performed to compare whether there was a statistically significant difference between monopolar and Laplacian derivation across all five tasks, each task repeated 125 times (5 tasks × 5 repetitions × 5 persons). The test demonstrated that there was no statistically significant differences between different derivations for all tasks p=0.2099. The same test was applied to compare between five different tasks for both derivations together, with 50 repetitions (2 derivations × 5 participants × 5 repetitions) resulting in nonsignificant differences among tasks, p=0.0712. When Friedman test was applied to only the first four tasks (without PostRelax which is

very similar to PreRelax, (see Section 3.4.1) it resulted in a statistically significant difference between tasks p=0.0277.

Linear regression was calculated for both derivations between the normalized amplitude of H reflex and EEG power in theta, SMR, beta 1, and beta 2 band for each task (25 measurements of Laplace derivation, and 25 for monopolar derivation). A statistically significant negative correlation was found in both cases between SMR and the H reflex for the PreRelax (Laplace p=0.038, R=-0.4172, monopolar $p=6\cdot10^{-6}$ and R=-0.7723) and NF (Laplace p=0.0173, R=-0.4717, monopolar p=0.0013, R=-0.6084). In monopolar derivation only, statistically significant negative correlation was also found for both MM and MI tasks ($p=4.2\cdot10^{-5}$, R=-0.7244 and $p=4.7\cdot10^{-5}$, R=-0.7214**)** respectively. Though the results of both derivations show similar trends, they are somewhat different from the results on 15 participants with monopolar derivation, probably due to the small number of participants. Although participants practiced NF with monopolar derivation this did not negatively influence their performance during NF with Laplace derivation. The average time to achieve 5 conditions for H reflex stimulation during NF was 16.7 ± 2.1s for monopolar and 15.6 ± 0.8s for Laplace.

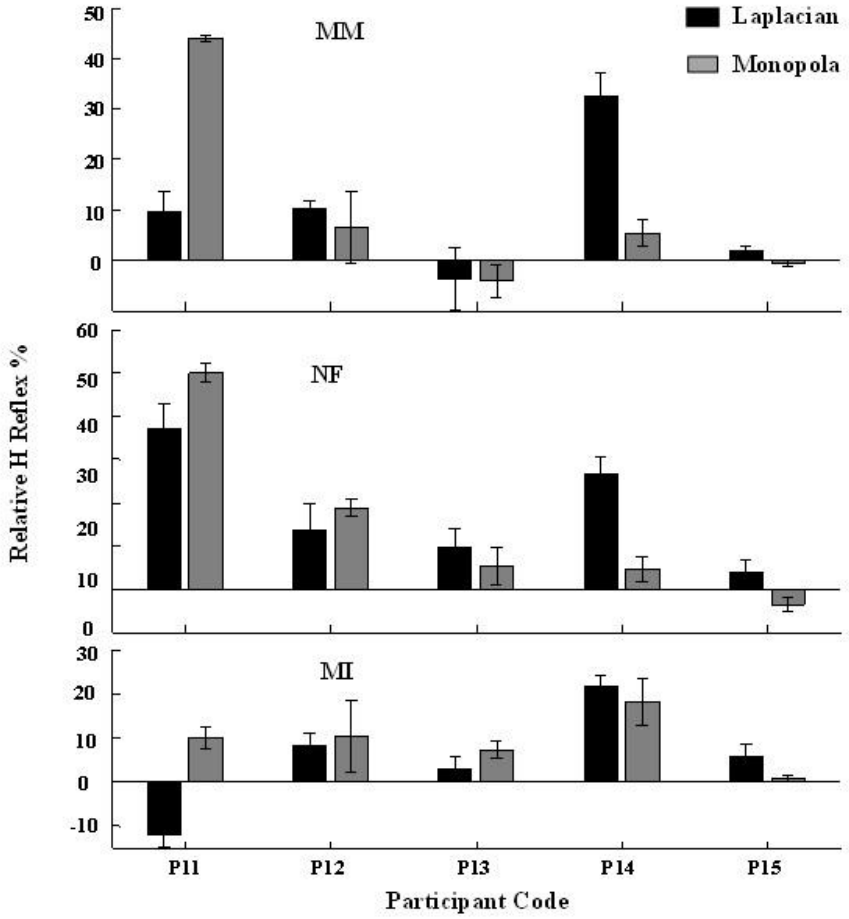


**Figure 3.8** Relative H wave amplitude for all three neuromodulation tasks (MM, NF and MI) during two EEG recording derivations (Laplacian and monopolar)

## 3.4.4 Kinaesthetic Imagery Scores

The mean value of KI scores across all 17 questions, including MI of different parts of the body, and across 12 participants (participants 6, 10 and 11 were not available for the test) was 3.2 ± 0.6, and it ranged from 1.95 to 4. These results show that on average participants had moderate kinaesthetic imagery (KI=3). To test the relation between the ability of the KI and the variation in H reflex amplitude during MI, a linear regression was calculated between KI score and the relative H reflex amplitude (Figure 3.9). The correlation coefficient was moderate (Pearson p=0.164, R=0.4282) but was not statistically significant.

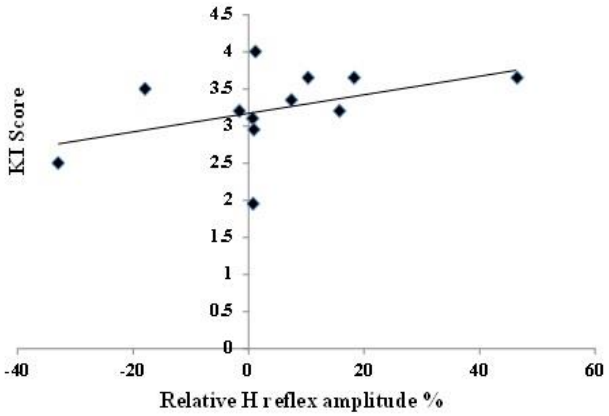


**Figure 3.9** A linear regression between KI score and the relative H reflex amplitude during MI across all 12 participants (3 out of 15 participants did not take part in this test)

### 3.4.5 Background Electromyography

The mean RMS value of background EMG in a period 100ms before each stimulus during all experimental conditions and across all participants was 3.49 ± 1.85μV (min 1.18μV, max 9.62μV). The mean RMS value of background EMG in a period 2 s before each stimulus was 3.42 ± 1.84μV (min 1.30μV, max8.72 μV). All values were under 10μV, which was a benchmark value to determine stability of background EMG in some previous studies[224], showing that H reflex was not modulated due to the modulation of the background EMG activity.

### 3.4.6 Modulation of Other EEG Frequency Bands during Mental Tasks

Figure 3.10 shows an example of Power Spectral Density (PSD) as a function of frequency over 2-30Hz range for PreRelax, MM, NF, and MI. PSD was calculated based on 1s of EEG before stimulation, providing 5s of recording for each condition. Although stimulation was based on 0.5s EEG, a period of 1s was chosen for computational reasons as 0.5s provided an overall EEG signal that was too short (only 2.5s). During MM and MI the power in 8-12Hz was smaller, and during NF it was larger than in PreRelax state.

While power was controlled in the SMR band only, it can be noticed that power was also modulated in other frequency bands, most notably in the theta and beta 1 band during MM and MI.

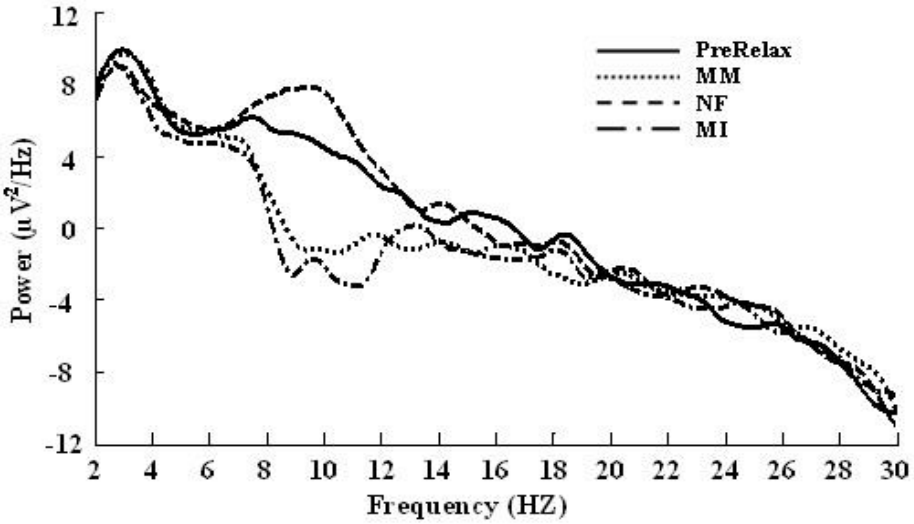


**Figure 3.10** EEG power as a function of frequency averaged across 15 participants in Experiment 1. PreRelax: relaxed state before the experiment; MI: motor imagery; NF: neurofeedback; MM: metal math

Figure 3.11 shows power in other frequency bands during modulation of SMR power, across different electrode locations at the central, parietal, and occipital cortex for different mental tasks. It also shows the baseline power across different cortical areas. Asterisks in Figure 3.11 mark statistically significant differences between the PreRelax and the various mental tasks across the frequency bands and electrodes, corrected for multiple comparisons. In the SMR band an increase in baseline power can be noticed, starting from the central area towards the parietal and occipital area, though it did not reach a statistically significant level ($p=0.0683$ Cz vs Oz). While the difference in SMR between the PreRelax and NF was statistically significant for Cz ($p=1\cdot10^{-11}$), it was not significant for Oz ($p=0.085$). This indicates that although EEG derivation was monopolar, it was the true SMR rather than wide-spread alpha being modulated during this task.

Significant decrease of the SMR during MM and MI can be noticed across all electrode locations. Wide spread posterior-occipital reduction in SMR activity during MM has been previously reported, and was related to modulation of the alpha rhythm[218]. Beta 1 power was also significantly reduced for MM at all electrode locations. A wide-spread reduction in SMR during MI can be attributed to aggregation of different processes involved in the transformation from seeing (a visual cue) to doing[227]. Beta 1 was significantly reduced ($p=0.035$) at Cz for MI. Theta band power was significantly reduced at Cz, C3, P4, and Oz during MM, and at Cz, P4, and Oz during MM. Beta 2 power was not significantly modulated by any of the mental tasks.

For Laplacian derivation at Cz, during MI, power was on average reduced in the SMR rhythm and theta and beta 1 band Figure 3.12. Although SMR and beta 2 are two nearby bands, MI did not result in reduced power in beta 2 band. During NF, the average power increased in SMR, beta 1 and beta 2, as compared to the baseline. Again, although SMR and theta are neighbouring frequency bands, theta band power decreased while SMR power increased. Finally, during MM, power decreased in SMR and theta bands, staying on a similar level as during the baseline in beta 1. On the contrary, beta 2 power decreased during MM. Compared to the monopolar montage, NF had a similar effect on the theta, SMR, beta 1 and beta 2 band, MI had the similar effect on the SMR, beta 1 and beta 2 band and MM had similar effect on SMR and theta band. It should however be noted, that largest differences between monopolar recording and Laplacian derivation were in bands in which there was no statistically significant differences between the baseline and the task, in case of monopolar montage shown in Figure 3.11.

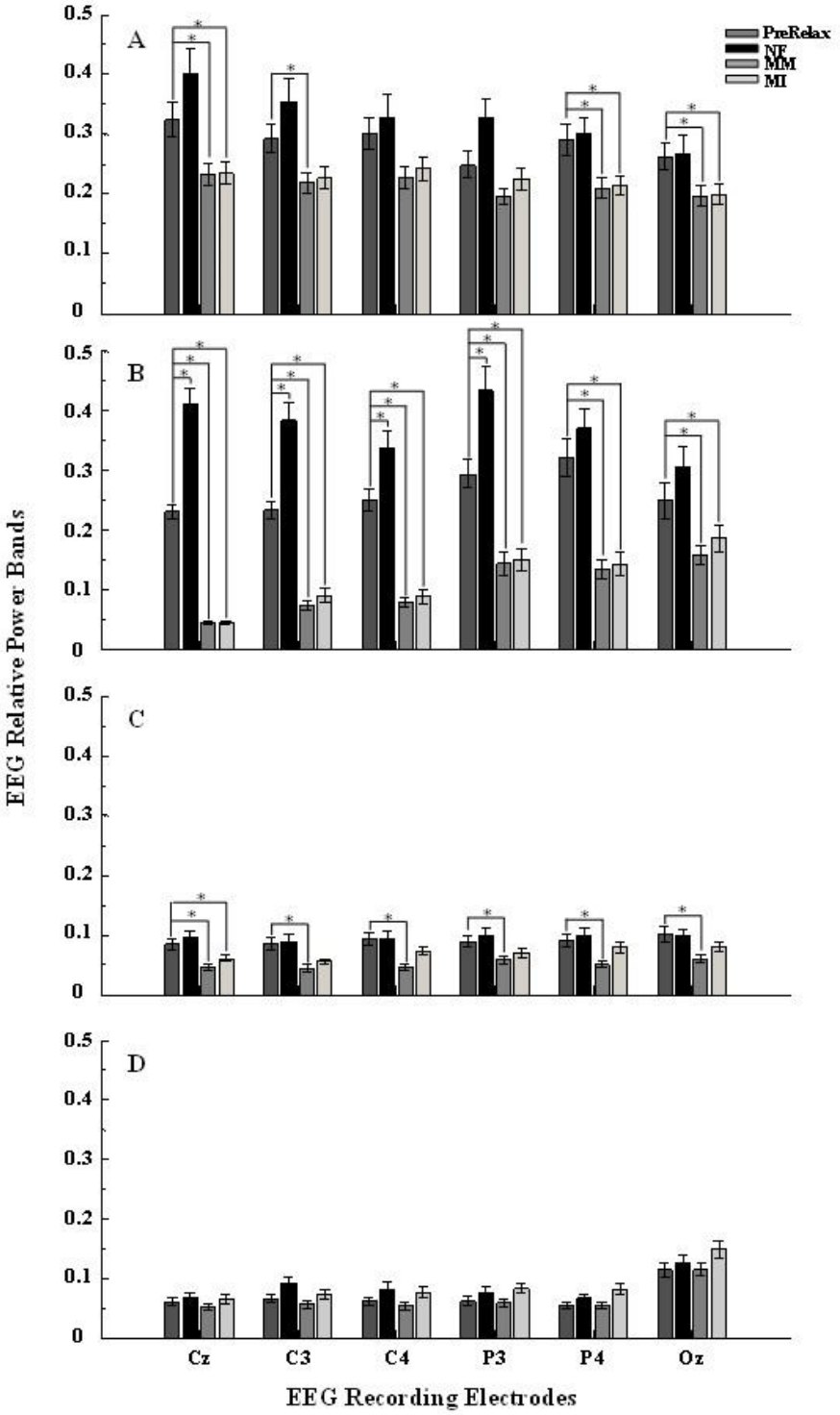


**Figure 3.11** Relative EEG power at different frequency bands (Fig A-D) during different mental tasks over several electrode locations. A: Theta band (4-8Hz), B: SMR (8-12Hz), C: Beta 1 (12-15Hz), D: Beta 2 (16-24Hz). PreBL: baseline power before the experiment, NF: neurofeedback, MM: mental math, MI: motor imagery. Asterisks above bars indicate tasks which significantly modulated power as compared to the baseline value. Initial statistical significance level p=0.05 was corrected for multiple comparisons for each single band/electrode.

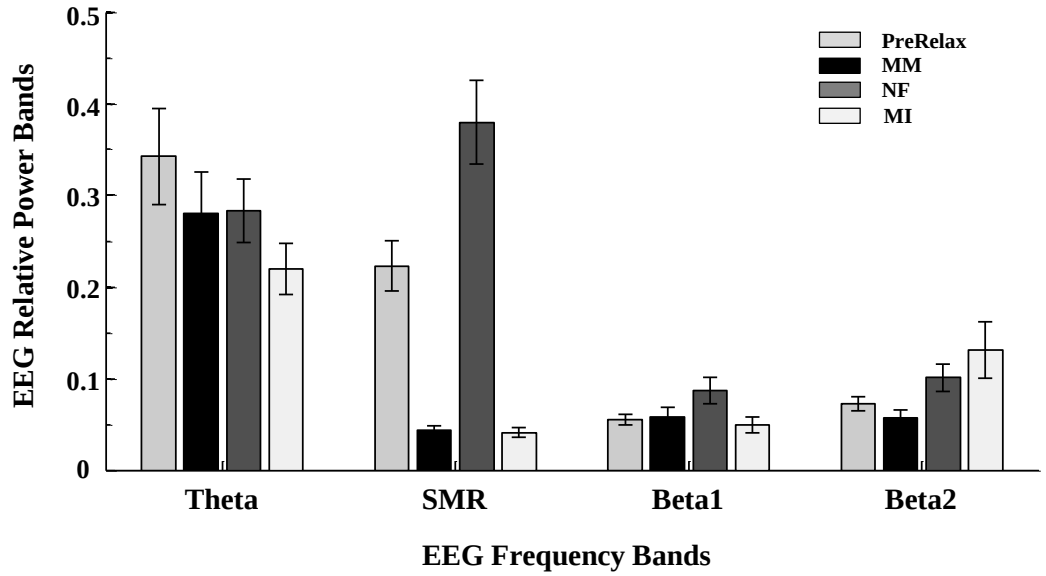


**Figure 3.12** Relative EEG power at different frequency bands during different mental tasks over Cz electrode location during Experiment 2. PreRelax: baseline power before the experiment, NF: neurofeedback, MM: mental math, MI: motor imagery.

## 3.5 Discussion

It is believed that the sensory-motor cortex presents the major supraspinal site for modulation of the H reflex[209,210]. However the effect of the self-induced modulation of SMR on the H reflex has not been sufficiently explored.

The present study explores the effect of short term modulation of SMR using different mental strategies on the H reflex amplitude of the soleus muscle. From the literature, it is known that mental tasks, including MI, can induce unspecific facilitation of motor evoked potential[235]. Our recent study shows that up-regulation of SMR power by NF over the motor cortex, results in increased SMR power primarily over the central areas of the cortex[44]. However, it is not known how it affects H reflex. In this study, the effect of MM and NF on the H reflex was excitatory despite the opposite direction of modulation of the SMR rhythm. Both tasks significantly increased the H reflex. MI also resulted in modulation of H reflex but in about one half of participants with significant modulation (amplitude change larger than ±5%) it caused an increase, while in the other half a decrease of H reflex amplitude. The comparable values of the baseline H reflex before and

after the experiment in the current study indicate that there was no carry-over effect following a single session of three mental tasks.

Modulation of H reflex was largest during NF. To the best of our knowledge, there is no published study providing information about the change in cortical excitability during NF task. However, Ros and Gruzelier studied the effect of suppression of monopolarly recorded 8-12 Hz rhythm over C3 on corticospinal tract excitability following 30 min NF training[233]. Motor evoked response to transcranial magnetic stimulation was used as a measure of excitability. They noticed no significant change in cortical excitability immediately after NF, followed by a significant increase in excitability 15 min after NF. In the current study, participants were asked to increase SMR power for 5 min only and no significant difference was noticed between PreRelax and PostRelax baseline H reflex.

An rTMS study showed that stimulation with 1Hz increased 8-12 Hz band power over the sensory-motor cortex as the result of ERS of neuronal activity[236], while stimulation with 5Hz caused ERD. Another rTMS study showed that stimulation with 1Hz caused increase in H reflex[237],while stimulation with 5Hz caused reduction of H reflex, resulting in reduced spasticity in patients with multiple sclerosis. Results of these studies show that 1Hz rTMS stimulation is related to both ERS and increase in H reflex. This indicates a possible relation between ERS (increased 8-12 Hz power) and increased H reflex. If we hypothesise that NF and rTMS result in a similar effect on SMR power, then the effect of NF would be similar to ERS, i.e. inhibition of cortical networks[229,238], which results in increased H reflex. In patients with spinal cord injury, total or partial loss of communication between the brain and monosynaptic loops in the spinal cord results in spasticity[239,240], which can manifest itself as an exaggerated H reflex[241]. In our recent NF study with spinal cord injury patients, we noticed increased spasm in legs during NF training from C3/C4 and Cz in people with an incomplete injury[44]. The NF protocol involved up-regulation of 8-12 Hz and down-regulation of theta and beta (20-30 Hz) band

power using monopolar EEG montage. A post hoc analysis revealed that 8-12 Hz rhythm was increased over the central area indicating that it was most likely the SMR rhythm.

It is of interest that while NF resulted in H reflex increase, largest increases were noticed for smaller increases of SMR. This apparent decoupling between the global effect of NF and a specific relation between SMR and H reflex might indicate that some more factors, apart from SMR, are involved in modulation of H reflex during NF.

During MM a significant increase in H reflex amplitude was noticed. It is believed that the mechanism for increasing H reflex during MM is caused by stress which heightens sympathetic outflow[242]. Sympathetic outflow enhances the stretch reflex response in the relaxed soleus muscle in humans[242]. It is of interest that reduced power during both MM and MI was noticed over the parieto-occipital region. It has previously been reported that mental math affects the widespread alpha rhythms over the parieto-occipital region[218]. This indicates that MM actually modulated the alpha rhythm rather than the SMR. However, in experiments with Laplacian derivate, which should reduce the influence of a widespread alpha rhythm on the stimulation-triggering SMR measurement, increase in H reflex during MM was noticed in some cases. Thus, MM probably modulated both SMR and alpha rhythms. On the other hand, a widespread cortical reduction of 8-12 Hz rhythm during MI over the central, parietal, and occipital regions might be the consequence of a volume-conduction effect or may reflect a complex process of transformation of seeing (a visual cue) into doing[227].

Previous studies demonstrated that the effect of MI on the H reflex depends on the level of fitness[212–214,216,217]. In our study the level of fitness was not measured, but participants belonged to a general population. However, a moderate, though non-significant, positive correlation ($R= 0.4282$, $p=0.164$) was noticed between the kinaesthetic imagery score and the H reflex amplitude during MI. Although we asked participants to perform MI at 60% of maximum contraction of the soleus muscle it is possible that this

varied among participants. Hale et al. found that MI practice rather than the intensity of imagination influenced H reflex amplitude, as it increased throughout the experiment including repeated MI sessions[213]. The inconsistent results on the influence of MI on H reflex indicate that although MI produces consistent decrease of SMR, the SMR power is likely not the only factor influencing the H reflex amplitude. In a recent study on rats by Boulay et al. two mechanisms were proposed through which the activity of the sensory-motor cortex may influence H reflex[243]. These two mechanisms were associated to a distinctive relation of H reflex with two frequency bands. The first, which is probably mediated by presynaptic inhibition, results in H reflex increase with increased activation of SMR (8-12 Hz). The second, which is probably mediated via the motoneuron itself as well as changes elsewhere in the spinal cord, has the opposite effect. A more active sensory-motor cortex in lower gamma band (40-85 Hz) results in lower H reflex. This could explain why, in some cases, H reflex was reduced during MI. A limitation of the current study is that gamma band activity was not recorded, making it impossible to test this hypothesis. In addition, it is not known to what extent results in humans and rats are comparable.

A recent study by Takemi et al. analyzed the influence of ERD during MI on the excitability of the human spinal motoneurons, as measured by the presence of F wave[244]. Although the intensity of ERD (5% or 15%) had no impact on the results, increasing SMR during MI task had an overall excitatory effect. A difference between F and H waves is that the F wave is elicited at supramaximal M wave amplitude and is caused by an antidromic stimulus in the motor pathways, meaning it requires higher current than H reflex and does not involve the sensory pathways. In our study H reflex activated both sensory and motor pathways, and intensity of ERD was 80% - much higher than that used by Takemi et al.[244].

Analysis of the power spectrum during all three tasks showed that modulation of SMR was accompanied by the modulation of EEG in other frequency bands. Significant reduction in theta and beta 1 power was noticed over the central cortex for MI, and over central, parietal, and occipital cortex for MM. These frequency bands might independently affect H reflex. We therefore calculated a correlation between the H reflex and modulation of power in different frequency bands over the central, parietal, and occipital cortex. A statistically significant negative correlation between H reflex and EEG power was found for SMR band only. It was present for all three mental tasks and PreRelax at electrode locations Cz and C4 located over the primary motor cortex. This effectively means that ERS was negatively and ERD positively related to the H reflex amplitude, confirming results of Boulay et al.[243].

A possible limitation of the study is that only NF included visual feedback and direct conscious self-regulation of SMR. This may have influenced wider cortical networks, including the occipital cortex; however in this study we found no significant modulation of 8-12Hz rhythm at Oz during NF. Since people use various mental strategies for NF, the set of mental tasks used to increase the SMR during NF is probably less homogeneous than mental tasks used to reduce SMR with MM and MI. To the best of our knowledge there is no verbalized rule that can be used to increase 8-12 Hz rhythm, apart from relaxation which typically affects the parieto-occipital alpha rhythm[245]. Additionally, the duration of NF training prior to the study was relatively short. We did however check the participants' ability to self-regulate their brain waves through post hoc analysis of PSD during NF.

Furthermore, another limitation is that we used monopolar montage for most of participants, which probably records a mixture of sensory-motor rhythm and alpha rhythm. In Experiment 2 of this study, the Laplacian derivation was used to exclude the effect of a widespread alpha rhythms modulation in 5 participants**.** A Friedman test failed to demonstrate a statistically significant difference between two montages, indicating that

either the modulation of relative H reflex amplitude was not clearly affected by the origin of 8-12 Hz rhythms, or that both montages recorded dominantly SMR. A regression analysis between SMR and H reflex amplitude showed a significant negative correlation for PreRelax and NF in both cases, while a negative correlation for MM and MI was found for monopolar montage only. The NF result confirm the result of our previous study in which we recorded multichannel EEG during NF[44], and showed that NF tasks predominantly modulated the central 8-12Hz rhythm, i.e. SMR. The absence of significant correlation for both MM and MI tasks for Laplacian derivation is probably a combination of two factors, the small number of participants and possibility that widespread alpha, rather than SMR was modulated. Unfortunately, due to the small number of participants we had to apply a nonparametric statistic which did not allow us to analyse between factors 'derivations' and 'tasks' to draw conclusions about which of five tasks was influence by different derivations.

The present study provides an important and novel first step in exploring the effect of modulation of SMR during neuromodulation tasks on H reflex amplitude in the able-bodied population. It is however based on the measurement of the immediate effect of a single session of neuromodulation. Repeated experiments over an extended period would be necessary to understand the long-term changes of H reflex induced via prolonged modulation of brain activity. The results of the study are also relevant for the design of brain-computer interface rehabilitation strategies, which are based on cortical activation to promote restoration of the neural activity in the cortico-spinal tract. Very often MI is combined with functional electrical stimulation (FES) to promote simultaneous activation of sensory and motor pathways[246–248]. Results of this study, in particular results concerning MI, should inform future design of such BCI-FES studies.

## 3.6 Conclusion

Short term voluntary modulation of SMR from Cz resulted in modulation of H reflex amplitude of the soleus muscle. The excitatory effect on H reflex was independent of the direction of modulation of the SMR rhythm. Increasing SMR through NF produced the largest increase in the H reflex. Decreasing SMR through MI had an inconsistent effect on the H reflex, indicating possible concomitant influence of other EEG rhythms present in the same area of the cortex or the influence of sub-cortical centres. All three mental tasks also resulted in modulation of the theta and lower beta band power in the central, parietal, and occipital cortex; however, a significant correlation with H reflex was found mainly for SMR. A single neuromodulation session produced only a short term modulation of the H reflex.

# 4

# Cortical Predictors of CNP in Sub-acute Patients with SCI

# Chapter 4 Cortical Predictors of CNP in Sub-acute Patients with SCI

## 4.1 Abstract

***Objective:*** to define dynamic EEG predictors of CNP in sub-acute SCI patients who have not developed physical symptoms of CNP.

***Methods***: Forty one participants took part in this study: 10 Able Bodied (AB), 11 Patient with CNP (PwP), 20 Patients with no CNP at the time of EEG recoding. Ten out of 20 developed CNP within six months after EEG recording (PdP) and 10 stayed pain free (PnP). EEG was recorded during cue-based motor imagery (MI) tasks involving the left arm (LA), right arm (RA) and feet (F) and during eyes opened (EO) and eyes closed (EC) relaxed state. Power spectral density (PSD) and time-frequency EEG analysis were performed on average brain response, analysed separately for each limb.

***Results:*** As predictors of CNP (preceding the physical symptoms of CNP), high theta PSD, shift of the dominant alpha peak towards lower frequencies and lower EEG reactivity during relax state as well as stronger alpha and beta ERD during MI were noticed in PdP group. Furthermore, the PwP group who already had pain at the time of EEG recording, had increased theta PSD during a relaxed state and a stronger ERD activity including lower frequency theta band during MI.

***Conclusion:*** This study demonstrated that changes in spontaneous and induced EEG can be both predictors and consequences of CNP following SCI.

## 4.2 Introduction

Central neuropathic pain (CNP) is one of the worst secondary consequences of SCI. More than 40% of SCI patients experience CNP, though the onset of its first symptoms might vary from weeks to years after injury[26]. As a consequence of CNP, patients' quality of sleep is reduced accompanied by a high level of anxiety and depression[249,250]. CNP not only affects patients' health status and quality of life, but has also an economic impact on the patient and the wider society[251].

CNP is refractory to most surgical, pharmacological, behavioural and physical interventions[252–254].This might be because patients are treated after considerable reorganisation and anatomical changes have occurred in the brain and spinal cord as a consequence of CNP[20,136,142,151,152]. Results from animal model studies suggested that CNP may be prevented by pre-emptive treatment early post injury in individuals with SCI[255,256]. Therefore, defining the predictor of CNP could lead to the development of the preventive treatment of CNP in SCI patients and possibly in other patient groups suffering from this type of pain.

An electroencephalographic (EEG) study by our research group demonstrated that chronic SCI patients with CNP have a characteristic 'signature' of pain, which can be detected while patients activate their sensory-motor cortex, by imagining moving the paralysed, painful part of the body. These signatures are particularly noticeable over the primary motor cortex (M1)[140] during motor imagination task and a known close relation between the over-activation of motor cortex and CNP[141]. It is however still debatable whether these signatures are predictors or consequences of CNP.

Studies demonstrating cortical and subcortical reorganisation in patients with long-standing pain indicate that changes in the brain are a consequence of long standing pain[136,138–140]. Typically, patients who experience CNP for more than 6 months are

included in these studies, in order to treat pain as chronic[12]. However multiple non-pharmacological treatments[44,88,169,176], including a neurofeedback treatment by our research group[44], demonstrated that the modulation of brain activity results in reduced intensity of pain and also reverse cortical activity. These results indicate that changes in brain activity might be a cause rather than a consequence of pain.

This study was conducted to explore the causal relation between EEG and CNP in the transitional period of early symptoms of CNP. Patients with SCI present a good model to explore CNP because of the well-defined location of CNP at or under the level of injury and because of the distinctive burning and shooting sensation which accompany this type of pain. In addition, most SCI patients have reduced, and in some case absolutely no sensation below the level of injury, which would in general reduce their sensation of nociceptive pain. Finally CNP responds to anticonvulsants and antidepressants, which are not effective in the treatment of nociceptive pain providing additional evidence of neuropathic origin of pain. For these reasons, we could also include in this study patients with CNP which persisted for less than 6 months, in order to investigate the effect of a relatively short-term presence of CNP on the activity of brain.

We compare both spontaneous and induced EEG activity of sub-acute SCI patients with and without CNP, as well as with able bodied participants. We also perform a retrospective study on the group of patients with no pain at the time of EEG recording, by separating them into two groups of those who did or did not develop pain within 6 months following the recording. In this way we were able to capture a transition from just before the onset of pain until a period just after the onset of pain.

# 4.3 Methods

## 4.3.1 Participants

Forty one adult participants were recruited for this study. Participants were categorized into four groups:

1. Ten able-bodied volunteers (**AB**) (3 Female (F), 7 Male (M), age 35.2±7.2)
2. Eleven sub-acute SCI patients with CNP (**PwP**) (4 F, 7M, age 44.9±16.9)
3. Twenty sub-acute SCI patients with no CNP at the time of EEG recoding were divided into:
   - **a)** Ten developed CNP within six months after EEG recording (**PdP**) (1 F, 9 M, age 46.9±15.9).
   - **b)** Ten stayed pain free within the first year after EEG recording (**PnP**) (1 F, 9 M, age 42.1±13.3)

All participants gave their informed consent. The study was approved by the University of Glasgow, College of Science and Engineering ethical committee for the able-bodied participants and by the National Health Service for Greater Glasgow and Clyde ethical committee for patients. American Spinal Injury Association (ASIA) Impairment Classification was used to determine the neurological level of SCI. The inclusion criteria for SCI patients with pain were intensity of CNP $\geq$ 4 VAS and pharmacological treatment of CNP ongoing for at least 6 weeks. The general inclusion criteria for all groups were adults aged between 18 and 75 years, no history of brain disease or injury and normal or corrected to normal vision. The general exclusion criteria for all groups were chronic or acute pain $\geq$ 3, diagnosed mental health problems. Table 4.1 shows the demographic information of the patient with CNP (PwP), patients with no pain (PnP) and patients developed CNP (PdP).

**Table 4.1** Demographic information of SCI patients groups

***Patients with CNP (PwP)***

| No. | Level of injury | ASIA | Weeks after SCI | Weeks with CNP | Pain intensity (VAS) | Medication |
|---|---|---|---|---|---|---|
| 1 | T12 | B | 20 | 20 | 9 | Pregabalin |
| 2 | T7/T8 | A | 12 | 12 | 6 | Gabapentin |
| 3 | C3/C4 | D | 16 | 16 | 7 | Tramadol |
| 4 | C5/C6 | A | 17 | 15 | 5 | Tramadol |
| 5 | T3 | A | 24 | 6 | 5 | / |
| 6 | T10 | A | 12 | 12 | 7 | Pregabalin |
| 7 | T8 | C | 26 | 26 | 5 | / |
| 8 | C3 | D | 6 | 6 | 6 | / |
| 9 | T6 | B | 28 | 28 | 8 | Pregabalin |
| 10 | C4 | A | 6 | 6 | 7 | Gabapentin |
| 11 | T6 | C | 6 | 6 | 7 | Gabapentin |

***Patients with no pain (PnP)***

| No. | Level of injury | ASIA | Weeks after SCI |
|---|---|---|---|
| 1 | T7,T10 | B | 12 |
| 2 | L1 | C | 12 |
| 3 | T11 | B | 7 |
| 4 | T12 | A | 4 |
| 5 | T6 | A | 12 |
| 6 | T6/T7 | B | 21 |
| 7 | L1 | D | 7 |
| 8 | L1 | B | 4 |
| 9 | T3,T5 | D | 10 |
| 10 | T6 | C | 10 |

***Patients developed CNP (PdP)***

| No. | Level of injury | ASIA | Weeks after SCI | Weeks Developing CNP after EEG Recording | Location of the CNP |
|---|---|---|---|---|---|
| 1 | C3/C4 | D | 12 | 8 | At and below level CNP |
| 2 | C3/C4 | B | 8 | 12 | At and below level CNP |
| 3 | T7/T8 | D | 9 | 6 | below level CNP |
| 4 | T12 | A | 6 | 10 | At and below level CNP |
| 5 | C5/C6 | A | 12 | 4 | At and below level CNP |
| 6 | L2 | B | 6 | 4 | At and below level CNP |
| 7 | T3 | A | 24 | 8 | At and below level CNP |
| 8 | T5 | A | 6 | 7 | At level CNP |
| 9 | T6 | A | 4 | 2 | At and below level CNP |
| 10 | C3 | A | 6 | 4 | At and below level CNP |

## 4.3.2 EEG Recording

Three modules of a modular biosignals amplifier (g.USBamp, Guger Technologies, Austria) were used to record 48 EEG channels. EEG electrodes were placed according to the international 10-10 standard system of electrode placement[257], shown on Figure 4.1. An ear-linked reference was used and ground was placed on AFz location. EEG was recorded with a sampling frequency of 256 Hz and band-pass filtered between 0.5 and 60 Hz (and notch filtered at 50 Hz) using $5^{th}$ order IIR digital Butterworth filters within the g.USBamp device. Filters could be set through a graphical user interface of a Simulink module of gUSBamp proprietary software. EEG recoding was performed using Simulink and MATLAB (MATLAB R2010a, The MathWorks Inc., USA). The electrodes impedance was also monitored through a proprietary Simulink block and was kept under 5 kΩ.

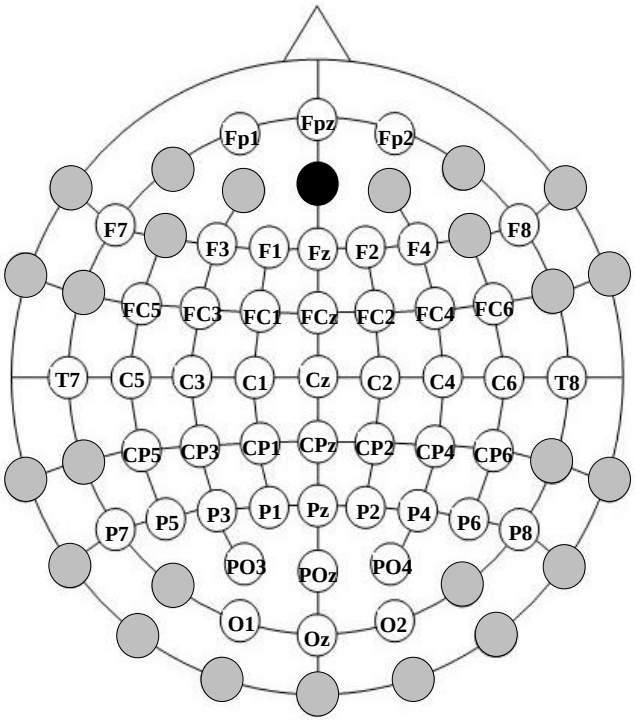


**Figure 4.1** The international 10-10 standard system of electrode placement used for this study, the black circle shows the position of the ground electrode and the gray circles show unused electrode locations.

### 4.3.3 Experimental Protocol

Prior to the start of EEG recording, patients with CNP (PwP) were asked to fill out a Brief pain inventory[33] questionnaire to collect information about their pain intensity, location of pain and medications. Figure 4.2 shows patient's perceived pain locations.

The sensory profiles of patients with no pain at the time of EEG recording were evaluated by testing the perceptual threshold (PT) using monofilaments. This test was performed in addition to the ASIA test which also involves testing the sensory threshold over different dermatomes. PT can be defined as the lowest stimulus intensity at which SCI patients reported sensation[37]. They were examined for mechanical wind-up by using monofilaments no. 6.65. Mechanical wind-up is a repeatable mechanical stimulus of identical intensity which causes a gradually increasing pain[20]. Stimulus was applied 4 consecutive times on their foot and shank of both legs. Patients ware asked if the stimulus was painful and to rate the intensity of pain after the first and fourth stimulus on VAS. It is believed that those patients for whom the sensation is painful are at a high risk of developing CNP[20]. They were tested every two months while in the hospital or until they developed CNP.

### 4.3.4 EEG Recoding during Relaxed State

Spontaneous EEG activity was recorded during eyes opened (EO) and eyes closed (EC) relaxed states for 2 min each and repeated twice alternating between EO and EC conditions. During EO relaxed state, participants were instructed to stay still and to focus on a small cross presented in the middle of a computer screen to avoid eyes movement, while during EC relaxed state, they were asked to close their eyes and relax.

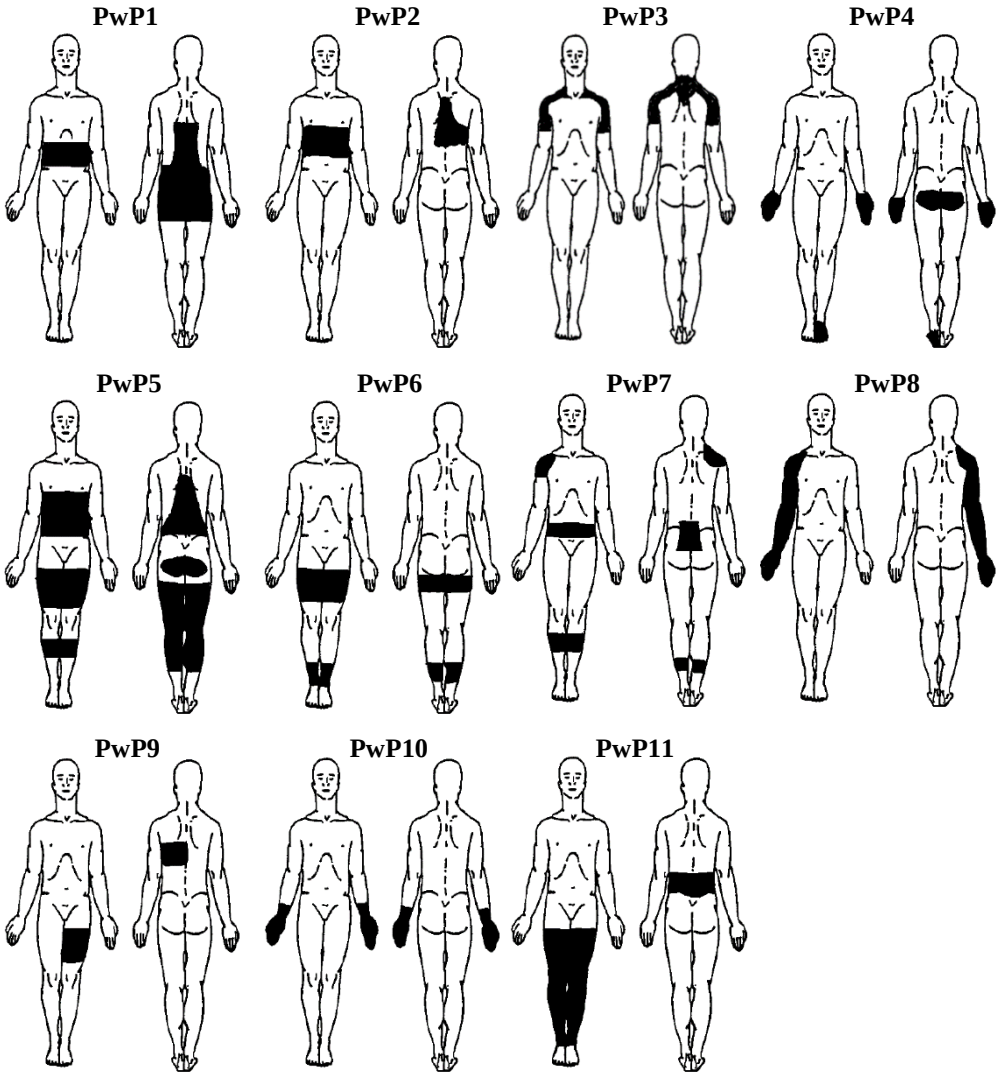


**Figure 4.2** Perceived location of pain as reported by patients in PWP group (black shaded areas)

### 4.3.5 EEG Recoding during Motor Imagery Task

Induced EEG activity was recorded during a cue based motor imagery (MI) task. The paradigm of the MI task was implemented using rtsBCI[258]. Participants were seated at a desk in the front of a computer screen at a distance of about 1.5m. They were instructed to imagine waving with their right hand (RH), left hand (LH) or both feet (F). Each MI trial lasted for 5s, as shown in Figure 4.3.

The MI trial started at t=-2s, when a black screen was presented, followed by a warning cue (a cross) at t=-1 s to give participants indication to get ready for MI. The cross was

presented for 4s (from -1 s to 3s (end of the trail)). At t=0 s, an arrow (initiation cue) was presented on the screen for 1.25s, overlapping with a cross. The arrow pointed to the right for RA MI, left for LA MI or down for F MI. The participants were instructed to keep imagining a movement until the cross disappeared, i.e. for 3s in total. The resting period between trials was semi-random and varied between 3-5 s, to avoid expectation of a predictable stimulus. Participants performed 6 MI sessions which lasted 5 min each. Each MI session included 30 trails (10 trails for each condition in semi-randomized sequences). In total, each participant performed 180 trails (60 trails for each condition).

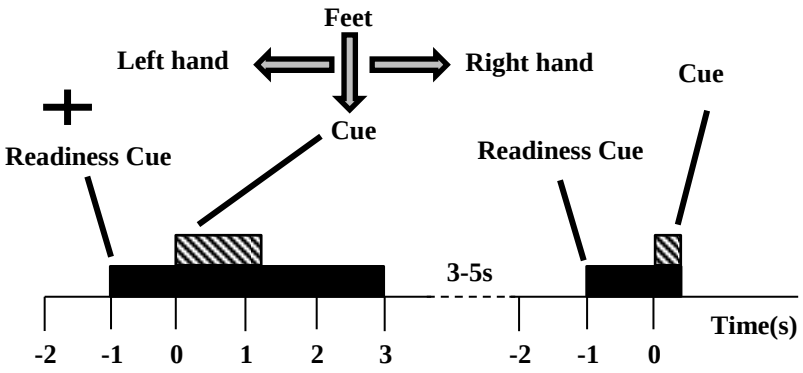


**Figure 4.3** Experimental protocol for a cue-based motor imagery task

## 4.3.6 Pre-Processing of EEG data

Both spontaneous and Induced EEG were exported to EEGlab toolbox[99]. EEG signals were then visually inspected and the signals with artifact or which had an amplitude ≥ 100 μV were manually removed. The EEG signal was then re-referenced to an average reference and decomposed into 48 independent temporal components using infomax independent component analysis (ICA) algorithm[113] implemented in EEGlab for further noise removal. The non-EEG components were identified and removed by considering their characteristic morphology, spatial distribution and frequency content. On average, no more than 3 out of 60 trials had been removed.

### 4.3.7 PSD Analysis for Spontaneous EEG

The group analysis was performed by utilising EEGLab structure 'study' in order to compare the power spectral density (PSD) of the spontaneous EEG between different groups (AB, PnP, PdP and PwP) and between different conditions (EO and EC). The averaged power over participants within the same group for each condition for a single frequency band, including theta (4-7Hz), alpha (8-12Hz) and beta (13-30Hz), was used for group analysis. That provided 3 EEG power analyses for EO and 3 for EC state. To assess the differences between and within the groups and between the conditions the statistical non-parametric method with a significance level p=0.05 was used. The comparison of the power and frequency of the dominant peak between and within the groups and during EO and EC relaxed state was performed using nonparametric Wilcoxon rank-sum test. A correction of multiple comparison was performed using the False Discovery Rate (FDR)[259].

### 4.3.8 ERD/ERS analysis for Induced EEG

The group analysis was performed by utilising EEGLab structure 'study' in order to compare the event related desynchronisation / event related synchronisation (ERD/ERS) induced by MI between different groups (AB, PnP, PdP, and PwP) and between different conditions (RA, LA and F). ERD/ERS was computed using EEGlab. ERD/ERS analysis was performed on the EEG data within a frequency range (3 to 45Hz) using Morlet Wavelet transform[103] with Hanning-tappered window applied and with a minimum of 3 wavelet cycles per window at lower frequency. The baseline period used for ERD/ERS analysis was (t=-1.9 to -1.1s). The averaged ERD/ERS over trails and participants within the same group for each MI condition was used for group analysis. A scalp map based on averaged ERD/ERS over a short time window and specific frequency bands was also used for group analysis. The statistical non-parametric two way ANOVA method with significance level p=0.05 was used in order to assess the differences between the groups

and conditions. A correction for multiple comparison was performed using the False Discovery Rate (FDR)[259].

### 4.3.9 sLORETA Localisation for Spontaneous and Induced EEG

sLORETA analysis was performed on spontaneous EEG data (EO and EC relax state) and on induced EEG data (MI tasks) for all 4 groups. sLORETA has been used to estimate the cortical three dimensional distribution of the EEG sources current density[69].

For spontaneous EEG, data for each subject of each group was split into 4s long time epochs. Each of these epochs was exported to sLORETA. The current source density was computed in sLORETA for each of these epochs in three frequency bands including theta 4-7Hz, alpha 8-12Hz and beta 13-30Hz. The frequency dependent changes in brain activation at surface and deep cortical structures were compared between the groups during EO and EC state. A non-parametric t test implemented in sLORETA package with 5000 randomisation of statistical analysis was used to compute corrected p values. The statistical significant level was set at p=0.05.

For induced EEG, the trials were split into 1s long epochs and exported to sLORETA. The current source density was computed in sLORETA for each of these 1s epochs in four frequency bands including theta 4-8Hz, alpha 8-12Hz, beta SMR 16-24Hz and beta 20-30Hz. The baseline was taken for 1s from the baseline period of each MI trial (-2 to -1s). The frequency dependent changes in brain activation at surface and deep cortical levels were compared between the groups for all three MI conditions (F, LH and RH). A non-parametric t test implemented in sLORETA package with 5000 randomisation of statistical analysis was used to compute corrected p values. The statistical significant level was set at p=0.05.

## 4.4 Results

Due to a considerable length of this chapter a summary of results will be presented to help the reader to understand the overall structure of results. Results are divided in a brief section reporting on mechanical stimuli followed by EEG results. EEG analysis is divided into spontaneous EEG analysis in EO and EC state and in analysis of induced EEG activity during motor imagination task. Each of these two is divided into EEG based analysis and sLORETA analysis. Results section comprise mostly of statistically significant results and where necessary, to preserve the consistency of data, also of non-significant results. However, for the majority of non-significant results that were presented in this chapter related figures are shown in Appendix A. A summary of the results is provided in section (4.4.7).

Section 4.4.2 Spontaneous EEG analysis is divided into:

- Comparison between PSD in EO and EC state for each single group separately.
- Comparison of PSD between each pair of groups for EC and for EO state, for theta, alpha and beta band.
- The analysis of inter-subject PSD variability in EO and EC state for each single group.
- Comparison of dominant alpha peak power and dominant alpha peak frequency between each pair of groups.

Section 4.4.3 sLORETA comparison of the spontaneous cortical activity between groups is divided into:

- sLORETA comparison of spontaneous cortical activity between groups in the theta band
- sLORETA comparison of spontaneous cortical activity between groups in the alpha band
- sLORETA comparison of spontaneous cortical activity between groups in the beta band

Section 4.4.4. Induced EEG during motor imagery (MI) tasks is divided into

- Analysis of ERD/ERS for all groups at representative electrodes
- Comparison of ERD/ERS scalp maps between PnP and PdP
- Statistical analysis of differences in ERD/ERS maps between all groups

Section 4.4.5. Spatio-temporal dynamics of ERD/ERS during MI task is divided into:

- Spatio-temporal dynamics of theta band ERD/ERS
- Spatio-temporal dynamics of alpha band ERD/ERS
- Spatio-temporal dynamics of beta band ERD/ERS

Section 4.4.6 sLORETA comparison of the cortical activity between groups during MI tasks is divided into:

- sLORETA comparison of the cortical activity between groups in the theta band during MI task.
- sLORETA comparison of the cortical activity between groups in the alpha band during MI task.
- sLORETA comparison of the cortical activity between groups in the beta band during MI task.

## 4.4.1 Response to Mechanical Stimulus

All patients in PnP and PdP have been tested for wind-up effect. Only one patient, who also verbally reported unpleasant altered sensation in his sole (touching a sand paper), reported pain during this test.

## 4.4.2 Spontaneous EEG Analysis

Spontaneous EEG was analyzed in both eyes opened (EO) and eyes closed (EC) conditions and compared among each of the groups. Two major features were adopted as a measure of spontaneous EEG, the power spectral density (PSD) and the dominant alpha frequency. The PSD has been analysed for different frequencies within a 2-30Hz band which covers theta, alpha and beta rhythms. Previous studies showed that these three rhythms are most affected by the presence of CNP[24,138–140]. The PSD was analysed in the

form of scalp maps for a selected frequency band as well as a full spectrum PSD over selected individual electrodes. For the later analysis, 5 representative electrode locations over frontal (Fz), central (C3, C4 and Cz) and occipital (Oz) regions were chosen. The 3 central representative electrodes located over the primary motor cortex of arms and legs cover the sources of the mu rhythm[260] while the other two cover the frontal and the occipital sources of the alpha rhythm[57,90].

#### *4.4.2.1 Comparison between PSD in EO and EC State for Each Single Group*

This analysis was performed for theta, alpha and beta band, separately for each frequency band. The scalp maps based on PSD on each of 48 electrodes in theta (4-7Hz), alpha (8-12Hz) and beta (13-30Hz) EEG frequency bands for all groups are shown in Figure 4.4, Figure **4.5**, and Figure **4.6**, respectively. Figure 4.4 shows that the AB group has lower theta PSD over the whole scalp in both EO and EC states compared to patient groups. The highest theta PSD was noticed in PwP and PdP groups. The statistically significant differences (without correction for multiple comparisons) between the groups were found over central, parietal and occipital regions during EO. Significantly larger theta PSD in EC state compared to EO state were found in AB and PnP groups over most of the 48 electrodes locations. PwP group also show significantly larger theta PSD in EC compared to EO over frontal and parieto-occipital regions. There was no significant difference in theta PSD between EO and EC states in PdP group.

In the alpha band (8-12Hz), AB exhibited lower PSD over central area than in all three patient groups during EC state (Figure 4.5). During EC state, all groups exhibited higher occipital alpha power compared to EO state. Significantly higher alpha PSD in EC state compared to EO was noticed over all 48 electrode locations in the AB group. The group of PnP show a significantly higher alpha PSD in EC state compared to EO state over frontal and occipital regions. Comparing between EC and EO state, PdP and PwP also exhibited a significantly higher alpha PSD (without correction for multiple comparison). The

comparison between all groups during EO or EC state showed that there was no significant difference in the alpha band PSD. In the beta band (13-30Hz), the comparisons between EO and EC states show that AB had significantly larger PSD during EC over most of the electrode locations and PnP had significantly larger PSD over the occipital region (Figure 4.6). Larger, but not significantly, beta PSD during EC state was noticed in PdP and PwP compared to EO state. The comparison between all the groups during EO or EC state showed no statistically significant difference in the beta band PSD.

#### *4.4.2.2 Comparison of PSD between each pair of groups for EC and EO state, for theta, alpha and beta bands*

The analysis was performed for the theta, alpha and beta frequency band, separately for each bands. The comparisons of scalp maps based on PSD between each pair of groups during EO and EC states of each of 48 electrodes in theta (4-7Hz), alpha (8-12Hz) and beta (13-30Hz) frequency bands are shown in Figure 4.7. The largest differences were noticed in the PwP group when compared to the AB group. The comparison shows that PwP exhibited a significantly higher theta PSD compared to the AB group in both EO and EC state over most of the 48 electrode locations. It can be also noticed that PdP had significantly higher theta PSD over frontal and parieto-occipital regions compared to AB in both EO and EC. The comparison between AB and PnP group shows that PnP had higher theta PSD over several electrode locations at the frontal and parieto-occipital regions during EC state. The comparison between all three patient groups during EO or EC state and for all three frequency bands showed no statistically significant difference except over two electrode locations (P7 and P8) which showed significantly higher beta PSD in PdP compared to the PnP group and over three electrode locations (P2, PO4 and POz) which showed significantly higher theta PSD in PwP compared to PnP during EO state. The comparison between AB and all three patient groups in alpha and beta bands and in EO and EC show the patient groups had a higher PSD over several electrode locations over the

scalp. None of these differences reached the adjusted p value after FDR correction of multiple comparisons.

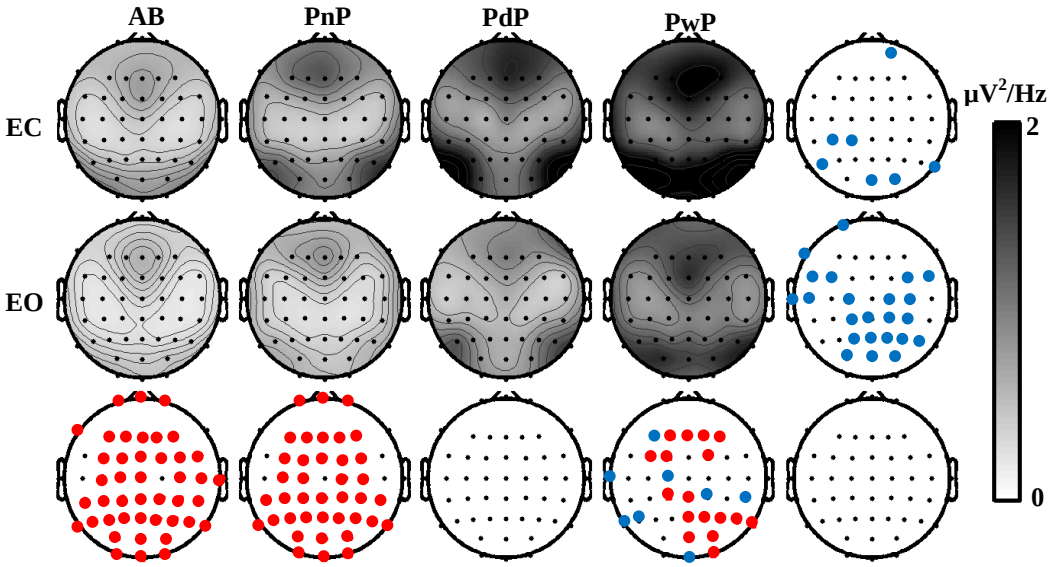


**Figure 4.4** The scalp maps based on PSD average over theta 4-7Hz frequency band for all groups (AB: able bodied, PnP: patients with no pain, PdP: patients developed CNP and PwP: patients with CNP) and eyes opened (EO) and eyes closed (EC) relaxed states. The statistical significant differences between the EO and EC of the same group are shown on the last bottom raw while the statistical significant differences among the groups for EO or EC state are shown on the last right column (p = 0.05). Red circles marked statistical significant differences with FDR correction of multiple comparisons while blue circles marked statistical significant differences without FDR.

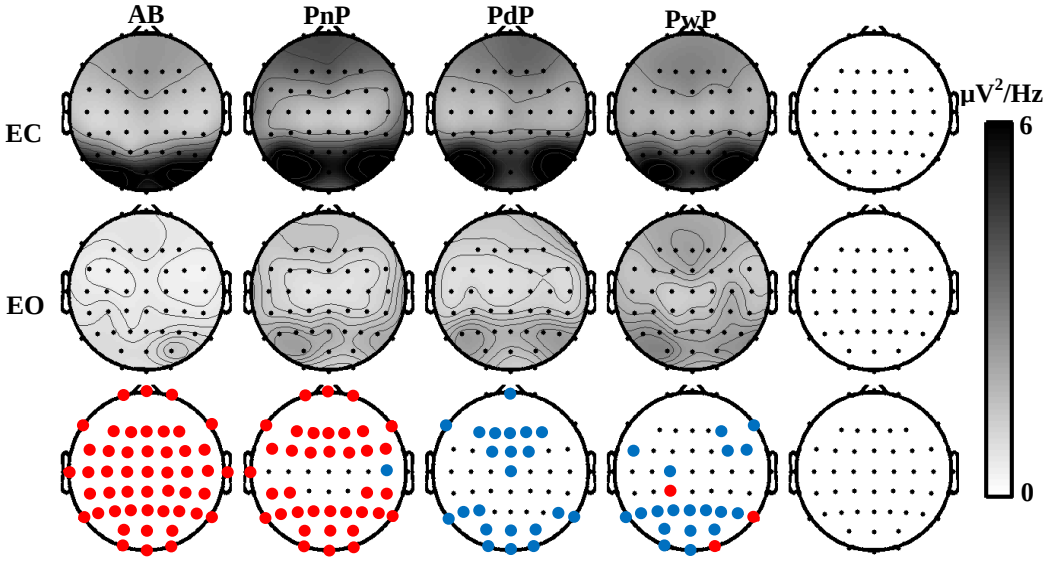


**Figure 4.5** The scalp maps based on PSD average over alpha 8-12Hz frequency band for all groups (AB: able bodied, PnP: patients with no pain, PdP: patients developed CNP and PwP: patients with CNP) and eyes opened (EO) and eyes closed (EC) relaxed states. The statistical significant differences between the EO and EC of the same group are shown on the last bottom raw while the statistical significant differences among the groups for EO or EC state are shown on the last right column (p = 0.05). Red circles marked statistical significant differences with FDR correction of multiple comparisons while blue circles marked statistical significant differences without FDR.

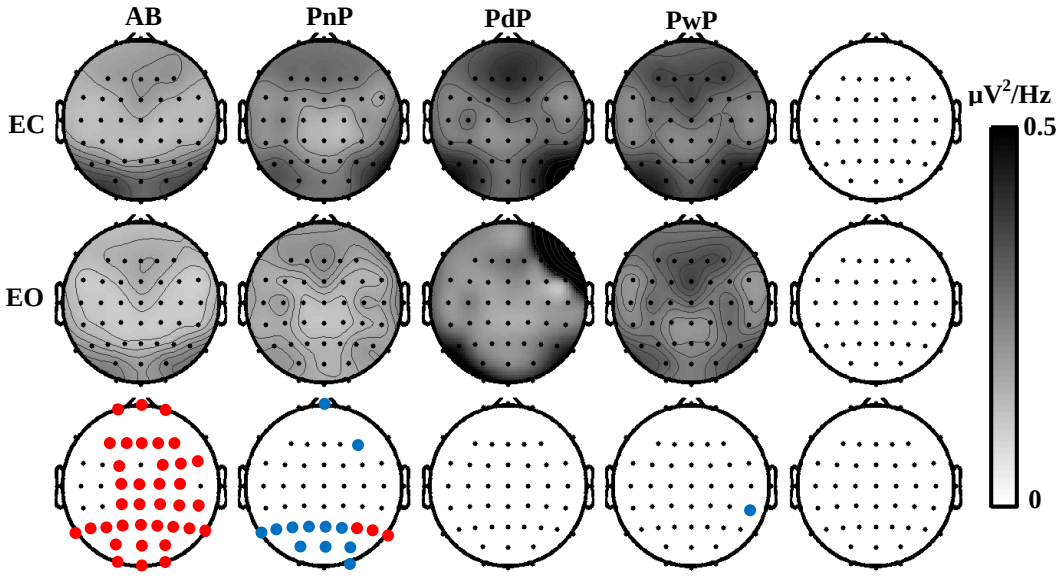


**Figure 4.6** The scalp maps based on PSD average over higher beta 13-30Hz frequency band for all groups (AB: able bodied, PnP: patients with no pain, PdP: patients developed CNP and PwP: patients with CNP) and eyes opened (EO) and eyes closed (EC) relaxed states. The statistical significant differences between the EO and EC of the same group are shown on the last bottom raw while the statistical significant differences among the groups for EO or EC state are shown on the last right column ($p = 0.05$). Red circles marked statistical significant differences with FDR correction of multiple comparisons while blue circles marked statistical significant differences without FDR.

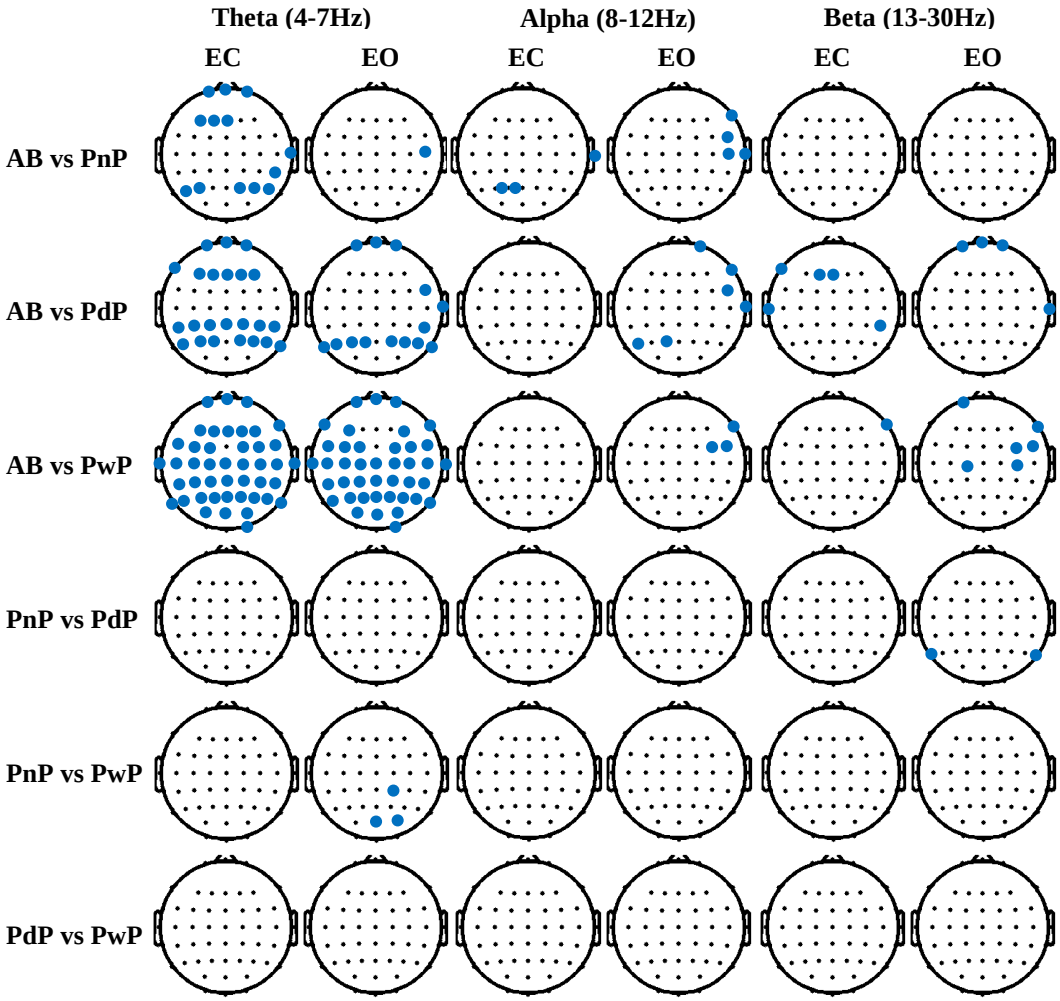


**Figure 4.7** The comparison of scalp maps based on PSD between each pair of groups; able bodied (AB), patients with no pain (PnP), patients developed pain (PdP), and patients with pain (PwP) during eyes opened (EO) and eyes closed (EC) relaxed states in theta (4-7Hz), alpha (8-12Hz) and beta (13-30Hz) EEG frequency bands. Blue circles marked statistical significant differences (p=0.05) without FDR correction of multiple comparison.

#### *4.4.2.3 Analysis of Inter-subject PSD Variability in EO and EC State for Each Single Group*

Power spectrum density of a group is typically presented as the average value. This however does not account for inter-subject variability. This section looks into the variability of PSD of individual participants within each group and compares this variability between different groups. The PSD of each subject and the averaged PSD for these 5 representative electrode locations for AB, PnP, PdP and PwP groups are shown in Figure 4.8, Figure 4.9, Figure 4.10 and Figure 4.11, respectively. These figures show that

there are large variations between the subjects within the same group in terms of the dominant peak frequency.

During EO state the largest variations across all 48 electrode locations can be noticed in both the PwP group (variance (VAR) = 2.12) and PdP (VAR = 2.07) compared to AB (VAR= 0.99) and PnP (VAR = 1.02). The F test was used to compare the variance between the groups. No significant difference between groups during EO was noticed (AB vs. PnP p=0.96, AB vs PdP p=0.28, AB vs. PwP p=0.26, PnP vs PdP p=0.3, PnP vs PwP p=0.28 and PdP vs PwP p=0.98). During EC state, although the variations between the subjects of the same groups are smaller than in EO state, PwP still exhibits the largest variations (VAR=1.77) compared to AB (VAR=0.27), PnP (VAR=0.92) and PdP (1.03). During EC state the variance of the PwP group was significantly larger compared to AB (p=0.009) but there were no significant differences between other groups AB vs. PnP (p=0.07), AB vs PdP (p=0.06), PnP vs PdP (p=0.85), PnP vs PwP (p=0.34) and PdP vs PwP (p=0.48). Due to this variability between subjects, the power and the frequency of the dominant peak for each of the 48 electrode locations was calculated individually for each subject.

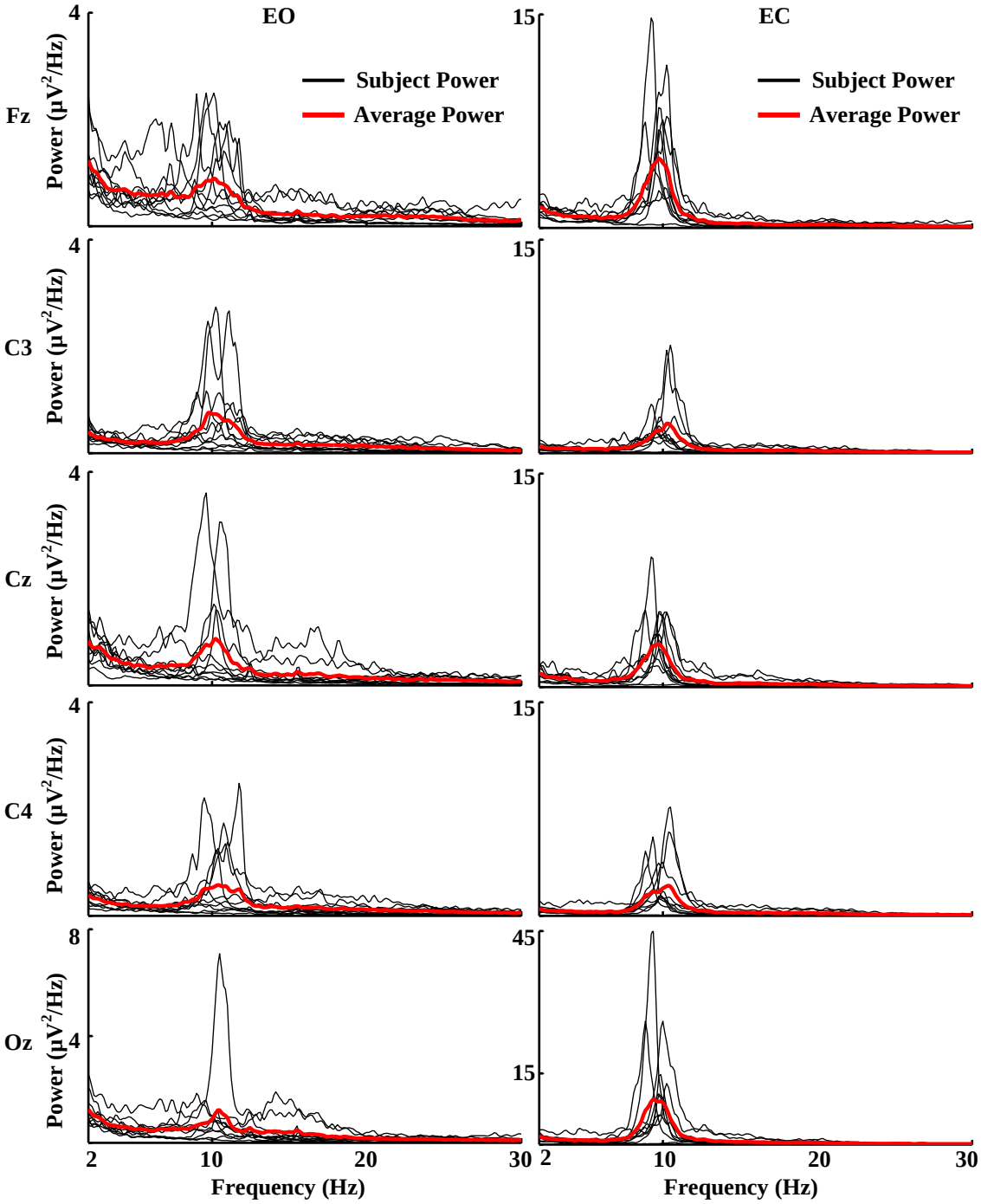


**Figure 4.8** The power spectral density (PSD) of each subject (thin black line) and the average PSD across all subjects (red thick line) in able bodied group (AB) during eyes opened (EO) and eyes closed (EC) relaxed states and for Fz, C3, Cz, C4 and Oz electrode locations.

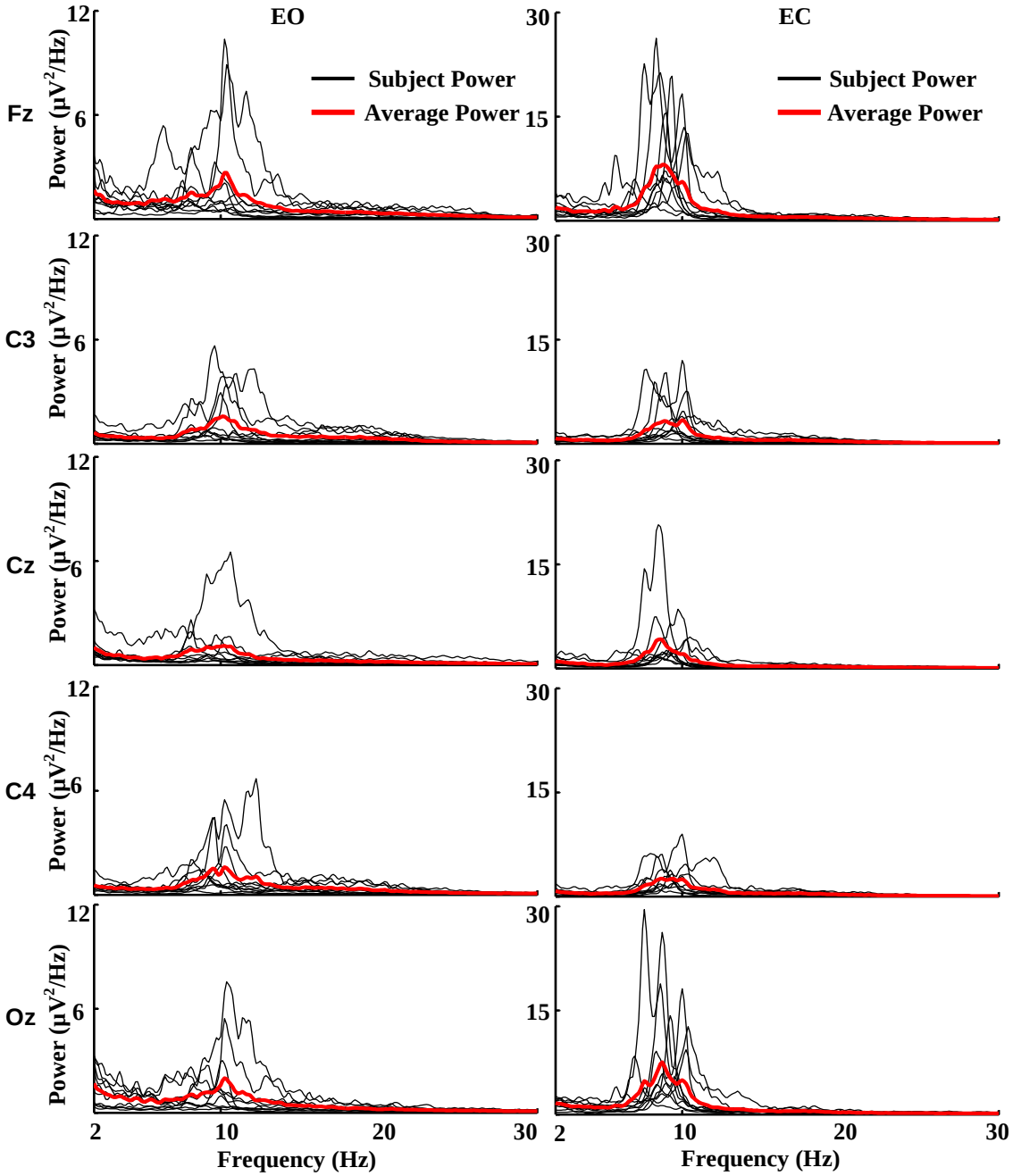


**Figure 4.9** The power spectral density (PSD) of each subject (thin black line) and the average PSD across all subjects (red thick line) in patients with no pain group (PnP) during eyes opened (EO) and eyes closed (EC) relaxed states and for Fz, C3, Cz, C4 and Oz electrode locations.

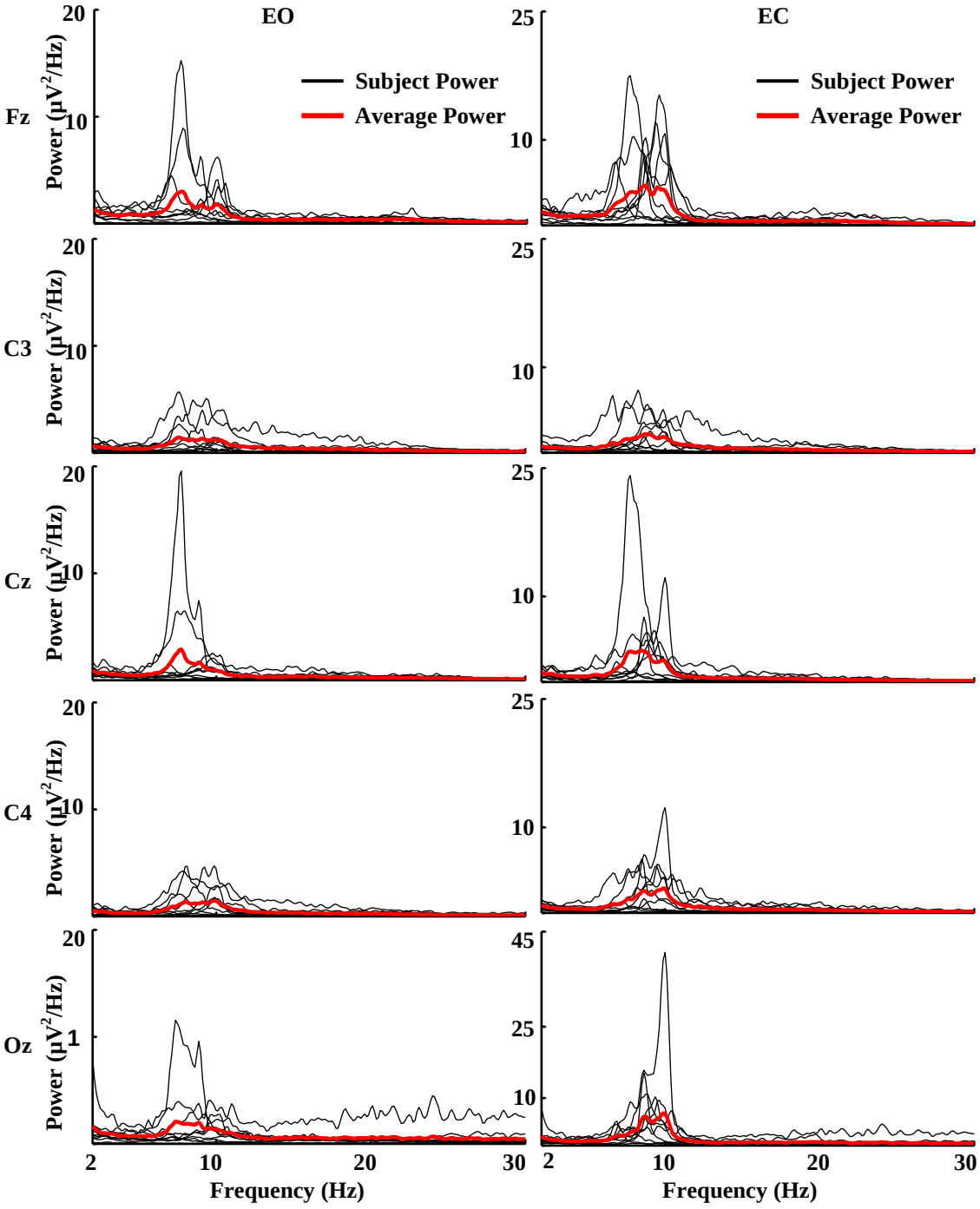


**Figure 4.10** The power spectral density (PSD) of each subject (thin black line) and the average PSD across all subjects (red thick line) in patients developed CNP group (PdP) during eyes opened (EO) and eyes closed (EC) relaxed states and for Fz, C3, Cz, C4 and Oz electrode locations.

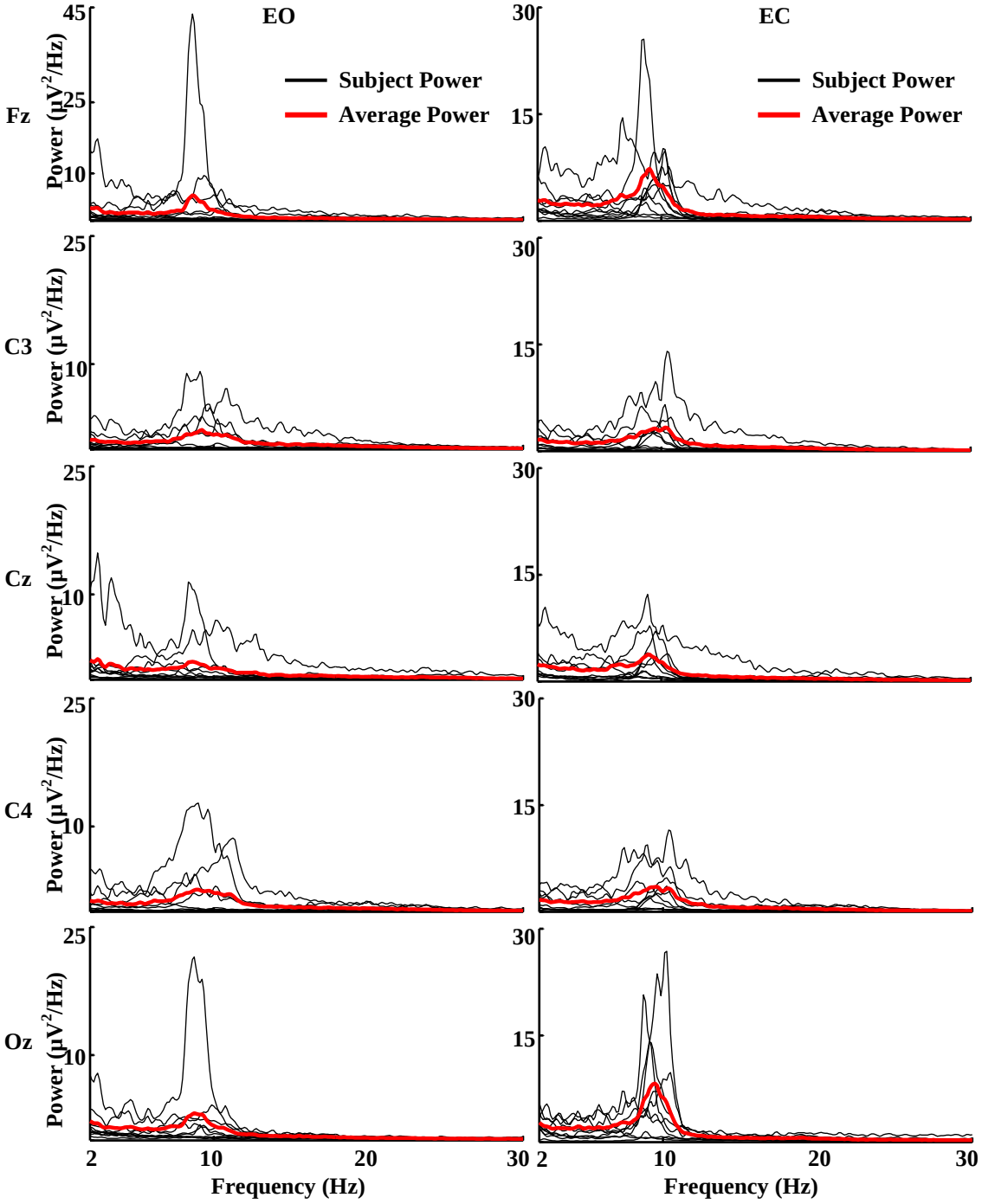


**Figure 4.11** The power spectral density (PSD) of each subject (thin black line) and the average PSD across all subjects (red thick line) in patients with CNP group (PwP) during eyes opened (EO) and eyes closed (EC) relaxed states and for Fz, C3, Cz, C4 and Oz electrode locations.

#### *4.4.2.4 Comparison of Dominant Peak Power and Dominant Peak Frequency between Each Pair of Groups*

A dominant peak in PSD graphs, such as one shown in Figures 4.8-4.11 is the 'peak' e.g. highest amplitude point which is typically located in alpha (8-12 Hz) range. This peak value is defined by its frequency and by the average power in PSD graph, for a narrow frequency band (peak±2Hz) surrounding the dominant peak, as described in the Method section.

The comparisons between the power of the dominant peak for each of the 48 EEG electrode locations during EO and EC state and for each group are shown in Figure 4.12. The comparison shows that AB and PnP had higher power during EC state compared to EO over most of the 48 electrode locations. PwP also show higher power during EC compared to EO state over frontal, parietal and occipital regions. Only several electrode locations with significantly higher power in EC compared to EO were noticed in the PdP group. The higher power during EO state was noticed in the PdP group compared to other groups (Table 4.2). None of the electrode locations in both PwP and PdP groups reached the adjusted p value after FDR correction of multiple comparisons (Figure 4.12). The increase of alpha power (alpha synchronisation) during EC state can reflect the idling status of the cortical (cognitive default state)[261].

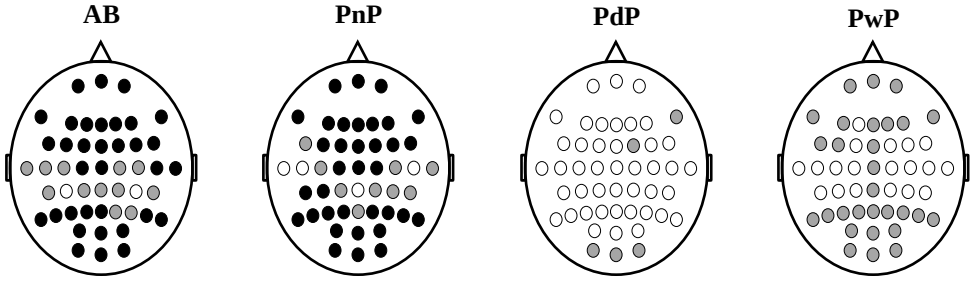


**Figure 4.12** The comparison between the power of the dominant peak for each 48 EEG electrode location during EO and EC state and for each group, AB: able bodied, PnP: patients with no pain, PdP: patients developed pain and PwP: patients with pain. Electrodes with statistically significant differences (p =0.05) and FDR correction of multiple comparisons are presented with black dots while grey dots mark electrodes with statistically significant differences without FDR correction.

The EC/EO power ratio of the dominant peak for each of the 48 EEG electrode locations was compared amongst the groups. The EC/EO power ratio of the dominant frequency was computed in order to investigate the EEG reactivity between EO and EC state[139,262]. Figure 4.13 shows the comparison of EC/EO power ratio of dominant peak over all 48 electrode locations between each pair of groups (AB vs. PnP, AB vs. PdP, AB vs. PwP, PnP vs. PdP, PnP vs. PwP, and PdP vs. PwP). The EC/EO ratio of the PdP group was significantly lower than the ratio in the AB and PnP groups, predominantly over the frontal and parieto-occipital regions. PwP demonstrated significantly lower EC/EO power ratio over FC3, P7, P5, O1 and Oz electrodes compared to AB. Statistically higher EC/EO power ratio of the dominant peaks were also noticed in PnP over Cp3 and P3 and statistically lower in PdP over Fpz and P1 compared to PwP. No significant difference in the EC/EO ratio of dominant peaks was found between AB and PnP. Over all 48 electrode locations PdP exhibited the lowest EC/EO ratio compared to other groups AB, PnP and PwP, as shown in Table 4.2. The deficiency in EC/EO power ratio has previously reported in SCI patients with CNP suggested that the reduction in EC/EO ratio can be an indicator of the thalamo-cortical dysrhythmia[139].

A shift of the dominant alpha frequency towards the lower frequencies was noticed in all patient groups compared to AB during both EO and EC state. This confirmed the results of the previous studies reporting 'slowing down' of EEG in chronic SCI patients with CNP[138–140] and with no pain[263] compared to the able-bodied controls. During EO state and over all 48 electrodes, PdP showed the lowest dominant frequency compared to AB, PnP and PwP (see Table 4.2). Comparisons of dominant frequency among the groups during EO and EC states and over all 48 electrode locations are shown in Figure 4.14 and Figure 4.15, respectively. The largest number of electrodes which show a significant difference between groups (before correction for multiple comparisons) was located in the occipital region, which is the source of the wide-spread alpha activity. During EO state, the

lowest dominant frequency of PdP was significantly different than AB and this 'low frequency shift' was present mostly over the central and parietal regions (Figure 4.14), which indicated that the source of this 8-12 Hz rhythm presents a mixture of the central mu and the wide spread alpha rhythm. PwP also showed a significantly lower dominant frequency compared to AB. Group PnP had a significantly lower dominant frequency over P7 and P3 electrodes compared to AB. No significant difference among the patient groups in dominant frequency for EO was found. Across all 48 electrodes and during EC state no significant difference in dominant frequency was found between all groups.

During EC state and over all 48 electrodes, PdP also showed lowest dominant frequency compared to AB, PnP and PwP (see Table 4.2). The significantly lower dominant frequency during EC state was found on most of the EEG electrode locations (45 out of 48 electrodes) between PdP and AB (Figure 4.15). PnP and PwP also showed a statistically significant difference in dominant frequency compared to AB. No significant difference was found in EC dominant frequency among patient groups, except between PdP and PwP over a single electrode location, FC6 (Figure 4.15). Across all 48 electrodes and during EC state, the dominant frequency of PdP and PwP groups were significantly lower than in AB (PdP vs AB $p= 0.0021$, and PwP vs AB $p= 0.0265$). No significant difference in dominant frequency was found between any other groups.

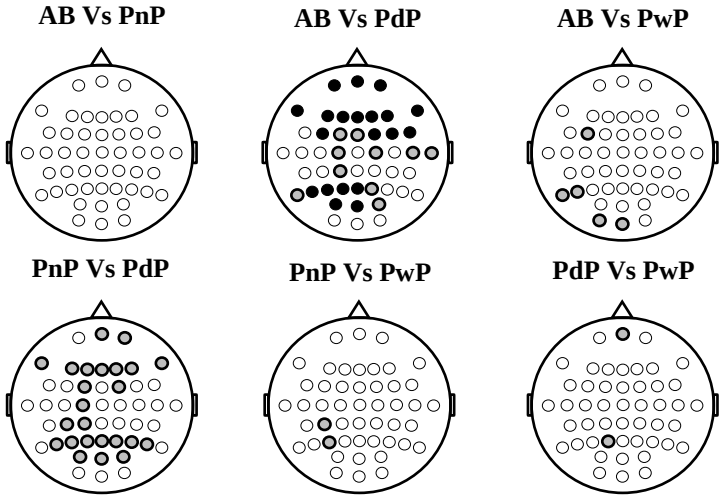


**Figure 4.13** The comparison of EC/EO ratio of the amplitude of the dominant peak between pair of groups (AB vs. PnP, AB vs. PdP, AB vs. PwP, PnP vs. PdP, PnP vs. PwP, and PdP vs. PwP). Electrodes with statistically significant differences (p =0.05) and FDR correction of multiple comparisons are presented with black dots while grey dots mark electrodes with statistically significant differences without FDR correction.

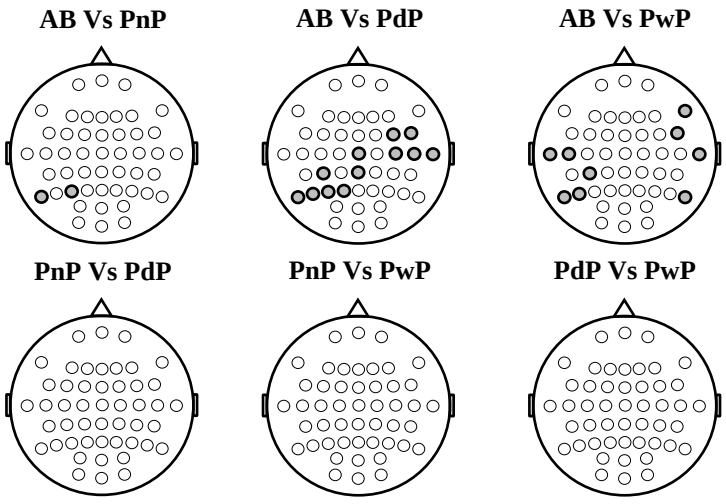


**Figure 4.14** The comparison of the dominant peak frequency between pair of groups (AB vs. PnP, AB vs. PdP, AB vs. PwP, PnP vs. PdP, PnP vs. PwP, and PdP vs. PwP) during EO state. Electrodes with statistically significant differences (p=0.05) are presented with grey dots mark electrodes. All statistical results without FDR correction.

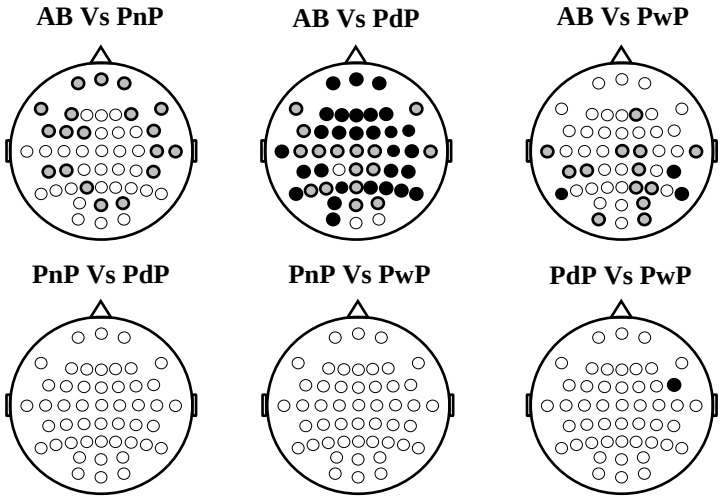


**Figure 4.15** The comparison of the dominant peak frequency between pair of groups (AB vs. PnP, AB vs. PdP, AB vs. PwP, PnP vs. PdP, PnP vs. PwP, and PdP vs. PwP) during EC relaxed state. Electrodes with statistically significant differences (p =0.05) and FDR correction of multiple comparisons are presented with black dots while grey dots mark electrodes with statistically significant differences without FDR correction.

**Table 4.2** The power and frequency of the dominant peak during EO and EC relaxed states and the EC/EO power ratio of the dominant peak across all 48 electrode location and for all 4 groups.

| **Group** | Power of the dominant peak (Mean ± SD) **$\mu V^2$/Hz** | | EC/EO power ratio (Mean ± SD) | Frequency of the dominant peak (Mean ± SD) **Hz** | |
|---|---|---|---|---|---|
| | **EO** | **EC** | **EC/EO** | **EO** | **EC** |
| **AB** | 1.4±1.0 | 7.8±4.3 | 8.3±7.4 | 10.4±1.0 | 10.0±0.6 |
| **PnP** | 3.2±3.2 | 14.2±10.2 | 10.5±11.2 | 9.6±1.1 | 9.2±1.0 |
| **PdP** | 5.5±3.5 | 11.0±5.9 | 2.6±1.5 | 9.3±1.4 | 8.6±1.0 |
| **PwP** | 4.7±7.0 | 10.5±8.0 | 5.1±5.8 | 9.5±1.5 | 9.0±1.4 |

**EO**: Eyes Opened Relaxed State, **EC**: Eyes Closed Relaxed State, **AB**: Able bodied, **PnP**: Patients no Pain, **PdP**: Patients Developed Pain, **PwP**: Patients with Pain.

### 4.4.3 sLORETA Comparison of the Spontaneous Cortical Activity between Groups

This subsection presents figures of statistically significant results only, while the rest of the analysis is provided in the Appendix A. The comparison of the cortical activity between all 4 groups and during EO and EC states are shown in Figures A.1 and A.2 (Appendix A) for theta band (4 to 7Hz), Figure 4.16 and Figure **4.17** for alpha band (8 to 12Hz), and Figure 4.18 and A.3 for beta band (13 to 30Hz).

#### 4.4.3.1 sLORETA Comparison of Spontaneous Cortical Activity between Groups in The Theta Band

None of the differences reach a statistical significance (p=0.05), therefore all figures are presented in Appendix A. In the theta band (4-7Hz), the comparisons between AB and patient groups are shown in Figure A.1 while the comparisons among the patients groups are shown in Figures A.2. Figure A.1 shows that the AB group exhibited higher activation over the central area during EO compared to the PnP group but this difference diminished during EC. Compared to the PdP group, AB showed higher theta activation over frontal and occipital regions during EO state and lower theta activation over central and parietal areas during EC state. The widespread lower theta activation was also noticed in the AB group compared to PwP. In other words, PdP and PwP had higher theta activation while PnP had lower theta activation compared to AB groups during both EO and EC states. Figure A.2 shows that PnP had lower theta activity compared to both PdP and PwP groups over the central area particularly during EC for the PdP group and both EO and EC for the PwP group. The comparisons between the PdP and the PwP groups show that PdP had lower theta activity over frontal and occipital regions and higher activity over the central area.

#### 4.4.3.2 sLORETA Comparison of Spontaneous Cortical Activity between Groups in The Alpha Band

In the alpha band (8-12Hz), the comparisons between the AB group and patient groups are shown in Figure 4.16. It shows that AB had higher activity over the parietal and occipital areas compared to PdP and PwP groups and the strongest activity of the AB group was noticed over the parietal area compared to the PdP group during EC state. The comparisons between patient groups show that the PnP group had higher activity over parietal and occipital areas compared to both PdP and PwP groups during EC state and the stronger differences were noticed over the parietal area (Figure 4.17). The strongest

differences of alpha activity with statistical significance (p=0.05) were noticed during EC state between AB and PdP groups, PnP and PdP, and PnP and PwP. Table 4.3 shows the brain area and the number of the voxels with significant differences between AB vs PdP, PnP vs PdP, and PnP vs PwP during EC state. There was no statistically significant difference between any other pair of groups in the EC state. There was also no statistically significant difference between any pair of groups in EO state.

#### *4.4.3.3 sLORETA Comparison of Spontaneous Cortical Activity between Groups in The Beta Band*

In the beta band (13-30Hz), AB exhibited stronger activity expanding from central to occipital regions compared to patient groups during EO and these differences were reduced in the EC state (Figure 4.18). PwP had higher beta activity over central region compared to AB during EO and EC states. The higher beta activity during the EC state can also be noticed over the central region in PdP compared to AB. The comparisons between the patient groups show that PnP exhibited lower beta activity over the central area compared to both PdP during EC and PwP groups during EO and EC states (Figure A.3). The lower beta activity over frontal and central regions was also noticed in the PdP group compared to the PwP group during EO state and this difference was reduced in the EC state. A significantly larger beta activity (p=0.05) was noticed during the EO state in AB compared to all three patient groups. Table 4.4 shows the brain area and the number of the voxels with statistically significant differences between AB vs PnP, AB vs PdP, and AB vs PwP during EO state.

**Table 4.3:** Areas with significant differences in cortical activity between AB vs PdP, PnP vs PdP and PnP vs PwP in alpha (8-12Hz) EEG frequency band during eyes closed (EC) relaxed state.

| Groups | Brain Lobe | Brodmann area | Brain Hemisphere | Number of Voxel | Voxel with maximum t value | | | |
|---|---|---|---|---|---|---|---|---|
| | | | | | Statistics t-values | MNI Coordinate | | |
| | | | | | | x | y | z |
| **AB vs PdP** | Parietal | 7 | **L** and R | 39 | 4.96 | 10 | -80 | 45 |
| | Parietal | 19 | **R** | 1 | 4.42 | 15 | -85 | 40 |
| **PnP vs PdP** | Parietal | 7 | **L** | 28 | 5.02 | -25 | -60 | 50 |
| | Parietal | 40 | **L** | 1 | 4.38 | -35 | -55 | 55 |
| **PnP vs PwP** | Parietal | 7 | **L** | 8 | 5.07 | -25 | -50 | 55 |
| | Parietal | 40 | **L** | 2 | 4.62 | -35 | -50 | 55 |

MNI: the Montreal Neurological Institute and Hospital (MNI) coordinate system. R, Right; L, Left. The brain hemisphere with bold font is the hemisphere with higher contribution in the number of significant voxel.

**Table 4.4:** Areas with significant differences in cortical activity between AB and patients groups, in beta (13-30Hz) EEG frequency band during eyes opened (EO) relaxed state.

| Groups | Brain Lobe | Brodmann area | Brain Hemisphere | Number of Voxel | Voxel with maximum t value | | | |
|---|---|---|---|---|---|---|---|---|
| | | | | | Statistics t-values | MNI Coordinate | | |
| | | | | | | x | y | z |
| **AB vs PnP** | Parietal | 7 | **R** | 5 | 4.65 | 20 | -80 | 45 |
| **AB vs PdP** | Parietal | 7 | **R** | 5 | 3.90 | 15 | -65 | 65 |
| **AB vs PwP** | Parietal | 7 | **L** and R | 11 | 4.40 | -10 | -65 | 65 |

MNI: the Montreal Neurological Institute and Hospital (MNI) coordinate system. R, Right; L, Left. The brain hemisphere with bold font is the hemisphere with higher contribution in the number of significant voxel.

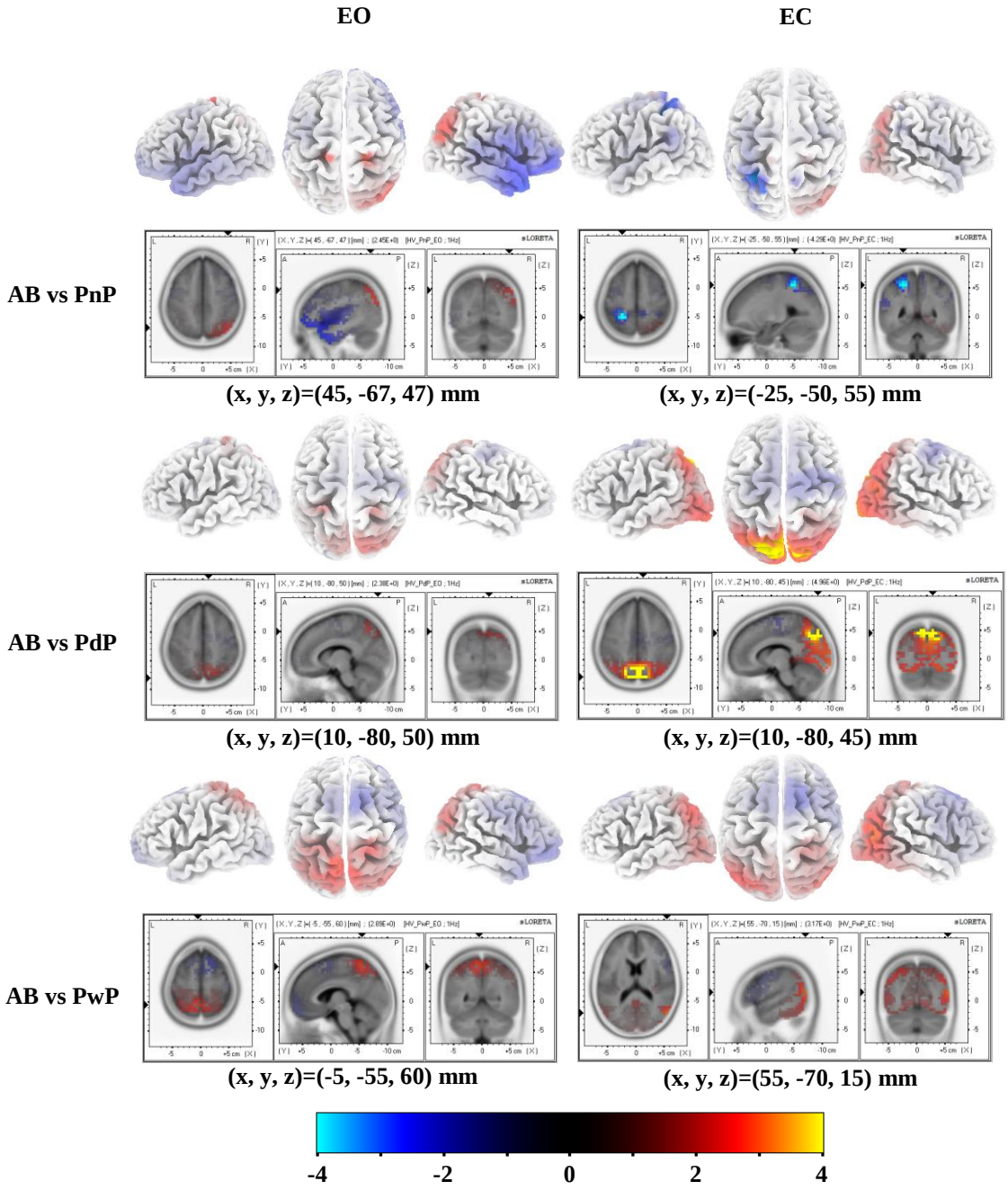


**Figure 4.16** sLORETA localisation for eyes open (EO) and eyes close (EC) relaxed state for able bodied (AB) group compared with patients groups: patients with no pain (PnP), patients developed CNP (PdP) and patients with CNP (PwP) in alpha EEG frequency band (8-12Hz). The first raw of each figure represents 3D map of the localisation while the second raw represents the 3D slice at the displayed of the voxel with negative or positive strongest activity. The (x, y, z) under each figure represent the Montreal Neurological Institute and Hospital (MNI) coordinate system of the voxel with strongest activity.

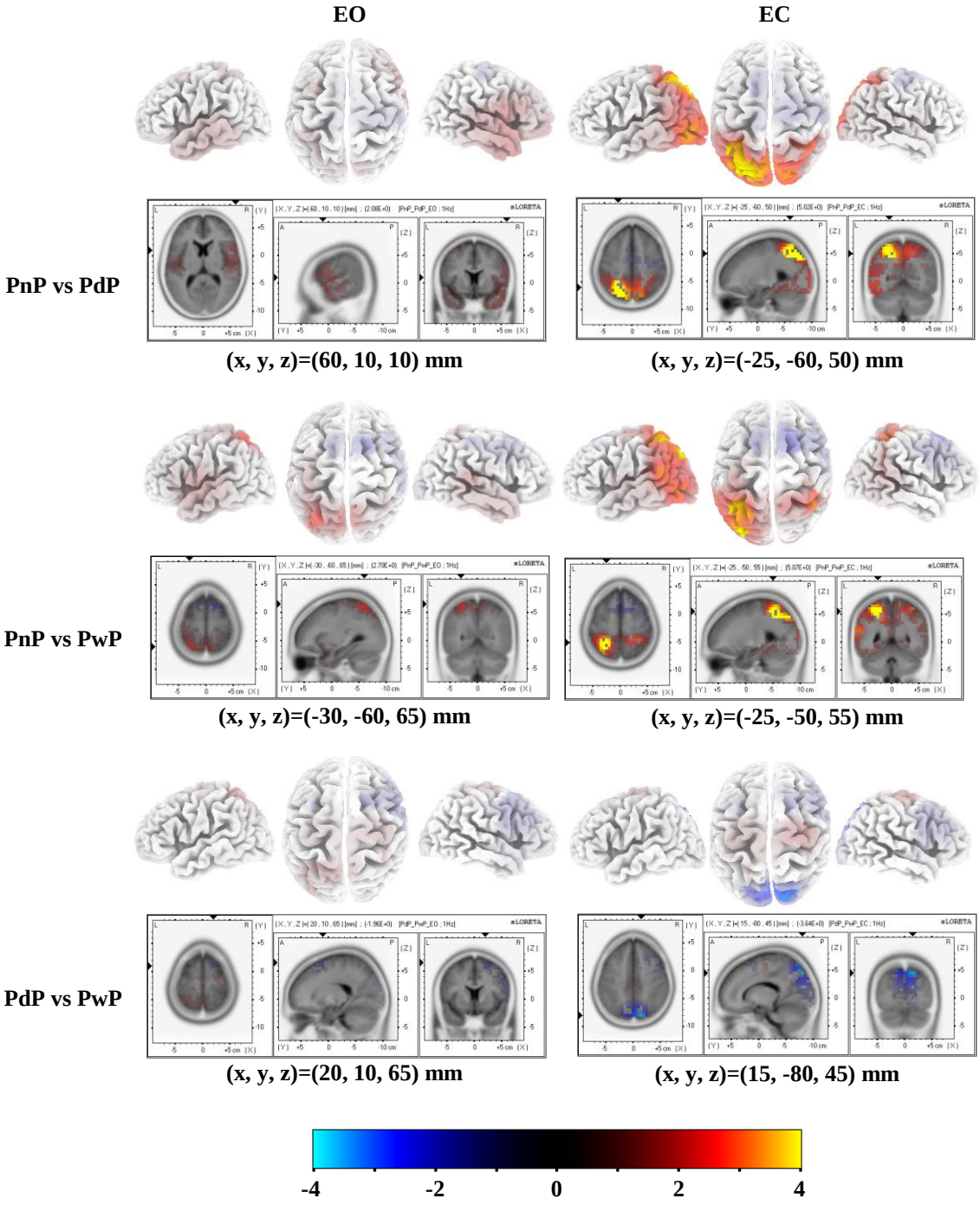


**Figure 4.17** sLORETA localisation for eyes open (EO) and eyes close (EC) relaxed state compared among the patients groups: patients with no pain (PnP), patients developed CNP (PdP) and patients with CNP (PwP) in alpha EEG frequency band (8-12Hz). The first raw of each figure represents 3D map of the localisation while the second raw represents the 3D slice at the displayed of the voxel with negative or positive strongest activity. The (x, y, z) under each figure represent the Montreal Neurological Institute and Hospital (MNI) coordinate system of the voxel with strongest activity.

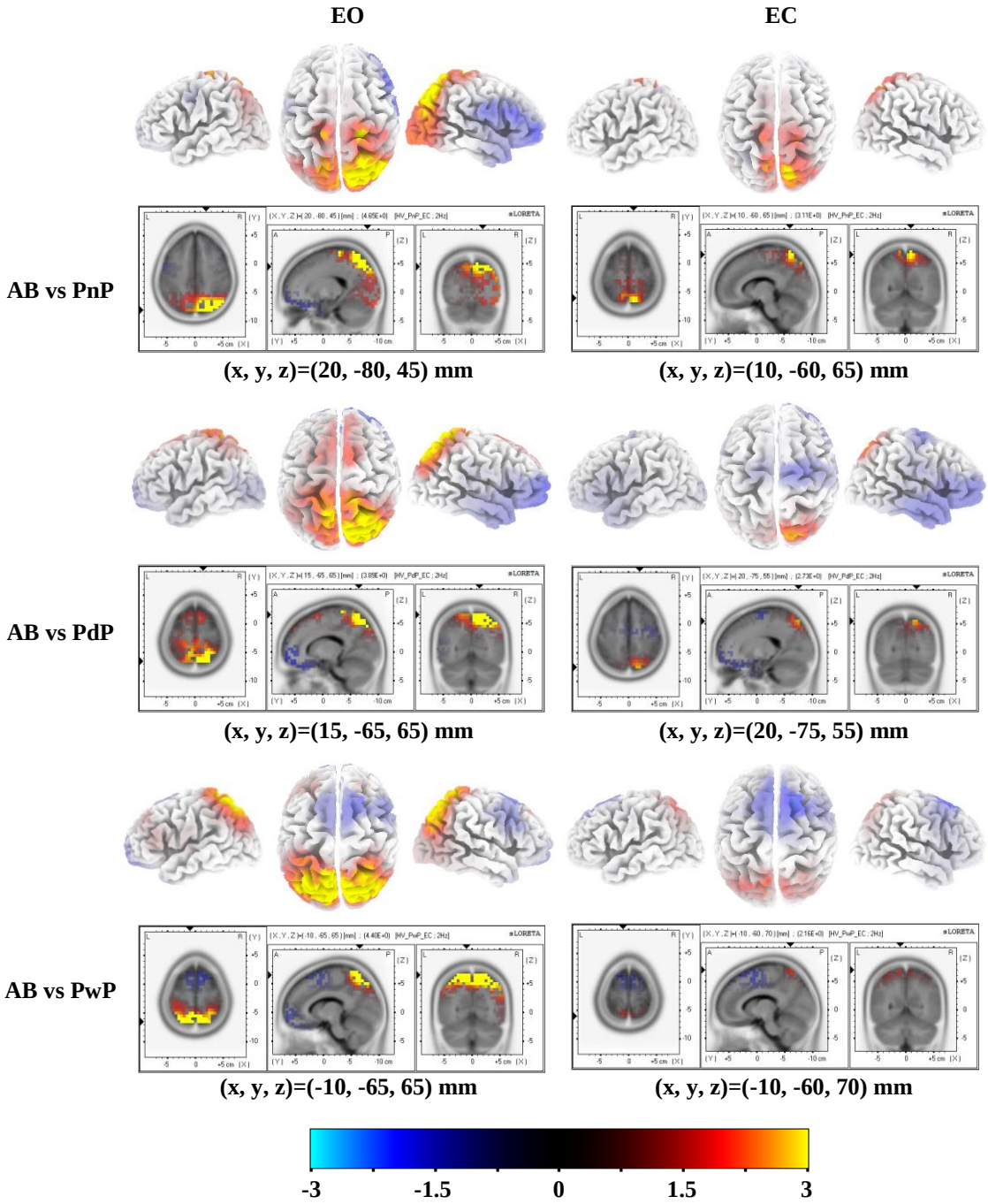


**Figure 4.18** sLORETA localisation for eyes open (EO) and eyes close (EC) relaxed state for able bodied (AB) group compared with patients groups: patients with no pain (PnP), patients developed CNP (PdP) and patients with CNP (PwP) in beta EEG frequency band (13-30Hz). The first raw of each figure represents 3D map of the localisation while the second raw represents the 3D slice at the displayed of the voxel with negative or positive strongest activity. The (x, y, z) under each figure represent the Montreal Neurological Institute and Hospital (MNI) coordinate system of the voxel with strongest activity.

## 4.4.4 Induced EEG during Motor Imagery (MI) Tasks

### *4.4.4.1 Analysis of ERD/ERS for all Groups at Representative Electrodes*

The ERD/ERS maps were averaged across all participants and trials for each group (AB, PnP, PdP and PwP) over three electrode locations, which are located over the primary cortex of the left hand (C4), feet (Cz) and right hand (C3), and are shown in Figure 4.19. The ERD/ERS maps were analysed at Cz for MI of feet, at C4 for MI of the left hand and at C3 for MI of the right hand. Negative values (blue color) represent the ERD, i.e. activation while positive values (red color) represent ERS, i.e. deactivation. The statistically significant differences among all four groups are shown in Figure 4.19 in the column furthest to the right. At approximately 0.3 s after both warning (t=-1) and execution (t=0) cues, the ERS can be noticed in all groups and all conditions at low frequency which is possibly related to the visual processing of a sensory input. At approximately 0.5 s after the MI execution cue, ERDs can be noticed for all groups and all conditions. PwP show a large ERD which spreads over most frequency bands in the first second post cue at C3 and C4 electrode locations but it is only sustained until t=1s. For t >1s, ERD can be noticed in alpha and beta bands. This activation pattern for PwP is characteristic for the electrode location rather than for a task and also exists at C3 and C4 for MI of feet as shown in Figure 4.21, Figure 4.22 and Figure **4.23**. PdP also show larger ERD expanding over a wide frequency range, sustained throughout the whole trial in the alpha and lower beta range. The largest difference between PdP and PnP can be noticed in the higher beta band at 20 to 30 Hz and time window 0.5 to 1.5 s for each of three conditions of MI. As shown in Figure 4.19, the ERD/ERS comparisons between each pair of groups (AB vs. PnP, AB vs. PdP, and AB vs. PwP) over Cz for F MI, C4 for LH MI and C3 for RH MI are shown in Figure 4.20.

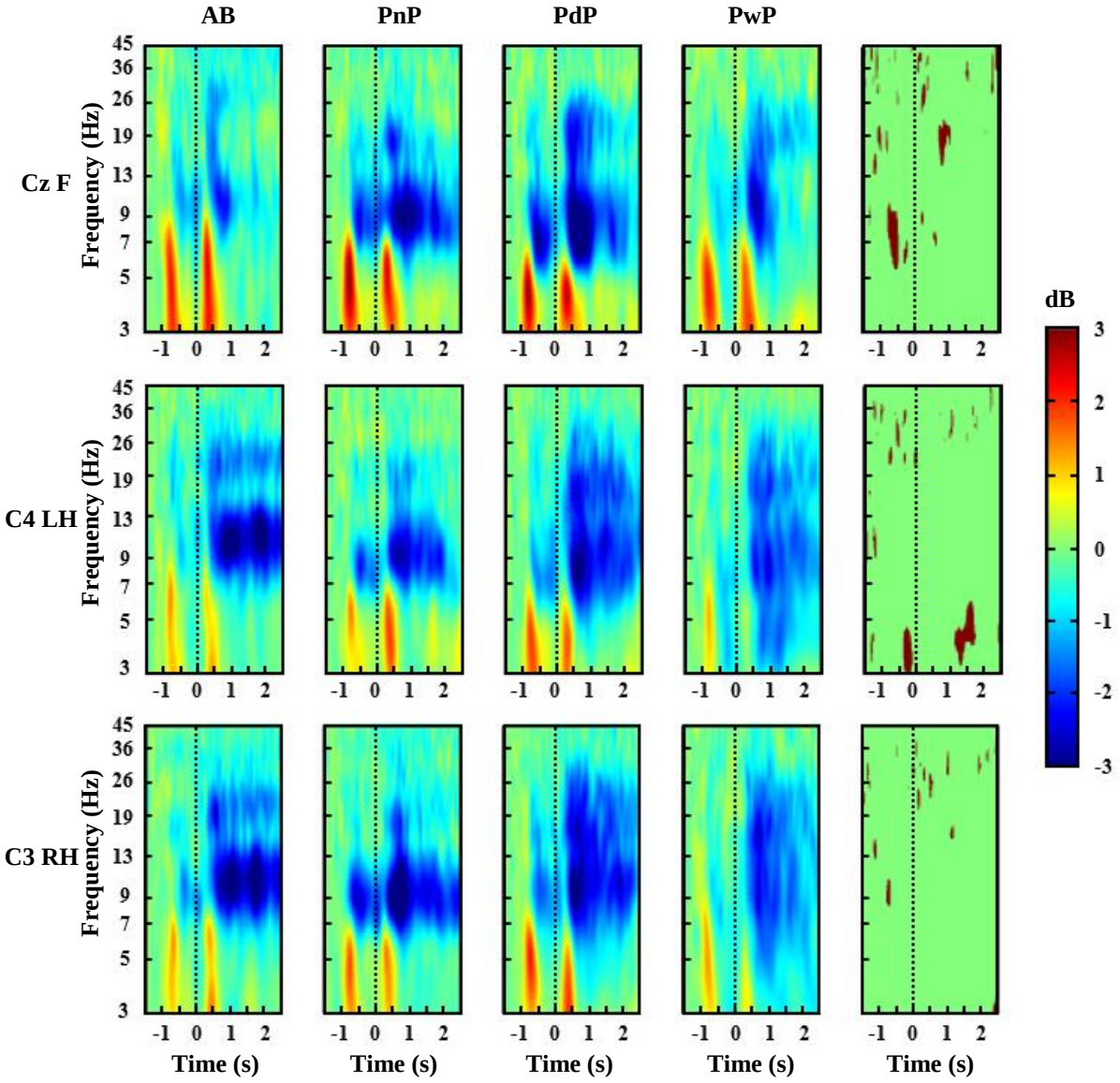


**Figure 4.19** ERD/ERS maps of electrode locations Cz for F: feet, C4 for LH: left hand and C3 for RH: right hand averaged across all participants and trials in each group (AB: able bodied, PnP: patients with no pain, PdP: patients developed pain and PwP: patients with pain) during MI task. The statistical significant differences among all four groups are shown on the last right column (p = 0.05). At t=-1 s, a warning cross appears, while at t=0 s (the vertical dashed line) participants start with motor imagery. The ERD/ERS maps are shown for t= -1.5 s to 2.5 s and frequency 3 Hz to 45 Hz.

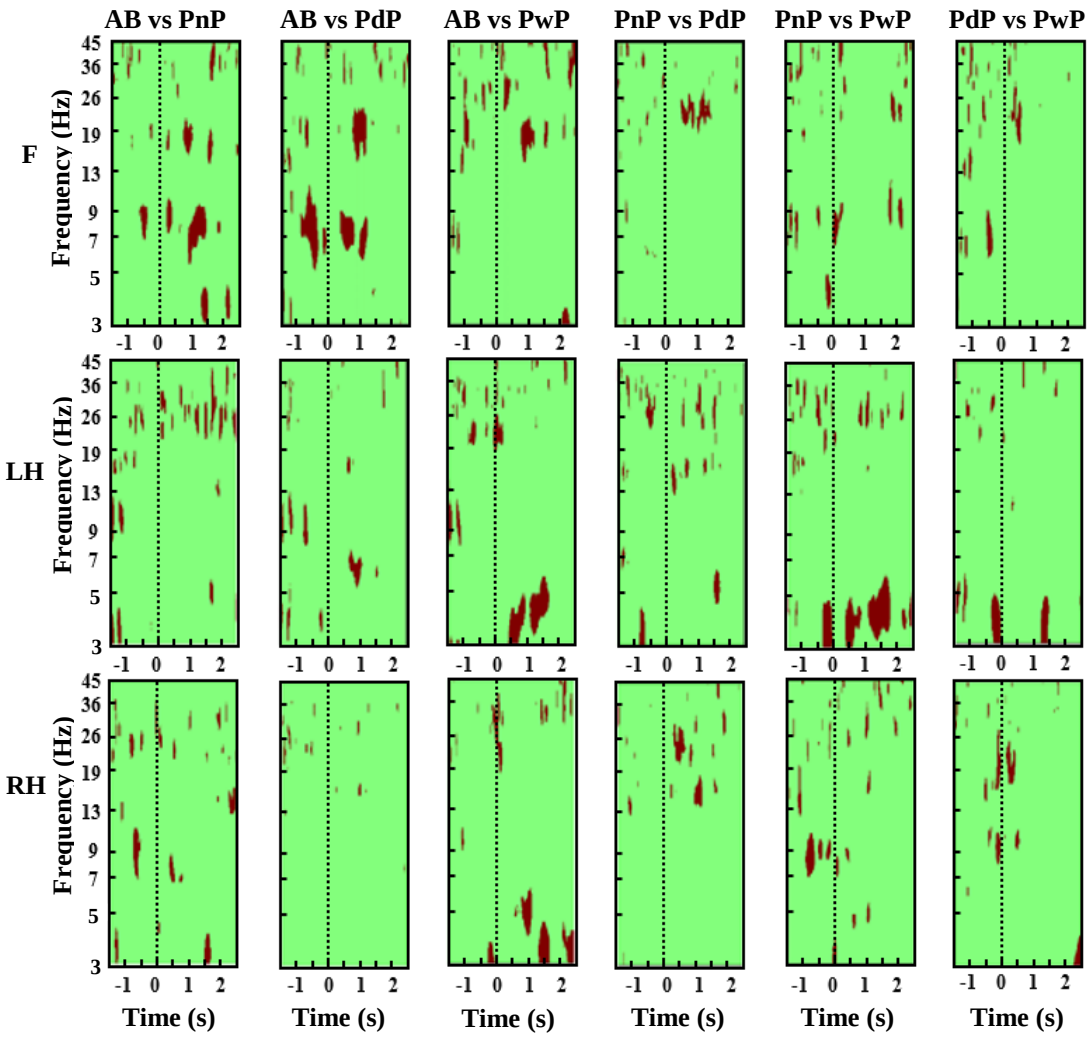


**Figure 4.20** ERD/ERS comparisons between each pair of groups (AB vs. PnP, AB vs. PdP, and AB vs. PwP) over Cz for F: foot, C4 for LH: left hand and C3 for RH: right hand during MI task. At t=-1 s, a warning cross appears, while at t=0 s (the vertical dashed line) participants start with motor imagery. The statistically significant differences were calculated using non-parametric ANOVA with p value =0.05. The ERD/ERS maps are shown for t= -1.5 s to 2.5 s and frequency 3 Hz to 45 Hz.

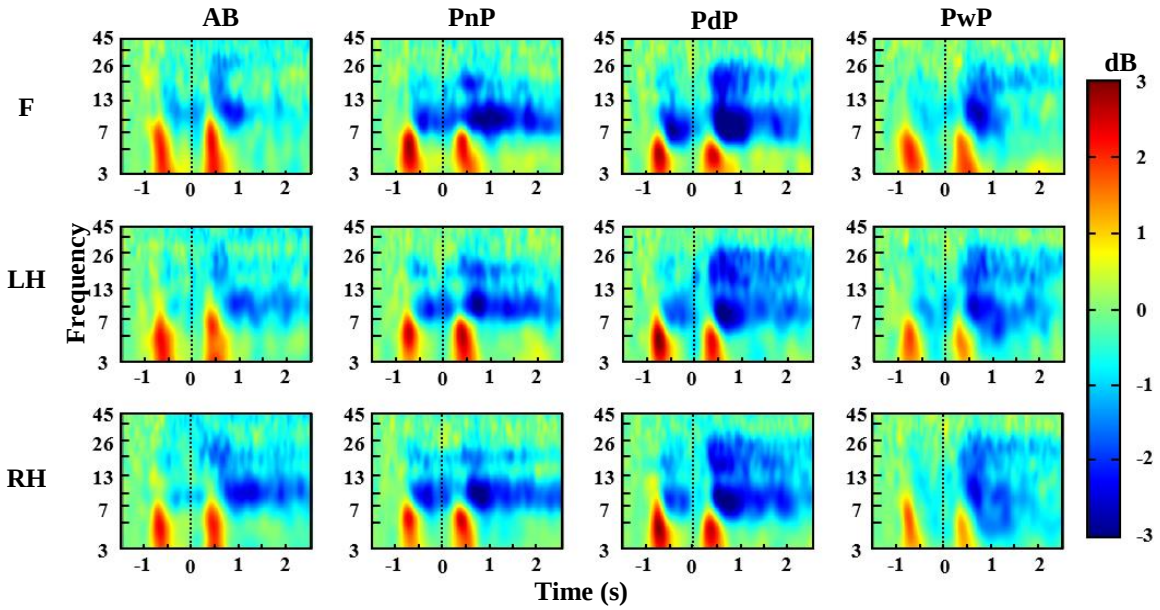


**Figure 4.21** ERD/ERS maps of electrode locations Cz for F: feet, LH: left hand and RH: right hand averaged across all participants and trials in each group (AB: able bodied, PnP: patients with no pain, PdP: patients developed pain and PwP: patients with pain) during MI task. At t=-1 s, a warning cross appears, while at t=0 s (the vertical dashed line) participants start with motor imagery. The ERD/ERS maps are shown for t= -1.5 s to 2.5 s and frequency 3 Hz to 45 Hz.

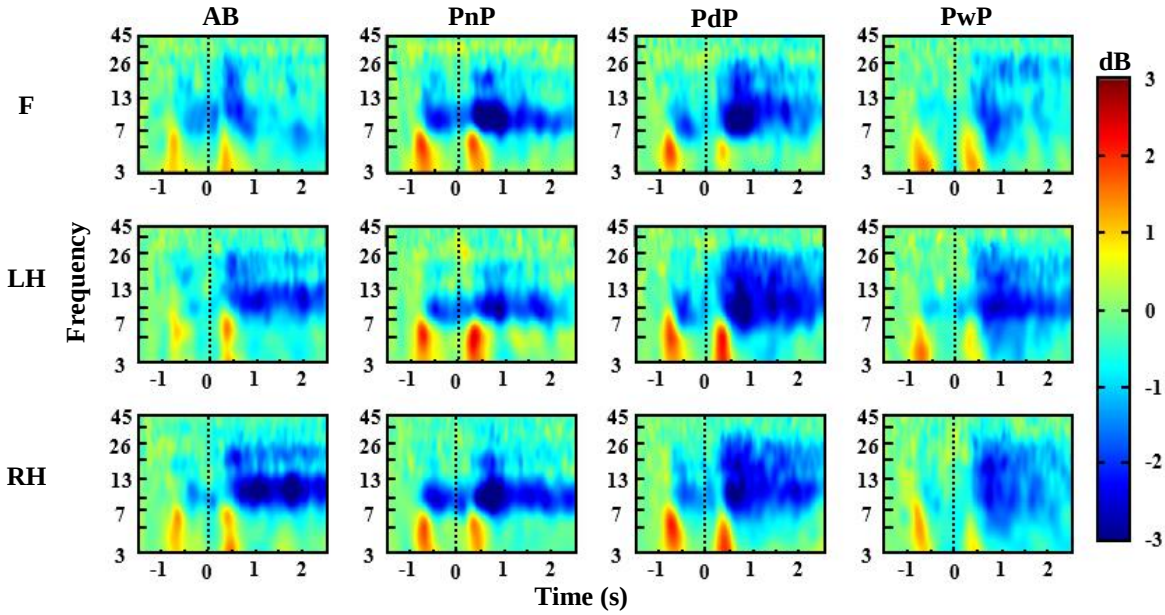


**Figure 4.22** ERD/ERS maps of electrode locations C3 for F: feet, LH: left hand and RH: right hand averaged across all participants and trials in each group (AB: able bodied, PnP: patients with no pain, PdP: patients developed pain and PwP: patients with pain) during MI task. At t=-1 s, a warning cross appears, while at t=0 s (the vertical dashed line) participants start with motor imagery. The ERD/ERS maps are shown for t= -1.5 s to 2.5 s and frequency 3 Hz to 45 Hz.

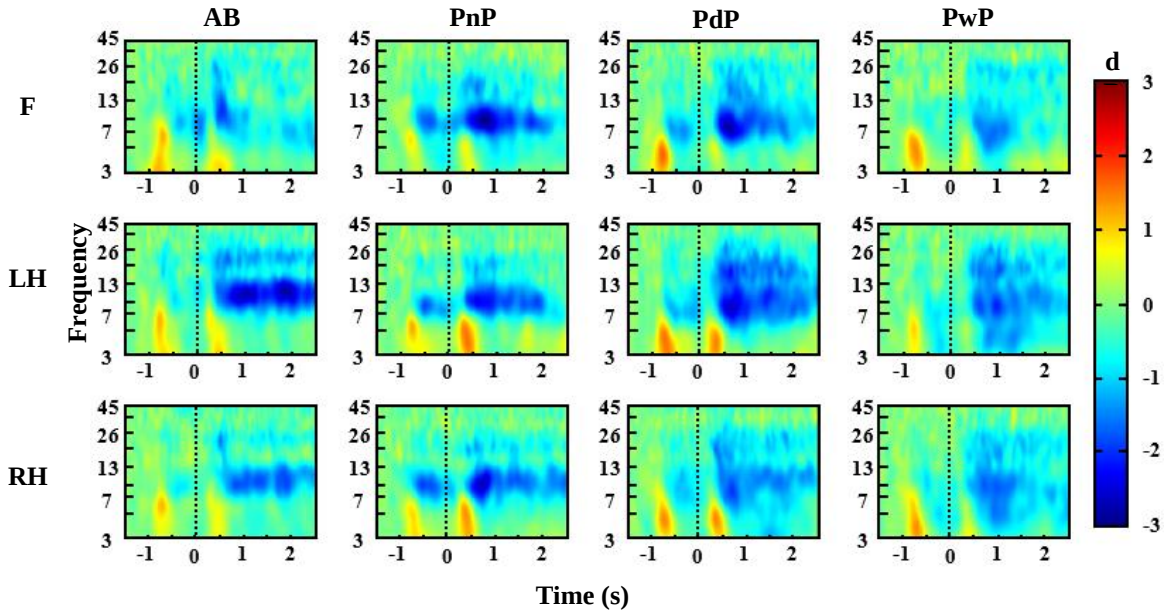


**Figure 4.23** ERD/ERS maps of electrode locations C**4** for F: feet, LH: left hand and RH: right hand averaged across all participants and trials in each group (AB: able bodied, PnP: patients with no pain, PdP: patients developed pain and PwP: patients with pain) during MI task. At t=-1 s, a warning cross appears, while at t=0 s (the vertical dashed line) participants start with motor imagery. The ERD/ERS maps are shown for t= -1.5 s to 2.5 s and frequency 3 Hz to 45 Hz.

### *4.4.4.2 Comparison of ERD/ERS Scalp Maps between PnP and PdP*

In this section a detailed comparison of ERD/ERS between PnP and PdP groups will be presented. ERD/ERS scalp maps are compared separately for each frequency band, theta (4-8Hz), alpha (8-12Hz), beta SMR (16-24Hz) and beta (20-30Hz) over a time window between t=0.5 to 1.5s. Results are shown in Figure 4.24, Figure **4.25**, Figure **4.26** and Figure **4.27**, respectively. In the theta band, significant differences were noticed over C5, CP1, CP3 and CP5 during LH MI. No statistical difference between the PnP and PdP groups was found in the alpha band, Figure 4.25. In the beta SMR band, significant differences were found over C3, CP5 and CP3 during MI of LH and over F3, FC3, FC5 and T7 during MI of RH Figure 4.26. The largest difference between the PnP and PdP groups is noticed in the beta band during MI of the left hand over premotor, motor, and sensory cortices ipsilateral to the MI task (Figure 4.27). As corresponding to Figure 4.27, Cp3 electrode location has been chosen because it shows the largest difference in ERD/ERS between PnP and PdP compared to other electrode locations. The ERD/ERS map over Cp3 electrode location for PnP and PdP groups during the three MI conditions

are shown in Figure 4.28. The strongest ERD is noticed in Theta (4 to 8 Hz) and beta (20 to 30 Hz) specifically during motor imagery of the left hand (LH) at time 0.5 to 1.5s.

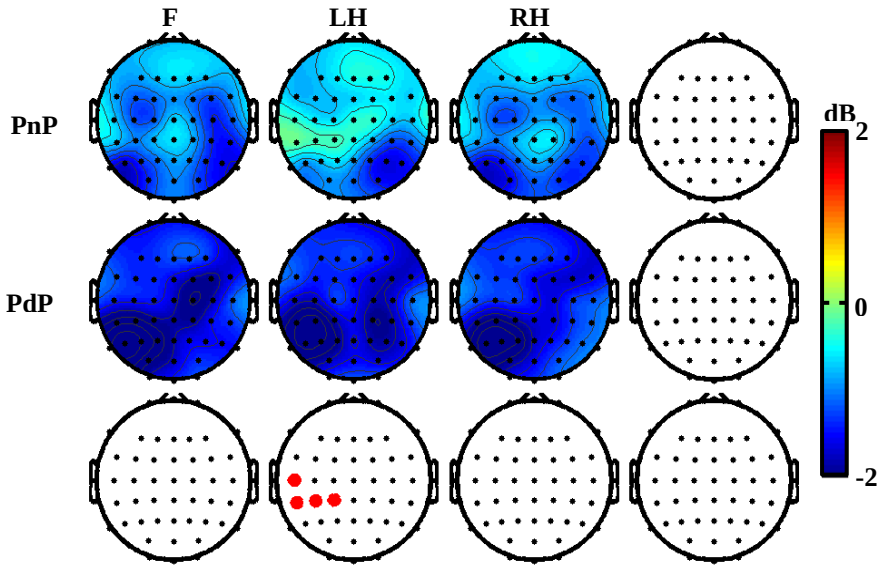


**Figure 4.24** The comparison of scalp maps based on ERD/ERS between PnP and PdP groups. The cortical activity averaged in theta (4-8Hz) frequency band and over 0.5 to 1.5 s and for MI of F, LH and RH. The statistical significant differences between the groups are shown on the last bottom raw while the statistical significant differences among the conditions within the same group are shown on the last right column (p = 0.05). All statistical results without FDR correction.

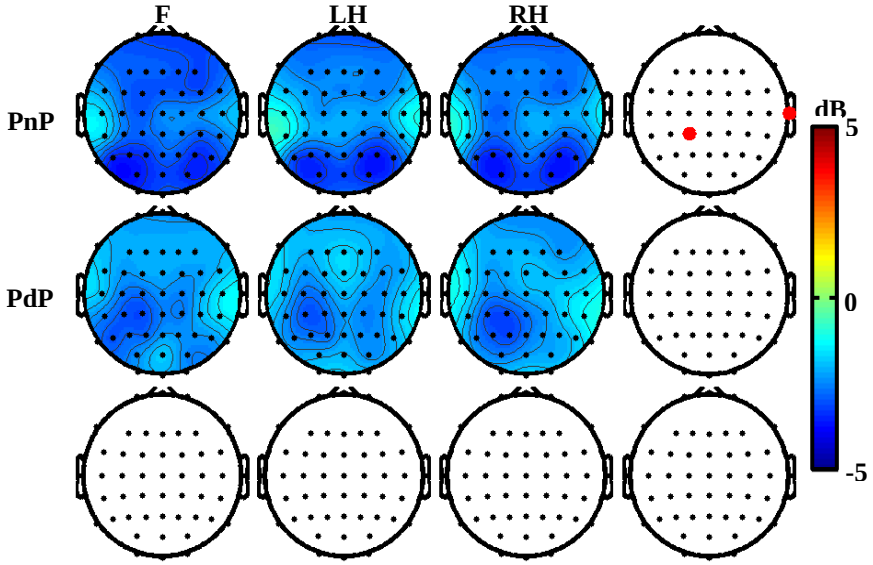


**Figure 4.25** The comparison of scalp maps based on ERD/ERS between PnP and PdP groups. The cortical activity averaged in alpha (8-12Hz) frequency band and over 0.5 to 1.5 s and for MI of F, LH and RH. The statistical significant differences between the groups are shown on the last bottom raw while the statistical significant differences among the conditions within the same group are shown on the last right column (p = 0.05). All statistical results without FDR correction.

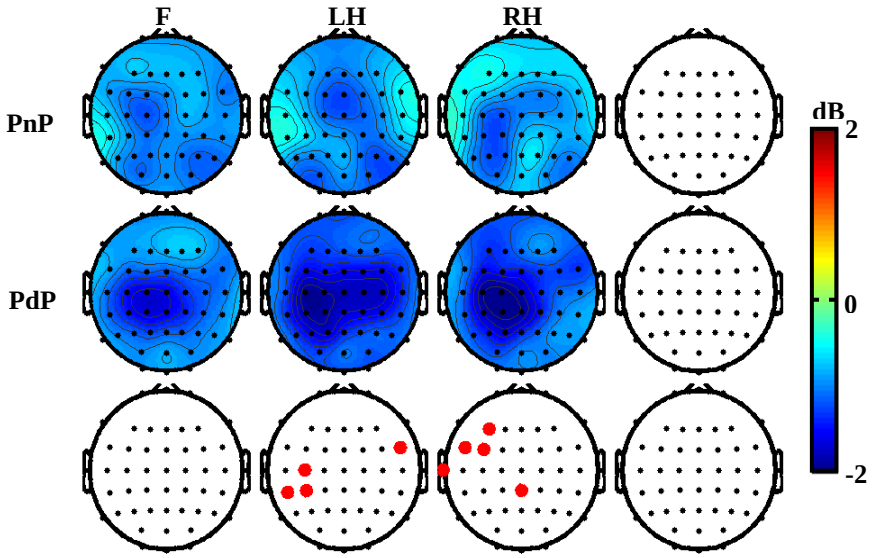


**Figure 4.26** The comparison of scalp maps based on ERD/ERS between PnP and PdP groups. The cortical activity averaged in beta SMR (16-24Hz) frequency band and over 0.5 to 1.5 s and for MI of F, LH and RH. The statistical significant differences between the groups are shown on the last bottom raw while the statistical significant differences among the conditions within the same group are shown on the last right column (p = 0.05). All statistical results without FDR correction.

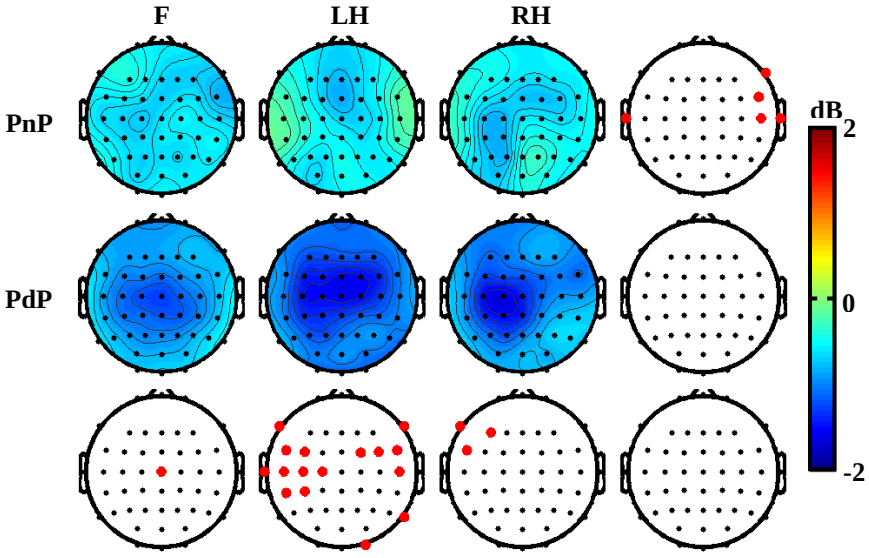


**Figure 4.27** The comparison of scalp maps based on ERD/ERS between PnP and PdP groups. The cortical activity averaged in beta 20-30Hz frequency band and over 0.5 to 1.5s and for MI of F, LH and RH. The statistical significant differences between the groups are shown on the last bottom raw while the statistical significant differences among the conditions within the same group are shown on the last right column (p = 0.05). All statistical results without FDR correction.

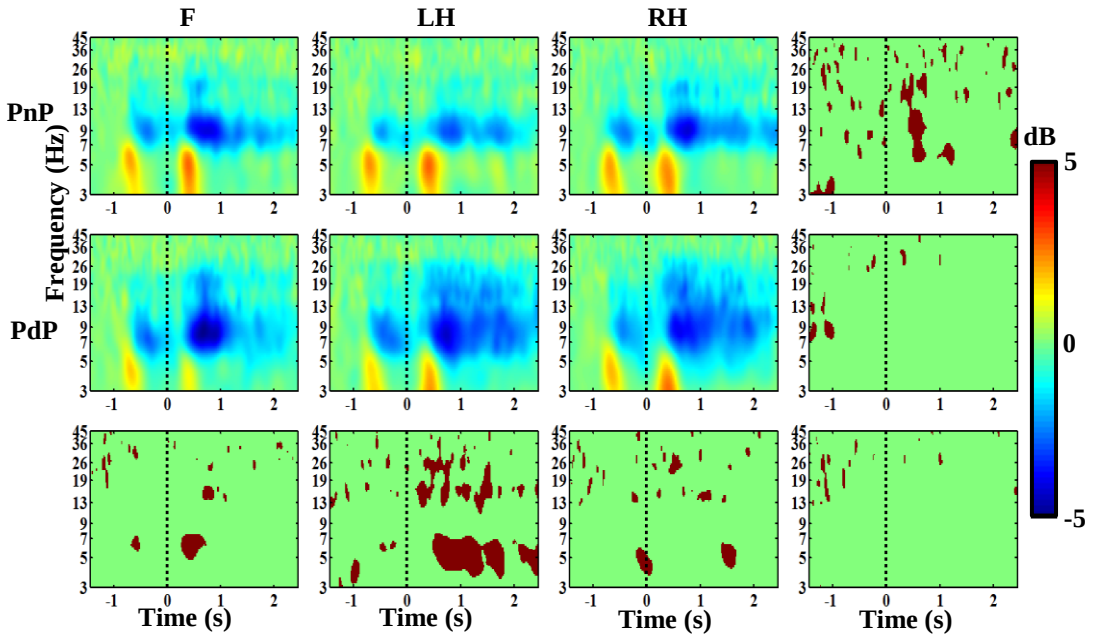


**Figure 4.28** ERD/ERS maps of electrode locations Cp3 for F: feet, LH: left hand and RH: right hand averaged across all participants and trials in each group (PnP: patients with no pain and PdP: patients developed pain) during MI task. The statistical significant differences between the two groups are shown on the last bottom raw while the statistical significant differences among the conditions within the same group are shown on the last right column (p = 0.05). At t=-1 s, a warning cross appears, while at t=0 s (the vertical dashed line) participants start with motor imagery. The ERD/ERS maps are shown for t= -1.5 s to 2.5 s and frequency 3 Hz to 45 Hz.

### *4.4.4.3 Statistical Analysis of Differences in ERD/ERS Maps Between all Groups*

In this section ERD/ERS maps in theta, alpha and beta bands were compared between each pair of groups. Results show only electrode locations of statistically significant differences rather than original ERD/ERS scalp maps.

The comparison of scalp maps based on ERD/ERS between each pair of groups and for all three MI conditions averaged over theta (4-8Hz), alpha (8-12Hz), beta SMR (16-24Hz) and higher beta (20-30Hz) frequency bands and over a time window 0.5 to 1.5s are shown in Figure 4.29, 4.30, Figure 4.31 and Figure 4.32, respectively. In the theta band, the difference between AB and PnP was noticed over Fc3, C4, C6, P5 and P7 electrode

locations during MI of feet, while between AB and PdP it was found over Cp3, Cp5 and P3 electrode locations during MI of the left hand (Figure 4.29). No difference was noticed between AB vs PwP, PnP vs PwP and PdP and PwP groups. In the alpha band, the largest differences were found during MI of feet (paralysed limbs in all patients). PnP exhibited the largest difference over the most electrode locations, particularly over the frontal, parietal and occipital region compared to the AB group. Compared to the AB group, PdP also showed statistical differences over several frontal electrode locations (Fp1, Fpz and Fp2) and over the parieto-occipital area (Cp1, Cp2, Cp3, Pz, P1 and P5). The comparison between patient groups shows that PwP had the largest difference over frontal (Fpz, Fz, F1, F2, F4, F8 and Fc4) parietal (P3, P5 and P7) and occipital area (Poz, Po3, Oz, and O1) during MI of feet compared to the PnP group. No difference between PnP and PdP was found. For the beta SMR frequency band the largest difference was noticed between AB and PdP over central and parieto-occipital regions during MI of feet; between PnP and PdP over C3, Cp3 and Cp5 during MI of left hand; and over T7, Fc3, Fc5, F3, and Cpz during MI of right hand (Figure 4.31). In the beta band as mentioned previously, the largest difference was noticed between PnP and PdP during MI of the left hand over the premotor, motor, and sensory cortices ipsilateral to the MI task.

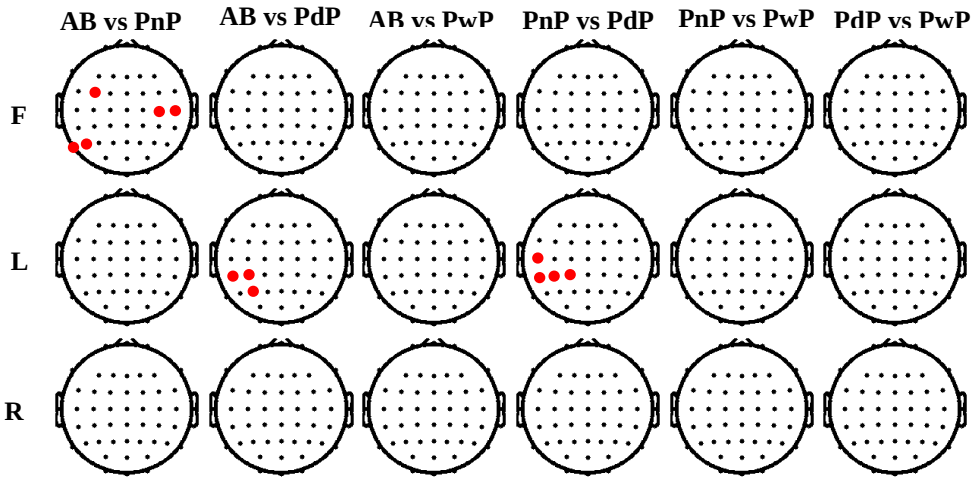


**Figure 4.29** The comparison of scalp maps based on ERD/ERS between each pair of groups and for all conditions of cortical activity averaged in theta (4-8Hz) frequency band and over 0.5 to 1.5s. The electrode locations with statistical significant differences are shown in red dots (p = 0.05).

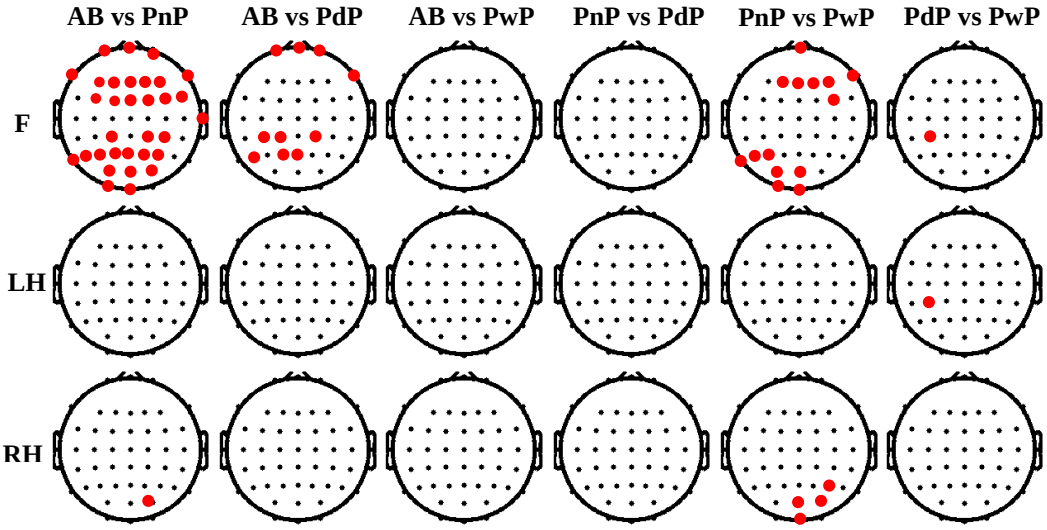


**Figure 4.30** The comparison of scalp maps based on ERD/ERS between each pair of groups and for all conditions of cortical activity averaged in alpha (8-12Hz) frequency band and over 0.5 to 1.5s. The electrode locations with statistical significant differences are shown in red dots (p = 0.05).

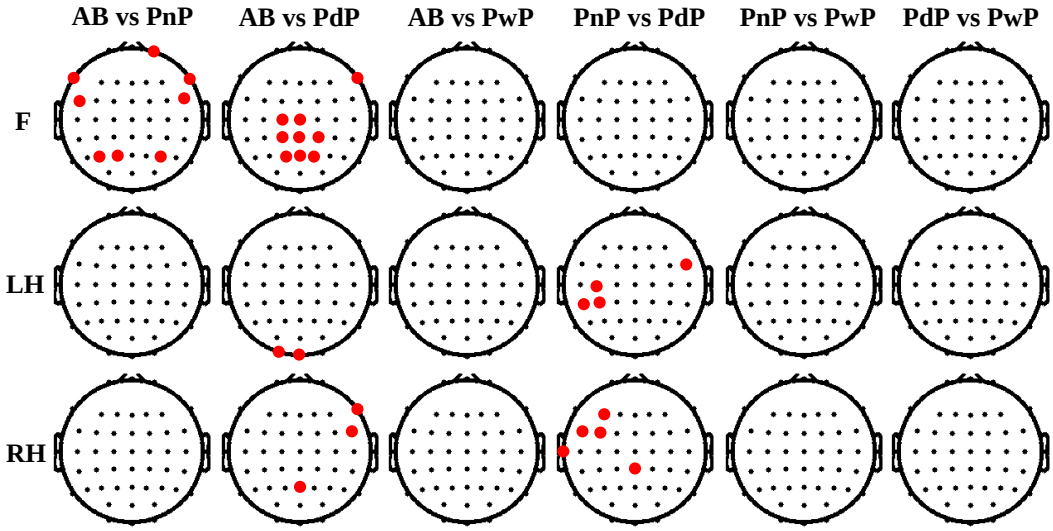


**Figure 4.31** The comparison of scalp maps based on ERD/ERS between each pair of groups and for all conditions of cortical activity averaged in beta SMR (16-24Hz) frequency band and over 0.5 to 1.5s. The electrode locations with statistical significant differences are shown in red dots (p = 0.05).

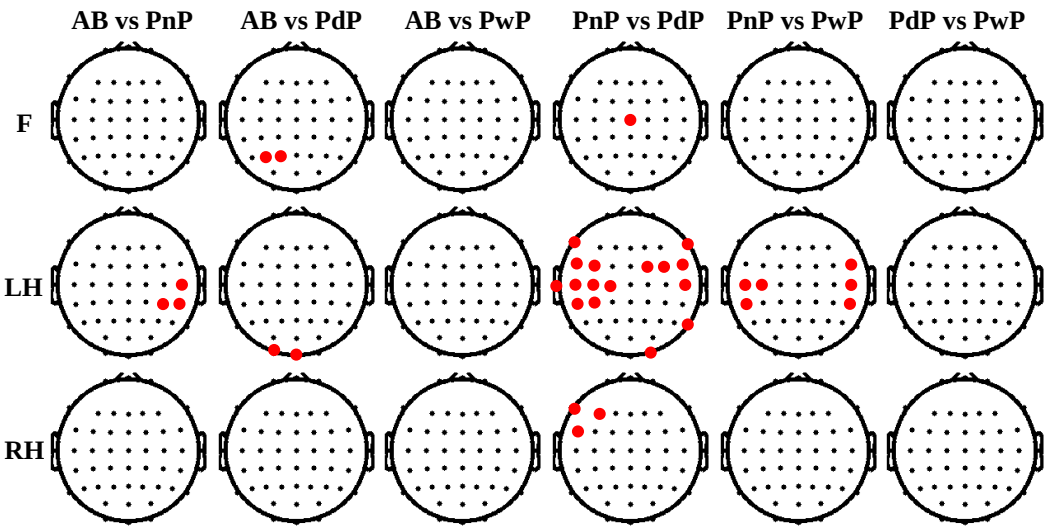


**Figure 4.32** The comparison of scalp maps based on ERD/ERS between each pair of groups and for all conditions of cortical activity averaged in higher beta (20-30Hz) frequency band and over 0.5 to 1.5s. The electrode locations with statistical significant differences are shown in red dots (p = 0.05).

### 4.4.5 Spatio-temporal Dynamics of ERD/ERS during MI task

The changes of cortical activity during a motor imagery task (MI) as a function of time can be visualized as spatio-temporal patterns of ERD/ERS. To achieve this, ERD/ERS in a selected frequency band were calculated over 0.5s time windows ranging from 0.5s to 3s. This time range covers the early onset of ERD at t=0.5s and last till the end of imagined movement at t=3s. The purpose of this analysis is to visually compare time-course and lateralization of ERD between different groups for all three frequency bands. Under time-course, one considers the duration of visible ERD while lateralization describes the intensity of ERD contralateral to the hand that performed MI. In case of the right hand shown here, ERD should be stronger on the left side of the cortex. This analysis is informative of the effect of paralysis and presence of CNP[140] on spatio-temporal dynamics of ERD.

### 4.4.5.1 Spatio-temporal Dynamics of Theta Band ERD/ERS

The spatio-temporal changes of the cortical activity of all groups during motor imagery of the right hand (a dominant hand for all participants) for different frequency bands (theta 4-8Hz, alpha 8-12Hz, beta SMR 16 to 24Hz and beta 20-30Hz) are shown in Figure 4.33, Figure **4.34**, Figure **4.35**, and Figure **4.36**, respectively. In the theta band (4-8 Hz), all patient groups exhibit stronger ERD than AB at the period 0.5 to 1.0s, particularly over central, parietal and occipital areas, as shown in Figure 4.33. The strongest and most widespread ERD is noticed in the PdP group. The ERD of the PdP and PwP groups lasted longer than in AB and PnP, over the central-parietal areas of the right hemisphere. No particular lateralization pattern could be observed.

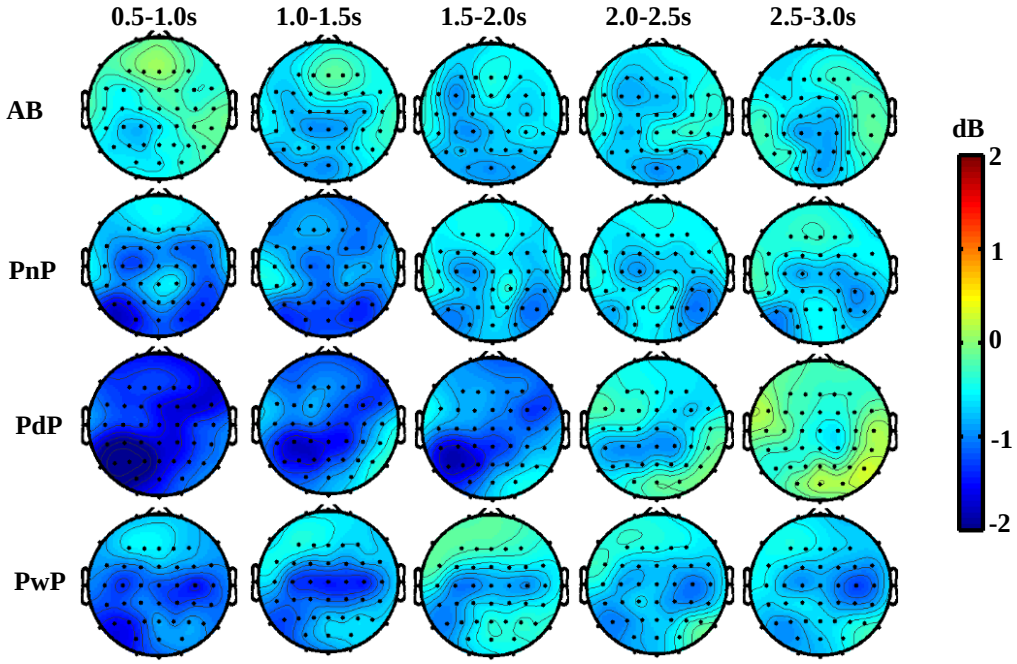


**Figure 4.33** The changes of scalp maps based on ERD/ERS with time (from t=0.5s post the MI cue till t=3s the end of the MI trial and with time window 0.5 s) in all four groups (AB: able bodied, PnP: Patients with no pain, PdP: patients developed pain and PwP: patients with pain) and for **Theta (4-8Hz)** during motor imagery of the **RH: right hand**.

### 4.4.5.2 Spatio-temporal Dynamics of Alpha Band ERD/ERS

In the alpha band (8-12 Hz), all three patient groups show stronger widespread ERD compared to AB in a time period 0.5 to 1.0s post cue (Figure 4.34). However, the PdP group shows distinctive ERD over the central area of the cortex compared to PnP and PwP,

which was lateralised over the contralateral cortex. The ERD in the PnP group is sustained longer than in the PdP and PwP groups but it is not lateralised as it can be observed on both hemispheres. The AB group also exhibited typical ERD dominantly located over the central area of the cortex in the left hemisphere which is contralateral to the motor imagery task (RH).

#### *4.4.5.3 Spatio-temporal Dynamics of Beta Band ERD/ERS*

In the beta SMR band (16 to 24Hz), PdP and PwP have the stronger ERD compared to AB and PnP at the time interval between t=0.5 to 2.0s (Figure 4.35). PdP and PwP also show sustained and lateralised ERD compared to the PnP group of the same beta SMR band and compared to their ERD in the alpha band (Figure 4.34). PnP only has strong ERD in a period 0.5 to 1.0s without clear lateralisation. The ERD in PnP group ceases shortly after the first second. AB, PdP and PwP show more sustained ERD until the end of the MI trial at t=3s. The AB group also shows particularly strong lateralised ERD over the cortical area that represents the right hand. In the beta band (20-30Hz), PdP exhibited stronger ERD compared to other groups (Figure 4.36). The ERD of PdP is not only stronger but also lasted longer than the trial over the central areas of the left hemisphere. Similar to the alpha and beta SMR band, the AB group had typical ERD dominantly located over the central area of the cortex in the left hemisphere which is contralateral to the motor imagery task (RH). The lowest ERD was noticed in the PnP group. PwP exhibited widespread beta activity which lasted longer until the end of the MI trial at t=3s.

In summary, judging by the scale of the side bar, the intensity of ERD for all groups was strongest for alpha band and the overall difference in ERD between PnP and PdP was strongest in beta (20-30 Hz) band in a period t=0.5 to 1s.

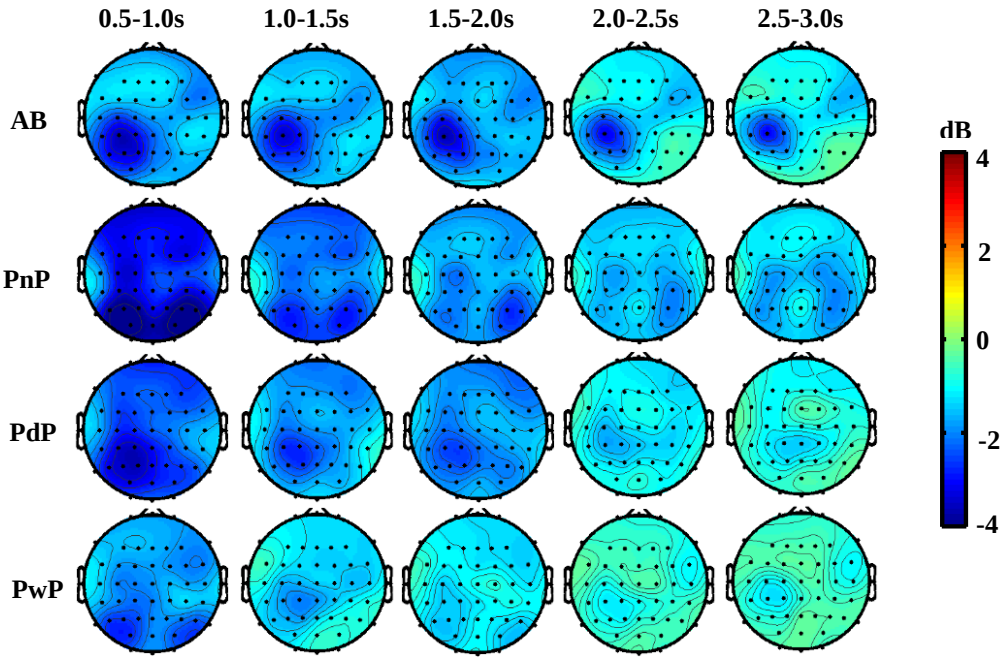


**Figure 4.34** The changes of scalp maps based on ERD/ERS with time (from t=0.5s post the MI cue till t=3s the end of the MI trial and with time window 0.5 s) in all four groups (AB: able bodied, PnP: Patients with no pain, PdP: patients developed pain and PwP: patients with pain) and in **Alpha (8-12Hz)** during motor imagery of the **RH: right hand**.

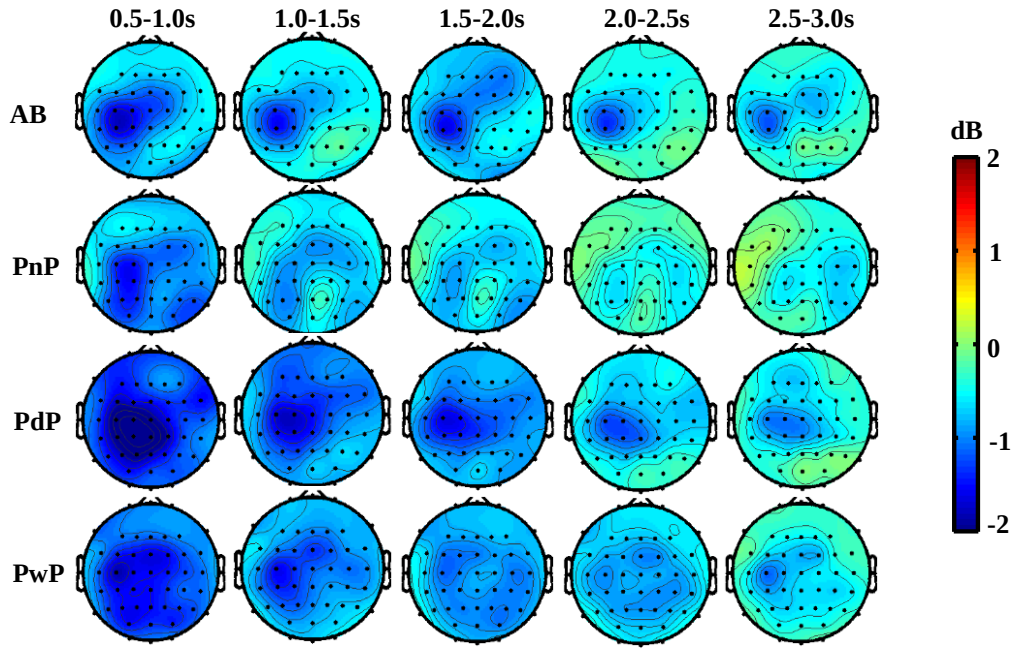


**Figure 4.35** The changes of scalp maps based on ERD/ERS with time (from t=0.5s post the MI cue till t=3s the end of the MI trail and with time window 0.5 s) in all four groups (AB: able bodied, PnP: Patients with no pain, PdP: patients developed pain and PwP: patients with pain) and in **beta SMR (16-24 Hz**) during motor imagery of the **RH: right hand**.

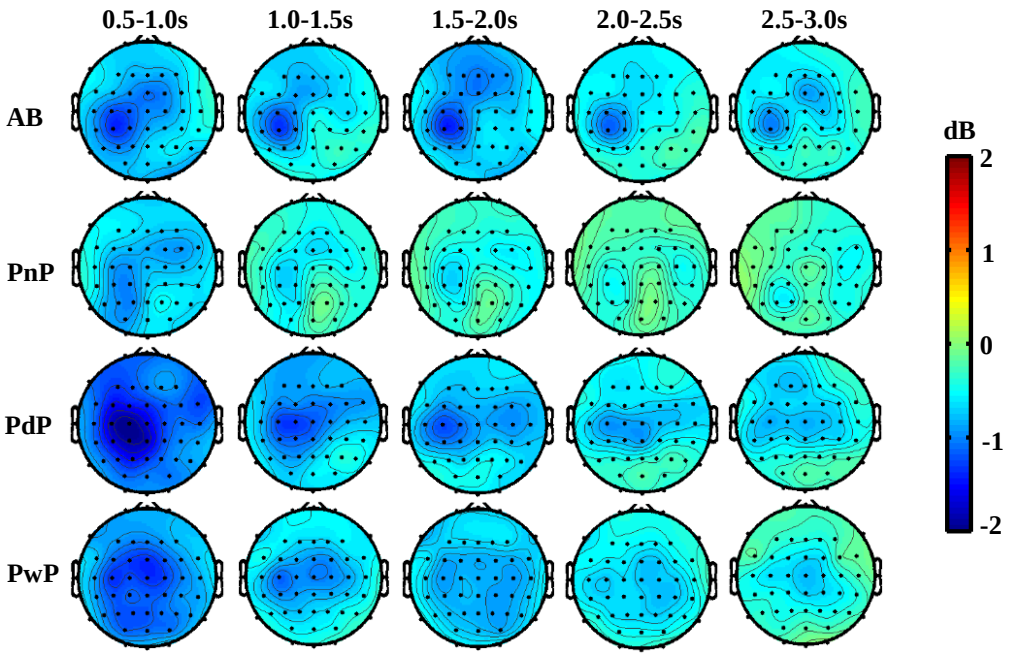


**Figure 4.36** The changes of scalp maps based on ERD/ERS with time (from t=0.5s post the MI cue till t=3s the end of the MI trial and with time window 0.5 s) in all four groups (AB: able bodied, PnP: Patients with no pain, PdP: patients developed pain and PwP: patients with pain) and in **beta (20-30 Hz)** during motor imagery of the **RH: right hand**.

### 4.4.6 sLORETA Comparison of the Cortical Activity Between Groups During MI Tasks

The comparison of the changes in the cortical activity during a motor imagery MI task between all four groups over a time window (t=0.5 to 1.5s) are shown in Figure 4.37 and Figure 4.38, and Figures A.4-A.9 (Appendix A). Only statistically significant results are shown in the main text. Figures A.4 and A.5 show results for the theta band (4-8Hz). Figure A.4 shows differences between AB and patient groups while Figure A.5 shows differences between 3 patient groups. In a similar manner, Figure 4.37 and Figure 4.38 show the alpha band, Figure A.6 and A.7 show beta SMR, and Figure A.8 and A.9 show the beta band. From the previous section, it can be observed that a time period t=0.5s to 1.5s corresponds to strongest ERD. A one second long time window was based on sLORETA analysis recommendations.

#### 4.4.6.1 sLORETA Comparison of the Cortical Activity Between Groups in the Theta Band During MI Task

Analysis of the activity in the theta band show no statistical significance (p=0.05) between groups, therefore all figures are presented in the Appendix A. In the theta band, AB shows higher activation over the parietal and occipital regions during MI of the feet and left hand compared to PnP group (Figure A.4). Group PdP exhibited higher theta activity over the frontal and central regions during all 3 MI conditions compared to AB group. Higher theta activity over the parietal region can be noticed in PwP compared to the AB group during MI of the left hand and right hand while during MI of the feet AB had higher theta activation over the frontal and central regions compared to PwP group (Figure A.4). Figure A.5 shows the comparison of the cortical activation during MI tasks between patient groups in the theta band. The comparison between PnP and PdP groups show that PdP had higher theta activity over the frontal, central and occipital regions and the highest activation can be noticed over the occipital region of the left hemisphere. PwP also shows high theta activity over the occipital region particularly in the left hemisphere (Figure A.5). It can also be noticed that PdP had higher activation over the frontal and central regions compared to the PwP group. Although these differences did not reach statistically significant level, they are worthwhile mentioning because strong theta ERD was considered a signature of CNP in patients with chronic SCI[140].

#### 4.4.6.2 sLORETA Comparison of the Cortical Activity Between Groups in the Alpha Band During MI Task

The results of comparing cortical activity in the alpha band (8-12Hz) between AB and each single patients group during MI tasks are shown in Figure 4.37. It can be noticed that the PnP group show higher widespread activation compared to the AB group particularly during MI of the feet. The AB group exhibited higher alpha activity over the right hemisphere occipital region during both right hand and left hand MI compared to both PdP

and PwP groups. Cross sections showing largest differences between the patients groups are shown in Figure 4.38. PnP group had higher occipital alpha activity compared to both PdP and PwP during all three MI conditions. The significant differences between the groups in the alpha band are shown in Table 4.5.

#### *4.4.6.3 sLORETA Comparison of the Cortical Activity Between Groups in the Beta Band During MI Task*

Beta band activity was compared in SMR band (16-24 Hz), most reactive to MI task, and for consistency with the remaining results also in beta (20-30 Hz) band, None of the difference between groups in neither beta bands reached the level of statistical significance (p=0.05), therefore all figures are presented in the Appendix A. In the beta SMR band (16-24Hz), PwP exhibited stronger activation compared to the AB group particularly during MI of the right hand over the central and occipital regions (Figure A.6). PnP and PdP also show higher beta SMR activation over the frontal and occipital regions compared to the AB group. The comparisons of the beta SMR activity between the patient groups are shown in Figure A.7. It can be noticed that PwP had higher activation compared to PnP over both the central and occipital regions. Higher beta SMR activity is also noticed over the central and occipital regions in PwP compared to the PdP group.

In the beta band (20-30Hz), PwP also shows the strongest activation over the central and occipital regions compared to the AB group specifically during MI of the right hand (Figure A.8). It can also be noticed that PdP has higher beta activity over the central and occipital regions during MI of the right hand and left hand compared to the AB group and PnP has lower activity over the occipital region during MI of the feet compared to AB. Comparisons between patient groups show that both PdP and PwP have higher beta activation compared to the PnP group over the central and occipital regions and PwP have the strongest beta activity (Figure A.9).

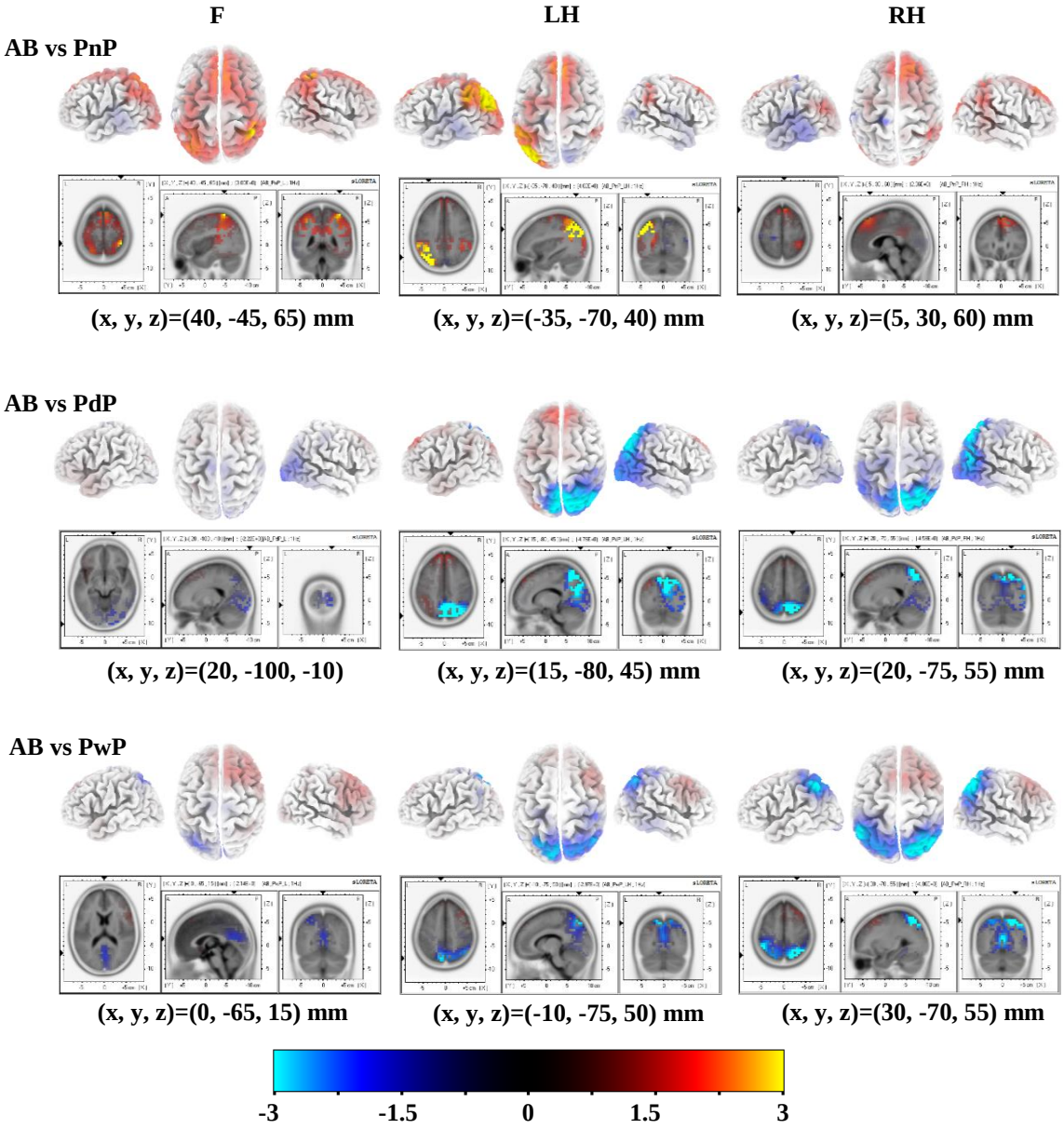


**Figure 4.37** sLORETA localisation for motor imagery (MI) during F: feet, LH: left hand and RH: right hand MI and for able bodied (AB) group compared with patients groups: patients with no pain (PnP), patients developed CNP (PdP) and patients with CNP (PwP) in alpha EEG frequency band (8-12Hz) over time window (0.5 to 1.5s). The first raw of each figure represents 3D map of the localisation while the second raw represents the 3D slice at the displayed of the voxel with negative or positive strongest activity. The (x, y, z) under each figure represent the Montreal Neurological Institute and Hospital (MNI) coordinate system of the voxel with strongest activity.

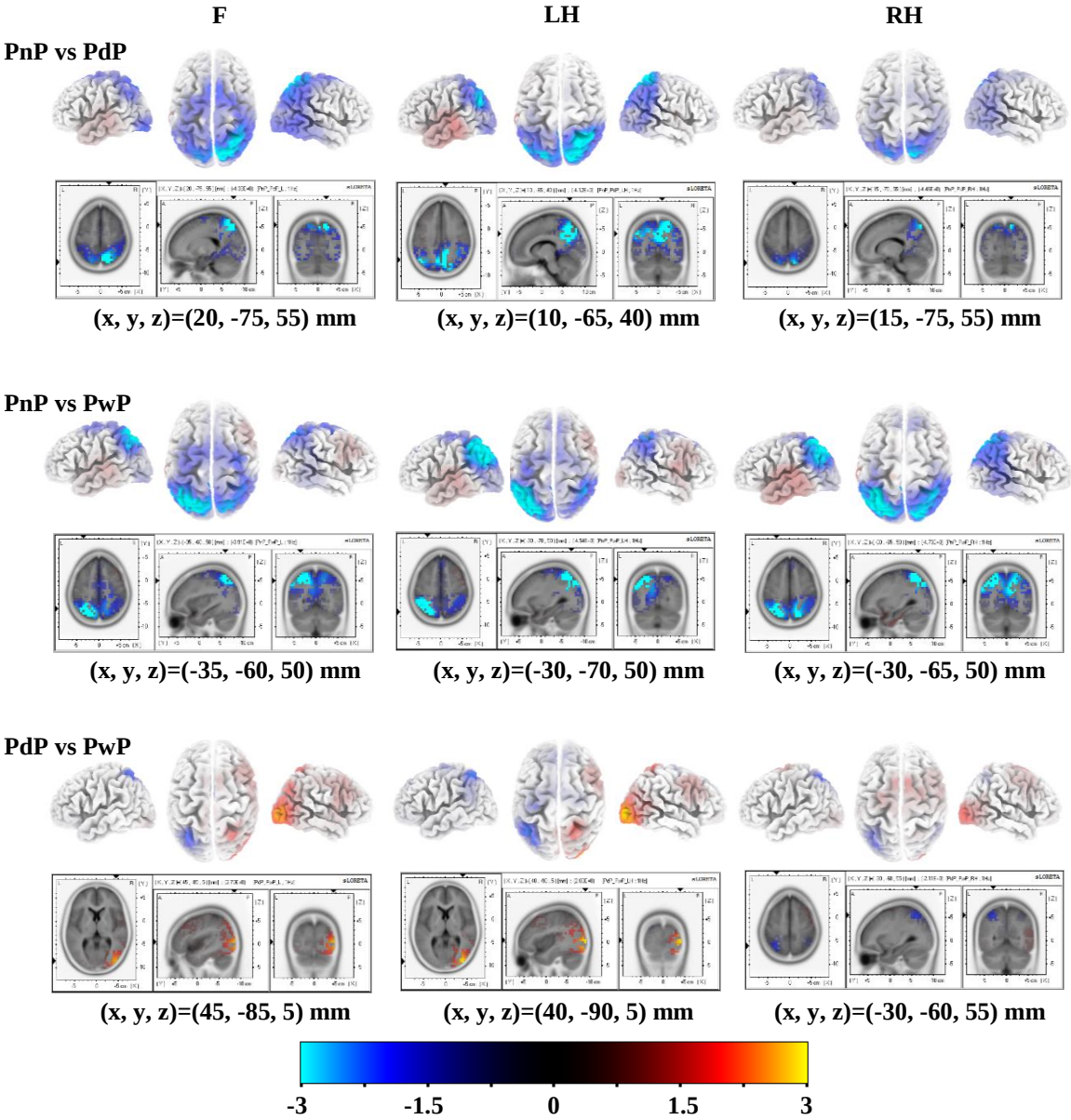


**Figure 4.38** sLORETA localisation for motor imagery (MI) during F: feet, LH: left hand and RH: right hand MI compared between the patients groups: patients with no pain (PnP), patients developed CNP (PdP) and patients with CNP (PwP) in alpha EEG frequency band (8-12Hz) over time window (0.5 to 1.5s). The first raw of each figure represents 3D map of the localisation while the second raw represents the 3D slice at the displayed of the voxel with negative or positive strongest activity. The (x, y, z) under each figure represent the Montreal Neurological Institute and Hospital (MNI) coordinate system of the voxel with strongest activity.

**Table 4.5:** Areas with significant differences in cortical activity between all 4 groups, in alpha (8-12Hz) EEG frequency band during MI tasks.

| Groups | MI task | Brain Lobe | BA | Brain Hemisphere | Number of Voxel | Voxel with maximum t value | | | |
|---|---|---|---|---|---|---|---|---|---|
| | | | | | | Statistics t-values | MNI Coordinate | | |
| | | | | | | | x | y | z |
| **AB vs PdP** | LH | Parietal | 7 | **R** | 32 | -4.76 | 15 | -80 | 45 |
| **AB vs PdP** | RH | Parietal | 7 | **R** | 18 | -4.58 | 20 | -75 | 55 |
| **AB vs PwP** | RH | Parietal | 7 | **R** | 1 | -4.06 | 30 | -70 | 55 |
| **PnP vs PdP** | F | Parietal | 7 | **R** | 6 | -4.37 | 20 | -75 | 55 |
| **PnP vs PdP** | LH | Parietal | 7 | **R** | 11 | -4.12 | 10 | -65 | 40 |
| **PnP vs PdP** | RH | Parietal | 7 | **R** | 6 | -4.46 | 15 | -75 | 55 |
| **PnP vs PwP** | F | Parietal | 7 | **L** | 5 | -3.91 | -35 | -60 | 50 |
| **PnP vs PwP** | LH | Parietal | 7 | **L** | 15 | -4.54 | -30 | -70 | 50 |
| **PnP vs PwP** | RH | Parietal | 7 | **L** | 27 | -4.73 | -30 | -65 | 50 |
| | | | 40 | **L** | 2 | -4.37 | -35 | -55 | 60 |

MNI: the Montreal Neurological Institute and Hospital (MNI) coordinate system. R, Right; L, Left. The brain hemisphere with bold font is the hemisphere with higher contribution in the number of significant voxel. F: feet, RH: right hand, LH: left hand. MI: motor imagery. BA: Brodmann area.

### 4.4.7 Summary of the results

EEG between three groups of patients and a group of able bodied people was compared during relaxed state and motor imagery task. In a relaxed, eyes open and eyes closed state, parameters such as EEG power in different frequency bands, the ratio of EEG power between eyes open and eyes closed states and the frequency of dominant alpha peaks were compared between groups, while during motor imagery tasks, the time-frequency analysis was computed and compared between groups.

The results of spontaneous EEG show that all three patient groups had a higher theta band PSD compared to the able bodied group and the highest theta band power was noticed in groups which already had pain (PwP), or have eventually developed pain (PdP). The statistically significant differences in theta band PSD (without correction of multiple comparisons) between all four groups was noticed in open eyes state over central, parietal and occipital regions. There were no significant differences between all groups in the alpha

and beta bands. In terms of the dominant alpha peak, both eyes opened and eyes closed relax states showed a similar tendency. A shift of the dominant alpha frequency towards a lower frequency was noticed in all patient groups compared to AB. The largest difference, over most of the 48 recorded electrodes, was found between PdP and AB during eyes closed state. EEG reactivity, which is an indicator of thalamo-cortical connectivity, was lower in the PdP group compared to the other three groups. A significantly lower EEG reactivity in PdP was noticed over most of the 48 electrode locations compared to the AB group and over 24 electrode locations (without correction of multiple comparisons) compared to the PnP group.

The results of sLORETA analysis of spontaneous EEG show that PdP and PwP had higher, though not statistically significant, theta activity compared to AB and PnP in the eyes closed state. In the alpha frequency band, AB and PnP exhibited significantly higher activity compared to PdP, and the PnP group also showed significantly higher alpha activity compared to PwP. Significantly higher beta activity was noticed in AB compared to patient groups. All statistically significant differences between groups in the alpha and beta bands were found in the parietal region, a part of the secondary sensory cortex. These results show that while some CNP signatures, such as lower dominant frequency, reduced reactivity and lower alpha power, are common to early and chronic CNP, as shown in literatures, other signatures of chronic CNP, such as higher theta power, are not so prominent in early CNP. These results provide us with an insight into the order of changes in EEG activity.

The results of the induced EEG compared event related desynchronisation/ synchronisation (ERD/ERS) scalp maps at time window t=0.5s to 1.5s and showed that PdP had significantly larger ERD in the theta, beta SMR and beta bands over the central area of the left hemisphere, particularly during MI of the left hand, compared to PnP. In the alpha band the significantly larger ERD over the frontal, parietal, and occipital regions was

noticed in PnP compared to AB and PwP during MI of the feet. The results of spatio-temporal analysis showed that PdP and PwP had larger and more widespread theta, beta SMR and beta ERD predominantly over the centro-parietal region of the left hemisphere, which last longer until the end of the motor imagery trial. The PnP group showed weaker beta band ERD which was not lateralised during motor imagery tasks compared to other groups.

The results of sLORETA analysis of induced EEG showed that alpha band desynchronisation is the best indicator of both future and present pain. In the alpha band, significantly higher activities were noticed in AB groups predominately over the parietal region of the right hemisphere compared to PdP and PwP during both right and left hand MI tasks. The PnP group also showed significantly higher alpha activity over the parietal region of the right hemisphere compared to PdP and over the left hemisphere compared to PwP during all thee MI tasks. Although PdP and PwP had more theta, beta SMR and beta power than PnP and AB, these results did not reach statistical significance.

## 4.5 Discussions

It is believed that SCI patients can experience CNP  weeks or even years after injury[26] and it has a severe impact on the patients' quality of life and health status[249,250]. Several animal model studies reported that the development of CNP can be avoided by preventive treatment in the early stages after SCI[255,256]. Therefore, defining reliable EEG predictors of CNP can lead to development of a preventive treatment. However, to the best of our knowledge, there is no published study defining an EEG predictor of CNP following SCI. The present study aims to define EEG predictors of CNP in sub-acute SCI patients who have not developed physical symptoms of CNP. To achieve this aim, the cortical EEG activities, recorded during relax state and during motor imagery tasks in three groups of SCI patients (PnP, PdP and PwP) as well as able bodied (AB) control group were

investigated and compared. The results of spontaneous EEG during EO and EC relaxed states will be discussed first followed by the results of induced EEG during motor imagery tasks. Worth to mention is that all but one patient in PdP group had no painful response to mechanical wind-up, which is believed to be an early predictor of CNP in SCI patients[20]. This indicates that changes in EEG occur before altered peripheral sensation. Thermal test was not applied in this study and it would be interesting to see whether changes in EEG precede changes in thermal sensation, which are also considered predictors of pain[205]. Testing EEG against thermal sensation would be maybe more relevant than mechanical stimulus test because of parallel neural pathways of pain and temperature sensations from periphery to the CNS.

### 4.5.1 Spontaneous EEG during EO and EC Relaxed States

In terms of EEG power, the largest differences between all 4 groups were noticed in the theta band (4-7Hz). In the theta (4-7Hz) band, in both EO and EC states, PdP and PwP had higher power compared to PnP and AB groups. Although higher theta power was presented in both PdP and PwP, it was clearly higher in PwP, which had consistent, significantly higher theta power at most of the 48 electrode locations compared to AB group. Furthermore, in comparison to AB group, the PdP group showed significantly higher theta power at 14 electrode locations during EO and at 23 electrode locations during EC over the frontal and central regions. On the contrast, compared to the able bodied, PnP had significantly higher theta power at only one electrode location during EO and at 13 electrode locations during EC. Association between increased theta power and the presence of CNP was reported in previous studies[138,139,205], but here we demonstrate that this occurs actually even before the appearance of the physical symptoms of pain . Increased theta power in patients with pain is related to thalamo-cortical dysrhythmia. Results of this study confirm that thalamo-cortical dysrhythmia precedes and possibly causes CNP.

The comparison between power of EO and EC state showed that PdP and PwP exhibited the lowest difference in all three frequency bands compared to PnP and AB groups. This was caused by the lack of reactivity i.e. insufficient increase in EEG power when closing eyes. Although power reactivity due to transition from EC to EO state has been most studied in the alpha band, results of published literature as well as our results, show that this is not a phenomena restricted to this band[264].

Similar results have also been noticed by comparing the power of the dominant alpha peak between the EO and EC states which showed that PdP and PwP had smaller differences compared to PnP and AB groups. Functional significance of alpha band reactivity has been explored by previous studies[139,265]. Rowe et al. reported that the difference in EEG activity between EO and EC can be used to explore the function of thalamo-cortical networks[265]. Boord et al. suggested that the neural networks in able bodied individuals and patients with no pain were able to adjust the change in sensory input between EO and EC but the patients with CNP were unable to adjust this change[139]. Boord et al. also suggested that the dynamic mechanisms adjusting the change in sensory input were highly affected by the presence of CNP[139]. Although in this study, both AB and PnP exhibited significantly higher alpha PSD in EC compared to EO state, PnP does not show this difference over the central region. This particular result might be a less relevant finding because the main sources of alpha activity are in the occipital region while combination of mu and alpha rhythm at the same 8-12 Hz frequency exists over the central areas.

The lower EEG reactivity measured by the EC/EO power ratio was noticed in the PdP group compared to the other three groups. A statistically significantly lower EC/EO ratio was noticed at a large number of the electrode locations predominantly over the frontal and parieto-occipital regions. The group of PdP showed a lower increase in PSD during EC state compared to EO state, resulting in a smaller difference in PSD between EC and EO

compared to the other groups. The deficiency in the EC/EO power ratio previously reported in SCI patients with CNP suggested that the reduction in EC/EO ratio can be an indicator of the thalamo-cortical dysrhythmia[139]. "Slowing-down" of the dominant alpha peak (i.e. shifting towards the lower frequencies closer to the theta band) was noticed in this study in SCI patient groups compared to the AB control. Although slowing-down of the dominant alpha peak was present in all three SCI patient groups, it was greater in the PdP group, which had consistently significant lower alpha dominant frequency at 45 electrode locations in comparison to the AB group during EC and over the central and parietal regions during EO.

The comparison of the cortical and deep cortical activity by sLORETA, between all 4 groups and for all four frequency bands shows that PdP and PwP exhibited higher but not statistically significant activations in both theta (4-7Hz) and beta (13-30Hz) bands predominantly over the frontal, central and parietal particularly during EC state compared to both AB and PnP groups. The over activation in the theta and beta bands was noticed in patients with chronic neurogenic pain specifically over the cortical pain matrix including insular (IC), anterior cingulate (ACC), prefrontal, and inferior posterior parietal cortices, and primary (S1), secondary (S2), and supplementary somatosensory (SSA) cortices in comparison to healthy controls[266]. Stern et al. also reported that these theta and beta over activations was reduced specifically over IC and ACC after a therapeutic lesion in the thalamus[266]. Therefore, they suggested that the higher theta and beta activity was associated with thalamo-cortical dysrhythmia. In the alpha band (8-12Hz), PdP showed statistical significant lower activity predominantly over the parietal region (Brodmann area 7) of the left hemisphere compared to AB and PnP groups during EC state. The PwP group also exhibited significantly lower alpha (8-12Hz) activity over the parietal region (Brodmann area 7) of the left hemisphere compared to the PnP group. Previous studies

showed that SCI patients with CNP exhibited lower alpha power compared to the control group[138,139,194].

### 4.5.2 Induced EEG during Motor Imagery (MI) Tasks

The time-frequency analysis of the EEG data recorded during MI tasks showed that PdP and PwP exhibited larger ERD over alpha and beta bands sustained throughout the 3s (a whole trial) compared to AB and PnP groups. PwP also exhibited larger ERD in the theta band compared to all of the other three groups but it was only sustained for 1s post MI cue. The larger and long lasting ERD in the PdP and PwP groups was characteristic for the electrode locations rather than for the MI tasks; as it was present for all three conditions of MI at the central cortex. A previous study of our research group found that during imagination of movement, SCI patients with long standing CNP had strong theta and alpha ERD compared to able-bodied people and SCI patients with no pain groups over the central and parietal regions which were not restricted to somatotopic arrangement of the painful area of the body[140]. The reduction of these theta and alpha over-activations were associated with the reduction of CNP[267]. The fMRI study by Gustin et al. also revealed that SCI patients with CNP exhibited strong activation over the central region during imagination of movement compared to healthy controls[141]. In comparison to the AB group, PnP exhibited lower beta SMR and beta ERD in particular during MI of left and right hand.

The comparison of scalp maps based on ERD/ERS between all four groups and at time window t=0.5 to 1.5s for all selected frequency bands (theta, alpha, beta SMR and beta) showed that PdP had significantly larger ERD over electrode locations at the central and parietal regions in the theta band compared to both AB and PnP groups; and in the beta band compared to the PnP group specifically during MI of the left hand. The PdP group also exhibited significantly larger ERD predominantly over the central region in alpha and beta SMR bands during MI of feet. The PnP group showed significantly larger ERD over

most of 48 electrode locations compared to the AB group and over the frontal and central regions compared to the PwP group in alpha band during MI of the feet. However, all results of the ERD/ERS scalp maps did not reach the adjusted p value after FDR correction for multiple comparisons. FDR is known to reduce false positive at a cost of inducing false negative results, and although it is widely used in EEG analysis, it is not best suited for analysis where spatial distribution of significant values should be taken into account.

Spatio-temporal analysis of scalp maps based on ERD/ERS analysis between all four groups showed that both PdP and PwP had stronger and widespread ERD in the theta band predominantly over the centro-parietal region of the left hemisphere which lasted longer until the end of the MI trial at t=3s. The intensity of ERD is proportional to the activity of neuronal substrates[268], in this study indicating stronger activity.

The changes in the cortical activity during motor imagery MI tasks between all four groups over time window (t=0.5 to 1.5s) have been compared by sLORTEA. sLORETA results showed that PdP showed higher, but not statistically significant theta activity over the centro-parietal region during all three MI tasks compared to AB and PnP groups, but it was lower compared to the PwP group. The highest theta activity was noticed in PdP and PwP groups over the parietal region of the left hemisphere during MI of the left hand compared to the PnP group. Both AB and PnP groups showed significantly higher widespread alpha activity over the parietal region compared to both PdP and PwP groups. In beta SMR and beta (20-30 Hz) bands, PwP showed the highest but not statistically significant activations over the central-parietal region compared to all other groups.

In summary, in the relaxed state, the comparison of PSD between EC and EO shows that the AB group had significantly higher theta, alpha and beta bands PSD and the PnP group had significantly higher theta and alpha bands PSD in EC compared EO state. The PwP group also exhibited significantly higher theta band PSD in EC compared to EO. In terms of the dominant alpha peak, AB and PnP groups showed significantly higher power

of dominant alpha peak in EC compared to EO state. The PdP group exhibited a significantly smaller EC/EO power ratio of the dominant peak as well as a significant shift towards the lower frequency of the dominant alpha peak during EC predominantly over the frontal and parieto-occipital regions compared to the AB group. The results of sLORETA during a relaxed state show that AB and PnP groups had significantly higher alpha activity over the parietal area of the left hemisphere compared to the PdP group. PnP exhibited significantly higher alpha activity over the parietal area of the left hemisphere compared to the PwP group during EC state. Additionally, the AB group showed significantly higher beta activity over the parietal area of the right hemisphere compared to PnP and PdP groups, and over the parietal areas of both right and left hemispheres compared to the PwP group during EO state.

During MI, the results of sLORETA show that the AB group exhibited significantly higher activity in the alpha band over the parietal region of the right hemisphere compared to PdP during MI of left hand. The AB group also had significantly higher alpha activity compared to both PdP and PwP during MI of right hand. The PnP group also showed significantly higher activity in the alpha band over the parietal region of the right hemisphere compared to PdP and over the parietal region of the left hemisphere compared to PwP during all three MI conditions.

In this study the PnP group showed weaker beta band ERD which was not lateralised during MI tasks compared to other groups. Similar findings were noticed in the chronic PnP group[140]. However, in the relaxed state, there was no significant difference in alpha PSD between PnP, and both AB and PwP. In contrast to this, the chronic PnP group showed significantly lower alpha PSD compared to AB and chronic PwP[140]. The results of PdP show that changes in EEG precede the onset of pain and they became even more pronounced once the patients start experiencing pain as noticed in the PwP group. The results of PwP are very similar to PwP group with long standing CNP[140]. During the

relaxed state, the high theta activity and lower frequency of the dominant alpha peak can be noticed in both PwP groups. During MI both PwP with short and long standing CNP showed large ERD spreading over most of the frequency bands. Additionally, PwP in this study show larger beta band ERD predominantly over the parietal region which has also been found in chronic PwP[140]. In this study however this result was not only found in the PwP group but also in PdP. These results indicate that changes in both relaxed and induced EEG can precede the onset of pain and happen much faster than previously thought.

## 4.6 Conclusion

This study demonstrated that changes in spontaneous and induced EEG can be both predictors and consequences of CNP following SCI. As predictors of CNP (preceding the physical symptoms of CNP), shift of the dominant alpha peak towards lower frequencies and lower EEG reactivity during the relaxed state as well as stronger alpha and beta ERD during MI can be noticed in the PdP group. In patients who already develop pain in PwP group, an increase in theta PSD during the relaxed state and stronger ERD activity that extended towards the lower frequency (theta band) during MI can be noticed.

# 5

# Neurofeedback Treatment of Central Neuropathic Pain in Sub-Acute Patients with Spinal Cord Injury

# Chapter 5 Neurofeedback Treatment of Central Neuropathic Pain in Sub-Acute Patients with Spinal Cord Injury

## 5.1 Abstract

***Objective:*** Exploring the effectiveness of the NF therapy on treatment of CNP in sub-acute patient with SCI (several months after injury).

***Methods***: Eleven sub-acute SCI patients with CNP $\geq$ 4 VAS participated in this study. Patients were divided into two groups: a treatment group (n=7, 5 male and 2 female, age 43.4±16.3 years) and a control group (n=4, 1 male and 3 female, age 43.8±12.8 years). Patients in the treatment group received NF therapy as well as medication while patients in control group received medication only. The intensity of pain of the control group was monitored within a 2 month follow up period. The NF protocol was to enhance alpha (9 to 12Hz) and suppress theta (4 to 8Hz) and higher beta (2o to 30Hz) band relative powers for 10% above/below the pre-determined baseline threshold over electrode location C4 for 30mins. EEG was recorded during EO and EC relaxed states and during motor imagery task before the first and after the last NF session in order to assess the long-time effect of the NF therapy.

***Results:*** Only Four out of seven patients in the treatment group completed multiple neurofeedback sessions 14, 14, 8, and 12 NF sessions. Clinically and statistically significant lower pain intensity as well as a reduction in painful areas was noticed in three patients out of four in the treatment group. The reduction of pain was accompanied by a reduction in ERD, reflecting the reduction of the over-activation of M1.

***Conclusion:*** The results of this study demonstrate that the NF treatment has a positive effect on the reduction of pain, at least over the period of the study. However, numerous factors, and in particular patients' low prioritization of pain, indicate that early NF of CNP in SCI patients might not be a practical solution.

## 5.2 Introduction

Treatments of the CNP can be divided into pharmacological[38] and non-pharmacological[41–44]. The pharmacological treatments of CNP may have side-effects on the patients, such as dizziness, sedation, drowsiness and constipation[39], and only 40-60 % of the patients with CNP can achieve relief of pain[40]. Therefore, non-pharmacological treatments of CNP such as repetitive Transcranial Magnetic Stimulation (rTMS), transcranial Direct Current Stimulation (tDCS) and Neurofeedback (NF) have been used to treat CNP[41–43,192]. A common denominator for all non-pharmacological treatments, including rTMS, tDCS and NF, is that they modulate the activity of the primary motor cortex (M1) to treat CNP[41–44].

In this study NF therapy was suggested as a non-invasive neuromodulatory technique. Although the effect of NF has lots of similarities to rTMS in the sense that it modulates the activity of the motor cortex at one site and causes wide spread modulation of the cortical activity[191,192], it does not require an external stimulating device. NF provides users with information about their brain activity and enable them to modulate that activity at will[56,73]. During NF training a person is provided with feedback information on a selected brain wave feature from the selected location of the cortex[57,58].

Neurofeedback information is provided in an auditory or a visual form, the latter typically being a graphical user interface presented on a computer screen. Most often neurofeedback is based on EEG because of its relative inexpensiveness and good temporal resolution providing fast feedback of the cortical activity. With the aid of a neurofeedback

technique, individuals can learn to voluntarily control or modify their EEG[56,57]. NF can be based on non-verbalised strategy[44],where subjects learn how to voluntarily control or modify their behaviour based on visual or audio feedback which reflects that behaviour, or verbalised strategy[269], where subjects learn how to modulate their behaviour based on verbal strategies, such as motor imagery. Neurofeedback therapy has been used for several neurological and psychological disorders such as attention deficit hyperactivity disorder (ADHD), epilepsy, cognitive enhancement, anxiety and alcohol dependence[56,57]. At least 20 NF sessions are required for NF to be effective as a therapy[44,57].

A set of selected features and locations defines a NF protocol. The NF protocol used in this study was the same protocol that was used in a previous study by our group[44]. Although the previous NF CNP study showed that NF can effectively treat pain[44], only patients with long standing pain were included. Knowing that prolonged presence of chronic CNP pain causes measurable changes in cortical activity[16,140], we hypothesise that early NF treatment of CNP might be more effective in both the reduction of pain and in the prevention of a maladaptive cortical plasticity. This study was conducted to explore the effectiveness of an early NF treatment of CNP following SCI in patients in the sub-acute phase, still hospitalised after the injury.

## 5.3 Methods

### 5.3.1 Participants

Eleven hospitalized SCI patients with recently developed symptoms of CNP (6 male (M) and 5 female (F), age 42.6±15.2 years) participated in this study. They were divided into two groups: a treatment group and a control group. All patients started receiving pharmacological treatment a few weeks before this study. These types of medication take several weeks to achieve the full effect so pain could be reduced over the period of NF study because of the cumulative effect of the pharmacological treatment. To separate the

effect of NF on CNP from the effect of medications, two groups of patients with CNP were compared: a treatment group (5 M and 2 F, age 43.4±16.3 years) that received NF and pharmacological treatment and a monitoring group (1 M and 3 F, age 43.8±12.8 years) that received pharmacological treatment only. The pharmacological treatment was a part of their standard treatment (independent of this study). Because of the small number of patients, randomization was performed before starting the study. Five red and five blue marbles were taken out of a box and the order of the marbles corresponds to the order in which patients were assigned to the treatment (blue marbles) and to the control (red marbles). A medical doctor not directly involved in the NF treatment randomly assigned patients into one of the groups. All participants had symptoms indicative of NP: injury to somatosensory system a few weeks/months preceding the onset of pain, burning/stinging/shooting sensation below the level of injury, intensity of pain was not related to movement (most patients were not able to move part of body perceived as being painful)[270]. Allodynia and hyperalgesia were not systematically tested because 7 out of 11 participants had complete sensory and motor paralysis.

All participants gave their informed consent. The study was approved by the National Health Service for Greater Glasgow and Clyde ethical committee. The American Spinal Injury Association (ASIA) Impairment Classification was used to determine the neurological level of SCI[18]. The inclusion criteria for both groups were: the intensity of CNP $\geq$ 4 on the Visual Analogue Scale (VAS, 0=no pain, 10=worst pain imaginable), CNP ongoing for at least 6 weeks, age between 18 and 75 years, no history of brain disease or injury and normal or corrected to normal vision. The exclusion criteria were chronic or acute muscular or visceral pain $\geq$ 4 VNS, epilepsy, diagnosed mental health problems. Table 5.1 shows the demographic information of the patient in treatment (PwP_NF) and control (PwP_C) groups.

**Table 5.1** Demographic information of SCI patients in a treatment and control groups

| ***Patients NF Treatment Group (PwP_NF)*** | | | | | | | |
|---|---|---|---|---|---|---|---|
| No. | Level of injury | ASIA | Weeks with SCI/Pain | Pain intensity (VAS) | Number of NF sessions | Medication | wearing braces |
| 1 | T12 | B | 20/20 | 6 | 7 | Pregabalin | Yes |
| 2 | T7/T8 | A | 12/12 | 4 | 2 | Gabapentin | Yes |
| 3 | C3/C4 | D | 16/16 | 7 | 14 | Tramadol | No |
| 4 | C5/C6 | A | 17/15 | 5 | 14 | Tramadol | No |
| 5 | T3 | A | 24/4 | 5 | 8 | / | Yes |
| 6 | T10 | A | 12/12 | 6 | 2 | Pregabalin | Yes |
| 7 | T8 | C | 26/20 | 5 | 12 | / | No |
| ***Patients Monitoring Group (PwP_C)*** | | | | | | | |
| No. | Level of injury | ASIA | Weeks with SCI/Pain | Pain intensity (VAS) | | Medication | wearing braces |
| 1 | T7/T8 | A | 12/12 | 4 | | Gabapentin | Yes |
| 2 | T12 | A | 20/2 | 4 | | Gabapentin | No |
| 3 | T7/T10 | D | 8/8 | 6 | | Pregabalin | No |
| 4 | T10 | A | 12/12 | 5 | | Pregabalin | Yes |

ASIA: American Spinal Injury Association (ASIA) Impairment Classification
VAS : Visual Analogue Scale (VAS, 0=no pain, 10=worst pain imaginable

## 5.3.2 EEG Recording during Assessment Phases

During the assessment phase, performed before the first and after the last NF training session, multichannel EEG was recorded using the same procedures as in study on the predictors of CNP (section 4.3.2).

## 5.3.3 EEG Recording during NF Training

During NF treatment, EEG was recoded from 6 electrode locations (F3, F4, C3, C4, O1 and O2) according to the international 10-10 standard system[257]. The EEG activity from the C4 electrode was used as feedback during the visual NF training session, while EEG activity from the remaining 5 electrodes was recorded for off-line analysis purposes. The rationale for choosing these electrodes was to modulate the central 9-12 Hz rhythm with NF while monitoring the frontal and the occipital alpha rhythm. This enables testing

whether NF modulates the wide spread alpha or the central SMR. This question is relevant because of the close relation between CNP and the activity of the primary motor cortex.

One module of a biosignals amplifier (g.USBamp, Guger Technologies, Austria) was used to record the 6 EEG channels with a sampling frequency of 256 Hz. The EEG was band-pass filtered between 0.5 and 60 Hz (and notch filtered at 50 Hz) using $5^{th}$ order IIR digital Butterworth filters within the g.USBamp device during recording. Reference and ground electrodes were connected to the right and left ear lobes, respectively. Simulink and MATLAB (MATLAB R2010a, The MathWorks Inc., USA) were used to perform EEG recording. The electrode-skin impedance was kept under 5kΩ.

### 5.3.4 NF GUI and Online EEG Analysis during NF Training

The NF graphical user interface (GUI) was created in LabVIEW (Robotics 2001 SP1, National Instruments, USA). A communication between Simulink and LabVIEW was performed using Simulation Interface Toolkit (version5). The EEG neurofeedback training features (a relative power in a selected frequency band) was calculated online in Simulink using a proprietary software g.RTanalyzer (Guger Technologies, Austria), and then sent to LabVIEW GUI for visualization purposes. The relative powers of the selected bands were computed with respect to 2-30Hz EEG band (Equation 5.4). The NF training feature was averaged over a 0.5s moving average window (corresponding to 128 EEG samples) and updated for every sample (1/256 s). The GUI consisted of three bars, the middle bar represented the dominant band (the alpha band) while the left and right bars represented the theta and beta bands respectively, as shown in Figure 5.1. The height of the bar was proportional to the relative power while the color represented the status of the patients according to the threshold. When the condition of the threshold was satisfied the color turned to green otherwise it was red. Therefore, patients were instructed to “do whatever

necessary" to keep the bars green in order to achieve successful training. This type of non-verbalized training is called 'operant conditioning'.

$$P_{Relative}(F) = \frac{P_{absolute}(F)}{\sum_{f=f1}^{f2} P_{absolute}(f)} \quad 5.4$$

Where
$P_{relative}\ (F)$ = Relative power of specific frequency (F)
$P_{absolute}\ (F)$ = Absolute power of specific frequency (F)
$P_{absolute}\ (f)$ = Absolute power of specific frequency band; f1 and f1 are lower and higher frequency of the frequency band, respectively.

The NF protocol (training site and EEG features) was based on a previous NF study by our group[44]. Relative power values from theta (4-8Hz), alpha (9-12Hz) and higher beta (20-30Hz) over electrode location C4 were used as online EEG training features for the visual NF training session, while during the audio relaxation feedback session alpha (7-10Hz) relative power over electrode location O1 was used as the EEG feedback feature. The relative power of the lower alpha band 7-10Hz was used for audio relaxation session because studies reported that patients with CNP had a lower dominant alpha frequency compared to the able bodied control[139,194]. During the audio relaxation session, relative power of the alpha band was used as a measure of relaxation. When the relative power of the alpha band was higher than the threshold (10%); the intensity of the music was lower, and vice versa. The relaxation session is standard general procedure recommended for the start of any NF. The purpose of the audio feedback, provided from the occipital cortex, was relaxation while the primary purpose of the visual feedback training was the reduction of pain.

During the visual NF training session, the patient was instructed to suppress the theta and higher beta band and to enhance the alpha band relative power for 10% above/below the pre-determined baseline threshold. Studies reported that the increase in theta[139,140,194] and beta[194] bands were associated with presences of CNP. Moreover, a previous NF study showed that an increase in the alpha band power can lead to reduced CNP[44,88]. The pre-

determined baseline threshold was calculated as the relative power of each EEG band recorded during 2 min eyes opened (EO) or eyes closed (EC) relaxed state. The 10% threshold above or below the baseline was calculated using Equation 5.5 and 5.6, respectively.

$$TH_{\boldsymbol{dominant}} = P_{\boldsymbol{dominant}} \times 1.1 \quad 5.5$$

$$TH_{\boldsymbol{inhibitory}} = P_{inhibitory} \times 0.9 \quad 5.6$$

Where,
$P_{dominate}$ and $P_{inhibit}$ are mean relative power for dominant and inhibitory bands, respectively.
$TH_{dominate}$ and $TH_{inhibit}$ are threshold values for dominant and inhibitory bands, respectively.

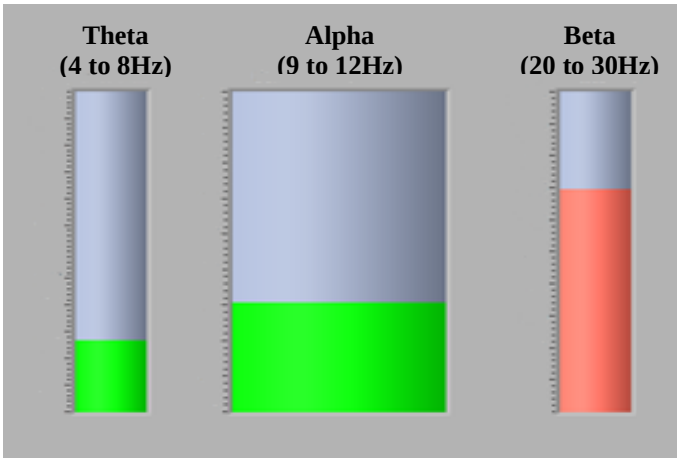


**Figure 5.1** Graphical user interface for NF treatment. Patients were instructed to 'do whatever necessary to keep bars green'.

## 5.3.5 Study Procedures

### *5.3.5.1 Pain Monitoring of Control Group*

Patients with CNP that did not receive NF treatment were recruited in order to separate the effect of NF treatment from that of medications. They were asked to fill out a Brief Pain Inventory questionnaire[33] every two weeks, over a period of two-months, to establish if their pain level changed and if there were any changes in their medications. A two month period was chosen as it is the longest period that patients from the treatment group would stay on the NF treatment.

#### *5.3.5.2 Assessment phase of Treatment Group*

The assessment phase was organized before the first and after the last NF session. It comprised of a Brief Pain Inventory questionnaire[33] , and EEG recording during both a relaxed state (spontaneous EEG activity) and a cue-based motor imagination task (induced EEG activity). The Brief Pain Inventory was used to assess the level of pain measured with VAS and its influence on mood and sleep[33]. The procedures and the experimental protocol of EEG recording during a relaxed state and a motor imagination task were the same as described in sections (4.3.4) and (4.3.5), respectively. This assessment phase was introduced to measure the long-term effect of the NF treatment on cortical activity.

#### *5.3.5.3 NF Treatment Phase*

Twenty NF treatment sessions were planned for each patient to attend. The number of sessions was based on previous research in the area of NF[44,57]. Each NF treatment session consisted of relaxation audio feedback followed by visual feedback for treatment of pain. At the beginning and the end of each NF training session, the EEG baseline activity during EO and EC relaxed stated was recorded. Each NF session consisted of 1 sub-session of audio NF which lasted 3 min followed by 6 sub-sessions of visual NF, each lasting 5 min. The 2min EO and 2min EC EEG baseline recordings were performed in order to assess the short-term effect of the NF treatment on the EEG activity.

During the audio NF, patients were instructed to listen to a relaxing piece of music keeping their eyes closed. The intensity of the music had two levels (high and low) and was inversely proportional to the relative power of the alpha (7-10Hz) band. Patients were asked to close their eyes, relax and decrease the intensity of the music. Following the single session of audio NF, patients were provided with 30 min (6*5min) of visual NF training. During visual NF, patients sat in front of a computer screen with a GUI, which

displayed the visual feedback of their brain activity. Patients were instructed to "do whatever necessary" to keep the bars green in order to achieve successful training.

### 5.3.6 Off line Analysis of EEG Recorded during NF training

The EEG recording during Pre_NF, NF and Post_NF sessions which contained blinking, muscle activity or amplitudes exceeding 100μV were removed. The PSD of the EEG data was computed using the Welch modified method under Matlab with 4s window with 50% overlapping. For visualisation purposes a logarithmic PSD was computed.

For statistical analysis, the EEG recording during Pre_NF, NF and Post_NF sessions were divided into 4 second long epochs. The Welch modified method was used to calculate the PSD for each epoch. For each 1 Hz of the whole PSD (2-30Hz), the comparison between Pre_NF and NF and between Pre_NF and Post_NF were computed using a non-parametric Wilcoxon paired test (p value=0.05), in order to find the statistically significant difference between before, during and after the NF session over the full PSD.

Relative changes in PSD during NF with respect to pre training EO relax state (Pre_NF) were calculated using Equation 5.7. For each NF training session, the PSD was averaged over all NF sub-sessions for NF training electrode C4. A non-parametric Wilcoxon paired test (p value=0.05) was used to find the statistically significant difference in PSD during each NF training session compared to the PSD of its Pre_NF session.

$$\Delta PSD_i = \frac{PSD_{NFi} - PSD_{Pre\_NFi}}{PSD_{Pre\_NFi}} \times 100 \qquad 5.7$$

Where
i= 1, 2, 3 …. n (n= total number of NF session)
$\Delta PSD_i$ = Percentage changes in PSD for $i^{th}$ NF session
$PSD_{NFi}$ = Average PSD over all NF sub-session for $i^{th}$ NF session
$PSD_{Pre\_NFi}$ = PSD in Pre_NF in $i^{th}$ NF session

### 5.3.7 Off line Analysis of EEG Recorded during Initial and Final Assessment

The EEG data of 48 electrodes during both relaxed state and motor imagery tasks were imported into EEGlab toolbox[99]. The EEG recordings in which the amplitude exceeded 100 μV over most electrodes at the same time were removed. A re-referencing to an average reference was performed. The independent component analysis (ICA) algorithm[113] was also performed on the EEG data for further noise and artifact removal. Components containing recognizable artifacts originating from 50Hz mains, electrooculogram, or muscular activity were set to zero and an inverse ICA was performed to get back to the EEG domain. The PSD analysis was performed on the relaxed EEG data, while ERD/ERS analysis was performed on the EEG data recorded during a cue based motor imagery task (4.3.5). Both PSD and ERD/ERS analysis was computed using EEGlab toolbox.

sLORETA analysis was performed on spontaneous EEG data (relaxed state). sLORETA has been used to estimate the cortical three dimensional distribution of the EEG sources current density[69]. Spontaneous EEG data for each patient was split into 4s long time window epochs. Each of these epochs was exported to sLORETA. The current source density was computed in sLORETA for each of these epochs in three frequency bands including theta 4-8Hz, alpha 8-12Hz and beta 20-30Hz. The frequency dependent change in brain activation at cortical and deep cortical structures was compared between the EO relaxed state before the first and after the last NF session. A non-parametric t test implemented in the sLORETA package with 5000 randomisation of statistical was used to compute corrected p values. The statistical significant level was set at p=0.05.

For Statistical analysis and to measure the long-term effect of NF treatment the statistical non-parametric method with a significance level p=0.05 was performed to compare between pre and post NF values of parameters such as ERD/ERS maps or PSD. A correction of multiple comparison was performed using the False Discovery Rate (FDR)[259].

### 5.3.8 Changes in Pain intensity

Patient was asked to express intensity of pain before and after each NF training session using VAS. The pain intensity after the last NF session was compared to the initial pain intensity value (before the first NF session) in order to find the clinically change relevant in pain intensity for each patient. For each patient, the pain intensities before and after each NF session were compared to calculate statistically significant changes in pain intensity. The comparison was computed using a non-parametric Wilcoxon paired test (p value=0.05).

## 5.4 Results

The result section is organized as follows: Demographic information about patients and pain levels before and after therapy is presented first. This is followed by the analysis of the power spectral density (PSD) of the EEG signal at an electrode location used for NF training on one representative NF session and over the whole training period. The effect on NF training on the resting state EEG is presented next, followed by the analysis of the effect of NF on the EEG response during imagination of movement.

Four out of seven patients in the treatment group (PwP_NF 3, 4, 5 and 7) completed multiple NF sessions 14, 14, 8, and 12, respectively. None of the patients completed 20 planned treatment sessions though they reported the reduction of pain. Pain was reduced immediately during NF training. The duration of the post training effect varied and lasted from two to Five hours. Three patients withdrew from the study after several NF session (two had 2 and one had 7 NF sessions). The reasons for terminating the study early were: one patient was discharged from the hospital before completing the therapy, and two patients felt uncomfortable during NF due to wearing neck and abdominal braces. The two patients who withdrew from the NF group (PwP_NF2 and PwP_NF6) decided to move to the control group (PwP_C1 and PwP_C4). Other patients who completed more than 10

sessions decided to terminate NF therapy before completing all 20 treatments because of inconvenient circumstances that accompany any study organised in a hospital setting. For example, inconveniences included times available for therapy, e.g. before a morning physiotherapy session, during a lunch break or between a morning and afternoon physiotherapy session, after afternoon physiotherapy (and before 5 pm when it was dinner time) when most patients were tired. The fact that EEG recoding often left some gel in patients' hair was an additional inconvenience, as ward nurses had to be asked to wash it. Last though not the least, patients with sub-acute SCI were overwhelmed by the new condition of their body, i.e. paralysis, compared to which pain was not perceived as a priority. Because pain which most people are familiar with is of a nociceptive nature, and can be successfully treated by medications, most patients were more keen using medications as a simpler, less time consuming solution.

Changes in pain intensity and perceived location before and after NF therapy as well as the comparison between changes in pain intensity in PwP_NF and PwP_C groups will be shown. Secondly, the short-term effect of the NF on EEG activity (changing in PSD) of the patients in the treatment group during the NF session will be explained. Finally, the long-term effect (up to a week after therapy) of the therapy on patients' EEG activity measured during a relaxed state and during cue based motor imagery task will be discussed. A summary of the results is provided in section (5.4.6).

### 5.4.1 Pain Intensities and the Perceived Pain Locations

The pain intensity before the first and after the last NF session of the patients in the treatment group are shown in Table 5.2. The reduction of pain intensity was noticed in all four patients compared to their baseline. However, the reduction of pain intensity in PwP_NF5, who had only 8 NF sessions, did not reach the clinically significant level (≥30%). Several studies of pain have reported that a reduction of pain between 30% to

50% as a clinical improvement[271–273]. Patients in the PwP_NF group showed both a clinically significant and also a statistically significant (non-parametric Wilcoxon paired p-value=0.05) reduction of pain by comparing the pain intensities before and after NF therapy over all training days (Table 5.4).

The perceived pain locations before the first and after the last NF therapy are shown in Figure 5.2 indicating a reduction of painful areas, specifically in patients who finished ≥ 12 NF sessions. Results demonstrate the importance of reporting not only intensity but also the location of pain, because either of these two can change over time. Although 'at level' and 'below level' pain was not discriminated in this study, it can be noticed that the 'band' of pain in patients PWP_NF5 and PWP_NF7, which probably presents 'at level' pain, has disappeared. The average pain intensities of the patients in the control group **(**PwP_C) are shown in Table 5.3 and indicate that there were no large changes in their pain intensities over a period of 8 weeks. Additionally, no reduction in the painful area was noticed in patients of the control group after two months compared to the first session and two of the patients even showed an increase in the size of the area in pain (PwP_C2 and PwP_C4) as shown in Figure 5.3. The perceived pain locations of the three patients who withdrew from NF group are shown in Figure 5.4.

**Table 5.2** Changing in pain intensities of patients in treatment group (PwP_NF) before the first and after last NF session.

| **Patients** | **Pain Intensity** | | **Change in Pain Intensity (%)** |
|---|---|---|---|
| | **Before First NF (VAS)** | **After last NF (VAS)** | |
| **PwP_NF3** | 7 | 2 | **-71%** |
| **PwP_NF4** | 5 | 2 | **-60%** |
| **PwP_NF5** | 5 | 4 | -20% |
| **PwP_NF7** | 5 | 2 | **-60%** |

VAS : Visual Analogue Scale (VAS, 0=no pain, 10=worst pain imaginable)

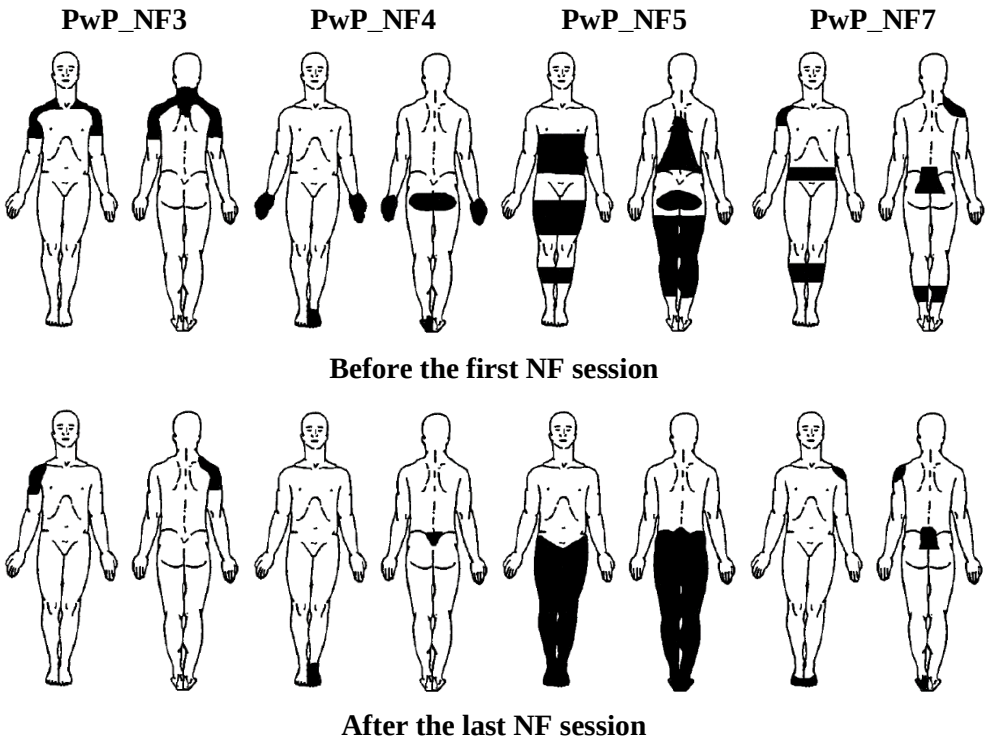


**Figure 5.2** Perceived location of pain (black shaded areas) as reported by patients in treatment group PwP_NF before the first and after the last NF training session

**Table 5.3** Averaged of pain intensities of patients in control group (PwP_C) over a period 8 weeks

| Patients | Averaged of pain intensities Mean±SD |
|---|---|
| **PwP_C1** | 4.0 ± 0.0 |
| **PwP_C2** | 4.7 ± 1.2 |
| **PwP_C3** | 5.0 ± 1.0 |
| **PwP_C4** | 5.2 ± 0.8 |

VAS : Visual Analogue Scale (VAS, 0=no pain, 10=worst pain imaginable)

**Table 5.4** Comparison in pain intensity of patients in treatment group (PwP_NF) before and after each NF session.

| Patients | Pain Intensity | | p-value |
|---|---|---|---|
| | Pre_NF (VAS) mean±SD | Post-NF (VAS) mean±SD | |
| **PwP_NF3** | 4.5±1.7 | 3.1±0.8 | **0.002** |
| **PwP_NF4** | 3.3±1.1 | 2.4±0.8 | **0.015** |
| **PwP_NF5** | 4.0±0.5 | 3.9±0.6 | 0.946 |
| **PwP_NF7** | 4.3±1.4 | 1.8±0.9 | **0.002** |

VAS : Visual Analogue Scale (VAS, 0=no pain, 10=worst pain imaginable); Pre_NF: before each NF session; Post_NF: after each NF session

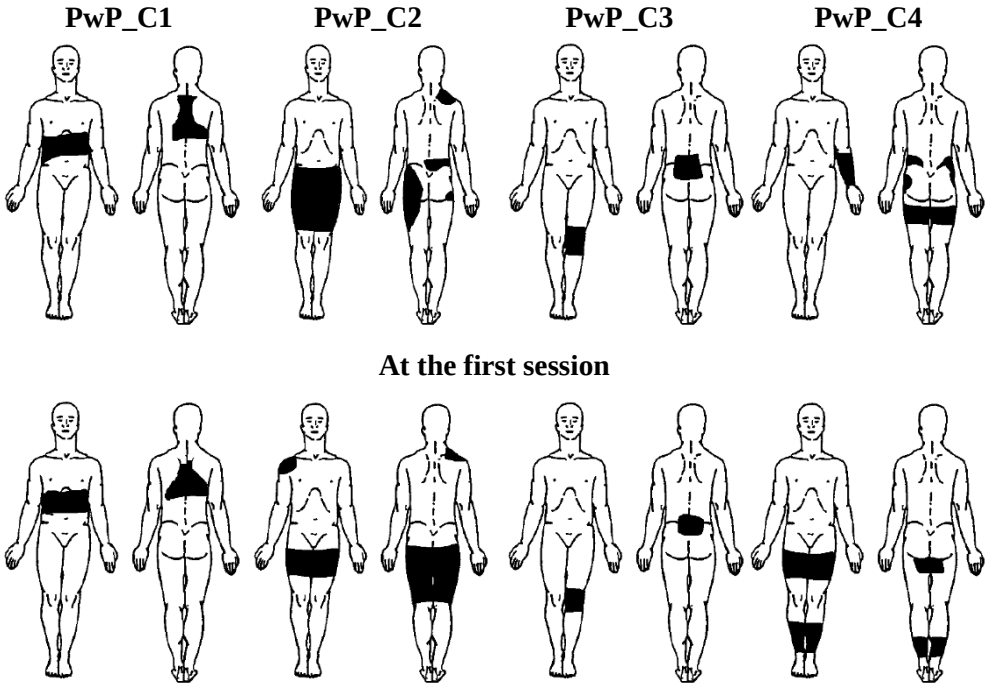


**Figure 5.3** Perceived location of pain (black shaded areas) as reported by patients in control group PwP_C at the first session and at the last session (two months later)

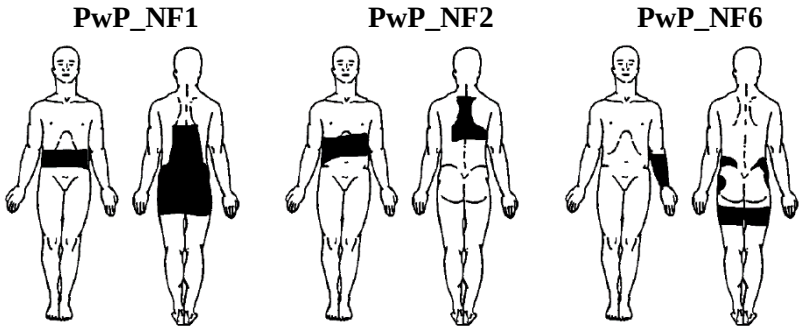


**Figure 5.4** Perceived location of pain (black shaded areas) as reported by patients who withdrew from NF group before the first NF training session

## 5.4.2 Changes in PSD during NF Training

In the following section, only results of four patients who completed multiple NF sessions will be presented.

Voluntary modulation of PSD during one representative NF sub-session (5 min NF training) compared to pre- and post- NF baseline PSD values are shown in Figure 5.5 for four patients in the treatment group. The change in PSD between Pre_NF and NF indicates the immediate effect of the NF training on the PSD, while the change between Pre_NF and Post_NF represents the short term carry-over effect of the NF training on PSD. It can be noticed that all 4 patients were able to modulate at least one frequency band during NF at the time, and this modulation still remained a few minutes after the NF training session. Most notably patients were not able to control PSD in all three frequency bands. In a previous study by our group, we noticed that most patients controlled alpha and beta bands simultaneously but only one controlled all three frequency bands at the same time[44]. Figure 5.5 shows the most consistent increase is in the alpha band power in PWP_NF4 and there is a decrease of beta band power in PWP_NF7, which remained during the post NF measurement. Interestingly, alpha and theta band power continued to increase in PWP_NF4 following the NF session.

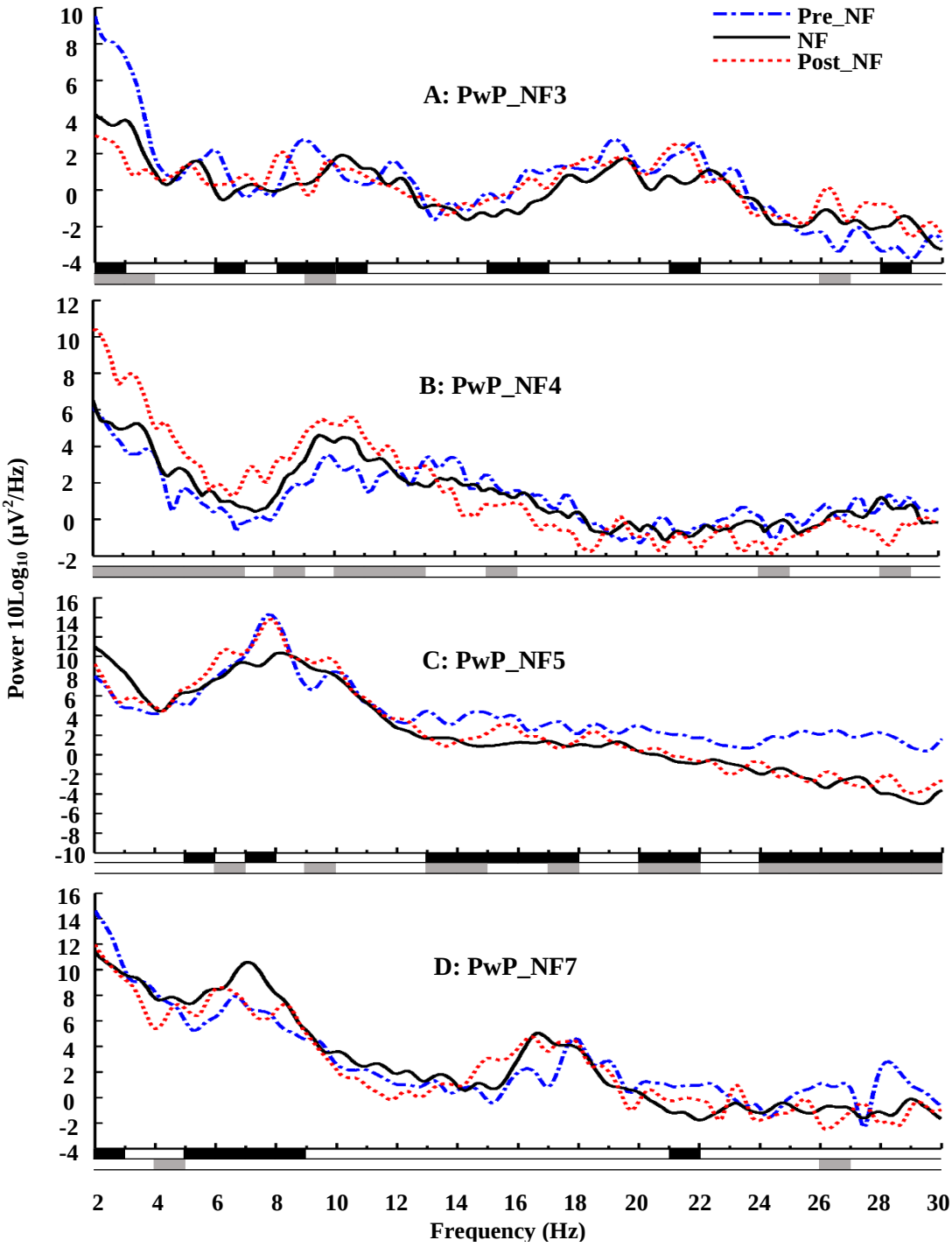


**Figure 5.5** Changes in PSD in pre-neurofeedback baseline (Pre_NF), NF training session (NF) and post-neurofeedback (Post_NF) at C4 NF training electrode location for all four patients. The statistically significant change between Pre_NF and NF is shown in thick horizontal black line while between Pre_NF and Post_NF is shown in thick horizontal grey line under the frequency axis. The statistically significant level is p=0.05.

## 5.4.3 Changes in Relative Power during NF Training

The relative changes in PSD with respect to pre training EO relaxed state (Pre_NF) for three frequency bands theta (4-8Hz), alpha (9-12Hz) and beta (20-30Hz) over all NF

training sessions and for all four patients are shown in Figure 5.6. The negative and positive bars represent the decrease and increase in PSD compared to the Pre_NF session, respectively. To remind the reader, patients were aiming to decrease theta and beta bands and to increase the alpha band power. Figure 5.6A shows that PwP_NF3 successfully decreased theta PSD for 11 out of 14 NF sessions. However, the decrease in theta PSD was larger than 10% during only during 4 NF sessions. PwP_NF3 showed an increase in alpha PSD and a decrease in beta PSD in only one NF session (session 4).

Figure 5.6B shows changes in PSD for PwP_NF4. PwP_NF4 achieved a decrease in theta PSD for 6 out of 14 NF sessions and in four of these six sessions the theta PSD was more that 10% below the baseline. In the alpha band, the PSD was higher than the baseline in 8 NF sessions (only 4 sessions >10%). The decrease in beta PSD was noticed in PwP_NF4 for 8 NF sessions with 5 of them >10%. The changes in PSD with respect to the Pre_NF for PwP_NF5 are shown in Figure 5.6C. PwP_NF5 exhibited a decrease in theta PSD for 3 NF sessions, and during only one NF session (session 5) the decrease in theta PSD was more than 10% compared to Pre_NF. The increase in alpha PSD and decrease in beta PSD was also noticed in PwP_NF4 during 3 NF sessions; an increase in alpha PSD (>10%) was noticed in sessions 5 and 6, and a decrease in beta PSD (>10%) occurred in sessions 2, 5 and 8.

Figure 5.6D shows the changes in PSD for PwP_NF7. PwP_NF7 showed a decrease in theta PSD in only one (session 10) out of 12 NF sessions. The increase in alpha PSD (>10%) was noticed in 8 NF sessions. In the beta band, the PSD decreased in 10 NF sessions and in 8 out of these 10 sessions the changes were more than 10%. Although all four patients were able to modulate their EEG PSD in required directions, only 2 of them were able to modulate the PSD in theta, alpha and beta bands (>10%) simultaneously during one NF session (PwP_NF5: session 5 and PwP_NF7: session 10).

Table 5.5 shows the relative change in PSD with respect to the Pre_NF averaged over all NF training sessions at electrode location C4 from which NF was provided. The PSD is presented for the theta, alpha and beta frequency bands for all four patients. It can be noticed that only PwP_NF3 had decreased theta PSD compared to Pre_NF and this decrease was statistically significant (p=0.05). In contrast, PwP_NF7 showed a significant increase in theta PSD compared to Pre_NF. In the alpha band, PwP_NF4 and PwP_NF7 showed increased PSD while PwP_NF3 and PwP_NF5 showed a decrease in alpha PSD. The significant decrease in alpha PSD was noticed in PwP_NF3 compared to Pre_NF. In the beta band, PwP_NF4, 5 and 7 exhibited a decrease in PSD but this decrease did not reach statistical significance (p=0.05). PwP_NF3 showed significantly increased beta PSD compared to Pre_NF. The inconsistency of the results is due to the small number of NF sessions and the fact that the first several sessions, while patients were still learning to use NF, have been included in the analysis.

**Table 5.5** Relative changes in PSD during NF with respect to pre training EO relax state (Pre_NF) averaged over all NF training sessions for C4 NF training electrode. Negative values mean a decrease while positive values mean an increase with respect to Pre_NF. The significant increase or decrease is shown in bold. The statistical significant level was set to p=0.05.

| **Patients** | **Theta (4-8Hz)** | | **Alpha (9-12Hz)** | | **Beta (20-30Hz)** | |
|---|---|---|---|---|---|---|
| | PSD (%) mean±SD | p value | PSD (%) mean±SD | p value | PSD (%) mean±SD | p value |
| **PwP_NF3** | -6.0 ± 9.7 | **0.024** | -5.0 ± 19.1 | **0.024** | 26.2 ± 35.9 | **$0.6e^{-3}$** |
| **PwP_NF4** | 3.0 ± 18.1 | 0.807 | 3.7 ± 15.3 | 0.625 | -4.57 ± 14.2 | 0.241 |
| **PwP_NF5** | 4.3 ± 14.3 | 0.981 | -3.5 ± 13.8 | 0.546 | -0.62 ± 23.3 | 0.945 |
| **PwP_NF7** | 16.6 ± 14.4 | **0.020** | 8.5 ± 12.3 | 0.129 | -12.5 ± 26.4 | 0.077 |

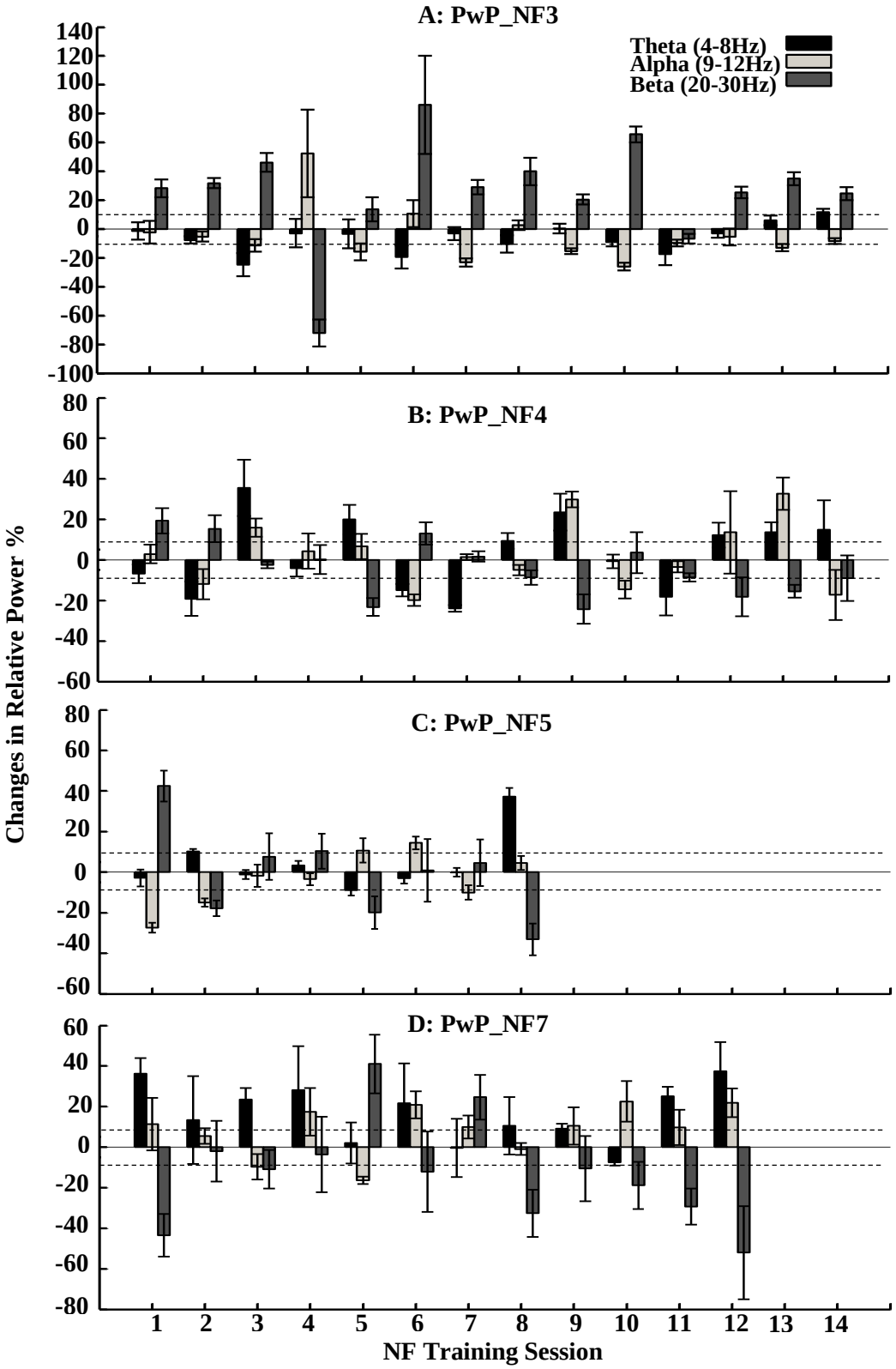


**Figure 5.6** The relative changes in PSD with respect to pre training EO relax state for three frequency bands theta (4-8Hz), alpha (9-12Hz) and beta (20-30Hz) over all NF training session and for all four patients PwP_NF 3, 4, 5 and 7. The horizontal dashed lines mark ±10% changes in relative power with respect to pre training EO relax state.

### 5.4.4 Long term effect of NF training on Spontaneous EEG

sLORETA localisation of the difference between eyes opened relaxed state after the last compared to before the first NF session for PwP_NF3 averaged over theta (4-8Hz), Alpha (8-12Hz) and Beta (20-30Hz) For PwP_NF3 (Figure 5.7), PwP_NF4 (Figure 5.8), PwP_NF5 (Figure 5.9) and PwP_NF7 (Figure 5.9).

Table B.1 (Appendix B) shows the areas with significant differences (p value=0.05) between eyes opened relaxed state after the last compared to before the first NF session for PwP_NF3 in theta (4-8Hz), alpha (8-12Hz) and beta (20-30Hz). It can be observed that statistically significant changes were present in all three frequency bands. For the same frequency band, both an increase and decrease were noticed, depending on the cortical region. It can be observed in Figure 5.7 that in the theta band PwP_NF3 had significantly lower activity over the frontal region, predominantly over the left hemisphere, and significantly higher activity over the parietal region, predominantly over right the hemisphere. In the alpha band, PwP_NF3 also exhibited significantly lower alpha activity over the frontal region, predominantly over the left hemisphere, while significantly higher activity over the parietal region as shown in Figure 5.7 and Table B.1. A significant decrease in beta activity was noticed over the frontal regions (BA: 11, 10 and 32) while a significant increase was noticed at the frontal region over Brodmann areas 6, 8, 9 and 32 over both left and right hemispheres (Figure 5.7 and Table B.1). In summary, a decrease in activity over a similar frontal region was widespread over theta, alpha and beta bands while at the same time theta and alpha activity increased over the parietal region.

Figure 5.8 and Table B.2 show results for patient PwP-NF4. This patient had a significant increase in theta activity over the parietal and frontal regions and a significant decrease in theta activity over the occipital region. Similar to the theta band, PwP_NF4 had significantly higher activity over the parietal and frontal regions and significantly lower activity over the occipital region. The increase and decrease in theta and alpha activities in

PwP_NF4 were predominantly over the right hemisphere. A significant increase in beta activity over the parietal, frontal and limbic areas was noticed in PwP_NF4 and significantly lower beta activity can be noticed over the occipital region, predominantly over the right hemisphere (Figure 5.8 and Table B.2).

The significantly higher theta, alpha and beta activity over the parietal region, predominantly over the right hemisphere, can be noticed in PwP_NF5 after NF compared to before NF as shown in Figure 5.9 and Table B.3. The significantly decreased theta activity in PwP_NF5 was noticed over the frontal and occipital region while in the alpha band the significant decrease was noticed over the occipital and limbic areas. Significantly lower beta activity can be noticed in PwP_NF5 over the parietal, occipital and temporal regions after NF compared to before NF (Figure 5.9 and Table B.3).

Figure 5.9 and Table B.4 show that PwP_NF7 had significantly higher theta activity over the parietal, occipital and temporal areas of the left hemisphere and significantly lower theta activity over the frontal areas, predominantly over the left hemisphere, after NF compared to before. In the alpha band, PwP_NF7 showed significantly higher activity over the frontal (BA: 4, 5 and 5) and parietal regions and significantly lower activity over the frontal (BA: 4, 7, 10, 11 and 46) area predominantly over the left hemisphere (Figure 5.9 and Table B.4). A significant increase in beta activity after NF compared to before NF can be noticed in PwP_NF7 over the frontal (BA: 4, 5 and 6) region, predominantly over the right hemisphere, while the significantly lower beta activity was observed over the frontal (BA: 10 and 11) and parietal areas, over both left and right hemisphere as shown in Figure 5.9 and Table B.4.

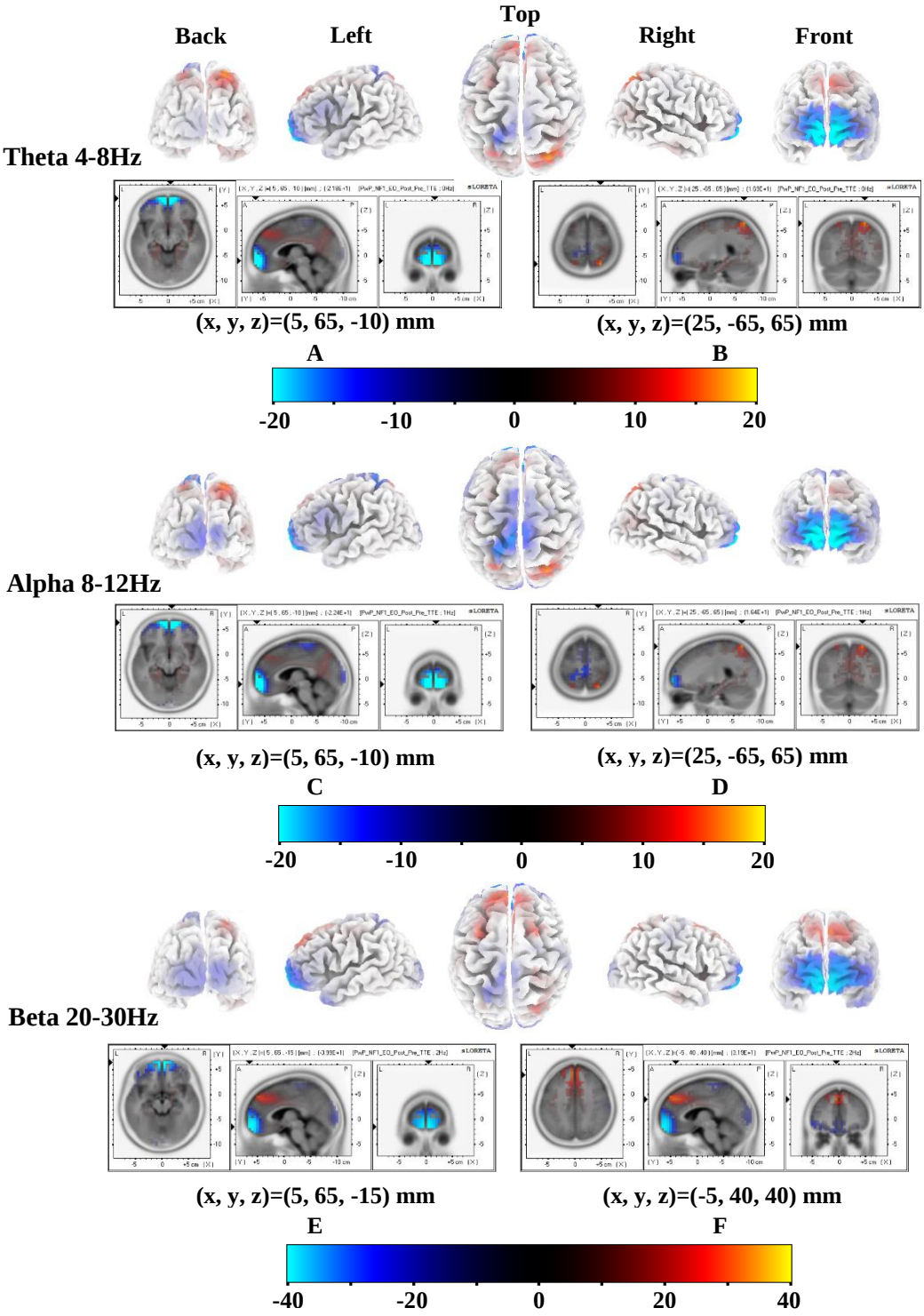


**Figure 5.7** sLORETA localisation of the different between eyes opened relaxed state after the last compared to before the first NF session for PwP_NF3 averaged over theta (4-8Hz) (A and B), Alpha (8-12Hz) (C and D) and Beta (20-30Hz) (E and F). The first raw of each figure represents 3D map of the localisation while the second raw represents the 3D slice at the displayed of the voxel with negative (A, C and E) and positive (B, D and F) strongest activity. The (x, y, z) under each figure represent the Montreal Neurological Institute and Hospital (MNI) coordinate system of the voxel with strongest activity.

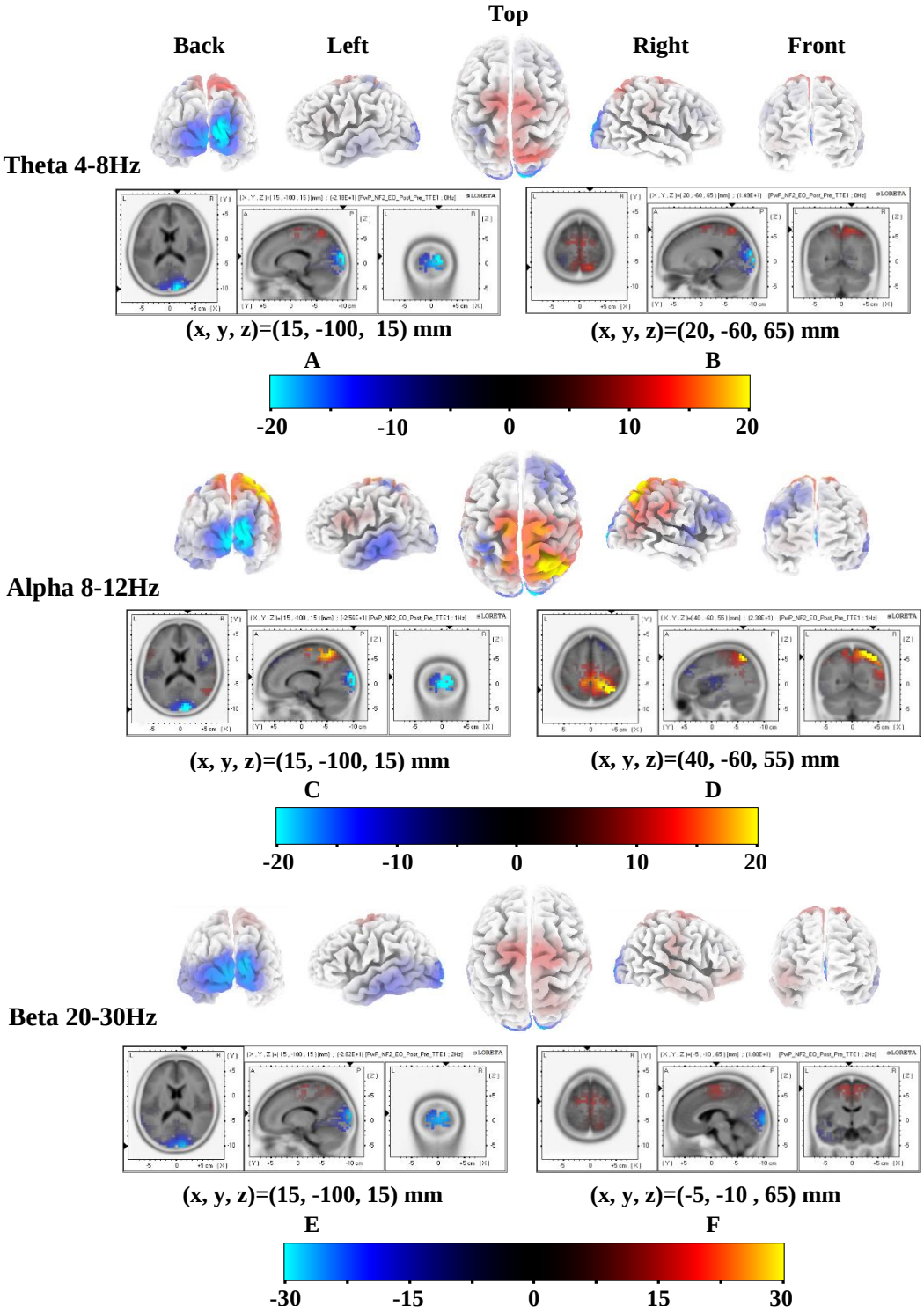


**Figure 5.8** sLORETA localisation of the different between eyes opened relaxed state after the last compared to before the first NF session for PwP_NF4 averaged over theta (4-8Hz) (A and B), Alpha (8-12Hz) (C and D) and Beta (20-30Hz) (E and F). The first raw of each figure represents 3D map of the localisation while the second raw represents the 3D slice at the displayed of the voxel with negative (A, C and E) and positive (B, D and F) strongest activity. The (x, y, z) under each figure represent the Montreal Neurological Institute and Hospital (MNI) coordinate system of the voxel with strongest activity.

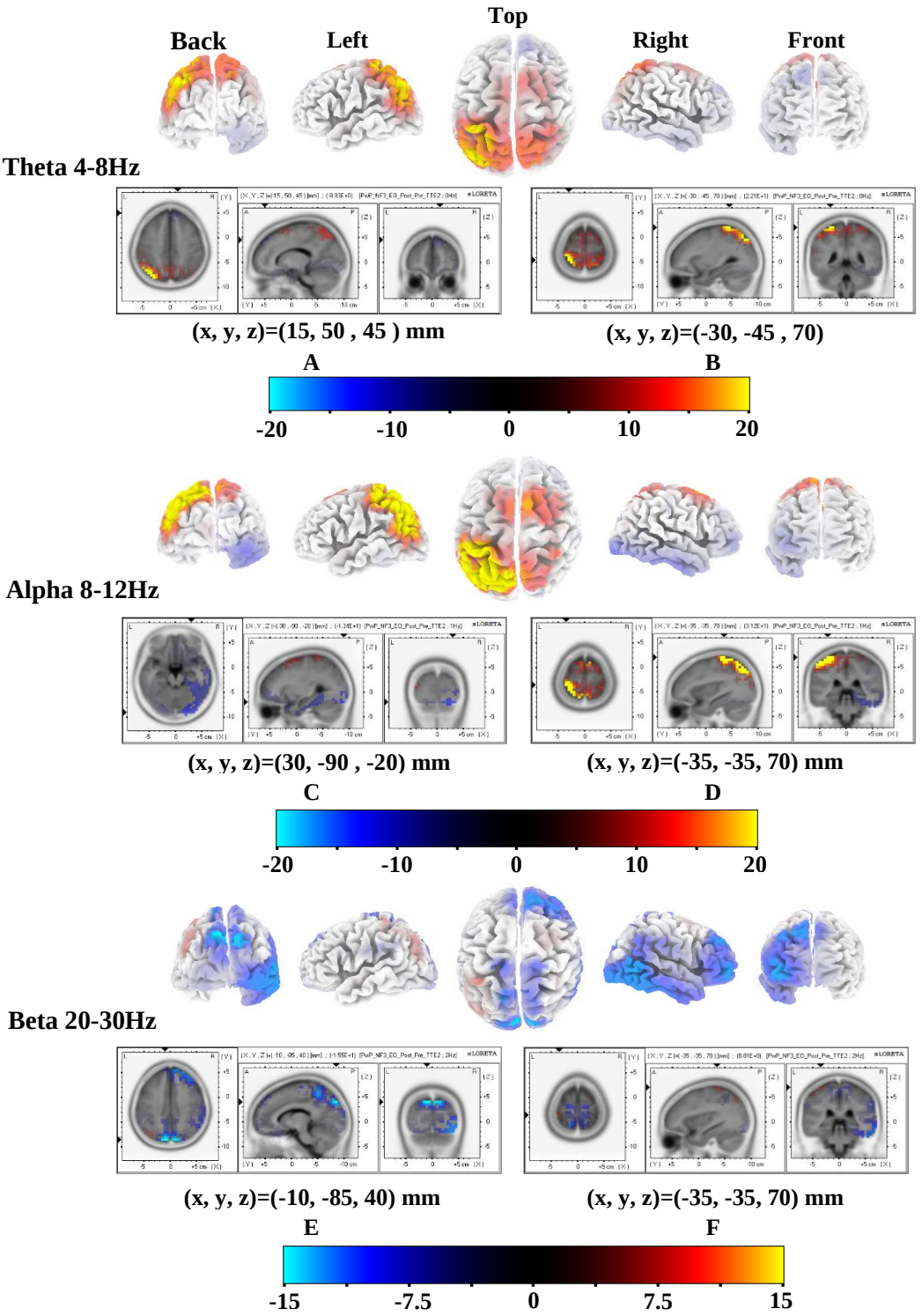


**Figure 5.9** sLORETA localisation of the different between eyes opened relaxed state after the last compared to before the first NF session for PwP_NF5 averaged over theta (4-8Hz) (A and B), Alpha (8-12Hz) (C and D) and Beta (20-30Hz) (E and F). The first raw of each figure represents 3D map of the localisation while the second raw represents the 3D slice at the displayed of the voxel with negative (A, C and E) and positive (B, D and F) strongest activity. The (x, y, z) under each figure represent the Montreal Neurological Institute and Hospital (MNI) coordinate system of the voxel with strongest activity.

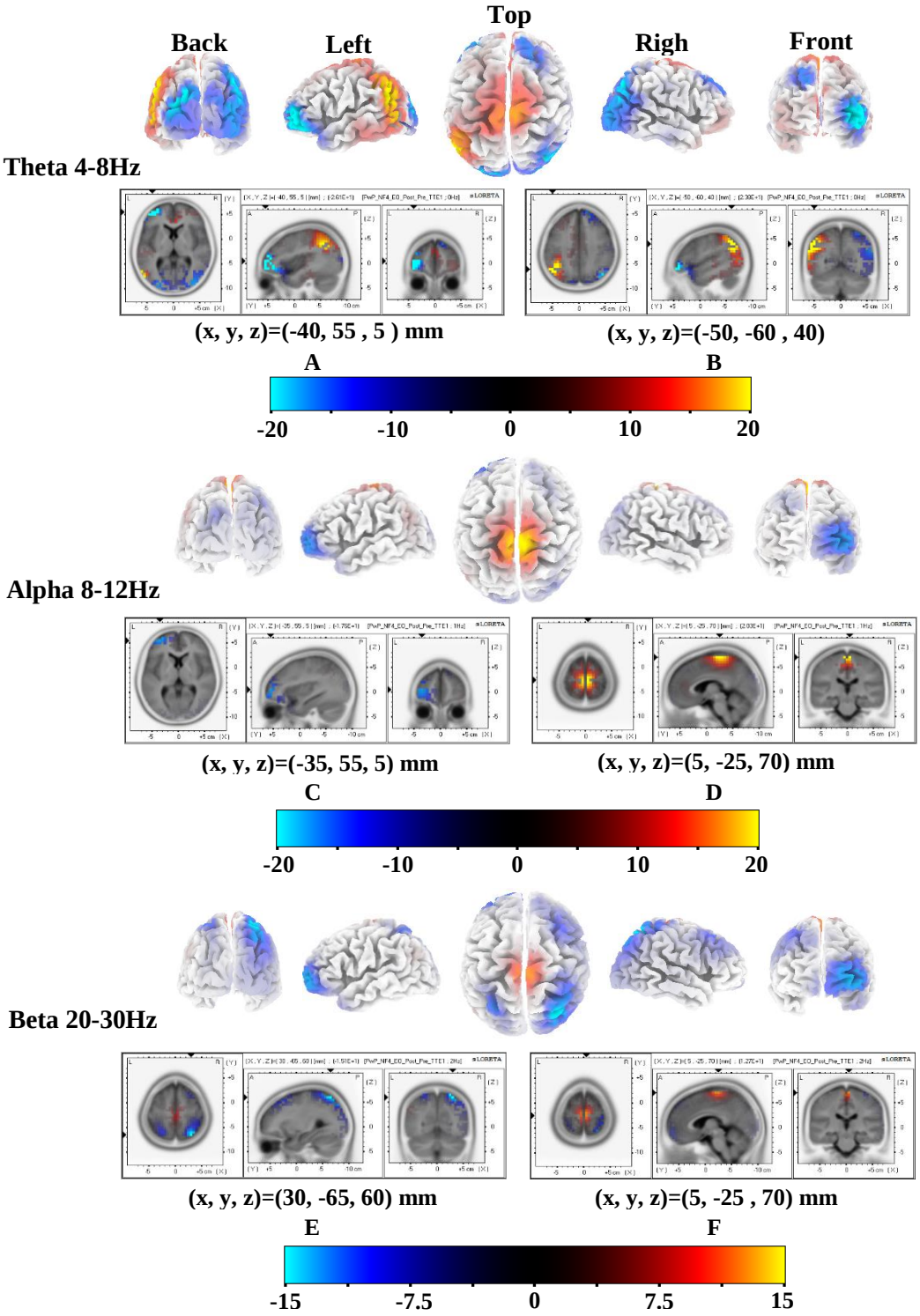


**Figure 5.10** sLORETA localisation of the different between eyes opened relaxed state after the last compared to before the first NF session for PwP_NF7 averaged over theta (4-8Hz) (A and B), Alpha (8-12Hz) (C and D) and Beta (20-30Hz) (E and F). The first raw of each figure represents 3D map of the localisation while the second raw represents the 3D slice at the displayed of the voxel with negative (A, C and E) and positive (B, D and F) strongest activity. The (x, y, z) under each figure represent the Montreal Neurological Institute and Hospital (MNI) coordinate system of the voxel with strongest activity.

## 5.4.5 Long term effect of NF training on ERS/ERD during MI task

The ERS/ERD maps for MI task of patients in the treatment group before the first and after the last NF training session over the primary motor cortex (M1) are shown in Figure 5.11-Figure 5.13. Figure 5.11 show the ERS/ERD maps during MI of feet over electrode location Cz located over M1 of the feet for all four patients. The vertical sold line represents a warning sign (a cross) appearing at t=-1s, while the vertical dashed line represents the MI execution cue at t=0s when patients started motor imagery. The EEG data during MI of feet of PwP_NF3 before the first NF session is not available because the MI data of the first assessment phase of this patient was taken from another study of our group which included only MI of the right and left hand. This data was taken from another study, which took place before NF training on the same patient for Ethical reasons, to minimize unnecessary discomfort to patients, as the assessment lasts about 2 hours. The patient was a control subject in a hand rehabilitation study.

It can be noticed that the level of desynchronisation (ERD, blue color), which is proportional to the level of activation of the motor cortex, was reduced in the post NF assessment compared to the first assessment, before starting NF therapy, in all patients. A significant reduction in theta and alpha ERD was noticed in PwP_NF5 and PwP_NF7. The reader should be reminded that in able-bodied individuals there should be no theta ERD, and that in general SCI patients with long standing CNP have stronger ERD (more active cortex during imagination of movement) than SCI patients with no pain[140].

During MI of the left hand over the electrode location C4 located over M1 of the left hand, a significant reduction in theta and alpha ERD can be noticed in PwP_NF3 (Figure 5.12). PwP_NF5 also exhibited a significant reduction in alpha ERD. As with MI of the left hand, PwP_NF3 also showed a significant decrease in theta and alpha ERD and PwP_NF5 showed a significant reduction in alpha ERD over electrode location C3 located over M1 of the right hand (Figure 5.13).

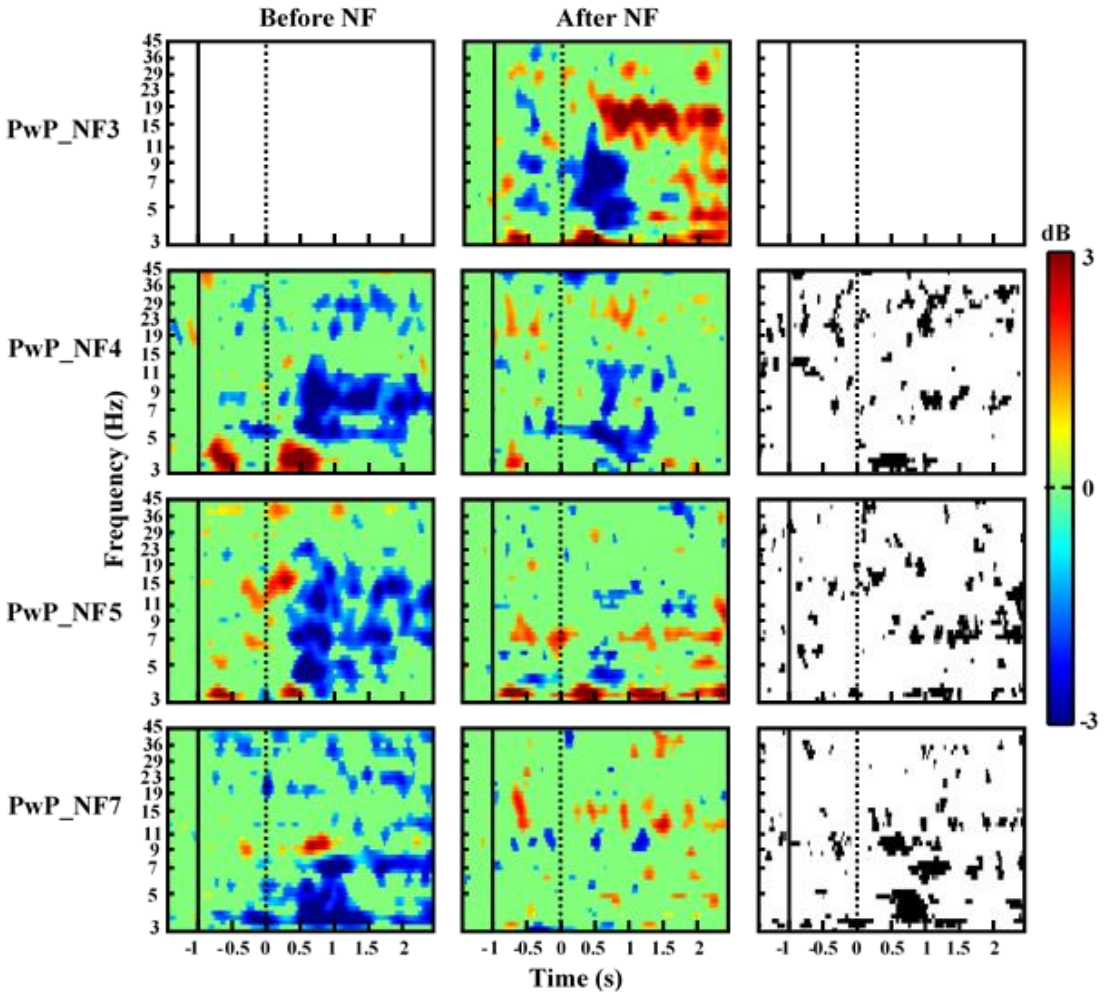


**Figure 5.11** ERD/ERS maps of electrode locations Cz for each patients in treatment group during motor imagery of feet. The first column shows before the first NF training session and the second column shows after the last NF training session. The last right column shows the areas of statistically significant (p=0.05) difference in ERD/ERS before and after neurofeedback training. At t=-1 s, a warning cross appears (the vertical sold line), while at t=0 s (the vertical dashed line) participants start with motor imagery. The ERD/ERS maps are shown for t= -1.5 s to 2.5 s and frequency 3 Hz to 45 Hz.

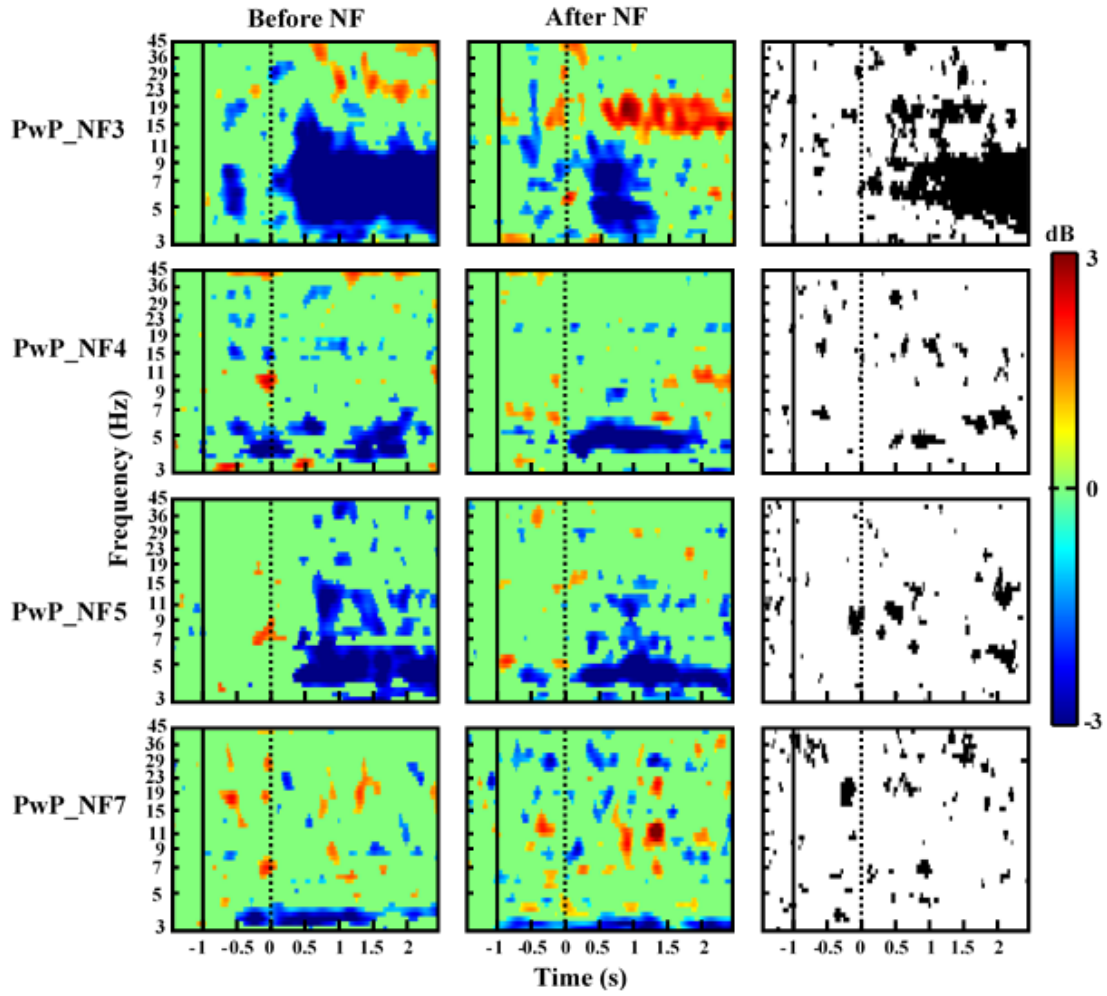


**Figure 5.12** ERD/ERS maps of electrode locations C4 for each patient in treatment group during motor imagery of left hand. The first column shows before the first NF training session and the second column shows after the last NF training session. The last right column shows the areas of statistically significant (p=0.05) difference in ERD/ERS before and after neurofeedback training. At t=-1 s, a warning cross appears (the vertical sold line), while at t=0 s (the vertical dashed line) participants start with motor imagery. The ERD/ERS maps are shown for t= -1.5 s to 2.5 s and frequency 3 Hz to 45 Hz.

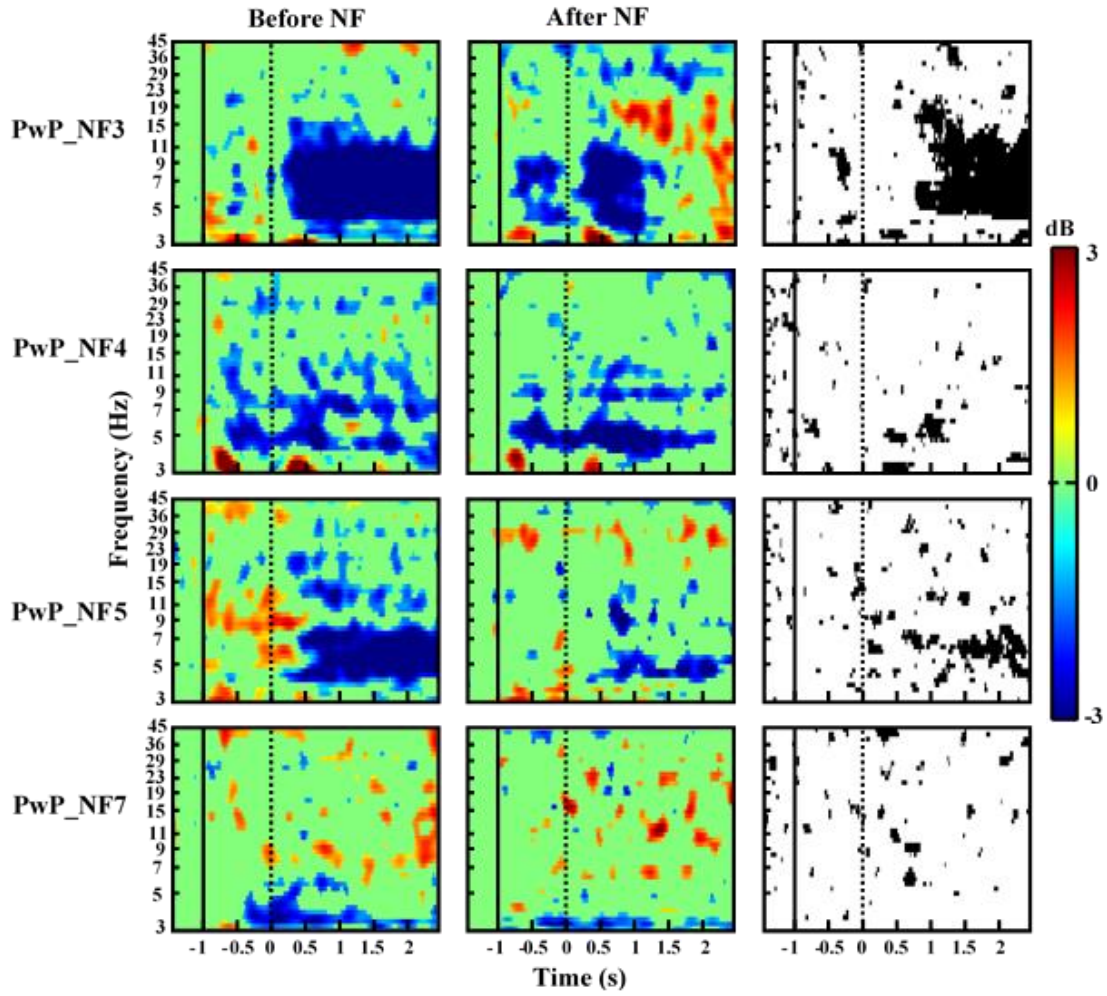


**Figure 5.13** ERD/ERS maps of electrode locations C3 for each patient in treatment group during motor imagery of right hand. The first column shows before the first NF training session and the second column shows after the last NF training session. The last right column shows the areas of statistically significant (p=0.05) difference in ERD/ERS before and after neurofeedback training. At t=-1 s, a warning cross appears (the vertical sold line), while at t=0 s (the vertical dashed line) participants start with motor imagery. The ERD/ERS maps are shown for t= -1.5 s to 2.5 s and frequency 3 Hz to 45 Hz.

## 5.4.6 Summary of the results

The results of pain intensities and perceived pain locations showed that NF affected both the overall intensity of the worst pain and the total area of the body which was perceived as being painful. Patients in the neurofeedback treatment group who finished ≥ 12 neurofeedback sessions had a clinically and statistically significant reduction in pain compared to the pain intensity before the neurofeedback treatment. The reduction of pain intensity of the treatment group was accompanied by reduction in the painful areas. In

contrast, there were no larger changes in the intensity of pain and in the area perceived as being painful in the control groups.

The analysis of the power spectral density during the neurofeedback training session showed that all 4 patients in the treatment group were able to modulate at least one or two frequency bands at the same time but none were able to simultaneously modulate all three frequency bands. The short-term effect of neurofeedback training session, measured by comparing the change in power spectral density during neurofeedback training session and a few minutes following the training showed the effects of the neurofeedback training session still remained for a few minutes after the neurofeedback training.

The results of the long-term effect of the neurofeedback treatment on spontaneous EEG showed that the activity of the theta band significantly decreased over the frontal region and significantly increased over the parietal region. In terms of activity of the alpha band, a significant increase was noticed over the parietal region while a significant decrease was noticed over the occipital and the frontal regions. Significantly increased beta activity over the frontal and the parietal regions was also noticed. In contrast, a significant decrease in beta activity was noticed over the parietal region.

The results of the long-term effect of the neurofeedback treatment on induced EEG showed that all patients had a reduction in event related desynchronisation compared (ERD) to the first assessment session. The significant reduction in theta and alpha ERD was noticed in PwP_NF3 during both right and left hand motor imagery. PwP_NF5 also exhibited a significant reduction in theta and alpha ERD, particularly during motor imagery of the right hand. PwP_NF7 showed a significant reduction in theta and alpha ERD and PwP_NF4 had a reduction in alpha ERD during motor imagery of feet.

## 5.5 Discussion

This study aims to explore the effectiveness of an early NF treatment of CNP in patients with SCI in a sub-acute phase (several months after injury). The intensity of pain and perceived pain locations in both PwP_NF and PwP_C groups will be discussed first followed by a discussion of the longer term effect of the NF on spontaneous and induced EEG activity.

### 5.5.1 Pain Intensities and the Perceived Pain Locations

The clinically and statistically significant lower pain intensity was noticed in three patients in a treatment group. The statistically significant reduction in pain intensity was accompanied by a reduction in painful areas as self-reported by patients. In the control group, pain varied by ±1 on the numerical analogue scale. Though this indicates that the pain level was stable it was not possible to perform statistical analysis due to only 4 measurements per patient being taken. However, in the control group there was not a large change in areas perceived as being painful.

Although PwP_NF demonstrated a reduction in pain intensity and pain location, none of them completed the whole planned 20 NF sessions. One reason for poor compliance with the study might be the lack of awareness that this type of pain is different from the nociceptive and often cannot be successfully treated by medications, which is a simpler and less time consuming solution. The other possible reason is that for patients, just learning to cope with various consequences of spinal cord injury, pain is not a high priority. This is a strong contrast with priorities of patients with long standing CNP, included in a previous study by our research group[44].

### 5.5.2 Immediate and Short-term Effect of NF training on EEG Activity

In all 4 patients who received multiple NF sessions, modulation of PSD during NF was noticed in at least one frequency band. The effect of the voluntary neuromodulation still remained for a few minutes (short-term effect) after the NF training session. However, none of the PwP_NF was able to modulate all three NF training bands simultaneously. The inability of the patients in the treatment group to control the three bands together might be due to the small number of NF sessions. Additionally, for a successful NF training, a certain level of concentration is required and patients should have good night's sleep; none of these two could be fulfilled for hospitalized patients with sub-acute injury. A simultaneous control of several frequency bands in different directions is considered a challenging task for NF training in general, independent of its purpose. Very often NF training produces a general increase or decrease of brain activity, which spreads beyond the targeted frequency band[274]. In this study we did not analyze the effect of neurofeedback from C4 on the rest of the cortex. Results of the previous study of our group[44] as well as results of neurofeedback in Chapter 3 of this thesis show that NF from one training site has a wide spread effect, therefore wide spread long term cortical changes should be expected as a result of NF training from a single electrode location.

### 5.5.3 Long-term effect of NF on spontaneous and induced EEG activity

The comparison of the sLORETA localisation results of the relaxed state between the first and after the last NF session showed a significant decrease in theta activity over the frontal region in three out of four patients. All patients showed significantly increased theta activity over the parietal region. A significant increase in alpha activity was noticed over the parietal region of the right hemisphere in 3 out of 4 patients and a significant decrease in alpha activity was noticed over the occipital region in two patients and over the frontal

region in the other two patients. In the beta band, three out of 4 patients showed a significant increase in power over the frontal region while one showed a significant increase over the parietal region. Significantly lower beta activity was noticed over the parietal region in 2 patients.

Parietal and frontal regions were most consistently affected by NF, and the increase in theta and alpha power over the parietal region was the most consistent result across all four patients. The parietal region is a part of the sensory cortex, which in the cortical pain matrix is responsible for discrimination of the sensory component[14,15]. A training electrode C4 was close to the parietal area and these changes might be directly related to modulation of the cortical activity over C4, though patients' performance during NF was not always consistent.

In all patients significant changes in cortical activity were also noticed over the frontal area but the trend of change was not consistent across patients. The frontal area is not close to C4 but it is functionally related to the parietal area in a sense that they both form a pain matrix, but the frontal area is responsible for the affective component of pain[275].

In chapter 4 of this thesis, we show that patients who recently developed pain have on average decreased alpha activity over the parietal cortex. Increase in the alpha band activity, following NF treatment indicates normalization of cortical activity, towards the activity of SCI patients who do not have CNP.

The ERD/ERS analysis of the EEG data recorded during MI tasks before the first NF training session showed that all patients had over-activation (strong ERD) over the motor cortex (M1). Previous fMRI and EEG studies reported overactive M1 in SCI patient with CNP compared to an able-bodied control during motor imagery tasks[140,141]. Additionally, the strong ERD was noticed during MI of both the painful and pain-free limbs. These results confirm the finding of a previous study of our group, which reported that CNP

affects wide spread cortical activity and the changes in ERD are not necessarily only related to M1 corresponding to the painful limbs[140]. The comparison of the ERD/ERS of the EEG data recorded during MI tasks before the first and after the last NF showed a significant reduction in ERD activity specifically over theta and beta bands. These results confirm the finding of our previous NF study on chronic SCI patients with CNP which showed reduction in ERD after NF therapy[267].

### 5.5.4 Limitation of the study:

The main limitations of the study are the small number of patients in both the control and treatment group and the small number of sessions. For the effect of any NF training to last beyond the duration of the study, it is necessary to have at least 20 sessions.

Another limitation is the lack of placebo testing, as performed in[44]. Placebo is normally tested once the patients learn to consistently regulate their brain activity in a desired direction during non-placebo training. Although testing for placebo was planned towards the end of 20 NF sessions, none of the patients got enough training to achieve these criteria.

## 5.6 Conclusion

The results of this study demonstrate that the NF treatment has a positive effect on the reduction of pain, at least over the period of the study. Most notably, even a relatively small number of training sessions resulted in statistically significant changes in brain activity in a direction towards the activity of patients with no pain. It would be interesting to know whether this effect would also be noticed in patients suffering from CNP for years or if it is due to the relatively short lasting nature of CNP in patients with sub-acute CNP.

Despite these encouraging results, numerous factors, and in particular patients' low prioritization of pain, indicate that early NF of CNP in SCI patients might not be a

practical solution. This conclusion could probably be extended to any non-pharmacological treatment of pain, which would require patients' active involvement and additional time.

# 6

# Central Neuropathic Pain in Paraplegia Alters Movement Related Potentials

# Chapter 6 Central Neuropathic Pain in Paraplegia Alters Movement Related Potentials

## 6.1 Abstract

***Objective:*** to define the influence of paralysis caused by spinal cord injury (SCI) and related central neuropathic pain (CNP) on movement related potentials in a cue-based motor imagination task.

***Methods***: Three groups were included in the study: 10 able bodied (AB), 9 SCI patients with no pain (PnP) and 10 SCI patients with CNP in lower limbs (PwP). They were asked to perform a cue dependent motor imagination task involving the feet (paralysed in both PnP and PwP, also painful in PwP), and the left and the right hand while their brain activity was recorded with multichannel EEG. Measure projection analysis, based on independent components and the equivalent dipoles, was used to define cortical areas which show high functional connectivity.

***Results:*** Three domains were identified: domain 1 consists of limbic cortex and some subcortical structures; domain 2 consists of sensory-motor cortex and BA 31, a part of the limbic cortex, and domain 3 covering the visual cortex. With respect to morphology, ERP in all three domains included peaks corresponding to cognitive processes related to visual cues. Only domain 2 contained movement related potentials while both domains 1 and 2 had reafferentation potential, related to kinesthetic sensory processing. The largest influence of CNP on ERP was noticed in domain 1 where only the earliest components were visible in PwP group. Compared to ERP in the AB and PnP groups, in the PwP group the component corresponding to P200 was significantly smaller in domain 1 and significantly larger in domain 2. The PnP group had ERPs similar to AB but with significant delays in domains 1 and 2.

***Conclusion:*** motor related potential is dominantly influenced by paralysis while both CNP and paralysis affect the reafferentation potential. Additionally, CNP influences cognitive processes in a manner that depends on the functional area of the cortex.

## 6.2 Introduction

Central Neuropathic Pain (CNP) is caused by an injury to the somatosensory system[11], affecting more than 40% SCI patients[270]. Several EEG and fMRI studies have shown a link between CNP and brain activity[16,136,139,194]. Most EEG studies of CNP analysed the influence of CNP on the resting state EEG, showing increased EEG power in the theta band and a shift of the dominant alpha frequency towards lower frequencies[139,194]. Functional MRI studies in addition demonstrated remapping of the sensory-motor cortex and an increase in activity over the primary motor cortex[16,136]. In addition to CNP, patients with SCI suffer from the impairment of sensory and motor functions which itself also affects brain activity, both in a resting state[263] and during a motor task[93,276,277].

To understand the effect of SCI on EEG during a motor task researchers have analysed both event-related synchronisation/desynchronisation (ERS/ERD)[228] and movement related cortical potential (MRCP)[95] as these two phenomena have different cortical origins. MRCP is a subtype of Event Related Potential (ERP) and presents the type of post-synaptic responses of main pyramidal neurons[278] triggered by an overt or covert motor action while ERS/ERD presents changes in parameters that control oscillations in neuronal networks[228]. Pfurtsheller et al. found that people with chronic SCI have altered and weaker ERS/ERD compared to able-bodied people[277]. Castro et al. analysed movement related potentials in people with SCI imagining the movement of a paralysed limb[93]. They found that people with SCI have lower readiness and movement related potentials while imagining moving paralysed limbs than able bodied subjects executing the same movement.

One of current problems in this research is that during imagination of movement both groups had comparable motor potentials over the primary motor cortex. Xu et al. analysed movement related cortical potential (MRCP) over the central cortical regions covering the primary motor cortex of arms and legs (C3, Cz and C4) in the same groups[92]. However, they could not find statistical differences between two groups of patients, even though they found differences between able-bodied and SCI patients in general. One of the reasons for this is that Xu and colleagues may have missed the macro-scale brain activation patterns because they used only three electrodes. In a recent EEG study by our group, using 61 channels EEG recording system, indicates the influence of CNP on wider cortical structures[140]. In that study, Vuckovic et al. analysed ERS/ERD during imagined movement in a group of patients with low level SCI (paraplegia) and CNP and compared them with a group of SCI with no pain and with a group of able-bodied people. They found that CNP resulted in a stronger ERS/ERD in theta, alpha and beta band with characteristic spatial distribution, that were present during the imagination of movement of both painful and non-painful limbs[140]. A group with SCI and no pain had similar but weaker ERS/ERD than the able-bodied group. Thus Vuckovic et al. showed that it is possible to distinguish between the influence of paralysis and of CNP on ERS/ERD analysis[140]. This lead us to expect that recent development of EEG analysis using multivariate signal processing and statistics should allow us to exploit more useful information from the 61-channel EEG data recorded from these patients to further characterize the influence of SCI on CNP.

In the present study, we applied a recently developed Measure Projection Analysis (MPA)[112], which is a post processing method after independent component analysis (ICA) and equivalent current dipoles, to determine the influence of SCI on CNP. MPA determines domains, which are defined as clusters of independent components with statistically proximate locations and similarity in measures, i.e. ERP in this case. The novelty of MPA approach is that it enables the analysis of a motor task in terms of

functionally rather than spatially distinctive domains. We hypothesise that each functionally distinctive domain will have characteristic morphology of ERP and that ERPs in different domains might be affected to a different degree by SCI and by CNP. The advantage of ERP over the ERS/ERD analysis is that it can distinguish between the cognitive, motor, and afferent sensory components by identifying the peaks of the corresponding ERP components. Thus we analysed the effect of CNP and SCI on each component separately. While Vuckovic et al.[140] defined the influence of CNP on different frequency bands, in this study we investigate the effect of CNP based on different phases of cue-based motor task.

## 6.3 Methods

### 6.3.1 Participants

Ten able bodied subjects (AB) (3 Female (F) , 7 Male (M), age 39.1 ±10.1), 10 patients with SCI with CNP (PwP) below the level of injury (3 F, 7 M, age 45.2 ± 9.1) and 9 patients with SCI and with no acute or chronic pain (PnP) (3 F, 6 M, age 44.4 ±8.1) participated in the study. The American Spinal Injury Association Impairment Classification scale[279] was used to determine the neurological level of injury. Inclusion criteria for PwP were the presence of pain ≥ 5 on the Visual Numerical Scale (0=no pain, 10=worst pain imaginable) and the presence of pain for at least 6 months. The inclusion criteria for both PwP and PnP groups were that they had a spinal lesion for at least 1 year post-injury at level T1 or lower. Exclusion criteria for all 3 groups were the self-reported presence of neurological disorders or brain injury which would influence EEG interpretation and the presence of any other chronic pain at the time of the experiment. The demography of PwP and PnP groups is shown in Table 6.1 and Table 6.2, respectively.

All participants provided informed consent for the study; the study was approved by the National Health Service ethical committee for SCI patient groups and by the University

ethical committee for able-bodied volunteers. The experiments were performed in accordance with the Declaration of Helsinki.

**Table 6.1** The demography of the SCI patients with CNP. G: Gabapentin, P: Pregabalin,

| No. | Level of Injury | ASIA* | Years After Injury | Intensity of Pain (VAS¥) | Year with Pain | Medication |
|---|---|---|---|---|---|---|
| 1 | T5 | A | 7 | 7 | 7 | G, carbamzepine |
| 2 | T5/T6 | A | 11 | 6 | 11 | none |
| 3 | T5 | A | 7 | 8 | 7 | P,G |
| 4 | L1 | B | 15 | 7 | 15 | G |
| 5 | T6/T7 | D | 4 | 7 | 3 | P |
| 6 | T7 | B | 6 | 8 | 5 | none |
| 7 | T6/T7 | B | 25 | 10 | 24 | G |
| 8 | T1 | A | 25 | 5 | 10 | P |
| 9 | T5 | A | 14 | 5 | 13 | Amitriptyline |
| 10 | L1 | B | 5 | 5 | 4 | none |

* ASIA: The American Spinal Injury Association. ¥ VAS: Visual Numerical Scale

**Table 6.2** The demography of the SCI patients with no CNP

| No. | Level of Injury | ASIA* | Years After Injury |
|---|---|---|---|
| 1 | T7 | A | 7 |
| 2 | T7 | B | 7 |
| 3 | T12 | A | 7 |
| 4 | L1 | A | 6 |
| 5 | T2 | A | 2 |
| 6 | T5 | B | 15 |
| 7 | T11 | A | 11 |
| 8 | T4 | A | 9 |
| 9 | T7 | A | 15 |

* ASIA: The American Spinal Injury Association

## 6.3.2 EEG Recording

EEG signal was recorded using a 61 channel EEG device (Synamp$^2$, Neuroscan, USA). The electrodes were placed according to the standard 10-10 system[257]. An ear-linked reference was used and an electrode placed at AFz served as ground. The sampling frequency was 1 kHz and the electrode impedance was below 5kΩ. Electromyograms (EMG) were recorded from the right and left wrist extensor muscles and right shank using the bipolar inputs to the Synamp device. The only purpose of the EMG was to check that

there was no evidence of voluntary movements when subjects attempted motor imagination (MI).

### 6.3.3 Experimental Setup

Participants were instructed to perform a MI task which consisted of imagining waving with their right or left hand or tapping with both feet every time they saw a corresponding visual cue at a computer screen. The experimental protocol of the motor imagination task were the same as described in chapter 4 section (4.3.5).

### 6.3.4 EEG Signal Pre-Processing

The EEG signal was divided into epochs, starting at t=-1s and finishing at t=3s (4s long). The epoched EEG signal was high passed filtered at 0.1Hz (IIR, 12db cut-off frequency) and a notch filter (48Hz – 52Hz) was also applied in order to remove the line noise (50Hz). Then, the EEG signal was down-sampled to 250Hz. The down-sampled EEG signal was then exported to EEGLab[99]. In EEGLab, EEG signal was visually inspected and trials containing an amplitude larger than 100μV over all channels or that were accompanied with EMG were manually rejected. No more than 3-4 trials were rejected per participant. Following this, the EEG signal was re-referenced to an average reference and independent component analysis (ICA) decomposition was performed as described below. IC components containing biological or instrumental noise identified by their characteristic morphology, spatial distribution and frequency content were removed prior to further analysis.

### 6.3.5 ERP Measure Projection

The measure projection method comprises of[112]:

1. ICA decomposition and equivalent dipole localisation

2. Spatial smoothing of a given dynamic measure (in this case ERP) for the equivalent dipole-localised ICs.
3. Measure Projection Analysis: this comprises defining the subspace of brain voxel locations with significant local IC measures of similarity.
4. Creating spatial brain voxel domains which exhibit sufficient measure differences.

### 6.3.6 ICA Decomposition, Equivalent Dipole Localisation and Spatial Smoothing

ICA decomposes EEG from multiple channels into maximally temporary independent components by creating a set of spatial filters W. Independent components are then created from EEG using a simple linear transformation (6.1).

$$S = W.X \qquad \textbf{6.1}$$

Where S is the effective source EEG activation that is decomposed by ICA, W is an unmixing matrix, and X is the observed signal. The filters W have a fixed projection to recording electrodes and produce the maximally independent time courses of data. Thus ICA defines which independent processes contribute to data recorded on a scalp EEG and reveals their independent scalp projections. Some of the components represent non-brain 'artifact' sources i.e. 'noise', having either biological (EOG, ECG, EMG) or instrumental (e.g. line noise) origin and can be removed from the ICAs set. To calculate ICs, the Informix algorithm[280] with the extended-ICA algorithm[281] that extracts the mixed sub-Gaussian and super-Gaussian sources effectively was implemented in EEGLab[99].

Following noise removal, the location of dipoles corresponding to remaining ICs were determined for each IC based on the boundary element model MNI[282]. A single dipole location procedure was used to estimate the location of the ICs, as most IC originating from the brain can be modelled by a single dipole[283]. Compared to methods which estimate a dipole location from EEG scalp maps, that present the mixture of sources, the uncertainty

of dipole locations based on ICs is reduced due to the fact that each ICA presents a single source. The set of ICs with a low residual variance (<15%) and with equivalent dipoles located inside the Montreal Neurological Institute (MNI) brain volume were chosen for data analysis[112]. This allowed anatomical location over the cortex and defining the nearest Brodmann Areas (BA), as well as several subcortical areas.

The precise localisation of sources is possible only if a precise head model based on magnetic resonance imaging MRI of that subject is available[282]. The level of accuracy in this group analysis was somewhat reduced due to a fact that the cortical locations of multiple subjects were wrapped into a common head model to allow group Measure Projection (MP). Therefore the dipole localisation method may occasionally localise sources deeper than they are really located. A co-registration between channel locations and the head model surface was performed to align the dataset channel locations to a three-shell stored Boundary head model template montage, followed by dipoles fitting for the ICs.

A spatial smoothing was performed using a truncated 3-D Gaussian spatial kernel. A standard deviation for each 3-D Gaussian, representing each equivalent dipole location, was set to 12mm (full width half maximum). This value was recommended by creators of MPA method[112] and was chosen heuristically to minimise the ambiguity of equivalent dipole localisation arising from numerical inaccuracies, errors in measurement methods and in a head model. Each Gaussian was then truncated to a radius of 3 standard deviations (36mm) to prevent interfering influences from distant sources.

In this study, common ICs were calculated for EEG of all three conditions together (MI of right hand, left hand and of both feet) and common dipoles were defined. However, following this step, data from different conditions was separated for Measure Projection Analysis (MPA), because it was expected that they would have a distinctive ERP, different for MI of each motor task.

### 6.3.7 Measure Projections Analysis

This step is the core of the whole analysis. MPA is a method which compares EEG source locations and dynamics across different subjects and sessions in a 3-D brain space[112]. It is based on a probabilistic approach that treats source-resolved data as samples drawn from the distribution of source locations and dynamics. It focuses on a single dynamic measure (in this case ERP) and performs a statistical analysis on the grid of brain locations rather than on individual sources.

In order to define the subspace of brain voxel locations with significant local IC measures, a brain volume was presented as a cubic dipole source space grid with 8mm spacing. Voxels outside the MNI brain volume were discarded.

A measure vector *Mi(x)* was then obtained by vectorising the ERP time course associated with each single IC with an equivalent dipole *D(x)*. Based on this, the method estimates an interpolated measure vector *M(y)*, defined across all possible brain locations $y \in V$, and estimates the statistical significance (i.e. *p* value) of this assignment for each of these locations. The *p* value is associated with a null hypothesis that *M(y)* has a random spatial distribution in the brain.

Each estimated dipole *Dj*, *j*=1…n, is presented by a spherical truncated Gaussian kernel with covariance $\sigma^2 I$ at an estimated dipole location, $\hat{x}_j$ where standard deviation $\sigma$ encapsulates dipole localisation errors. The Gaussian is further normalised to ensure that densities in the different areas of brain volume (e.g. deep inside the brain and closer to the surface) have a unity mass within the brain volume.

A probability that an estimated dipole *Dj* is truly located at position *j* is presented by a normalised truncated Gaussian distribution $P_j(y) = TN(y; \hat{x}_j, \sigma^2 \cdot I, t)$. For an arbitrary location, the value of expected (projected) measure vector *M(y)* is (Equation 6.2):

$$E\{M(y)\} = \langle M(y) \rangle = \frac{\sum_{i=1}^{n} P_i(y) M_i}{\sum_{i=1}^{n} P_i(y)} = \sum_{i=1}^{n} \overline{P}(y) M_i \qquad \textbf{6.2}$$

Where $\overline{P}(y)$ (with a property $\sum_{i=1}^{n} \overline{P}_i = 1$) is a probability that the estimated location of measure vector $M_i(y)$ is truly $M(y)$

The next step upon obtaining an estimate measure vector $M(y)$ at each brain voxel location is to test against the null hypothesis that $M(y)$ is produced by a random set of measure vectors $M_i$. The overall goal of this is to identify brain areas, or 'neighborhoods' that exhibit statistically significant similarities in ERP based measure between IC of equivalent dipoles within the neighborhood. To do that it is necessary to calculate the measure of convergence $C(y)$ at each brain location $j \in V$ (Equation 6.3).

$$C(y) = E\{S(y)\} = \frac{\sum_{i=1}^{n} \sum_{j=1, j \neq i}^{n} P_i(y) P_j(y) S_{i,j}}{\sum_{i=1}^{n} \sum_{j=1, j \neq i}^{n} P_i(y) P_j(y)} \qquad \textbf{6.3}$$

Where $P_i(y)$ is the probability of dipole $D_i$ being at location $y$, and $P_j(y)$ is the probability of dipole $D_j$ being at location $y$, with an additional assumption that dipoles are independent, in order to factorise a joint probability. Factor $S_{i,j}$ is the degree of similarity associated with dipoles $D_i$ and $D_j$. Convergence $C(y)$ is the expected value of the measure of similarity at location $y$. The calculated value $C$ is a scalar which is larger in the area of homogenous (similar) ICs.

To check the statistical significance of $C(y)$, i.e. to calculate a Type I error, randomised surrogates were created and a nonparametric bootstrapping method to create a surrogate null distribution, was applied. The significance of convergence of $C(y)$ (a significant $p$ value) was obtained by comparing it to the right tail of a null distribution. After calculating $p$ values for each single voxel, a correction for multiple comparisons was applied using the False Discovery rate method[259].

The recommended measure of the degree of similarity $S_{i,j}$ in MPT toolbox is the signed mutual information $SMI$[284] ( Equation 6.4) between IC-pair ERP measure, which is based on a correlation CORR[112].

$$SMI = \frac{1}{2} sign(CORR) \log_2 (\frac{1}{1 - CORR^2})(bits / sample) \quad \textbf{6.4}$$

Once the significance of *C(y)* is found for each group and each task, they can be compared between tasks or between groups. This step requires that the size of each domain is defined as described in the next subsection. For now, let's assume that the number and the size of each domain have been defined. To determine a statistically significant difference between tasks/groups it is necessary to determine a weighted-mean measure *WM*, based on mean measures (here SMIs, Equation 6.4) across all voxels belonging to one domain. To achieve this we produce *WM* values for each task within a group (for example, MI of foot in PwP, MI of foot in PnP, MI of right hand in PnP etc) in order to compare between groups and tasks. Different tasks for different groups will be called a condition *c* further in the text. In this study we have 9 conditions (3 tasks and 3 groups).

Let's assume that a domain of interest *d* has $\nu$ voxels ($i$=1…$\nu$). For a condition *c*, a weighted-mean measure *WM(d,s,c)* across all $\nu$ voxels is (Equation 6.5)

$$WM(d,s,c) = \frac{\sum_{i-=1}^{\nu} M(c,i,d) \cdot D(i,s)}{\sum_{i=1}^{\nu} D(i,s)} \quad \textbf{6.5}$$

Where $D(i,s) = \sum_{j=1}^{n} P_j(i)$ **6.6**

Above, *n* is the number of component dipoles for a certain condition and $P_j(i)$ is a model probability that a dipole *j* is actually located at a domain voxel *i*. Once *WM* values

were obtained for each condition, a two-tailed student t-test was applied to reveal a statistically significant ERP difference between conditions within a domain.

### 6.3.8 ERP domain clustering

The method chosen for domain clustering in the MPT toolbox is Affinity Propagation Clustering[285]. The clustering step is only used to determine the granularity of segmentation of brain regions exhibiting significant measurement consistency obtained in the previous step and therefore does not change the projected source measurement values. It is based on the similarity matrix $S_{nxn}$ of pairwise correlations between n measure projection values at each voxel point. This method has the following properties:

1. It does not require a prior knowledge of the number of clusters. It automatically finds the appropriate number of clusters based on the maximum allowed correlation between the cluster exemplars. It increases the number of clusters until any potential cluster exemplar becomes too similar to one of the existing exemplars. In this study correlation was set to the recommended value of 0.8[112]. This means that the maximum allowed correlation between clusters is 0.8. Increasing the correlation value to 0.9 would result in increased number of clusters of smaller size (but they would cover the same 3D area as clusters in the case of correlation=0.8). Likewise, reducing correlation to 0.7 would result in a smaller number of clusters of larger size. For the outlier cluster, a correlation was set to the recommended value of 0.7.

2. Affinity propagation clustering determines outliers during the clustering process. This is achieved by adding an additional row and column to the pair-wise similarity matrix $S$ which now has $n+1$ rows and columns $S_{(n+1)x(n+1)}$. The $n+1^{st}$ column and row contain a fixed element $T_o$, and each point that is less similar than $T_o \in R$ to any cluster exemplar is assigned to the outlier cluster.

3. Clusters do not have a fixed geometric shape (e.g. a sphere as in k-mean clustering). In addition, spatially discontinuous regions of the brain can belong to the same cluster if they present highly functionally connected areas. Finally, because the MPA method is based on the probabilistic representation of dipole locations, it is not necessary that the IC of each single subject contributes to each domain.

To apply measure projection analysis, the Measure Projection Toolbox, which is operated as an EEGLab plug-in under MATLAB (The Mathworks, Inc, USA), was used. There were three groups in the study, AB, PwP and PnP. Each group has three experimental conditions, which corresponded to motor imagery of the right hand, left hand and feet. Data was grouped using a study structure in EEGLab for the purpose of further analysis.

## 6.4 Results

The results of spatial locations of domains are presented first followed by comparison of ERP between different conditions (tasks and groups). The ERP domains are shown in Figure 6.1. Figure 6.1a shows the spatial location of all three domains together, relative to each other. Figure 6.1 shows the contribution of different groups to different domains. It can be noticed that dipoles of all three groups are mixed showing no obvious clustering of one particular group within a domain.

### 6.4.1 Analysis of the Spatial Locations of Domains

Locations of domains with respect to corresponding BAs are shown in Table 6.3. Brodmann Areas (BA) with contributions less than 5% are not shown (thus explaining why probabilities do not add up to 100%). Subcortical areas are indicated as being closest to the BA of interest.

Domain 1 is located within the limbic system which is responsible for regulating sadness and affective components of pain over the subcortical regions responsible for control of movement and sensory processing, including pain. It covers three Brodmann areas BA25, BA23 and BA34 and subcortical regions such as the caudate, brainstem and putamen. The domain is slightly shifted towards the left hemisphere.

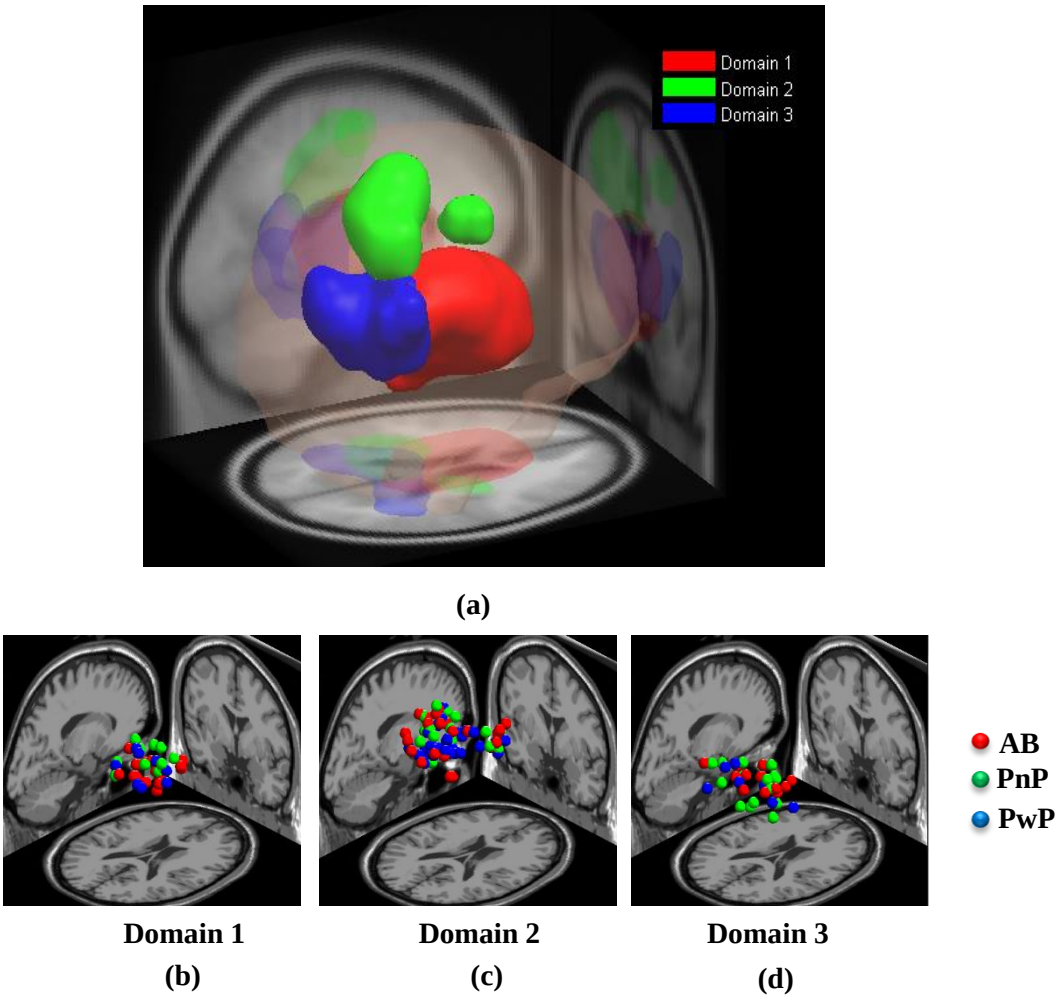


**Figure 6.1** MPT domains (a) Relative locations of domains, (b, c and d) Contributions of all groups in each domain; Red: able bodied (AB), Green: patients with no pain (PnP) and Blue: patients with central neuropathic pain (PwP)

Almost half of the domain belongs to BA25 which is located in the cingulate cortex and is responsible for serotonin transport, and neuroimaging studies indicate that this region of the brain is involved in processing sadness[286]. BA23 is located in the posterior cingulate cortex (PCC), which is, amongst other, involved in the affective component of

pain[275,287] and is believed to be a part of the Default Mode Network[288]. There is a functional relation between PCC and BA25 as they belong to the Default Mode Network and they both seem to be affected by depression in a similar [286,288]. Brodmann area BA34 is a part of the superior temporal gyrus.

**Table 6.3** BAs contributing to different domains with corresponding probabilities.

| Domain 1 | | Domain 2 | | Domain 3 | |
|---|---|---|---|---|---|
| Location | Probability | Location | Probability | Location | Probability |
| BA 25 | 0.47 | BA 31 | 0.29 | BA 30 | 0.27 |
| BA 23 | 0.16 | BA 3 | 0.17 | BA 19 | 0.22 |
| BA 34 | 0.16 | BA 4 | 0.14 | BA 37 | 0.08 |
| BA 29 | 0.06 | BA 6 | 0.12 | BA 23 | 0.08 |
| BA 28 | 0.06 | BA 40 | 0.08 | BA 27 | 0.07 |
| Caudate | | BA 2 | 0.06 | BA 18 | 0.07 |
| Brainstem | | BA 23 | 0.06 | | |
| Putamen | | | | | |

The rest of domain 1 covers subcortical structures but these areas should be interpreted with caution due to a known tendency of the head model used in EEGLab to locate dipoles deeper in the brain. The brainstem is an important pathway connecting the motor and sensory systems from the main part of the brain to the rest of the body. It contains both motor and sensory (touch, vibration) pathways, and pain and temperature pathways. Caudate and putamen are parts of the corpus striatum and are, among other functions, involved in the control of movements of the limbs and in processing of pain. Unlike the brainstem they do not contribute directly to the corticospinal tract[289].

A large part of Domain 2 belongs to BA 31 anatomically located at the postcentral gyrus, a part of the PCC (dorsal posterior cingulate area), which is a part of the limbic system. Other areas of domain 2 involve the primary somatosensory cortex (BA2 and 3), primary motor cortex (BA4) and supplementary and premotor cortex (BA6), areas of the

brain involved in high level sensory-motor control of movement. Domain 2 also involves BA40, which is responsible for spatial and semantic processing and has previously been found active in cue-based motor imagery tasks[290]. Although domain 2 includes two spatially disjointed areas, in fact these areas belong to neighboring BA (6, 4, 2, and 3).

Most of domain 3 belongs to the occipital cortex. The largest parts belong to BA30 and BA19, the former involves the agranular retrolimbic area and is responsible for a higher cognitive function, like audio-visual integration and, the later involves the associate visual cortex. The latter is also the part of the visual association area (V3) responsible for multimodal integration functions. The activity of Domain 3 is related to visual processing of the cue-based motor task.

### 6.4.2 Analysis of ERP

We first present ERP morphology in different domains in able-bodied people in Figure 6.2a-c and then compare it with ERP in other two groups. ERP is presented for each domain separately and compared pairwise among three groups for each MI task separately. The time delay of all peaks for all groups and for each MI condition for domains 1, 2 and 3 is shown in Table 6.4, Table **6.5** and Table **6.6**, respectively.

Figure 6.2a-c shows ERP in all three domains for a representative MI of left hand in AB group. We defined clearly visible peaks, present for all three types of motor imagination (the other two types of motor imagination are shown in Figures 6.3-6.5. Peaks larger than 0 were defined as positive and peaks smaller than 0 were defined as negative. Positive ‘peaks’ in between two negative peaks staying under 0 were not counted as real peaks. Consecutive positive and negative peaks beard the same numbers which increased consecutively from left to right on the time axis. In Tables 6.4-6.6, the delays of peaks were calculated with respect to the nearest event, i.e. the appearance of a warning sign at

t=-1s, the appearance of the execution cue at t=0s and the disappearance of the execution cue at t=1.25s. The vertical lines in the figures delineate between these events.

**Table 6.4** Delays of positive and negative peaks describing ERP in Domain 1 with respect to the nearest cue. Delays of peaks N1 and N2 correspond to the appearance of a warning cue at t=-1s. Delays of peaks N3 to P4 correspond to the appearance of the execution cue at t=0s and delays of peak N5 corresponds to the disappearance of the execution cue at t=1.25s.

| Group | MI condition | N1 | N2 | N3 | N4 | P4 | N5 |
|---|---|---|---|---|---|---|---|
| AB | LA | 220 | 440 | 250 | 330 | 720 | 255 |
| | RA | 220 | 420 | 250 | 350 | 730 | 250 |
| | F | 180 | 430 | 250 | 330 | 880 | 260 |
| PwP | LA | 220 | - | 215 | - | - | - |
| | RA | 205 | - | 220 | - | - | - |
| | F | 210 | - | 220 | - | - | - |
| PnP | LA | 210 | 460 | 290 | 430 | 1030 | - |
| | RA | 200 | 445 | 290 | 410 | 1080 | - |
| | F | 210 | 430 | 260 | 420 | 990 | - |

**Table 6.5** Delays of positive and negative peaks describing ERP in Domain 2 with respect to the nearest cue. Delays of peaks N1 and P1 correspond to the appearance of a warning cue at t=-1s. Delays of peaks P2, N2 and P3 correspond to the appearance of the execution cue at t=0s.

| Group | MI condition | N1 | P1 | P2 | N2 | P3 |
|---|---|---|---|---|---|---|
| AB | LA | 170 | 300 | 140 | 200 | 330 |
| | RA | 180 | 320 | 110 | 180 | 340 |
| | F | 190 | 310 | 115 | 190 | 335 |
| PwP | LA | 200 | 340 | 120 | 205 | 570 |
| | RA | 200 | 285 | 130 | 205 | 540 |
| | F | 195 | 280 | 115 | 205 | 635 |
| PnP | LA | 210 | 400 | 175 | 230 | 410 |
| | RA | 195 | 340 | 175 | 210 | 340 |
| | F | 200 | 355 | 155 | 210 | 600 |

**Table 6.6** Delays of positive and negative peaks describing ERP in Domain 3 with respect to the nearest cue. Delays of peaks N1 and P1 correspond to the appearance of a warning cue at t=-1s. Delays of peak N2 is with respect to the appearance of the execution cue at t=0s while the delay of peak N3 is with respect to the disappearance of the execution cue at t=1.5s.

| Group | MI condition | N1 | P1 | N2 | N3 |
|---|---|---|---|---|---|
| AB | LA | 175 | 265 | 210 | 260 |
| | RA | 175 | 290 | 195 | 250 |
| | F | 180 | 265 | 200 | 255 |
| PwP | LA | 180 | 270 | 205 | - |
| | RA | 175 | 270 | 200 | - |
| | F | 180 | 270 | 205 | - |
| PnP | LA | 190 | 280 | 210 | - |
| | RA | 190 | 290 | 205 | - |
| | F | 185 | 285 | 215 | - |

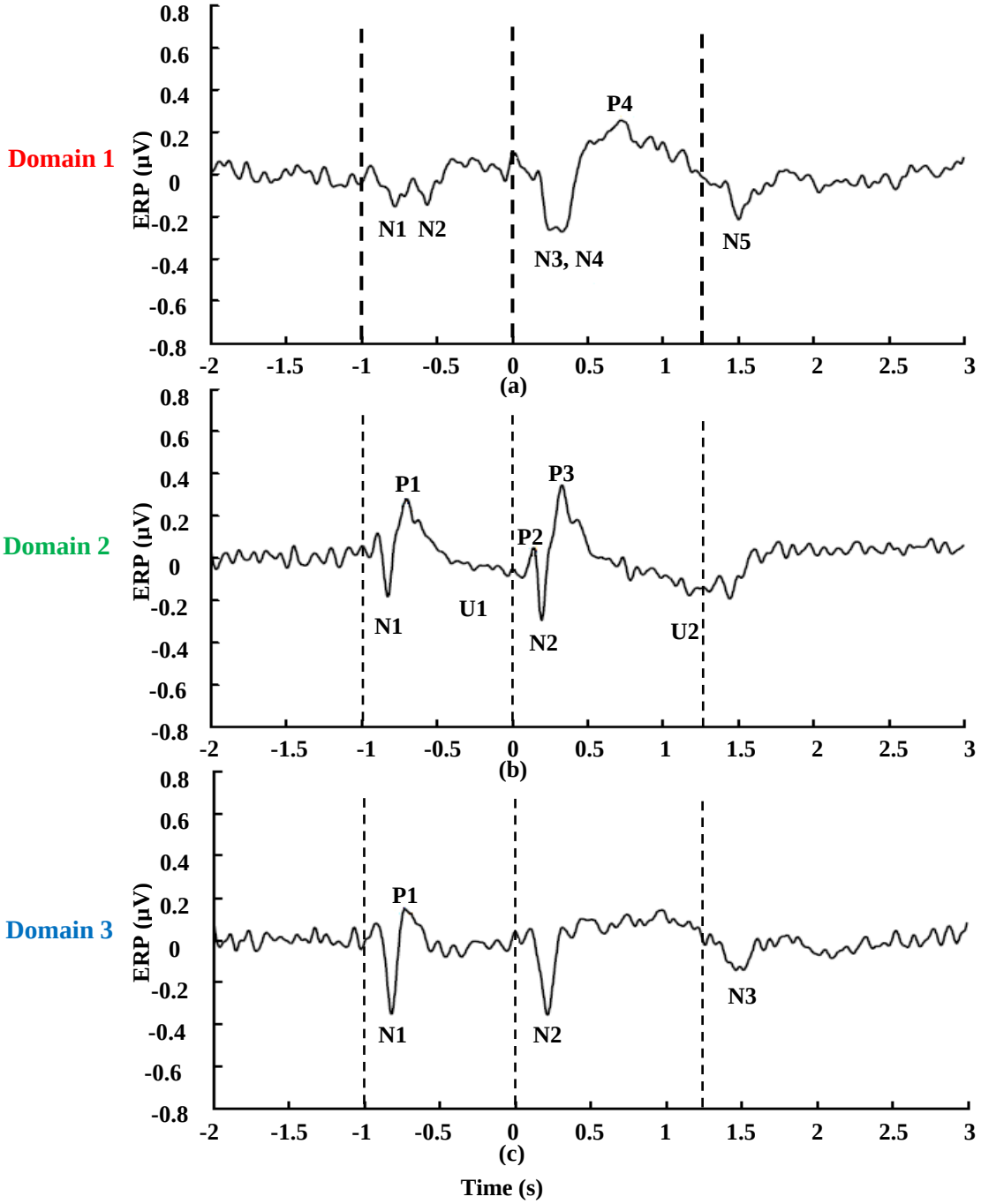


**Figure 6.2** ERP for AB during MI of Left Hand, the appearance of a warning sign at t=-1s, the appearance of the execution cue at t=0s and the disappearance of the execution cue at t=1.25s. Vertical lines in figures delineate between these events.

We start the analysis with domain 2, the part which includes the sensory-motor cortex and is therefore expected to be most similar to the ERP analysis of EEG signal over the motor cortex[92]. The main difference between EEG derived MRCP and ERP in Domain 2 is that ERP in Domain 2 is inverted, so positive peaks correspond to negative peaks in EEG MRCP and vice versa. This is due to IC derived dipole orientation. In a period between the warning and the execution cue, the ERP resembles a contingency negative variation (CNV) in an EEG signal. The first large, short duration negative peak N1 (t=170ms) caused by a visual stimulus is followed by a longer positive peak P1 (t=300ms) and a slow negative undershoot (U1) that lasts until the appearance of an execution cue. In a period following the execution cue, a positivity-negativity-positivity complex (P2 at t=140ms, N2 at t= 200ms and P3=330ms) is followed by a negative undershooting. While P2 and N2 most likely represent a cognitive response to a visual stimulus peak P3 corresponds to an inverted sign motor related potential (MRP) and a negative undershooting (U2) corresponding to the reafferentation potential of kinaesthetic sensory origin[98].

In domain 1 in a period between the warning and the execution cue, two consecutive brief negative peaks can be noticed (N1 at t=220ms and N2 at t=440ms), probably as a result of cognitive processing of a visual cue. A typical CNV is absent, which is not surprising, as its origin is in BA6 which is a part of domain 2. The morphology of the ERP following the execution cue contains a double negativity (N3 at t=250ms and N4 at t=330ms), followed by large longer lasting positivity P4 and then another smaller negativity N5. Judging by a post-stimulus delay N3 and N4 also represent a response to a visual stimulus, probably corresponding to P200 and P300 with inverted signs. Positivity P4 (at t=720ms) has a larger delay and is of longer duration than positivity P2 in domain 2. It most likely corresponds to the reafferentation potential in domain 2, but with an inverted sign. Bötzel et al. reported inverted reafferentation potentials between the central and parietal cortex[98], though they suggested its origin is in the primary somatosensory cortex

which belongs to domain 2. Finally, N5 follows disappearance of a cue (at t=1.25s) with a delay t=255ms.

ERP in domain 3 covering the occipital cortex has the simplest morphology. In a period following a warning sign a negativity N1 at t=175ms is followed by a positivity P1 at t=265ms and while following an execution cue a negativity N2 at t=210ms can be noticed. Finally another negativity at N3=260 following disappearance of the execution cue can be noticed. This peak is not visible in Domain2 but this might be because of the overlap with the undershooting U2.

Peaks which exist in all domains with comparable time delay are N1 in domains 1-3 and N3 (domain 1) and N2 in domains 2 and 3. These are the earliest responses, probably corresponding to P200 with an inverted sign.

Figures 6.3-6.5 show ERP in three groups over three domains, domain 1 Figure 6.3a-c, domain 2 Figure 6.4a-c and domain 3 Figure 6.5a-c. ERPs of all three groups for a single domain and a single type of motor imagination are shown in one graph. For all three domains, ERPs of different types of movement are shown in subplots a-c. Bars under the graphs indicate time instances when ERPs were statistically significant among each of the two groups (nonparametric permutation statistics, p=0.01). For each domain, we will first analyses a time period between the warning and execution cue followed by the analysis of ERP in a period following the execution cue.

In Domain 1, following the warning cue, both N1 and N2 can be noticed in the PnP and AB groups. Peak N2 lasts significantly longer and returns slower to the baseline in the PnP group. The PwP group has only N1 visible but significantly smaller than N1 in PnP. Unsurprisingly, similar results can be noticed across all three types of motor imagery because participants had the same warning sign for all three types of motor imagery and did not know in advance which execution cue will follow.

In a period following the execution cue, AB and PnP have a similar N3 while N4 is significantly delayed in PnP. Group PwP has only N3 and it is significantly smaller than in the other two groups. While in the AB group P4 is visible in all 3 types of motor imagery, in the PnP group it is noticeable only during MI of feet. Note that PnP had paralysed legs and neither sensory nor motor impairments in arms. PwP had pain and paralysis of legs and no pain nor paralysis in arms, yet peaks characteristic for the other two groups are absent for all three types of MI. Component N5 is visible in the AB group. Statistically significant difference between AB and PnP can be noticed, for all three types of MI in a period of N4 and P4 and later during N5.

In summary, ERP has the most similar morphology in AB and PnP group for MI of legs, but apart from the earliest peaks (N1, N3) other peaks are delayed in PnP group. Most peaks are absent in the PwP group, apart from the earliest two peaks N1 and N3.

In Domain 2, in a period following a warning cue in the PnP group, N1 is very weak or almost absent and P1 returns much slower to the baseline than in the AB group; Instead of undershooting the potential is positive following P1 due to the slow return to the baseline value. On the contrary the morphology of ERP in the PwP group is more similar to that of AB but with a significantly larger N1 than in the AB group.

In a period following the execution cue, all three groups have visible N2 and P2 but PwP and PnP do not have the undershooting U2, which would correspond to the reafferentation potential in ERP derived from EEG over the motor cortex. PwP group has a significantly larger N2 than the other two groups. This peak is probably of a similar origin as N1, which is also larger in PwP. P3 is delayed and lasts longer in patient groups as compared to AB. The whole period between t=0.5 and 1.5s is significantly different between AB and the two patient groups.

In summary, apart from the reafferentation potential, all three groups have similar peaks but they are delayed in patient groups. The earliest negative peaks (N1 and N2) in the PwP group are significantly larger than in the other two groups. EPR has comparable morphology for all three types of MI for all three groups.

In domain 3 in a period following the warning cue, all three groups have N1 and P1 of a comparable delay and intensity but PnP rebounds slower to the baseline compared to the other two groups. In a period following the execution cue, N2 is also similar in all three groups. Negativity N3 is visible in the AB group only, following the disappearance of the execution cue. In summary, judging by the delays and morphology, this domain has peaks mostly originating from visual processing. They are of comparable delay and intensity in all three groups. The largest difference between PnP and the other two groups is due to a slow rebound towards the baseline value.

All groups have the earliest negative peaks visible in all domains and with approximately the same delay both between groups and between domains. There is however a large difference in the amplitude of these peaks in PwP across different domains. As results, they are significantly smaller than in the other two groups in domain 1, significantly larger than in the other two groups in domain 2 and of comparable amplitude with the other two groups in domain 3. Domain 1 showed the largest variability between groups and also to some extent between types of MI in patient groups.

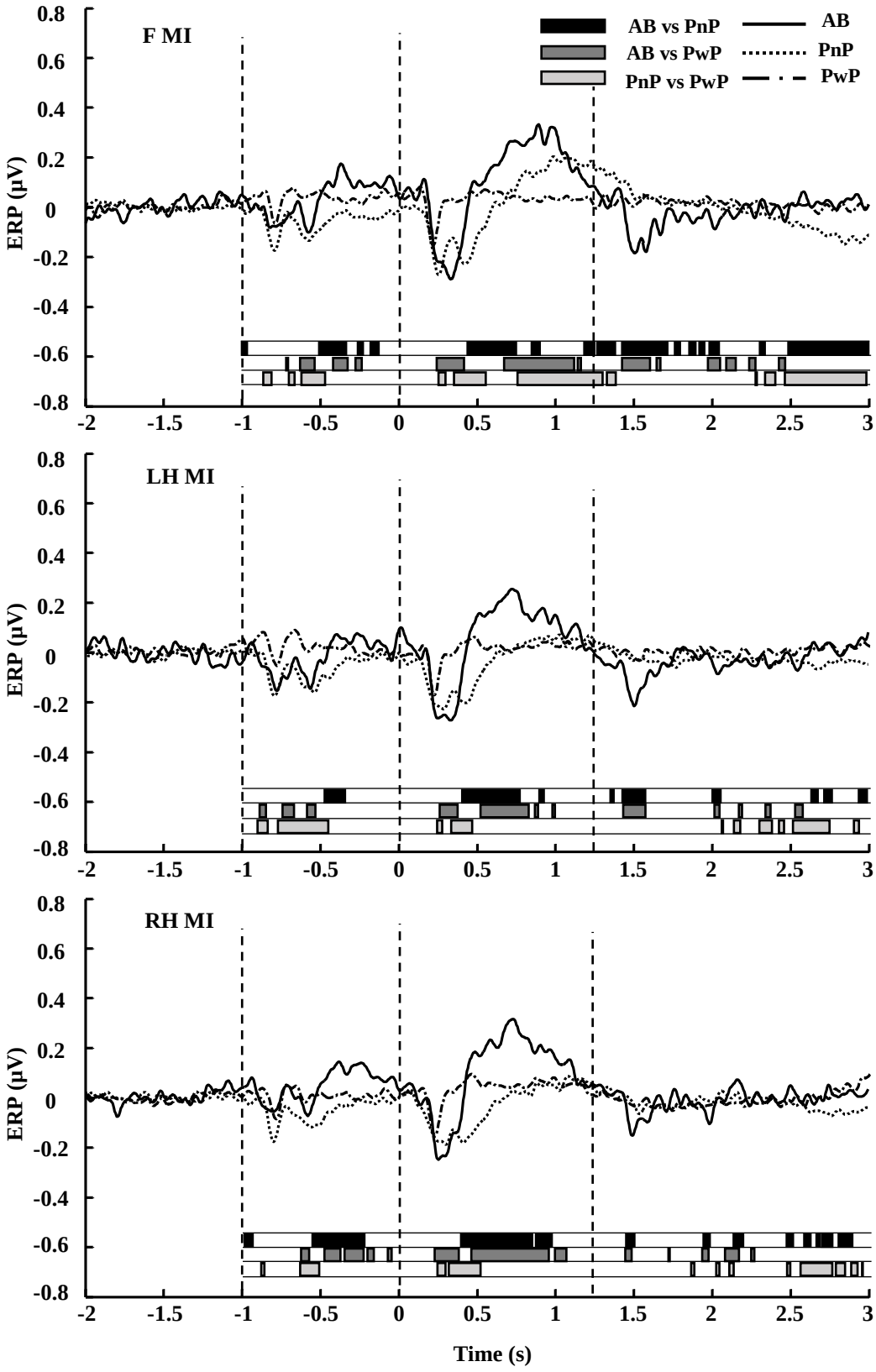


**Figure 6.3** Domain 1 MRCP during motor imagery of Feet: F, Left Hand: LH and Right Hand: RH for the three groups AB, PnP and PwP. Thick horizontal lines below the graphs represent the intervals in which the statistically significant difference between each pair of groups (Above: AB vs PnP, middle: AB vs PwP and below PnP vs PwP) with p value = 0.01.

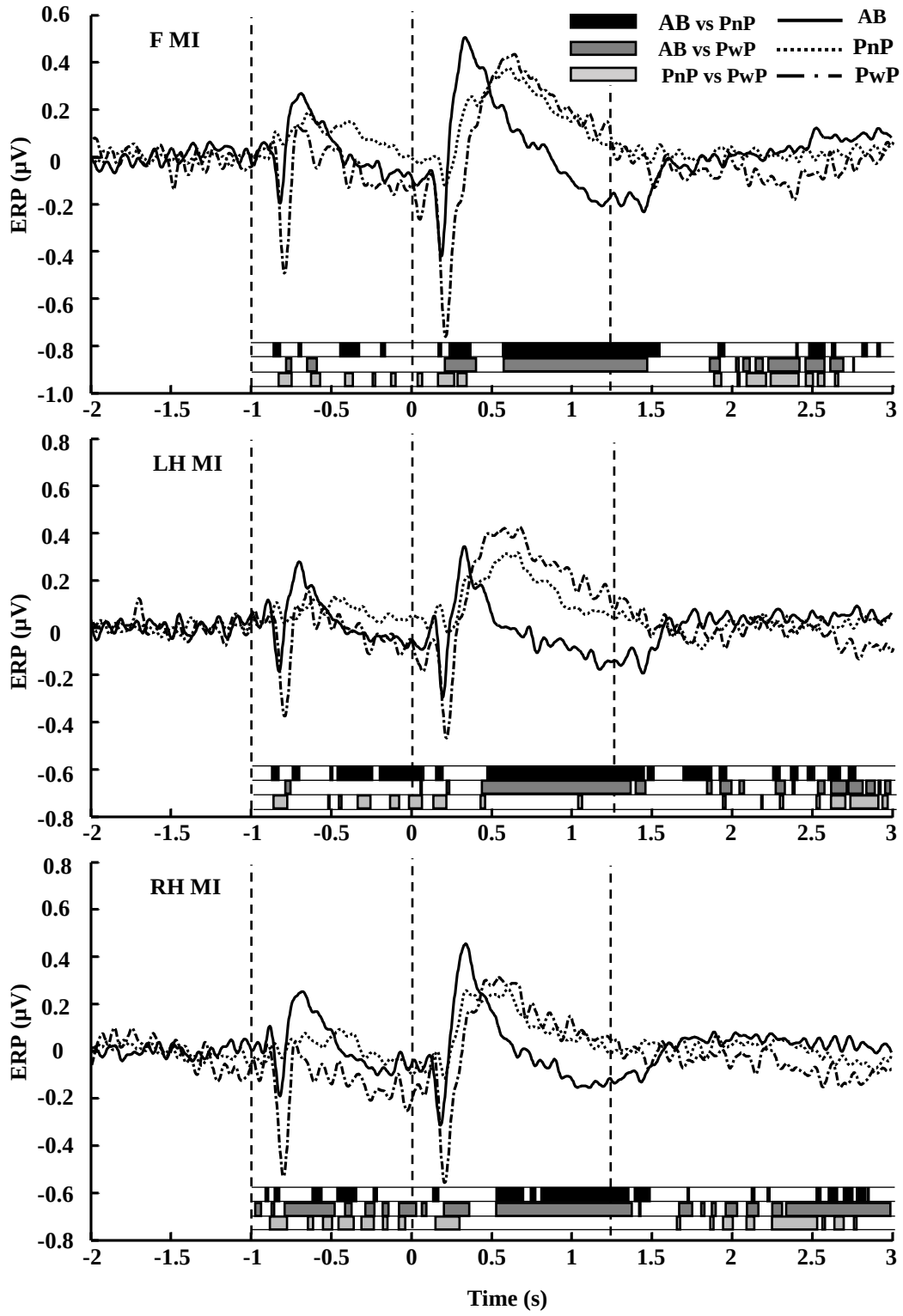


**Figure 6.4** Domain 2 MRCP during motor imagery of Feet: F, Left Hand: LH and Right Hand: RH for the three groups AB, PnP and PwP. Thick horizontal lines below the graphs represent the intervals in which the statistically significant difference between each pair of groups (Above: AB vs PnP, middle: AB vs PwP and below PnP vs PwP) with p value = 0.01.

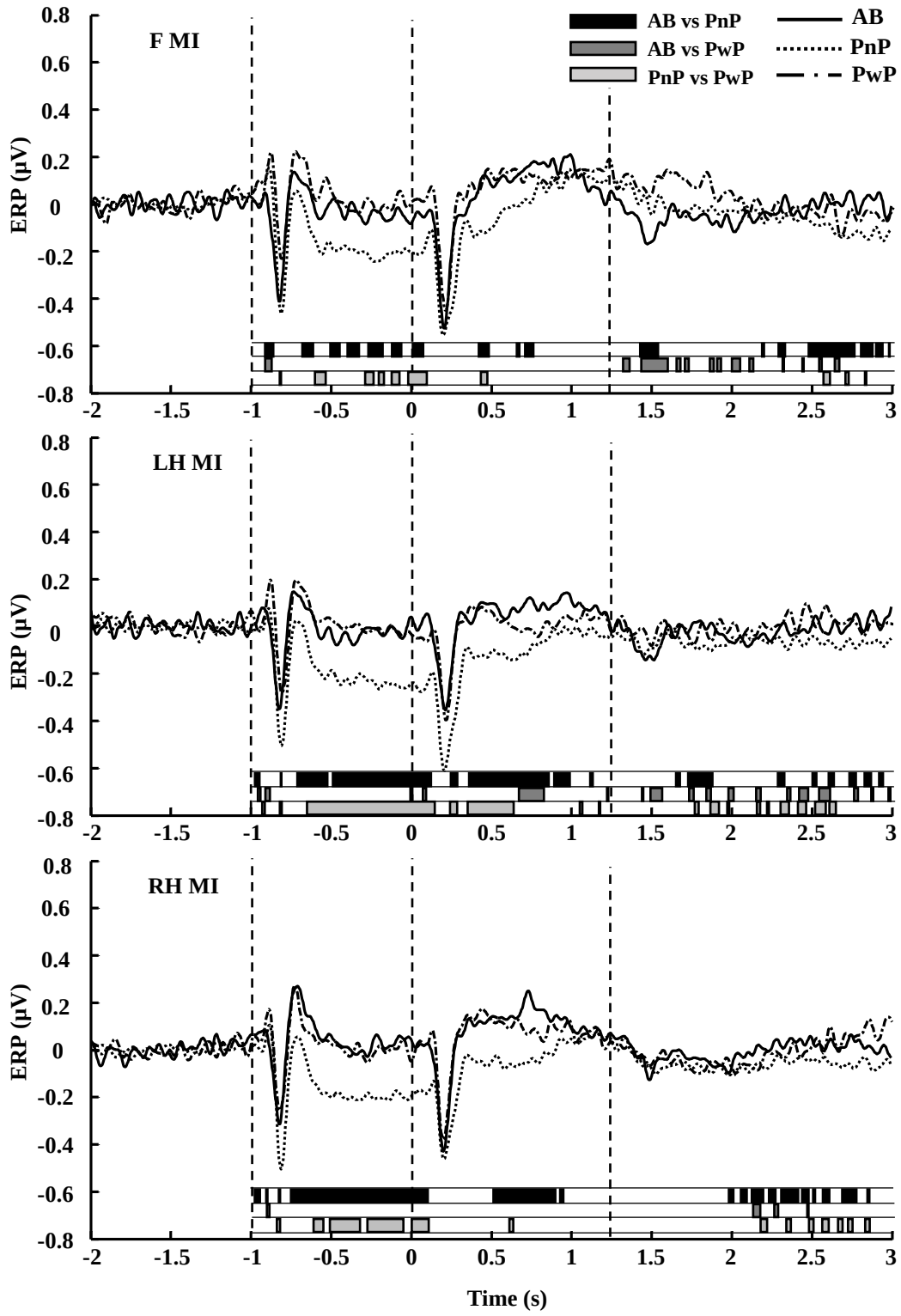


**Figure 6.5** Domain 3 MRCP during motor imagery of Feet: F, Left Hand: LH and Right Hand: RH for the three groups AB, PnP and PwP. Thick horizontal lines below the graphs represent the intervals in which the statistically significant difference between each pair of groups (Above: AB vs PnP, middle: AB vs PwP and below PnP vs PwP) with p value = 0.01.

## 6.5 Discussion

This study revealed three distinctive functional domains which were comparably represented by participants of all three groups. Each domain had a distinctive ERP during cue based motor imagination task. Presence of CNP and of SCI affected domains to a different degree, depending on their function and location. The first domain was located in the limbic cortex and some deeper cortical structures, at least apparently. The second domain showed a functional similarity between the sensory-motor cortex and some parts of the limbic system which in people with CNP regulate the affective component of pain. Thus the limbic cortex is distributed between two domains. The third domain was localized within the visual cortex due to a visual nature of the cue based task, and showed well-established and comparable morphology across the three groups. Because the visual cortex is not the primary target of this study, it will be excluded from the following discussion. Only the ERP in domain 2 has movement related potential while both domains 1 and 2 had reafferentation potential, related to sensory processing. All thee domains have early peaks similar to P200 and P300 with inverted sign reflecting cognitive processes with respect to the visuo-motor task.

The first domain includes anatomical areas within the cingulate cortex responsible for the affective component of pain. The ERP of AB and PnP in this domain consists of early components within the first 400ms reflecting cognitive processes and late components related to a sensory, reafferentation potential. While PnP had all peaks present but delayed, in the PwP group only earliest peaks were present. This indicates possibly general suppression of ERP related to early cognitive and sensory processing. Notably, these peaks are absent not only during motor imagination of painful and paralysed lower limbs but also during motor imagination of non-paralysed and non-painful upper limbs. Pain and paralysis thus have a distinctive effect on ERP in the limbic cortex, during a cue-based MI task. While paralysis causes delayed responses, presence of CNP causes suppression

similar to the general effect of chronic pain to cognitively related ERP responses in EEG signal[291,292].

The second domain covers the areas of the primary and secondary sensory and motor cortex. ERPs of able bodied people in this domain look like inverted EEG MRCP over the primary motor cortex. In both patient groups a reafferentation potential is missing, while a component related to movement preparation and execution is present but delayed and lasts longer than in AB group. Earliest peaks are significantly larger in PwP as compared to the other two groups, probably reflecting higher cognitive effort. Motor related potential is similar in PnP and PwP groups indicating that it is probably not influenced by CNP. The absence of the reafferentation potential in this domain (also seen in EEG MRCP[92]) in both patient groups might indicate that it is not influenced by CNP. However, considering that a similar ERP component is absent only in the PwP group in domain 1, it is more likely that both paralysis and presence of CNP contribute to reduced processing of kinaesthetic sensory feedback within this domain.

The difference of the amplitude of the earliest negativities in PwP across these domains is remarkable. It shows a complex mechanism through which CNP influences cognitive functions. Similar to the effect of the other types of chronic pain on P300[291,292], it reduces the amplitude of this peak as in domain 1. However an increased peak in domain 2 resembles phenomena seen in people with neurotic disorders[293], who have increased P300 amplitude when processing stimuli related to critical fear concern, which in this case might be the imagination of the movement of a painful limb. Finally a corresponding peak in domain 3 does not seem to be influenced by CNP.

## 6.6 Conclusion

In conclusion, CNP has the largest influence on ERP in a domain which includes the limbic system with no contribution from the sensory-motor cortex. In the domain including

the sensory-motor cortex MRCP of both patients groups is similar and delayed as compared to able bodied. Smaller differences exist in a domain which included the visual cortex. Both pain and paralysis affect the reafferentation potential while CNP influences cognitive processes in a manner that depends on the area of the cortex.

# 7
# General Discussion

# Chapter 7 General Discussion

This thesis has two parts, real time modulation of EEG activity over the central cortex and offline quantitative EEG analysis of pain signatures in sub-acute and chronic spinal cord injury (SCI) patients. The first part aims to explore the influence of neuromodulation strategies over the central cortex on the cortical excitability measured by H reflex in able bodied participants and on the central neuropathic pain (CNP) in patients with SCI. The second part aims to investigate the causal relationship between changes in EEG activity and the transitional period of early symptoms of CNP and also at the chronic phases of CNP following SCI. Four studies have been conducted to achieve these aims. The discussion section is organized as follows: real time neuromodulation strategies as chapters 3 and 5 and offline quantitative EEG analysis as chapters 4 and 6.

## 7.1 The Effect of Neuromodulation Strategies on Cortical Excitability and CNP

The objective of Chapter 3 was to explore the effectiveness of neuromodulation strategies (neurofeedback (NF), motor imagery (MI) and mental math (MM)) of sensory-motor rhythm (SMR: 8-12Hz) at Cz electrode location on modulation of the cortical excitability measured by soleus H reflex. MI and MM were used for decreasing SMR, while NF was used to increase SMR. From the literature, it has been shown that H reflex amplitude can be modulated during both MI[212–214,216,217] and MM[217] as well as during biofeedback (not directly related to brain activity)[209,224]. However, EEG activity and the H reflex have not been measured concurrently during these studies and there is no published study exploring the effect of NF strategy on modulation of the H reflex. To the best of our knowledge, this is the first study to define the relationship between the self-induced modulation of SMR and the amplitude of the H reflex during different neuromodulation strategies. The results of this study showed that MM and NF had excitatory (significantly

increased) effect on H reflex amplitude and MI had an inconsistent effect on the H reflex. The excitatory effect of NF and MM on the H reflex was independent of the direction of modulation of the SMR rhythm. The results of this study showed that self-induced neuromodulation of the EEG activity over the central cortex can influence motor functions in able bodied participants.

Induced EEG activity over the central cortex not only influences motor function but also influences sensory function. Several non-invasive stimulation treatments, including rTMS, tDCS and NF have been used to stimulate the central cortex to treat CNP[41–44]. In chapter 5 the NF therapy was used to manage CNP following SCI in patients in the sub-acute phase (several months after injury). A previous study conducted by our group demonstrated that NF has a positive result in the treatment of CNP in chronic paraplegic patients[267]. However, treating SCI patients with CNP in the sub-acute phase by NF might have more benefit in both the reduction of pain and the prevention of a maladaptive cortical plasticity. The objective of chapter 5 was to explore the effectiveness of NF therapy on the treatment of CNP in sub-acute patients with SCI. Four out of seven patients completed multiple NF sessions. None of the patients completed the whole planned 20 NF sessions. The clinically and statistically significant reduction of pain as well as a reduction in painful areas was noticed in three of the patients who had completed more than 12 NF sessions. The patients in the control group showed almost stable pain intensity over the period of two months and no large change in areas perceived as being painful.

Comparison of EEG activity during a relaxed state before the first and after the last NF session showed that there was an increase in theta and alpha activity over the parietal region in all four patients. Changes in induced EEG activity were also noticed after the last NF training session. Furthermore, patients showed a significant reduction in theta and alpha ERD over the central cortex during the MI task. The previous NF study by our group also showed a reduction in ERD after NF therapy[267]. The results of both chapters 3 and 5

demonstrated that NF strategy over the central cortex results in the modulation of sensory and motor function. Although the results of chapter 5 on the reduction of pain were encouraging, numerous factors, and in particular patients' low prioritization of pain, indicate that early NF of CNP in SCI patients might not be a practical solution.

## 7.2 The Causality between EEG and CNP in patients with SCI

Brain reorganization after SCI and after the presence of CNP following SCI has been investigated by neuroimaging studies[16,115,119,136–138]. It has been shown that the degree of brain reorganization has correlation with the intensity of CNP[136,140]. However, it is still debatable whether these brain reorganizations are causes or consequences of CNP. The objective of chapter 4 was to explore the causal relationship between EEG and CNP in the transitional period of early symptoms of CNP. The results of post hoc analysis of this study showed that SCI patients who developed pain (PdP) had higher theta power, lower EEG reactivity and a shift of the dominant alpha peak towards lower frequencies, in comparison to patients with no pain (PnP) and able bodied (AB) controls, during the relaxed state. The results of ERS/ERD analysis showed that PdP exhibited strong alpha and beta ERD during the motor imagery task. The differences in spontaneous and induced EEG activity in PdP compared to AB and PnP represent the predictors of CNP (preceding the physical symptoms of CNP). The SCI patients with CNP showed an increase in theta PSD, a lower frequency of the dominant alpha peak during the relaxed state and stronger ERD activity which extended towards the lower frequency (theta band) during the MI task. These results, which indicate differences between PdP and PwP represent consequences of CNP (following the symptoms of CNP). The results of chapter 4 confirmed that changes in EEG precede the onset of pain as noticed in the PdP group and these changes became even more pronounced after the presence of pain as noticed in the PwP group. It is also of interest to mention that 9 out of 10 patient in the PdP group had no response to the mechanical

stimulation test, indicating that changes in EEG can be seen before the onset of sensory changes.

The results of PwP in chapter 4 are very similar to the PwP group with long standing CNP in the previous study by our group[140]. This similarity indicated that changes in both spontaneous and induced EEG can precede the onset of CNP and occur much faster than previously thought. In the previous study by our group, ERS/ERD analysis showed that PwP had strong ERD spreading over most of the frequency bands with characteristic spatial distribution during the MI task of both painful and non-painful limbs and PnP had weaker ERD compared to AB[140]. Therefore, they were able to distinguish between the effectiveness of long standing CNP and paralysis using ERS/ERD analysis[140].

There are two cortical phenomena reflecting induced cortical activity during MI, ERS/ERD and movement related cortical potential (MRCP) that have different origins[95,228]. Therefore CNP might have different effects on these two phenomena. In previous studies by our group, Xu et al.[92] investigated the MRCP at only three electrode locations over the primary motor cortex (C3, C4 and Cz), while Vuckovic et al.[140] explored the change in ERS/ERD over the wider cortical structures. A difference in the MRCP was only seen between AB and patient groups with no differences shown between patient groups[92]. One of the reasons for this might be that, similar to ERS/ERD, the influence of CNP on MRCP is widespread and cannot be captured by only analyzing several isolated electrodes.

In Chapter 6, Measure Projection Analysis (MPA) was used to overcome the limitations of Xu et al.[92] study by investigating the MRCP of deeper cortical structures. MPA relies on independent component analysis and equivalent dipoles localization to define domains with high functional connectivity[112]. Three domains have been identified by MPA: domain 1 (limbic cortex and some subcortical structures), domain 2 (sensory-motor cortex and BA 31, a part of the limbic cortex), and domain 3 (visual cortex). The MRCP was only noticed in domain 2 while reafferentation potential, related to kinesthetic

sensory processing, was noticed in both domains 1 and 2. The largest influence of CNP on ERP was noticed in domain 1. Moreover, PwP exhibited significantly smaller P200 in domain 1 and significantly larger P200 in domain 2 compared to both PnP and AB participants. These results confirm that CNP influences cognitive processes in a manner that depends on the functional area of the cortex.

## 7.3 Limitations of the studies

A possible limitation of chapter 3 is that frequencies higher than 30 Hz were not measured. The results of chapter 3 on the influence of MI on the H reflex were inconclusive because only alpha SMR was controlled. An animal study showed that the influence of gamma band on the H reflex evoked during the motor task. Large numbers of evoked H reflexes in each task is required for statistical consideration. More electrode locations can be involved in order to investigate the change in EEG over a wider cortical structure and correlate it with changes in the H reflex.

In chapter 4 a larger sample size in SCI patients with pain and without pain groups as well as in the able bodied group will be beneficial to increase the power of statistical analysis. Thermal tests for cold and hot sensations, in addition to the mechanical stimulus sensory test, would provide more complete insight into the relation between sensory and EEG predictors of pain.

The small number of patients in both control and treatment groups as well as the small number of NF sessions is the main limitation of chapter 5. Moreover, there was a lack of sham NF training session which is required to distinguish between the effect of NF training and the placebo effect on CNP.

## 7.4 Suggestion for future studies

Repeated experiments in chapter 3 over a long period of time would be useful to understand the long-term modulation of H reflex induced via prolonged modulation of cortical activity. Moreover, including down regulation SMR protocol as well as the up regulation SMR protocol using NF would be worthwhile to understand how the NF strategy influences cortical excitably.

Further data analysis on the EEG data of chapter 4 using different analyses, such as Common Spatial Pattern and Source Information Flow analysis, can be useful to define more features of CNP predictors. It will also be worthwhile if the same study applied to other patient groups suffering from the same type of pain.

## 7.5 Conclusion

This PhD thesis studied the influence of neuromodulation strategies on cortical excitability measured by the H reflex in able bodied volunteers and on CNP in patients with SCI, as well as the causality between EEG and CNP. The results of the thesis revealed that neuromodulation strategies over the central cortex have an effect on both motor and sensory function. The effectiveness of the neuromodulation strategies on motor function was measured by the modulation of the H reflex. The results showed that it is possible to achieve a short-term modulation of the H reflex through short-term modulation of SMR. The effectiveness of the NF on the sensory function was noticed by reduction of CNP in patients with SCI after multiple sessions of NF training. Although a positive effect of the NF treatment was noticed on the reduction of pain, several factors indicated that early NF of CNP in SCI patients might not be a practical solution. The causal relationship between EEG and CNP was also defined in this thesis. The results demonstrated that changes in

spontaneous and induced EEG can be both predictors and consequences of CNP following SCI. It was also shown that MRCP in patients with SCI is influenced by paralysis while both CNP and paralysis affect the reafferentation potential. Furthermore, CNP was found to influence cognitive processes in a manner that depends on the functional area of the cortex.

# 8

# Appendices A and B

# Appendix A

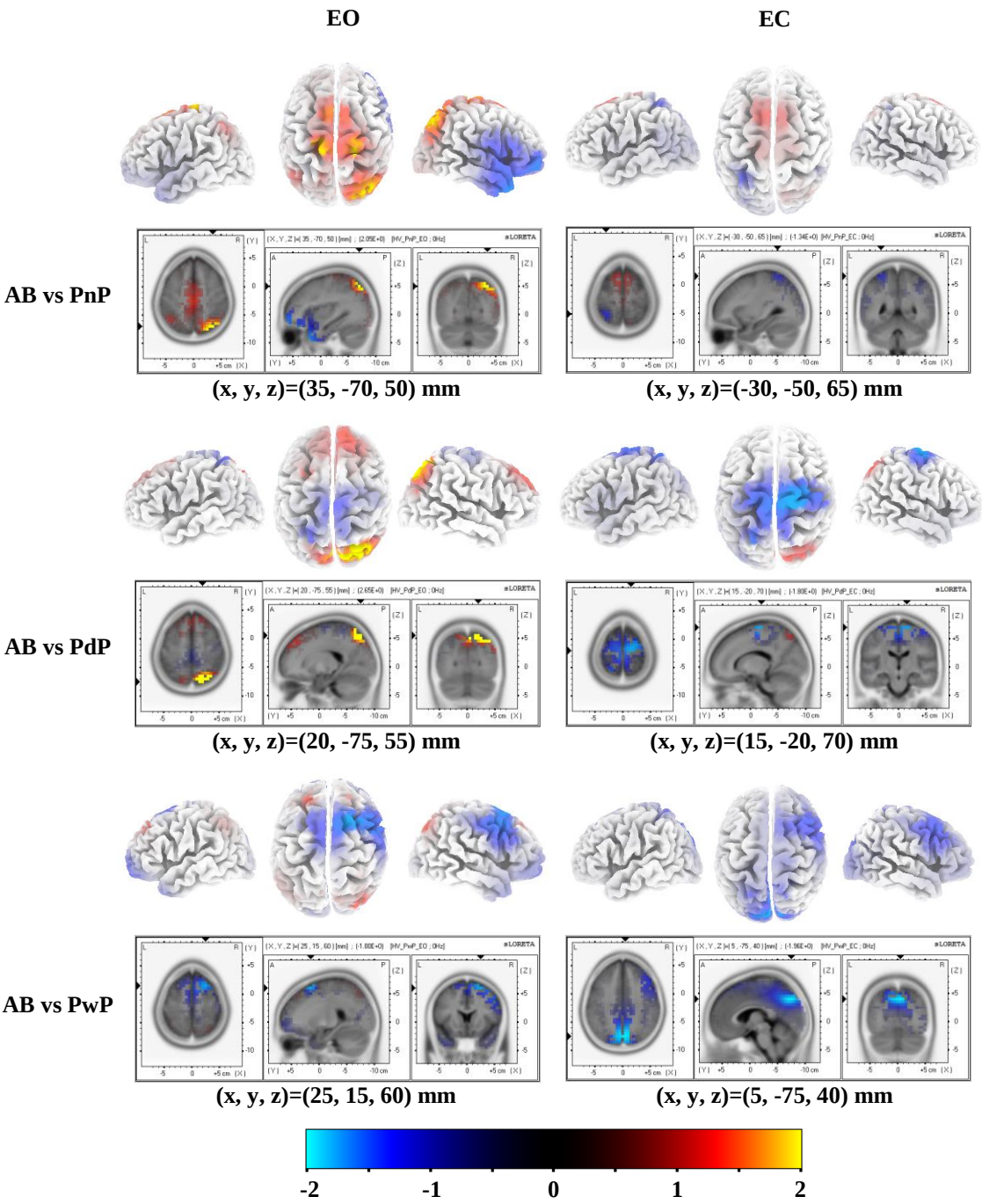


**Figure A.1** sLORETA localisation for eyes opened (EO) and eyes closed (EC) relaxed state for able bodied (AB) group compared with patients groups: patients with no pain (PnP), patients developed CNP (PdP) and patients with CNP (PwP) in theta EEG frequency band (4-7Hz). The first raw of each figure represents 3D map of the localisation while the second raw represents the 3D slice at the displayed of the voxel with negative or positive strongest activity. The (x, y, z) under each figure represent the Montreal Neurological Institute and Hospital (MNI) coordinate system of the voxel with strongest activity.

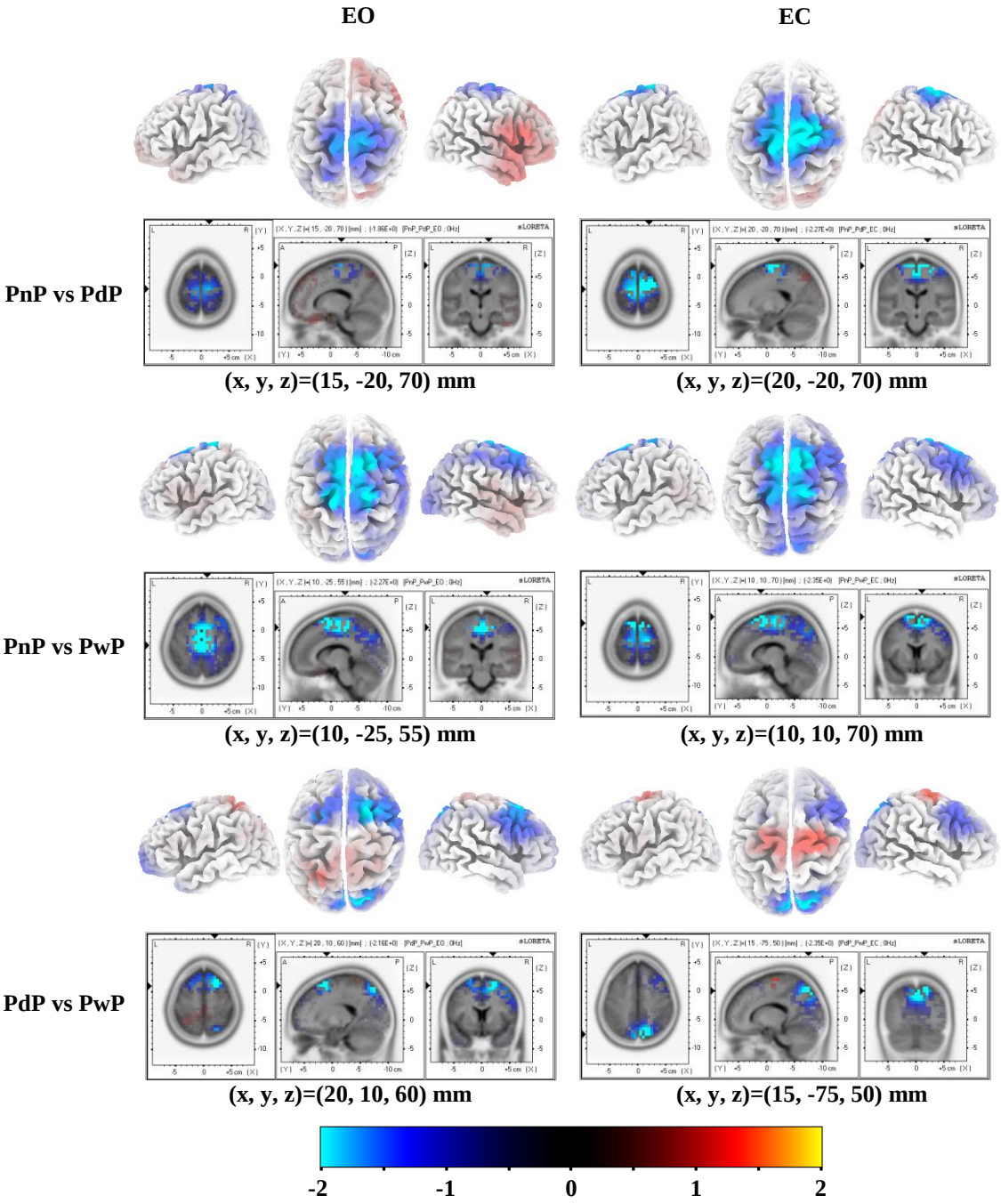


**Figure A.2** sLORETA localisation for eyes open (EO) and eyes close (EC) relaxed state compared among the patients groups: patients with no pain (PnP), patients developed CNP (PdP) and patients with CNP (PwP) in theta EEG frequency band (4-7Hz). The first raw of each figure represents 3D map of the localisation while the second raw represents the 3D slice at the displayed of the voxel with negative or positive strongest activity. The (x, y, z) under each figure represent the Montreal Neurological Institute and Hospital (MNI) coordinate system of the voxel with strongest activity.

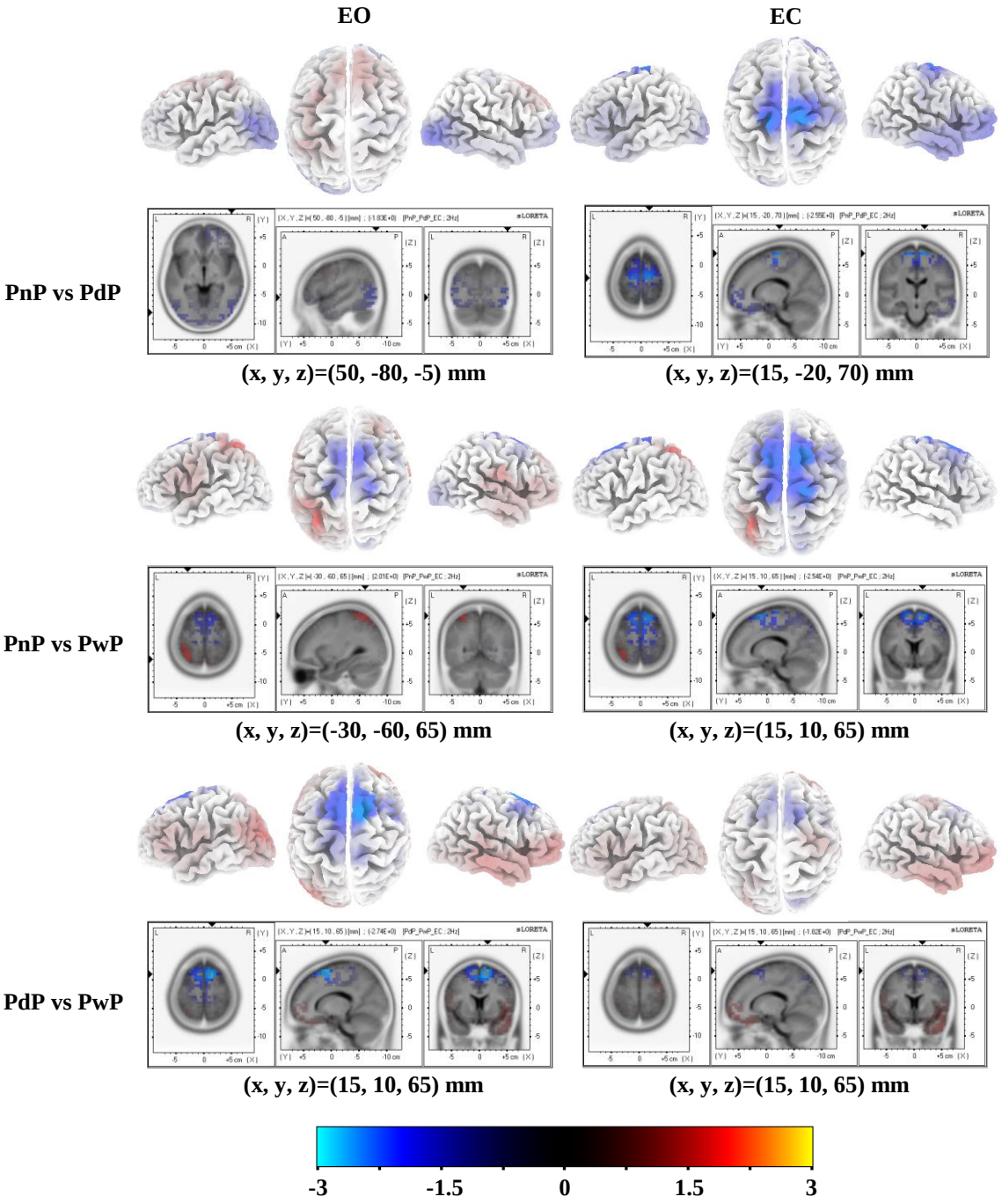


**Figure A.3** sLORETA localisation for eyes open (EO) and eyes close (EC) relaxed state compared among the patients groups: patients with no pain (PnP), patients developed CNP (PdP) and patients with CNP (PwP) in beta EEG frequency band (13-30Hz). The first raw of each figure represents 3D map of the localisation while the second raw represents the 3D slice at the displayed of the voxel with negative or positive strongest activity. The (x, y, z) under each figure represent the Montreal Neurological Institute and Hospital (MNI) coordinate system of the voxel with strongest activity.

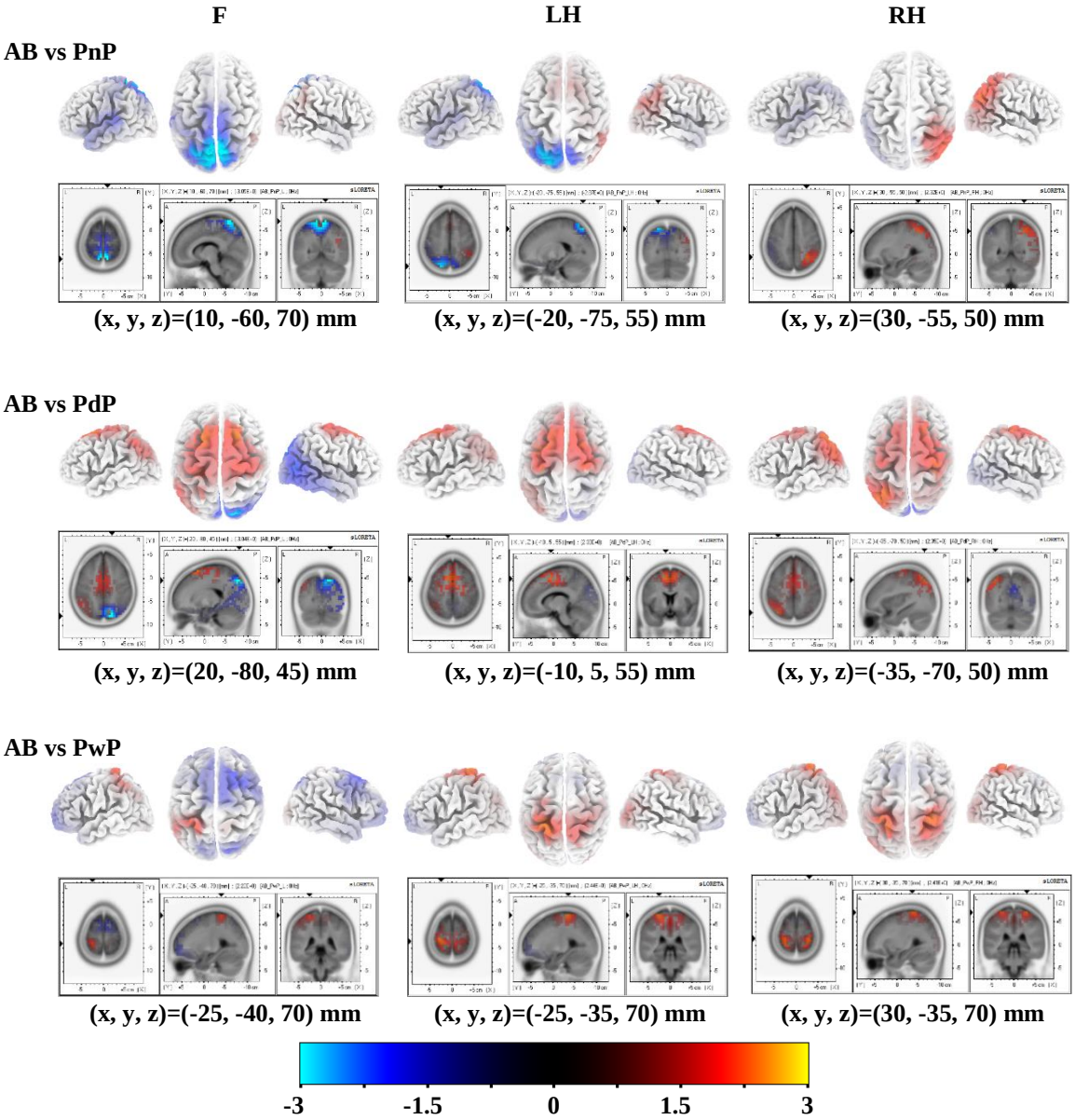


**Figure A.4** sLORETA localisation for motor imagery (MI) during F: feet, LH: left hand and RH: right hand MI and for able bodied (AB) group compared with patients groups: patients with no pain (PnP), patients developed CNP (PdP) and patients with CNP (PwP) in theta EEG frequency band (4-8Hz) over time window (0.5 to 1.5s). The first raw of each figure represents 3D map of the localisation while the second raw represents the 3D slice at the displayed of the voxel with negative or positive strongest activity. The (x, y, z) under each figure represent the Montreal Neurological Institute and Hospital (MNI) coordinate system of the voxel with strongest activity.

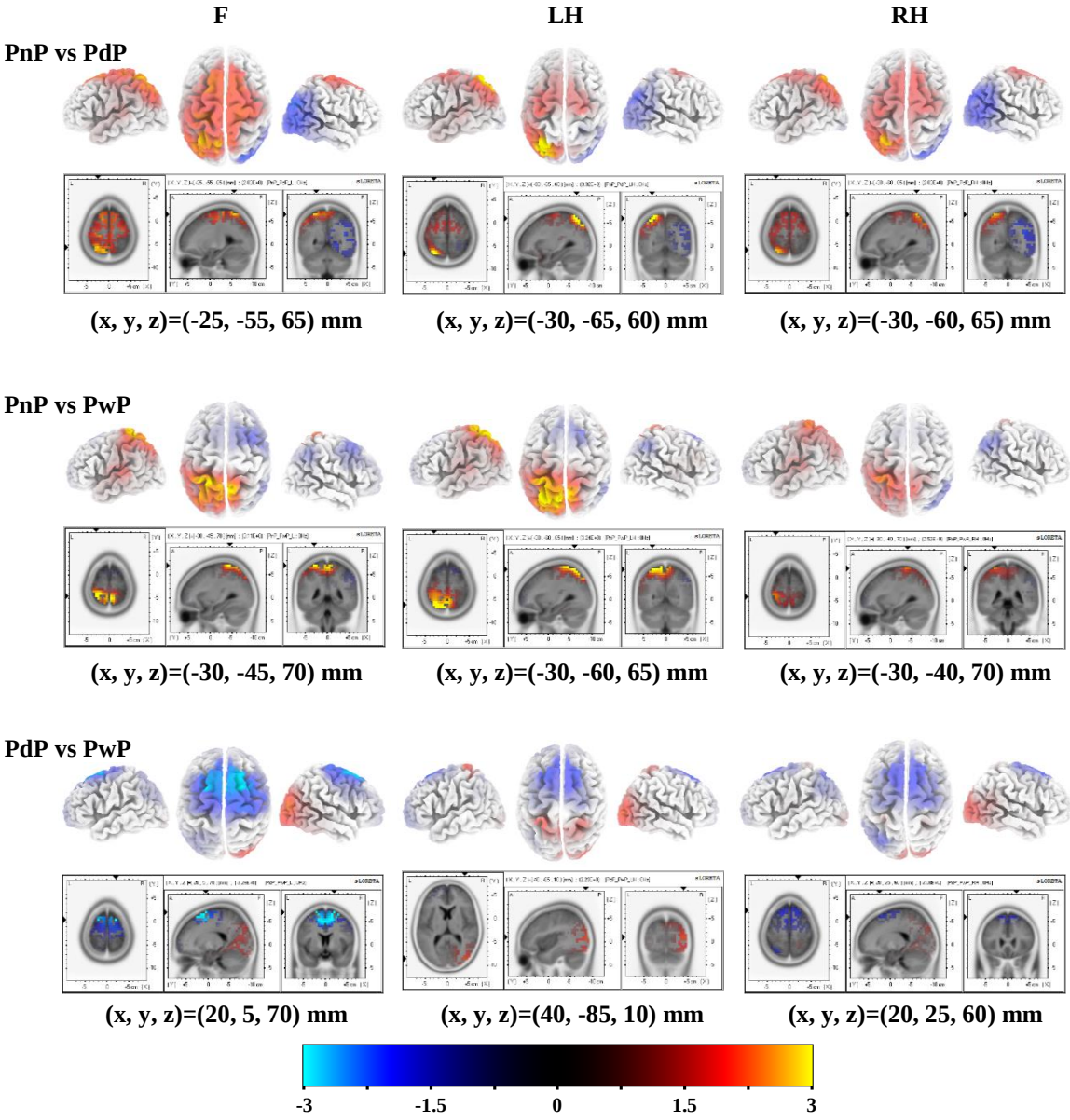


**Figure A.5** sLORETA localisation for motor imagery (MI) during F: feet, LH: left hand and RH: right hand MI compared between the patients groups: patients with no pain (PnP), patients developed CNP (PdP) and patients with CNP (PwP) in theta EEG frequency band (4-8Hz) over time window (0.5 to 1.5s). The first raw of each figure represents 3D map of the localisation while the second raw represents the 3D slice at the displayed of the voxel with negative or positive strongest activity. The (x, y, z) under each figure represent the Montreal Neurological Institute and Hospital (MNI) coordinate system of the voxel with strongest activity.

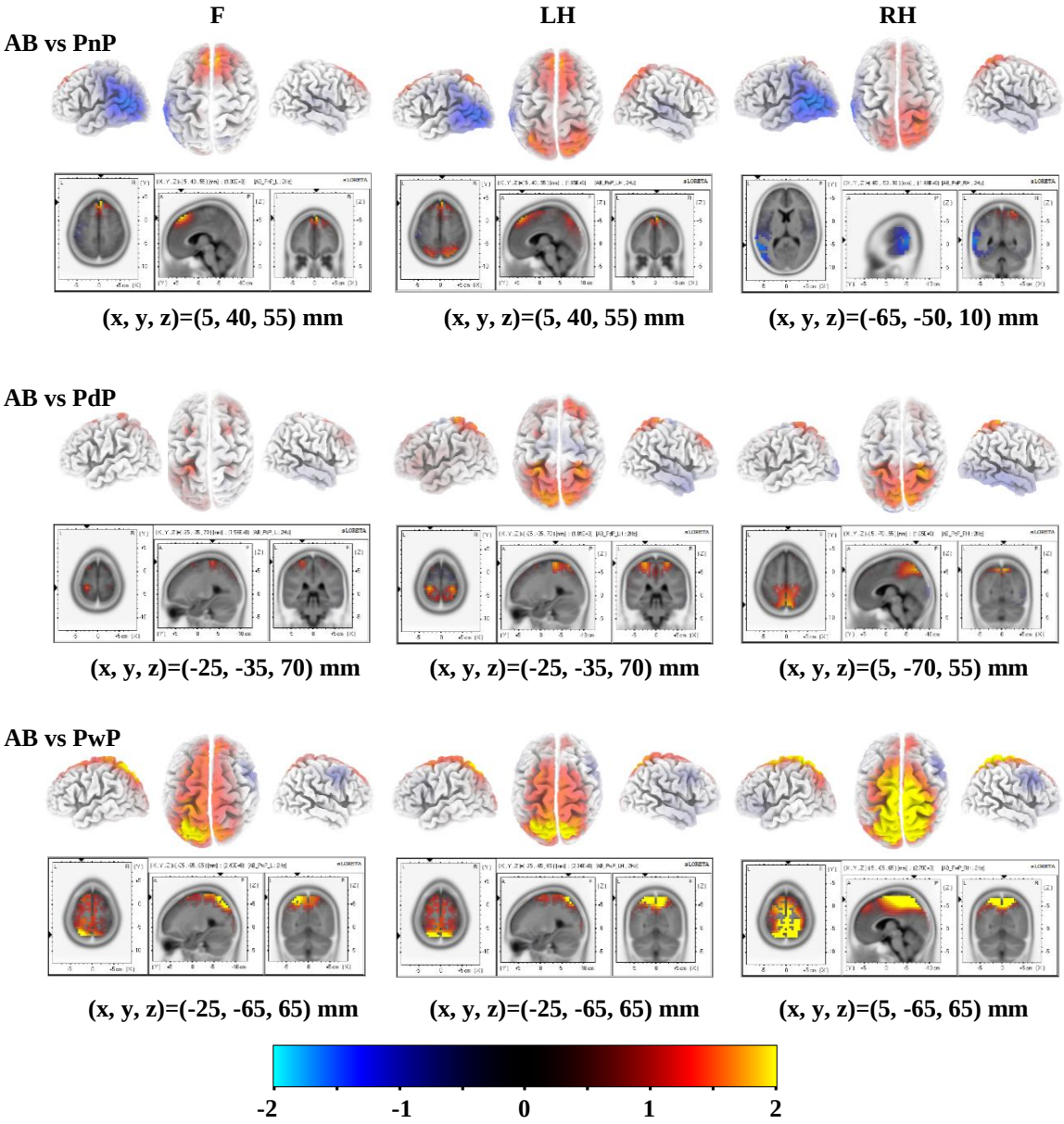


**Figure A.6** sLORETA localisation for motor imagery (MI) during F: feet, LH: left hand and RH: right hand MI and for able bodied (AB) group compared with patients groups: patients with no pain (PnP), patients developed CNP (PdP) and patients with CNP (PwP) in beta SMR EEG frequency band (16-24Hz) over time window (0.5 to 1.5s). The first raw of each figure represents 3D map of the localisation while the second raw represents the 3D slice at the displayed of the voxel with negative or positive strongest activity. The (x, y, z) under each figure represent the Montreal Neurological Institute and Hospital (MNI) coordinate system of the voxel with strongest activity.

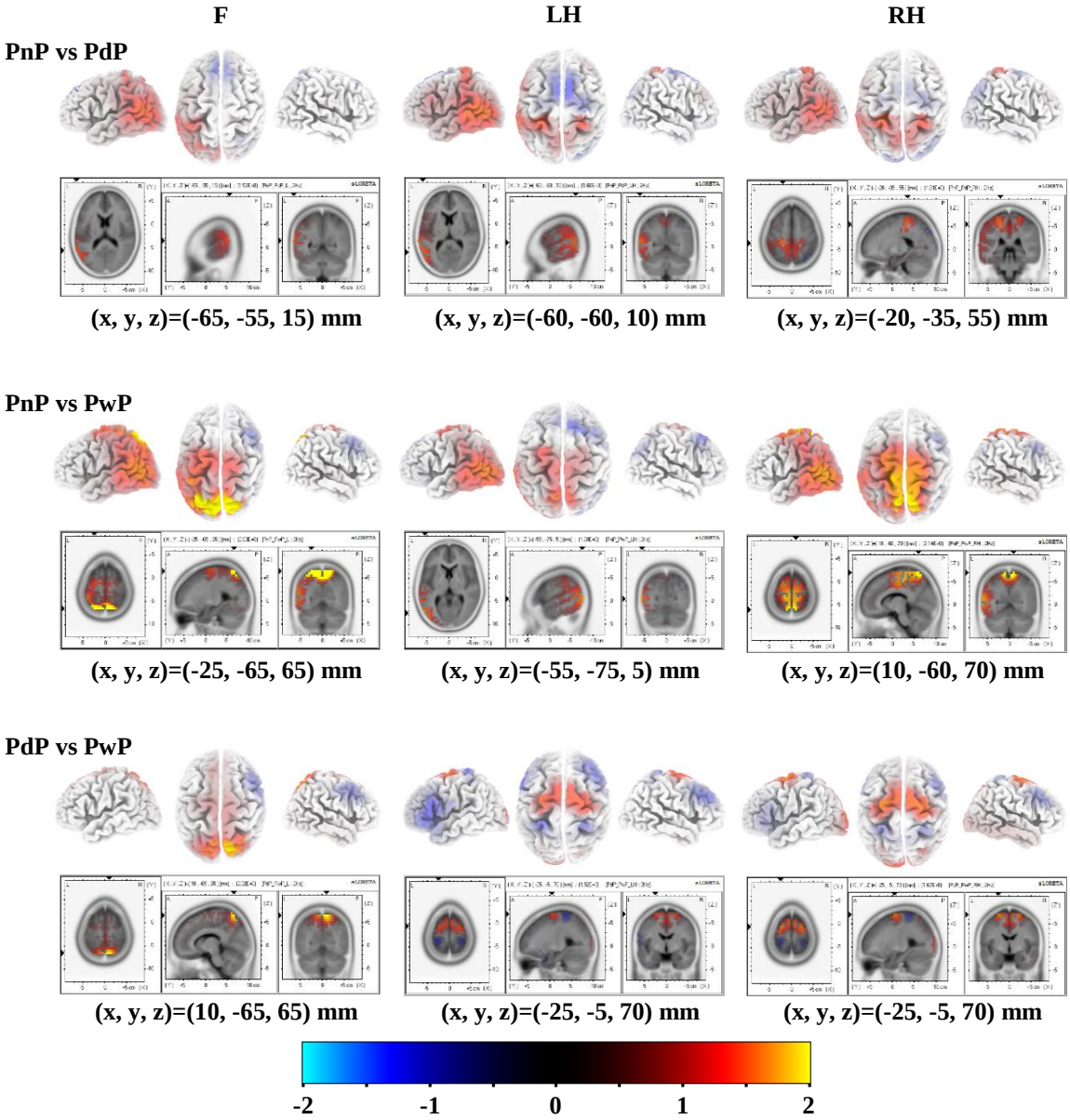


**Figure A.7** sLORETA localisation for motor imagery (MI) during F: feet, LH: left hand and RH: right hand MI compared between the patients groups: patients with no pain (PnP), patients developed CNP (PdP) and patients with CNP (PwP) in beta SMR EEG frequency band (16-24Hz) over time window (0.5 to 1.5s). The first raw of each figure represents 3D map of the localisation while the second raw represents the 3D slice at the displayed of the voxel with negative or positive strongest activity. The (x, y, z) under each figure represent the Montreal Neurological Institute and Hospital (MNI) coordinate system of the voxel with strongest activity.

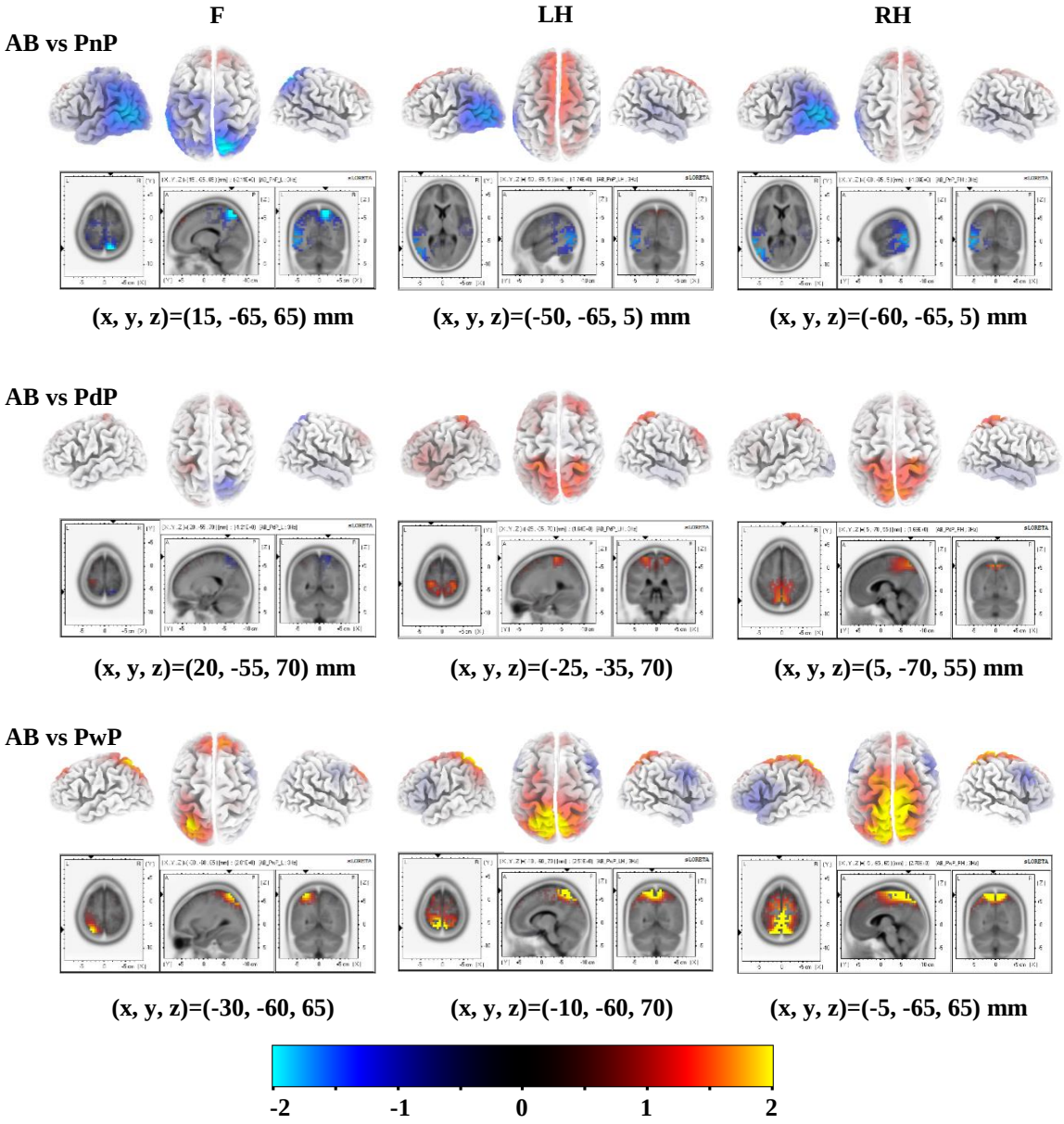


**Figure A.8** sLORETA localisation for motor imagery (MI) during F: feet, LH: left hand and RH: right hand MI and for able bodied (AB) group compared with patients groups: patients with no pain (PnP), patients developed CNP (PdP) and patients with CNP (PwP) in beta EEG frequency band (20-30Hz) over time window (0.5 to 1.5s). The first raw of each figure represents 3D map of the localisation while the second raw represents the 3D slice at the displayed of the voxel with negative or positive strongest activity. The (x, y, z) under each figure represent the Montreal Neurological Institute and Hospital (MNI) coordinate system of the voxel with strongest activity.

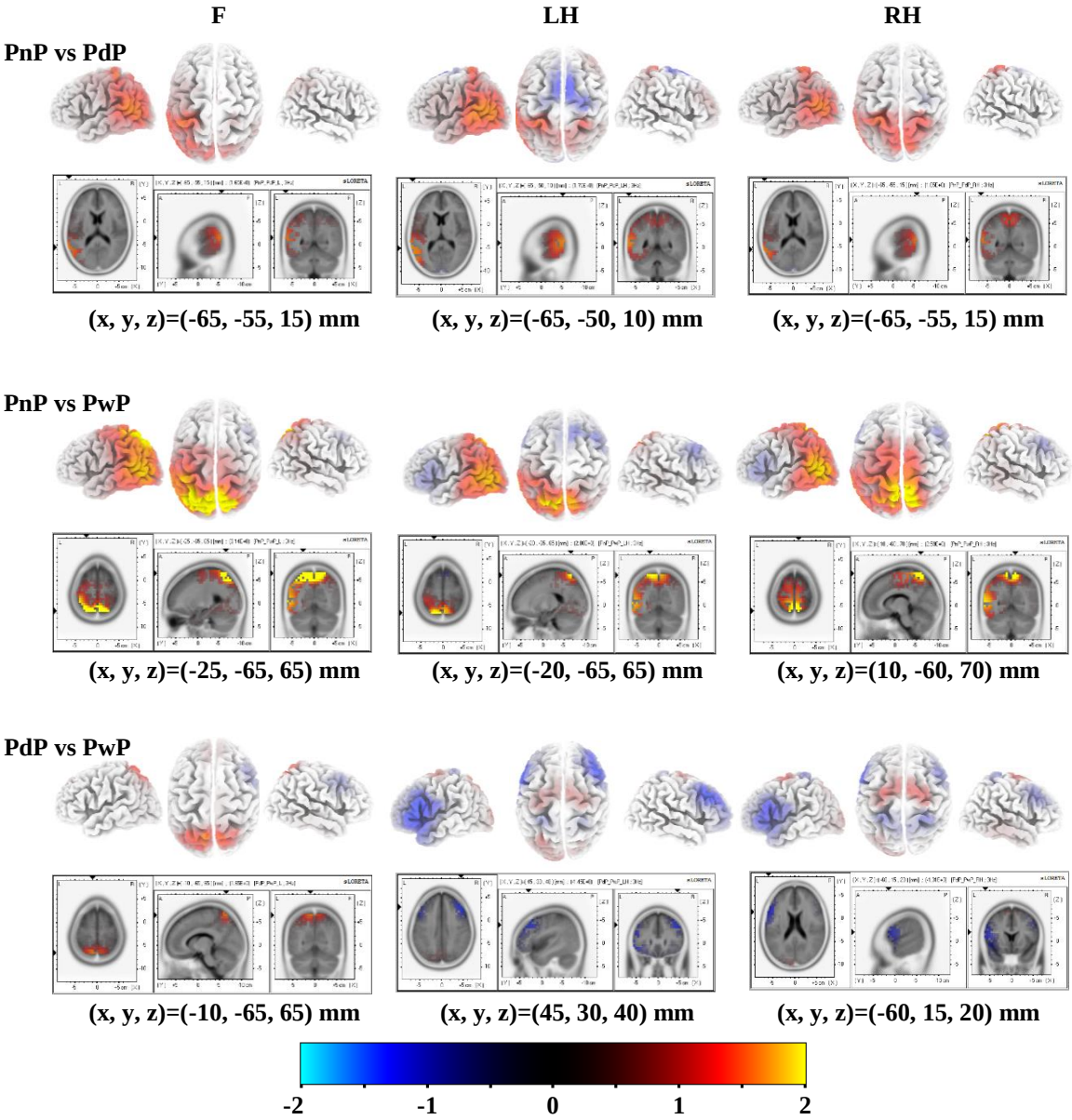


**Figure A.9** sLORETA localisation for motor imagery (MI) during F: feet, LH: left hand and RH: right hand MI compared between the patients groups: patients with no pain (PnP), patients developed CNP (PdP) and patients with CNP (PwP) in beta EEG frequency band (20-30Hz) over time window (0.5 to 1.5s). The first raw of each figure represents 3D map of the localisation while the second raw represents the 3D slice at the displayed of the voxel with negative or positive strongest activity. The (x, y, z) under each figure represent the Montreal Neurological Institute and Hospital (MNI) coordinate system of the voxel with strongest activity.

# Appendix B

**Table B.1:** Areas with significant differences between eyes opened relaxed state after the last compared to before the first NF session for PwP_NF3 in theta (4-8Hz), alpha (8-12Hz) and beta (20-30Hz).

| Band | Activity | Brain Lobe | BA | H | N.V. | Voxel with maximum t value | | | |
|---|---|---|---|---|---|---|---|---|---|
| | | | | | | Statistics t-values | MNI Coordinate | | |
| | | | | | | | x | y | z |
| Theta | Increase | Parietal | 7 | L and **R** | 280 | 16.9 | 25 | -65 | 65 |
| | | Frontal | 6 | **L** and R | 137 | 13.8 | -5 | 40 | 40 |
| | | Frontal | 8 | **L** and R | 115 | 13.5 | -5 | 50 | 45 |
| | | Frontal | 9 | **L** and R | 65 | 12.8 | -5 | 50 | 40 |
| | | Frontal | 32 | L and **R** | 17 | 11.9 | -5 | 25 | 40 |
| | Decrease | Frontal | 11 | **L** and R | 148 | -21.7 | 5 | 65 | -10 |
| | | Frontal | 10 | **L** and R | 210 | -21.5 | 5 | 65 | -5 |
| | | Limbic | 32 | **L** and R | 31 | -16.1 | 0 | 50 | 0 |
| Alpha | Increase | Parietal | 7 | L and **R** | 223 | 16.3 | 25 | -65 | 65 |
| | | Frontal | 6 | **L** and R | 93 | 10.9 | -5 | 40 | 40 |
| | | Frontal | 8 | **L** and R | 88 | 10.8 | -5 | 50 | 45 |
| | Decrease | Frontal | 11 | **L** and R | 154 | -22.4 | 5 | 65 | -10 |
| | | Frontal | 10 | L and **R** | 239 | -22.2 | 5 | 65 | -5 |
| | | Frontal | 6 | L and **R** | 172 | -16.8 | -5 | -35 | 70 |
| Beta | Increase | Frontal | 6 | **L** and R | 245 | 31.8 | -5 | 40 | 40 |
| | | Frontal | 8 | L and **R** | 152 | 31.1 | -5 | 50 | 45 |
| | | Frontal | 9 | L and **R** | 129 | 29.0 | -5 | 50 | 40 |
| | | Frontal | 32 | L and **R** | 21 | 27.2 | -5 | 25 | 40 |
| | Decrease | Frontal | 11 | **L** and R | 195 | -39.9 | 5 | 65 | -15 |
| | | Frontal | 10 | L and **R** | 240 | -39.4 | 5 | 60 | -5 |
| | | Limbic | 32 | **L** and R | 54 | -34.3 | 0 | 50 | 0 |

**MNI**: the Montreal Neurological Institute and Hospital (MNI) coordinate system. **BA**: Brodmann area. **H**: Brain Hemisphere. **R**, Right; **L**, Left. The brain hemisphere with bold font is the hemisphere with higher contribution in the number of significant voxel. **N.V.:** Number of Voxel.

**Table B.2:** Areas with significant differences between eyes opened relaxed state after the last compared to before the first NF session for PwP_NF4 in theta (4-8Hz), alpha (8-12Hz) and beta (20-30Hz).

| Band | Activity | Brain Lobe | BA | H | N.V. | Voxel with maximum t value | | | |
|---|---|---|---|---|---|---|---|---|---|
| | | | | | | Statistics t-values | MNI Coordinate | | |
| | | | | | | | x | y | z |
| **Theta** | **Increase** | Parietal | 7 | L and **R** | 192 | 14.9 | 20 | -60 | 65 |
| | | Frontal | 6 | L and **R** | 238 | 12.6 | -5 | -10 | 65 |
| | | Parietal | 5 | L and **R** | 24 | 10.9 | -5 | -50 | 70 |
| | | Frontal | 5 | L and **R** | 43 | 10.7 | -5 | -50 | 65 |
| | **Decrease** | Occipital | 18 | L and **R** | 292 | -21.8 | 15 | -100 | 15 |
| | | Occipital | 19 | L and **R** | 237 | -18.9 | 15 | -95 | 20 |
| | | Occipital | 17 | L and **R** | 76 | -17.7 | 10 | -100 | 0 |
| **Alpha** | **Increase** | Parietal | 7 | L and **R** | 261 | 23.7 | 40 | -60 | 55 |
| | | Parietal | 40 | L and **R** | 234 | 22.9 | 45 | -60 | 55 |
| | | Parietal | 5 | L and **R** | 28 | 19.7 | 25 | -50 | 65 |
| | | Frontal | 5 | L and **R** | 49 | 18.9 | 20 | -45 | 55 |
| | **Decrease** | Occipital | 18 | **L** and R | 245 | -25.5 | 15 | -100 | 15 |
| | | Occipital | 17 | L and **R** | 75 | -22.4 | 10 | -100 | 0 |
| | | Occipital | 19 | **L** and R | 107 | -21.6 | 15 | -95 | 20 |
| **Beta** | **Increase** | Frontal | 6 | **L** and R | 334 | 17.9 | -5 | -10 | 65 |
| | | Limbic | 24 | L and **R** | 106 | 15.1 | -5 | -10 | 50 |
| | | Parietal | 7 | L and **R** | 234 | 15.0 | 20 | -60 | 65 |
| | | Frontal | 31 | **L** and R | 17 | 14.6 | 0 | -15 | 50 |
| | | Limbic | 31 | L and **R** | 33 | 14.3 | -10 | -15 | 50 |
| | | Parietal | 2 | **R** | 36 | 14.1 | 65 | -25 | 35 |
| | | Parietal | 1 | **R** | 9 | 14.0 | 65 | -20 | 40 |
| | **Decrease** | Occipital | 18 | L and **R** | 314 | -28.1 | 15 | -100 | 15 |
| | | Occipital | 17 | L and **R** | 77 | -26.7 | 10 | -100 | 0 |
| | | Occipital | 19 | L and **R** | 231 | -25.5 | 15 | -95 | 20 |

**MNI**: the Montreal Neurological Institute and Hospital (MNI) coordinate system. **BA**: Brodmann area. **H**: Brain Hemisphere. **R**, Right; **L**, Left. The brain hemisphere with bold font is the hemisphere with higher contribution in the number of significant voxel. **N.V.:** Number of Voxel.

**Table B.3:** Areas with significant differences between eyes opened relaxed state after the last compared to before the first NF session for PwP_NF5 in theta (4-8Hz), alpha (8-12Hz) and beta (20-30Hz).

| Band | Activity | Brain Lobe | BA | H | N.V. | Voxel with maximum t value | | | |
|---|---|---|---|---|---|---|---|---|---|
| | | | | | | Statistics t-values | MNI Coordinate | | |
| | | | | | | | x | y | z |
| **Theta** | **Increase** | Parietal | 5 | **L** and R | 41 | 22.0 | -30 | -45 | 70 |
| | | Parietal | 2 | **L** and R | 17 | 21.1 | -30 | -40 | 70 |
| | | Parietal | 7 | **L** and R | 209 | 21.0 | -35 | -75 | 45 |
| | | Parietal | 19 | **L** | 23 | 19.8 | -40 | -75 | 40 |
| | | Parietal | 40 | **L** | 64 | 19.7 | -45 | -65 | 45 |
| | | Parietal | 39 | **L** | 16 | 19.3 | -45 | -70 | 40 |
| | **Decrease** | Frontal | 8 | **R** and L | 45 | -8.9 | 15 | 50 | 45 |
| | | Frontal | 9 | **R** and L | 71 | -8.8 | 15 | 55 | 40 |
| | | Occipital | 18 | **R** and L | 127 | -8.7 | 25 | -90 | -25 |
| **Alpha** | **Increase** | Parietal | 1 | **L** | 6 | 31.1 | -35 | -35 | 70 |
| | | Parietal | 7 | **L** and R | 172 | 30.4 | -40 | -70 | 45 |
| | | Parietal | 40 | **L** | 97 | 30.4 | -45 | -65 | 45 |
| | | Parietal | 2 | **L** and R | 22 | 29.5 | -30 | -40 | 70 |
| | | Parietal | 19 | **L** | 29 | 29.5 | -40 | -75 | 40 |
| | **Decrease** | Occipital | 18 | **R** | 68 | -13.3 | 30 | -90 | -20 |
| | | Occipital | 19 | **R** | 72 | -13.3 | 25 | -85 | -20 |
| | | Limbic | 30 | **R** | 14 | -12.0 | 20 | -65 | 5 |
| **Beta** | **Increase** | Parietal | 1 | **L** | 1 | 8.8 | -35 | -35 | 70 |
| | | Parietal | 2 | **L** | 10 | 8.3 | -40 | -40 | 65 |
| | | Temporal | 39 | **L** | 16 | 8.2 | -50 | -75 | 30 |
| | | Parietal | 19 | **L** | 5 | 7.8 | -40 | -75 | 40 |
| | | Parietal | 7 | **L** | 12 | 7.5 | -35 | -75 | 45 |
| | | Parietal | 5 | **L** | 5 | 7.0 | -40 | -45 | 65 |
| | | Parietal | 40 | **L** | 17 | 6.5 | -45 | -40 | 60 |
| | **Decrease** | Parietal | 19 | L and **R** | 25 | -15.5 | -10 | -85 | 40 |
| | | Parietal | 7 | L and **R** | 318 | -14.4 | -10 | -80 | 40 |
| | | Occipital | 19 | L and **R** | 210 | -14.0 | 10 | -90 | 35 |
| | | Temporal | 39 | **R** | 35 | -13.4 | 60 | -60 | 10 |
| | | Temporal | 21 | **R** | 125 | -13.3 | 65 | -55 | 0 |

**MNI**: the Montreal Neurological Institute and Hospital (MNI) coordinate system. **BA**: Brodmann area. **H**: Brain Hemisphere. **R**, Right; **L**, Left. The brain hemisphere with bold font is the hemisphere with higher contribution in the number of significant voxel. **N.V.:** Number of Voxel.

**Table B.4:** Areas with significant differences between eyes opened relaxed state after the last compared to before the first NF session for PwP_NF7 in theta (4-8Hz), alpha (8-12Hz) and beta (20-30Hz).

| Band | Activity | Brain Lobe | BA | H | N.V. | Voxel with maximum t value | | | |
|---|---|---|---|---|---|---|---|---|---|
| | | | | | | Statistics t-values | MNI Coordinate | | |
| | | | | | | | x | y | z |
| **Theta** | **Increase** | Parietal | 40 | **L** | 137 | 23.7 | -50 | -60 | 40 |
| | | Parietal | 39 | **L** | 17 | 23.4 | -55 | -65 | 35 |
| | | Occipital | 19 | **L** | 16 | 19.6 | -55 | -75 | 5 |
| | | Temporal | 37 | **L** | 62 | 19.3 | -60 | -65 | 5 |
| | | Temporal | 22 | **L** | 42 | 18.6 | -60 | -60 | 20 |
| | **Decrease** | Frontal | 10 | **L** and R | 82 | -26.1 | -40 | 55 | 5 |
| | | Frontal | 46 | **L** and R | 10 | -22.1 | -40 | 45 | 10 |
| | | Frontal | 11 | **L** | 45 | -21.9 | -45 | 50 | -10 |
| | | Frontal | 47 | **L** and R | 79 | -21.6 | -50 | 45 | -10 |
| **Alpha** | **Increase** | Frontal | 6 | **L** and R | 211 | 20.2 | 5 | -25 | 70 |
| | | Frontal | 4 | **L** and R | 30 | 19.0 | 10 | -30 | 70 |
| | | Frontal | 5 | **L** and R | 49 | 16.4 | 0 | -35 | 60 |
| | | Parietal | 3 | **L** and R | 41 | 16.3 | 10 | -40 | 70 |
| | **Decrease** | Frontal | 10 | **L** and R | 125 | -17.6 | -35 | 55 | 5 |
| | | Frontal | 11 | **L** and R | 80 | -15.8 | -40 | 55 | -10 |
| | | Frontal | 47 | **L** | 74 | -14.3 | -50 | 45 | -10 |
| | | Frontal | 46 | **L** | 7 | -13.1 | -40 | 45 | 10 |
| **Beta** | **Increase** | Frontal | 6 | L and **R** | 114 | 12.7 | 5 | -25 | 70 |
| | | Frontal | 4 | L and **R** | 14 | 10.0 | 10 | -30 | 70 |
| | | Frontal | 5 | L and **R** | 22 | 8.1 | 0 | -35 | 60 |
| | **Decrease** | Parietal | 7 | L and **R** | 163 | -15.1 | 30 | -65 | 60 |
| | | Frontal | 10 | **L** and R | 161 | -13.8 | -30 | 60 | 5 |
| | | Frontal | 11 | **L** and R | 114 | -12.9 | -30 | 60 | -10 |
| | | Parietal | 5 | L and **R** | 28 | -12.8 | 35 | -50 | 65 |

**MNI**: the Montreal Neurological Institute and Hospital (MNI) coordinate system. **BA**: Brodmann area. **H**: Brain Hemisphere. **R**, Right; **L**, Left. The brain hemisphere with bold font is the hemisphere with higher contribution in the number of significant voxel. **N.V.:** Number of Voxel.

# 9

# References

# References


1. Martini FH, Edwin F B. *Essentials of Anatomy & Phsiology*. 5th ed. Pearson Education, Inc.; 2010.

2. Martini FH, Nath JL. *Fundamentals of Anatomy & Physiology*. 8th ed. Pearson Education, Inc.; 2009.

3. Thomas H C. *Essential Clinical Neuroanatomy*. 1st ed. John Wiley & Sons, Ltd; 2016.

4. Brodmann K. *Brodmann's Localisation in the Cerebral Cortex*. 3rd ed. (Garey LJ, ed.). Springer Science+Business Media, Inc; 2006.

5. Sneel S. R. *Clinical Neuroanatomy*. .Ch 1, 7th. Lippincott William and Wilkins, a Wolter Kluwer; 2010.

6. VanPutte CL, Regan JL, Russo AF. *Essentials of Anatomy and Physiology*. 9th ed. New York: McGraw-Hill Education; 2016.

7. Rajagopal MR. Pain - Basic Considerations. *Indian J Anaesthesiol*. 2006;50(5):331-334.

8. Merskey H, Bogduk N. *Classification of Chronic Pain*.; 2002. doi:10.1002/ana.20394.

9. Bryce TN, Biering-Sørensen F, Finnerup NB, et al. International spinal cord injury pain classification: part I. Background and description. *Spinal Cord*. 2012;50:413-417.

10. Loeser JD TR. The kyoto protocol of IASP Basic Pain Terminology. *J Pain*. 2008;137(3):473-477.

11. Jensen TS, Baron R, Haanpää M, et al. A new definition of neuropathic pain. *Pain*. 2011;152(10):2204-2205.

12. Nicholson B. Differential diagnosis: nociceptive and neuropathic pain. *Am J Manag Care*. 2006;12:256-262.

13. Patestas MA, Gartner LP. *A Textbook of Neuroanatomy*. Oxford: Blackwell Publishing; 2006.

14. Garcia-Larrea L, Peyron R. Pain matrices and neuropathic pain matrices: a review. *Pain*. 2013;154:29-43.

15. Brooks J, Tracey I. From nociception to pain perception: imaging the spinal and supraspinal pathways. *J Anat*. 2005;207(1):19-33.

16. Gustin SM, Wrigley PJ, Siddall PJ, Henderson L a. Brain anatomy changes associated with persistent neuropathic pain following spinal cord injury. *Cereb cortex*. 2010;20(6):1409-1419.

17. Field-Fote EC. *Spinal Cord Injury Rehabilitation*. United State of America: F. A. Davis Company; 2009.

18. Maynard FM, Bracken MB, Creasey G, et al. International standards for neurological and functional classification of spinal cord injury. *Spinal Cord*. 1997;35(5):266-274.

19. Noordenbos W, Wall PD. Diverse sensory functions with an almost totally divided spinal cord. A case of spinal cord transection with preservation of part of one anterolateral quadrant. *Pain*. 1976;2:185-195.

20. Zeilig G, Enosh S, Rubin-Asher D, Lehr B, Defrin R. The nature and course of sensory changes following spinal cord injury: Predictive properties and implications on the mechanism of central pain. *Brain*. 2012;135(2):418-430.

21. Vasquez N, Gall A, Ellaway PH, Craggs MD. Light touch and pin prick disparity in the international standard for neurological classification of spinal cord injury (ISNCSCI). *Spinal Cord*. 2013;51(5):375-378.

22. Ballantyne JC. Diagnosis and classifi cation of neuropathic pain epidemiology and impact of neuropathic pain. *Pain*. 2010;XVIII(7):1-6.

23. Haanpää M, Attal N, Backonja M, et al. NeuPSIG guidelines on neuropathic pain assessment. *Pain*. 2011;152(1):14-27.

24. Wydenkeller S, Maurizio S, Dietz V, Halder P. Neuropathic pain in spinal cord injury: significance of clinical and electrophysiological measures. *Eur J Neurosci*. 2009;30(1):91-99.

25. Lee S, Zhao X, Hatch M, Chun S, Chang E. Central neuropathic pain in spinal cord injury. *Crit Rev Phys Rehabil Med*. 2013;25(3-4):159-172.

26. Siddall PJ, Taylor D a, McClelland JM, Rutkowski SB, Cousins MJ. Pain report and the relationship of pain to physical factors in the first 6 months following spinal cord injury. *Pain*. 1999;81:187-197. http://www.ncbi.nlm.nih.gov/pubmed/10353507.

27. D'Angelo R, Morreale A, Donadio V, et al. Neuropathic pain following spinal cord injury: what we know about mechanisms, assessment and management. *Eur RevMed Pharmacol Sci*. 2013;17:3257-3261.

28. Brix N, Baastrup C, Staehelin T. Neuropathic pain following spinal cord injury pain : mechanisms and treatment. *Scand J Pain*. 2009;1(1):3-11.

29. Finnerup N, Baastrup C, Jensen T. Neuropathic pain following spinal cord injury pain : mechanisms and treatment. *Scand J Pain*. 2009;1(1):3-11.

30. Hains BC, Waxman SG. Activated microglia contribute to the maintenance of chronic pain after spinal cord injury. *J Neurosci*. 2006;26(16):4308-4317.

31. Hains BC, Saab CY, Waxman SG. Changes in electrophysiological properties and sodium channel Nav1.3 expression in thalamic neurons after spinal cord injury. *Brain*. 2005;128:2359-2371.

32. Bouhassira D, Attal N, Fermanian J, et al. Development and validation of the Neuropathic Pain Symptom Inventory. *Pain*. 2004;108(3):248-257.

33. Tan G, Jensen MP, Thornby JI, Shanti BF. Validation of the brief pain inventory for chronic nonmalignant pain. *J Pain*. 2004;5(2):133-137.

34. Bennett M. The LANSS Pain Scale : the Leeds assessment of neuropathic symptoms and signs. 2001;92.

35. May S, Serpell M. Diagnosis and assessment of neuropathic pain. *Med reports*. 2009;1(76):1-4. doi:10.3410/M1-76.

36. Melzack R. The short-form McGill pain questionnaire. *Pain*. 1987;30:191-197.

37. Savic G, Bergström EMK, Davey NJ, et al. Quantitative sensory tests (perceptual thresholds) in patients with spinal cord injury. *J Rehabil Res Dev*. 2007;44(1):77-82.

38. Helme RD. Drug treatment of neuropathic pain. *Aust Prescr*. 2006;29(3):72-75. http://www.australianprescriber.com/magazine/29/3/72/5.

39. Baastrup C, Finnerup NB. Pharmacological management of neuropathic pain following spinal cord injury. *CNS Drugs*. 2008;22(6):455-475.

40. Dworkin RH, O'Connor AB, Backonja M, et al. Pharmacologic management of neuropathic pain: Evidence-based recommendations. *Pain*. 2007;132(3):237-251.

41. Ngernyam N, Jensen M, Auvichayapat N, Punjaruk W, Auvichayapat P. Transcranial direct current stimulation in neuropathic pain. *Natl Institutes Heal*. 2013;3:1-13.

42. Lefaucheur JP, Drouot X, Menard-Lefaucheur I, Keravel Y, Nguyen JP. Motor cortex rTMS restores defective intracortical inhibition in chronic neuropathic pain. *Neurology*. 2006;67:1568-1574.

43. Nardone R, Höller Y, Leis S, et al. Invasive and non-invasive brain stimulation for treatment of neuropathic pain in patients with spinal cord injury: a review. *J Spinal Cord Med*. 2014;37(1):19-31.

44. Hassan MA, Fraser M, Conway BA, Allan DB, Vuckovic A. The mechanism of neurofeedback training for treatment of central neuropathic pain in paraplegia: a pilot study. *BMC Neurol*. 2015;15(1):1-13.

45. Zeidan F, Martucci KT, Kraft RA, Gordon NS, McHaffie JG, Coghill RC. Brain mechanisms supporting the modulation of pain by mindfulness meditation. *J Neurosci*. 2011;31(14):5540-5548.

46. Adams MM, Hicks a L. Spasticity after spinal cord injury. *Spinal Cord*. 2005;43:577-586.

47. Biering-s F, Nielsen JB, Klinge K. Spasticity-assessment : a review. *Spinal Cord*. 2006;44:708-722.

48. Wolpaw JR. What can the spinal cord teach us about learning and memory? *Neurosci*. 2010;16(5):532-549.

49. Misiaszek JE. The H-reflex as a tool in neurophysiology: its limitations and uses in understanding nervous system function. *Muscle Nerve*. 2003;28(2):144-160.

50. Supraja M, Resident S. Study of quantitative assessment of spasticity by isokinetic dynamometry. *India J Phys Med Rehabil*. 2003;14:15-18.

51. Bohannon RW, Smith MB. Interrater reliability of a modified ashworth scale of muscle Spasticity. *Phys Ther*. 1987;67(2):206-207.

52. Lin C-C, Ju M-S, Lin C-W. The pendulum test for evaluating spasticity of the elbow joint. *Arch Phys Med Rehabil*. 2003;84(1):69-74.

53. Palmieri RM, Ingersoll CD, Hoffman MA. The hoffmann reflex: methodologic considerations and applications for use in sports medicine and athletic training research. *Jouranl Athl Train*. 2004;39(3):268-277.

54. Henneberg KA. *The Biomedical Engineering Handbook*. J. D. Bronzino, ed., CRC press LLC; 2000.

55. Frank DL, Khorshid L, Kiffer JF, Moravec CS, McKee MG. Biofeedback in medicine: who, when, why and how? *Ment Health Fam Med*. 2010;7(2):85-91.

56. Angelakis E, Stathopoulou S, Frymiare JL, Green DL, Lubar JF, Kounios J. EEG neurofeedback: a brief overview and an example of peak alpha frequency training for cognitive enhancement in the elderly. *Clin Neuropsychol*. 2007;21:110-129.

57. Demos J. *Getting Started with Neurofeedback*. New York USA: W.W. Norton & Company; 2005.

58. Escolano C, Aguilar M, Minguez J. EEG-based upper alpha neurofeedback training improves working memory performance. *33rd Annu Int Conf IEEE EMBS*. January 2011:2327-2330.

59. Budzynski TH, Budzynski HK, Evans JR, Abbarbanel A. *Introducation to Quantitative EEG and Neurofeedback Advanced Theory and Application*. Elsevier Inc; 2009.

60. Huettel SA, Song AW, McCarthy G. *Functional Magnetic Resonance Imaging*. 2nd ed. Sinauer Associates Inc; 2009.

61. Weiskopf N, Veit R, Erb M, et al. Physiological self-regulation of regional brain activity using real-time functional magnetic resonance imaging (fMRI): Methodology and exemplary data. *Neuroimage*. 2003;19(3):577-586.

62. Weiskopf N, Scharnowski F, Veit R, Goebel R, Birbaumer N, Mathiak K. Self-regulation of local brain activity using real-time functional magnetic resonance imaging (fMRI). *J Physiol Paris*. 2004;98:357-373.

63. Scharnowski F, Veit R, Zopf R, et al. Manipulating motor performance and memory through real-time fMRI neurofeedback. *Biol Psychol*. 2015;108:85-97.

64. Cohen D. Magnetoencephalography: evidence of magnetic fields produced by alpha-rhythm currents. *Science (80- )*. 1986;161:784-786.

65. Parkkonen L. *Clinical Systems Neuroscience*. (Kansaku K, Cohen LG, Birbaumer N, eds.). Tokyo: Springer; 2015.

66. Birbaumer N, Elbert T, Canavan a G, Rockstroh B. Slow potentials of the cerebral

cortex and behavior. *Am Physiol Soc*. 1990;70(1):1-41.

67. Gruzelier J. A theory of alpha/theta neurofeedback, creative performance enhancement, long distance functional connectivity and psychological integration. *Cogn Process*. 2009;10:101-109.

68. Congedo M, Lubar JF, Joffe D. Low-resolution electromagnetic tomography neurofeedback. *IEEE Trans Neural Syst Rehabil Eng*. 2004;12(4):387-397.

69. Pascual-Marqui RD. Standardized low-resolution brain electromagnetic tomography (sLORETA): technical details. *Methods Find Exp Clin Pharmacol*. 2002;24:5-12.

70. Lubar JF, Swartwood MO, Swartwood JN, O'Donnell PH. Evaluation of the effectiveness of EEG neurofeedback training for ADHD in a clinical setting as measured by changes in T.O.V.A. scores, behavioral ratings, and WISC-R performance. *Biofeedback Self Regul*. 1995;20(1):83-99.

71. Kropotov JD, Grin-Yatsenko VA, Ponomarev VA, Chutko LS, Yakovenko EA, Nikishena IS. ERPs correlates of EEG relative beta training in ADHD children. *Int J Psychophysiol*. 2005;55(1):23-34.

72. Lansbergen MM, Van Dongen-Boomsma M, Buitelaar JK, Slaats-Willemse D. ADHD and EEG-neurofeedback: A double-blind randomized placebo-controlled feasibility study. *J Neural Transm*. 2011;118(2):275-284.

73. Evans JR, Abarbane A. *Introduction to Quantitative EEG and Neurofeedback*. Academic Press; 1999.

74. Logemann HNA, Lansbergen MM, Van Os TWDP, B??cker KBE, Kenemans JL. The effectiveness of EEG-feedback on attention, impulsivity and EEG: A sham feedback controlled study. *Neurosci Lett*. 2010;479(1):49-53. doi:10.1016/j.neulet.2010.05.026.

75. Monastra VJ, Lynn S, Linden M, Lubar JF, Gruzelier J, LaVaque TJ. Electroencephalographic biofeedback in the treatment of attention-deficit/hyperactivity disorder. *Appl Psychophysiol Biofeedback*. 2005;30(2):95-114.

76. Arns M, Feddema I, Kenemans JL. Differential effects of theta/beta and SMR neurofeedback in ADHD on sleep onset latency. *Front Hum Neurosci*. 2014;8:1-10.

77. Hoedlmoser K, Pecherstorfer T, Gruber G, et al. Instrumental conditioning of human sensorimotor rhythm (12-15 Hz) and its impact on sleep as well as declarative learning. *Sleep*. 2008;31(10):1401-1408.

78. Finley WW, Smith HA, Etherton MD. Reduction of seizures and normalization of the EEG in a severe epileptic following sensorimotor biofeedback training: preliminary study. *Biol Psychol*. 1975;2:189-203.

79. Sterman MB. Basic concepts and clinical findings in the treatment of seizure disorders with EEG operant conditioning. *Clin Electroencephalogr*. 2000;31(1):45-55.

80. Walker JE, Kozlowski GP. Neurofeedback treatment of epilepsy. *Child Adolesc Psychiatr Clin N Am*. 2005;14:163-176.

81. Hammond DC. Neurofeedback treatment of depression and anxiety. *J Adult Dev*. 2005;12(2-3):131-137.

82. Elsa B, J. Peter R, Rufus B. Clinical use of an alpha asymmetry neurofeedback protocol in the treatment of mood disorders. *J Neurother*. 2001;4(4):11-18.

83. Peniston EG, Kulkosky PJ. Alpha-theta brainwave neuro-feedback therapy for Vietnam veterans with combat-related post-traumatic stress disorder. *Med Psychother*. 1991;4:47-60.

84. Coben R. Connectivity-guided neurofeedback for autistic spectrum disorder. *Biofeedback*. 2007;35(4):131-135.

85. Gannon L, Sternbach R. Alpha enhancement as a treatment for pain: a case study. *J Behav Ther Exp Psychiatry*. 1971;2(3):209-213.

86. Caro XJ, Winter EF. EEG biofeedback treatment improves certain attention and somatic symptoms in fibromyalgia: a pilot study. *Appl Psychophysiol Biofeedback*. 2011;36(3):193-200. doi:10.1007/s10484-011-9159-9.

87. Kayiran S, Dursun E, Dursun N, Ermutlu N, Karamürsel S. Neurofeedback intervention in fibromyalgia syndrome; a randomized, controlled, rater blind clinical trial. *Appl Psychophysiol Biofeedback*. 2010;35(4):293-302.

88. Jensen MP, Gertz KJ, Kupper AE, et al. Steps toward developing an EEG biofeedback treatment for chronic pain. *Appl Psychophysiol Biofeedback*. 2013;(1).

89. Picton TW, Lins OG, Scherg M. The recording and analysis of event-related potentials. *Handb Neuropsychol*. 1995;10:3-73.

90. Niedermeyer E, Silva FL da. *Electroencephalography: Basic Principles, Clinical Application, and Related Fields*. 5th ed. Lippincott William and Wilkins; 2005.

91. Landa L, Krpoun Z, Kolarova M, Tomas K. Event-related potentials and their applications. *J Neurocognitive Res*. 2014;56(1-2):17-23.

92. Xu R, Jiang N, Vuckovic A, et al. Movement-related cortical potentials in paraplegic patients: abnormal patterns and considerations for BCI-rehabilitation. *Front Neuroeng*. 2014;7:35.

93. Castro A, Díaz F, Sumich A. Long-term neuroplasticity in spinal cord injury patients: A study on movement-related brain potentials. *Int J Psychophysiol*. 2013;87:205-214.

94. Castro A, Díaz F, Van Boxtel GJM. How does a short history of spinal cord injury affect movement-related brain potentials? *Eur J Neurosci*. 2007;25:2927-2934.

95. Shibasaki H, Barrett G, Halliday E, Halliday a M. Components of the movement-related cortical potential and their scalp topography. *Electroencephalogr Clin Neurophysiol*. 1980;49:213-226.

96. Deecke L, Grözinger B, Kornhuber HH. Voluntary finger movement in man: Cerebral potentials and theory. *Biol Cybern*. 1976;23(2):99-119.

97. Deecke L, Scheid P, Kornhuber HH. Distribution of readiness potential, pre-motion

positivity, and motor potential of the human cerebral cortex preceding voluntary finger movements. *Exp Brain Res*. 1969;7:158-168.

98. Bötzel K, Ecker C, Schulze S. Topography and dipole analysis of reafferent electrical brain activity following the Bereitschaftspotential. *Exp brain Res*. 1997;114:352-361.

99. Delorme A, Makeig S. EEGLAB: an open source toolbox for analysis of single-trial EEG dynamics including independent component analysis. *J Neurosci Methods*. 2004;134:9-21.

100. Yi W, Qiu S, Qi H, Zhang L, Wan B, Ming D. EEG feature comparison and classification of simple and compound limb motor imagery. *J Neuroeng Rehabil*. 2013;10(106):1-12.

101. Neuper C, Klimesch W. *Event-Related Dynamics of Brain Oscillations*. 1st ed. Elsevier B.V.; 2006.

102. Sejdic E, Djurovic I, Jiang J. Time-frequency feature representation using energy concentration: an overview of recent advances. *Digit Signal Process A Rev J*. 2009;19(1):153-183.

103. Lee DTL, Yamamoto A. Wavelet analysis : theory and applications. *Hewlett-Packard*. 1994:44-52.

104. Grossmann A, Morlet J. Decomposition of hardy functions into square integrable wavelets of constant shape. *SIAM J Math Anal*. 1984;15(4):723-736.

105. Daubechies I, Grossmann A, Meyer Y. Painless nonorthogonal expansions. *J Math Phys*. 1986;27(5):1271-1283.

106. Roach BJ, Mathalon DH. Event-related EEG time-frequency analysis: an overview of measures and an analysis of early gamma band phase locking in schizophrenia. *Schizophr Bull*. 2008;34(5):907-926.

107. Arnon C. *Biomedical Signal Processing*. Volume 1. Florida: CRC press; 1986.

108. Metin A. *Biomedical Signal Processing*. California: Academic Press, Inc; 1994.

109. Challis RE, Kitney RI. Biomedical signal processing (in four parts) - Part 3 The power spectrum and coherence function. *Med Biol Eng Comput*. 1991;29:225-241.

110. Jung T-PP, Makeig S, Humphries C, et al. Removing electroencephalographic artifacts by blind source separation. *Psychophysiology*. 2000;37:163-178.

111. Comon P. Independent component analysis, a new concept? *Signal Processing*. 1994;36:287-314.

112. Bigdely-Shamlo N, Mullen T, Kreutz-Delgado K, Makeig S. Measure projection analysis: a probabilistic approach to EEG source comparison and multi-subject inference. *Neuroimage*. 2013;72:287-303.

113. Hyvarinen A, Oja E. Independent component analysis : algorithms and applications. *Neural Networks*. 2000;13:411-430.

114. Makeig S, Bell AJ, Jung T, Sejnowski TJ. Independent component analysis of electroencephalographic data. *Adv Neural Inf Process Syst*. 1996;8:145-151.

115. Ding YM, Kastin AJ, Pan WH. Neural plasticity after spinal cord injury. *Curr Pharm Des*. 2005;11(11):1441-1450.

116. Moore CI, Stern CE, Dunbar C, Kostyk SK, Gehi A, Corkin S. Referred phantom sensations and cortical reorganization after spinal cord injury in humans. *Proc Natl Acad Sci*. 2000;97(26):14703-14708.

117. Levy WJ, Amassian VE, Traad M, Cadwell J. Focal magnetic coil stimulation reveals motor cortical system reorganized in humans after traumatic quadriplegia. *Brain Res*. 1990;510(1):130-134.

118. Nakagawa H, Ninomiya T, Yamashita T, Takada M. Reorganization of corticospinal tract fibers after spinal cord injury in adult macaques. *Sci Rep*. 2015;5:1-9.

119. Kokotilo K, Eng J, Curt A. Reorganization and preservation of motor control of the brain in spinal cord injury: a systematic review. *J Neurotrauma*. 2009;26(11):2113-2126.

120. Lenz FA, Kwan HC, Dostrovsky JO, Tasker RR. Characteristics of the bursting pattern of action potentials that occurs in the thalamus of patients with central pain. *Brain Res*. 1989;496:357-360.

121. Calancie B, Lutton S, Broton JG. Central nervous system plasticity after spinal cord injury in man: interlimb reflexes and the influence of cutaneous stimulation. *Electroencephalogr Clin Neurophysiol*. 1996;101(4):304-315.

122. Dietz V. Neuronal plasticity after a human spinal cord injury: Positive and negative effects. *Exp Neurol*. 2012;235(1):110-115.

123. Alkadhi H, Brugger P, Boendermaker SH, et al. What disconnection tells about motor imagery: Evidence from paraplegic patients. *Cereb Cortex*. 2005;15(2):131-140.

124. Cramer SC, Lastra L, Lacourse MG, Cohen MJ. Brain motor system function after chronic, complete spinal cord injury. *Brain*. 2005;128(12):2941-2950.

125. Sabbah P, De SS, Leveque C, et al. Sensorimotor cortical activity in patients with complete spinal cord injury: a functional magnetic resonance imaging study. *J Neurotrauma*. 2002;19(1):53-60.

126. Sabre L, Tomberg T, Kõrv J, Kepler J, Kepler K, Asser T. Brain activation in the acute phase of traumatic spinal cord injury. *Spinal Cord*. 2016;54:65-68.

127. Curt A, Alkadhi H, Crelier GR, Boendermaker SH, Hepp-Reymond M-C, Kollias SS. Changes of non-affected upper limb cortical representation in paraplegic patients as assessed by fMRI. *Brain*. 2002;125:2567-2578.

128. Hotz-Boendermaker S, Funk M, Summers P, et al. Preservation of motor programs in paraplegics as demonstrated by attempted and imagined foot movements. *Neuroimage*. 2008;39(1):383-394.

129. Jurkiewicz MT, Mikulis DJ, McIlroy WE, Fehlings MG, Verrier MC. Sensorimotor

cortical plasticity during recovery following spinal cord injury: a longitudinal fMRI study. *Neurorehabilitation & Neural Repair*. 2007;21(6):527-538.

130. Curt A, Bruehlmeier M, Leenders KL, Roelcke U, Dietz V. Differential effect of spinal cord injury and functional impairment on human brain activation. *J Neurotrauma*. 2002;19(1):43-51.

131. Bruehlmeier M, Dietz V, Leenders KL, Roelcke U, Missimer J, Curt A. How does the human brain deal with a spinal cord injury? *Eur J Neurosci*. 1998;10:3918-3922.

132. Lacourse MG, Cohen MJ, Lawrence KE, Romero DH. Cortical potentials during imagined movements in individuals with chronic spinal cord injuries. *Behav Brain Res*. 1999;104:73-88.

133. Green JB, Sora E, Bialy Y, Ricamato A, Thatcher RW. Cortical motor reorganization after paraplegia: an EEG study. *Neurology*. 1999;53:736-743.

134. Gourab K, Schmit BD. Changes in movement-related b-band EEG signals in human spinal cord injury. *Clin Neurophysiol*. 2010;121:2017-2023.

135. Lopez-Larraz E, Montesano L, Gil-Agudo A, Minguez J, Oliviero A. Evolution of EEG motor rhythms after spinal cord injury: a longitudinal study. *PLoS One*. 2015;10(7):1-15.

136. Wrigley PJ, Press SR, Gustin SM, et al. Neuropathic pain and primary somatosensory cortex reorganization following spinal cord injury. *Pain*. 2009;141:52-59.

137. Pascoal-Faria P, Yalcin N, Fregni F. Neural markers of neuropathic pain associated with maladaptive plasticity in spinal cord injury. *Pain Pract*. 2015;15(4):371-377.

138. Jensen MP, Sherlin LH, Gertz KJ, et al. Brain EEG activity correlates of chronic pain in persons with spinal cord injury: clinical implications. *Spinal Cord*. 2013;51(1):55-58.

139. Boord P, Siddall PJ, Tran Y, Herbert D, Middleton J, Craig A. Electroencephalographic slowing and reduced reactivity in neuropathic pain following spinal cord injury. *Spinal Cord*. 2008;46(2):118-123.

140. Vuckovic A, Hasan MA, Fraser M, Conway BA, Nasseroleslami B, Allan DB. Dynamic oscillatory signatures of central neuropathic pain in spinal cord injury. *J Pain*. 2014;15(6):645-655.

141. Gustin SM, Wrigley PJ, Henderson L a, Siddall PJ. Brain circuitry underlying pain in response to imagined movement in people with spinal cord injury. *Pain*. 2010;148(3):438-445.

142. Yoon EJ, Kim YK, Shin HI, Lee Y, Kim SE. Cortical and white matter alterations in patients with neuropathic pain after spinal cord injury. *Brain Res*. 2013;1540:64-73.

143. Wall JT, Xu J, Wang X. Human brain plasticity: An emerging view of the multiple substrates and mechanisms that cause cortical changes and related sensory dysfunctions after injuries of sensory inputs from the body. *Brain Res Rev*. 2002;39:181-215.

144. Jutzeler CR, Huber E, Callaghan MF, et al. Association of pain and CNS structural changes after spinal cord injury. *Sci Rep*. 2016;6:1-13.

145. Freund P, Weiskopf N, Ward NS, et al. Disability, atrophy and cortical reorganization following spinal cord injury. *Brain*. 2011;134:1610-1622.

146. Gwak YS, Hulsebosch CE. GABA and central neuropathic pain following spinal cord injury. *Neuropharmacology*. 2011;60(5):799-808.

147. Hiersemenzel LP, Curt A, Dietz V. From spinal shock to spasticity: neuronal adaptations to a spinal cord injury. *Neurology*. 2000;54:1574-1582.

148. Mailis A, P. A, Ashby P. Alterations in group Ia projections to motoneurons following spinal lesions in humans. *J Neurophysiol*. 1990;64(2):637-647.

149. Lundell H, Barthelemy D, Skimminge A, Dyrby TB, Biering-Sørensen F, Nielsen JB. Independent spinal cord atrophy measures correlate to motor and sensory deficits in individuals with spinal cord injury. *Spinal Cord*. 2011;49(1):70-75.

150. Freund P, Weiskopf N, Ashburner J, et al. MRI investigation of the sensorimotor cortex and the corticospinal tract after acute spinal cord injury: A prospective longitudinal study. *Lancet Neurol*. 2013;12:873-881.

151. Gwak YS, Tan HY, Nam TS, Paik KS, Hulsebosch CE, Leem JW. Activation of spinal GABA receptors attenuates chronic central neuropathic pain after spinal cord injury. *J Neurotrauma*. 2006;23(7):1111-1124.

152. Hains BC, Klein JP, Saab CY, Craner MJ, Black J a, Waxman SG. Upregulation of sodium channel Nav1.3 and functional involvement in neuronal hyperexcitability associated with central neuropathic pain after spinal cord injury. *J Neurosci*. 2003;23(26):8881-8892.

153. Gao W, Yu LG, Liu YL, Wang YZ, Huang XL. Mechanism of GABA receptors involved in spasticity inhibition induced by transcranial magnetic stimulation following spinal cord injury. *J Huazhong Univ Sci Technol - Med Sci*. 2015;35(2):241-247.

154. Leis AA, Kronenberg MF, Sttetkarova I, Paske WC, Stokic D. Spinal motonuron excitability after acute spinal cord injury in humans. *Neurology*. 1996;47:231-237.

155. Gorassini MA, Knash ME, Harvey PJ, Bennett DJ, Yang JF. Role of motoneurons in the generation of muscle spasms after spinal cord injury. *Brain*. 2004;127:2247-2258.

156. D'Amico JM, Condliffe EG, Martins KJ, Bennett DJ, Gorassini MA. Recovery of neuronal and network excitability after spinal cord injury and implications for spasticity. *Front Integr Neurosci*. 2014;8:1-24.

157. Thompson AK, Wolpaw JR. Restoring walking after SCI: operant conditioning of spinal reflexes can help. *Neuroscientist*. 2015;21(2):203-2015.

158. Crone C, Johnsen LL, Biering-Sørensen F, Nielsen JB. Appearance of reciprocal facilitation of ankle extensors from ankle flexors in patients with stroke or spinal cord injury. *Brain*. 2003;126(2):495-507.

159. Barthélemy D, Willerslev-Olsen M, Lundell H, et al. Impaired transmission in the corticospinal tract and gait disability in spinal cord injured persons. *J Neurophysiol*. 2010;104:1167-1176.

160. Fagundes-Pereyra WJ, Teixeira MJ, Reyns N, et al. Motor cortex electric stimulation for the treatment of neuropathic pain. *Arq Neuropsiquiatr*. 2010;68(6):923-929.

161. Nguyen JP, Lefaucheur JP, Decq P, et al. Chronic motor cortex stimulation in the treatment of central and neuropathic pain. Correlations between clinical, electrophysiological and anatomical data. *Pain*. 1999;82(3):245-251.

162. Im S, Ha S, Kim D, Son B. Long-term results of motor cortex stimulation in the treatment of chronic, intractable neuropathic pain. *Stereotact Funct Neurosurg*. 2015;93(3):212-218.

163. Young RF, Kroening R, Fulton W, Feldman R a., Chambi I. Electrical stimulation of the brain in treatment of chronic pain. *J Neurosurg*. 1985;62(3):389–396.

164. Bittar RG, Kar-Purkayastha I, Owen SL, et al. Deep brain stimulation for pain relief: a meta-analysis. *J Clin Neurosci*. 2005;12(5):5-5.

165. Utz KS, Dimova V, Oppenlander K, Kerkhoff G. Electrified minds: transcranial direct current stimulation (tDCS) and galvanic vestibular stimulation (GVS) as methods of non-invasive brain stimulation in neuropsychology-A review of current data and future implications. *Neuropsychologia*. 2010;48(10):2789-2810.

166. Zaghi S, Heine N, Fregni F. Brain stimulation for the treatment of pain: a review of costs, clinical effects, and mechanisms of treatment for three different central neuromodulatory approaches. *J Pain Manag*. 2009;2(3):339-352.

167. Medeiros LF, de Souza ICC, Vidor LP, et al. Neurobiological effects of transcranial direct current stimulation: a review. *Front Psychiatry*. 2012;3:1-11.

168. Fregni F, Boggio PS, Lima MC, et al. A sham-controlled, phase II trial of transcranial direct current stimulation for the treatment of central pain in traumatic spinal cord injury. *Pain*. 2006;122:197-209.

169. Soler MD, Kumru H, Pelayo R, et al. Effectiveness of transcranial direct current stimulation and visual illusion on neuropathic pain in spinal cord injury. *Brain*. 2010;133(9):2565-2577.

170. Yoon EJ, Kim YK, Kim HR, Kim SE, Lee Y, Shin HI. Transcranial direct current stimulation to lessen neuropathic pain after spinal cord injury: a mechanistic PET study. *Neurorehabil Neural Repair*. 2014;28(3):250-259.

171. Wrigley PJ, Gustin SM, McIndoe LN, Chakiath RJ, Henderson LA, Siddall PJ. Longstanding neuropathic pain after spinal cord injury is refractory to transcranial direct current stimulation: a randomized controlled trial. *Pain*. 2013;154:2178-2184.

172. Ngernyam N, Jensen MP, Arayawichanon P, et al. The effects of transcranial direct current stimulation in patients with neuropathic pain from spinal cord injury. *Clin Neurophysiol*. 2015;126(2):382-390.

173. Boldt I, Eriks-Hoogland I, Brinkhof MW, De BR, Joggi D, Von EE. Non-

pharmacological interventions for chronic pain in people with spinal cord injury. *Cochrane Databasem Syst Rev*. 2014;(11):1-85.

174. O'Connell NE, Wand BM, Marston L, Spencer S, Desouza LH. Non-invasive brain stimulation techniques for chronic pain. *Cochrane Database Syst Rev*. 2010;(9):1-74.

175. Terao Y, Ugawa Y. Basic Mechanisms of TMS. *J Clin Neurophysiol*. 2002;19(4):322-343.

176. Defrin R, Grunhaus L, Zamir D, Zeilig G. The effect of a series of repetitive transcranial magnetic stimulations of the motor cortex on central pain after spinal cord injury. *Arch Phys Med Rehabil*. 2007;88(12):1574-1580.

177. Yilmaz B, Kesikburun S, Yasar E, Tan AK. The effect of repetitive transcranial magnetic stimulation on refractory neuropathic pain in spinal cord injury. *J Spinal Cord Med*. 2013;37(4):397-400.

178. Niv S. Clinical efficacy and potential mechanisms of neurofeedback. *Pers Individ Dif*. 2013;54(6):676-686.

179. Jensen MP, Grierson C, Tracy-Simth V, Bacigalupi SC, Othmer S. Neurofeedback treatment for pain associated with complex regional pain syndrome type I. *J Neurother*. 2007;11(1):45-53.

180. Stokes DA, Lappin MS. Neurofeedback and biofeedback with 37 migraineurs: a clinical outcome study. *Behav brain Funct*. 2010;6(9):1-10.

181. Jensen MP, Hakimian S, Sherlin LH, Fregni F. New insights into neuromodulatory approaches for the treatment of pain. *J Pain*. 2008;9(3):193-199.

182. Walker JE. QEEG-guided neurofeedback for recurrent migraine headaches. *Clin EEG Neurosci*. 2011;42(1):59-61.

183. Elkins G, Jensen M. Hypnotherapy for the management of chronic pain. *Int J Clin Exp Hypn*. 2007;55(3):275-287.

184. Jensen M, Patterson DR. Hypnotic treatment of chronic pain. *J Behav Med*. 2006;29(1):95-124.

185. Patterson DR, Jensen MP. Hypnosis and clinical pain. *Psychol Bull*. 2003;129(4):495-521.

186. Stoelb BL, Jensen MP. Hypnotic analgesia for combat-related spinal cord injury pain : a case study. *Am J Clin Hypn*. 2009;51(3):273-280.

187. Jensen MP, Romano JM, Patterson DR. Effects of self-hypnosis training and EMG biofeedback relaxation training on chronic pain in persons with spinal-cord injury. *Int J Clin Hypn*. 2009;57(3):239-268.

188. Jensen MP, Sherlin LH, Askew RL, et al. Effects of non-pharmacological pain treatments on brain states. *Clin Neurophysiol*. 2013;124(10):2016-2024.

189. Marchand WiR. Mindfulness-based stress reduction, mindfulness-based cognitive therapy, and Zen meditation for depression, anxiety, pain, and psychological

distress. *J Psychiatr Pract*. 2012;18(4):233-252.

190. Zeidan F, Martucci1 KT, Kraft RA, Gordon NS, McHaffie JG, Coghill RC. Brain mechanisms supporting modulation of pain by mindfulness meditation. *J Neurosci*. 2011;31(14):5540-5548.

191. Baeken C, De Raedt R. Neurobiological mechanisms of repetitive transcranial magnetic stimulation on the underlying neurocircuitry in unipolar depression. *Dialogues Clin Neurosci*. 2011;13(1):140-146.

192. Knoch D, Treyer V, Regard M, Müri RM, Buck A, Weber B. Lateralized and frequency-dependent effects of prefrontal rTMS on regional cerebral blood flow. *Neuroimage*. 2006;31(2):641-648.

193. Jensen MP, Day M a, Miró J. Neuromodulatory treatments for chronic pain: efficacy and mechanisms. *Nat Rev Neurol*. 2014;10(3):167-178.

194. Sarnthein J, Stern J, Aufenberg C, Rousson V, Jeanmonod D. Increased EEG power and slowed dominant frequency in patients with neurogenic pain. *Brain*. 2006;129:55-64.

195. Elbasiouny SM, Moroz D, Bakr MM, Mushahwar VK. Management of spasticity after spinal cord injury: current techniques and future directions. *Neuroehabilitaion and Neural Repair*. 2010;24(1):23-33.

196. Onushko T, Schmit BD. Reflex response to imposed bilateral hip oscillations in human spinal cord injury. *J Neurophysiol*. 2007;98(4):1849-1861.

197. Ping B, Chung H, Kam B, Cheng K. Immediate effect of transcutaneous electrical nerve stimulation on spasticity in patients with spinal cord injury. *Clin Rehabil*. 2010;24:202-210.

198. Oo WM. Efficacy of addition of transcutaneous electrical nerve stimulation to standardized physical therapy in subacute spinal spasticity: a randomized controlled trial. *Arch Phys Med Rehabil*. 2014;95(11):2013-2020.

199. Mills PB, Dossa F. Transcutaneous electrical nerve stimulation for management of limb spasticity: a systematic review. *Am J Phys Med Rehabil*. 2016;95(4):309-318.

200. Pinter MM, Gerstenbrand F, Dimitrijevic MR. Epidural electrical stimulation of posterior structures of the human lumbosacral cord: 3. Control Of spasticity. *Spinal Cord*. 2000;38:524-531.

201. Hofstoetter US, McKay WB, Tansey KE, Mayr W, Kern H, Minassian K. Modification of spasticity by transcutaneous spinal cord stimulation in individuals with incomplete spinal cord injury. *J Spinal Cord Med*. 2014;37(2):202-211.

202. Midha M, Schmitt JK. Epidural spinal cord stimulation for the control of spasticity in spinal cord injury patients lacks long-term efficacy and is not cost-effective. *Spinal Cord*. 1998;36(3):190-192.

203. Kumru H, Murillo N, Samso J, et al. Reduction of spasticity with repetitive transcranial magnetic stimulation in patients with spinal cord injury. *Neuroehabilitaion and Neural Repair*. 2010;24(5):435-441.

204. Levitan Y, Zeilig G, Bondi M, Ringler E, Defrin R. Predicting the risk for central pain using the sensory components of the international standards for neurological classification of spinal cord injury. *J Neurotrauma*. 2015;32:1684-1692.

205. Finnerup NB, Norrbrink C, Trok K, et al. Phenotypes and predictors of pain following traumatic spinal cord injury: a prospective study. *J Pain*. 2014;15(1):40-48.

206. Wasner G, Lee BB, Engel S, McLachlan E. Residual spinothalamic tract pathways predict development of central pain after spinal cord injury. *Brain*. 2008;131(9):2387-2400.

207. Cruz-Almeida Y, Felix ER, Martinez-Arizala A, Widerström-Noga EG. Decreased spinothalamic and dorsal column medial lemniscus-mediated function is associated with neuropathic pain after spinal cord injury. *J Neurotrauma*. 2012;29(17):2706-2715.

208. Lee JK, Oh CH, Kim JY, et al. Brain activation evoked by sensory stimulation in patients with spinal cord injury : functional magnetic resonance imaging correlations with clinical features. *J Korean Neurosurg Soc*. 2015;58(3):242-247.

209. Wolpaw JR. Spinal cord plasticity in acquisition and maintenance of motor skills. *Acta Physiol*. 2007;189(2):155-169.

210. Thompson AK, Wolpaw JR. Operant conditioning of spinal reflexes: from basic science to clinical therapy. *Front Integr Neurosci*. 2014;8:1-8.

211. Capaday C, Stein RB. Amplitude modulation of the soleus H-reflex in the human during walking and standing. *J Neurosci*. 1986;6(5):1308-1313.

212. Cowley PM, Clark BC, Ploutz-Snyder LL. Kinesthetic motor imagery and spinal excitability: the effect of contraction intensity and spatial localization. *Clin Neurophysiol*. 2008;119(8):1849-1856.

213. Hale BS, Raglin JS, Koceja DM. Effect of mental imagery of a motor task on the Hoffmann reflex. *Behav Brain Res*. 2003;142:81-87.

214. Bonnet M, Decety J, Jeannerod M, Requin J. Mental simulation of an action modulates the excitability of spinal reflex pathways in man. *Cogn brain Res*. 1997;5(3):221-228.

215. Jeannerod M. Mental imagery in the motor context. *Neuropsychologia*. 1995;33(11):1419-1432.

216. Oishi K, Kimura M, Yasukawa M, Yoneda T, Takashi M. Amplitude reduction of H-reflex during mental movement simulation in elite athletes. *Behav Brain Res*. 1994;62:55-61.

217. Oishi K, Maeshima T. Autonomic nervous system activities during motor imagery in elite athletes. *J Clin Neurophysiol*. 2004;21(3):170-179.

218. Yu X, Zhang J, Xie D, Wang J, Zhang C. Relationship between scalp potential and autonomic nervous activity during a mental arithmetic task. *Auton Neurosci*. 2009;146:81-86.

219. Fernandez T, Harmony T, Rodriguez M, et al. EEG activation patterns during the performance of tasks involving different components of mental calculation. *Electroencephalogr Clin Neurophysiol*. 1995;94(3):175-182.

220. Harmony T, Fernández T, Silva J, et al. EEG delta activity: an indicator of attention to internal processing during performance of mental tasks. *Int J Psychophysiol*. 1996;24:161-171.

221. Escolano C, Navarro-Gil M, Garcia-Campayo J, Congedo M, De Ridder D, Minguez J. A controlled study on the cognitive effect of alpha neurofeedback training in patients with major depressive disorder. *Front Behav Neurosci*. 2014;8:1-12.

222. Kober SE, Schweiger D, Witte M, et al. Specific effects of EEG based neurofeedback training on memory functions in post-stroke victims. *J Neuroeng Rehabil*. 2015;12(1):1-13.

223. Sollfrank T, Ramsay A, Perdikis S, et al. The effect of multimodal and enriched feedback on SMR-BCI performance. *Clin Neurophysiol*. 2016;127(1):490-498.

224. Thompson AK, Chen XY, Wolpaw JR. Acquisition of a simple motor skill: task-dependent adaptation plus long-term change in the human soleus h-reflex. *J Neurosci*. 2009;29(18):5784-5792.

225. Jasper HH. Report of the committee on methods of clinical examination in electroencephalography. *Electroencephalogr Clin Neurophysiol*. 1957;10(2):370-375.

226. Hjorth B. An on-line transformation of EEG scalp potentials into orthogonal source derivations. *Electroencephalogr Clin Neurophysiol*. 1975;39(5):526-530.

227. Pineda JA. The functional significance of mu rhythms: translating "seeing" and "hearing" into "doing." *Brain Res Rev*. 2005;50(1):57-68.

228. Pfurtscheller G, Lopes Da Silva FH. Event-related EEG/MEG synchronization and desynchronization: basic principles. *Clin Neurophysiol*. 1999;110:1842-1857.

229. Kuhlman WN. EEG feedback training: Enhancement of somatosensory cortical activity. *Electroencephalogr Clin Neurophysiol*. 1978;45(2):290-294.

230. Neuper C, Scherer R, Reiner M, Pfurtscheller G. Imagery of motor actions: Differential effects of kinesthetic and visual-motor mode of imagery in single-trial EEG. *Cogn Brain Res*. 2005;25(3):668-677.

231. Malouin F, Richards CL, Jackson PL, Lafleur MF, Durand A, Doyon J. The Kinesthetic and Visual Imagery Questionnaire (KVIQ) for assessing motor imagery in persons with physical disabilities: a reliability and construct validity study. *J Neurol Phys Ther*. 2007;31(1):20-29.

232. Holm S. A simple sequentially rejective multiple test procedure. *Scand J Stat*. 1979;6(2):65-70.

233. Ros T, Gruzelier JH. The immediate effects of EEG neurofeedback on cortical excitability and synchronization. *Neurofeedback Neuromodulation Tech Appl*. 2011:381-402.

234. Mizuki Y, Hashimoto M, Tanaka T, Inanaga K, Tanaka M. A new physiological tool for assessing anxiolytic effects in humans: frontal midline theta activity. *Psychopharmacology (Berl)*. 1983;80(4):311-314.

235. Rossi S, Pasqualetti P, Tecchio F, Sabato A, Rossini PM. Modulation of corticospinal output to human hand muscles following deprivation of sensory feedback. *Neuroimage*. 1998;8:163-175.

236. Brignani D, Manganotti P, Rossini PM, Miniussi C. Modulation of cortical oscillatory activity during transcranial magnetic stimulation. *Hum Brain Mapp*. 2008;29(5):603-612.

237. Centonze D, Koch G, Versace V, Mori F, Rossi S. Repetitive transcranial magnetic stimulation of the motor cortex ameliorates spasticity in multiple sclerosis. *Neurology*. 2007;68(13):1045-1050.

238. Neuper C, Wortz M, Pfurtscheller G. ERD/ERS patterns reflecting sensorimotor activation and deactivation. *Prog Brain Res*. 2006;159:211-222.

239. Decq P. Pathophysiology of spasticity. *Neurochirurgie*. 2003;49:163-184.

240. Pikov V. Spinal plasticity. In: Horsh K., Dhillon G., eds. *Neuroprosthetics Theory and Practice*. Singapore World Scientific; 2007:302-321.

241. Thomas CK, Field-Fotte E. Spasticity after human spinal cord injury. In: Filed-Fotte EC, ed. *Spinal Cord Injury Rehabilitation*. Philadelphia: CPR; 2009:445-466.

242. Kamibayashi K, Nakazawa K, Ogata H, Obata H, Akai M, Shinohara M. Invariable H-reflex and sustained facilitation of stretch reflex with heightened sympathetic outflow. *J Electromyogr Kinesiol*. 2009;19(6):1053-1060.

243. Boulay CB, Chen XY, Wolpaw JR. Electrocorticographic (Ecog) activity over sensorimotor cortex and motor function in awake behaving rats. *J Neurophysiol*. 2015;113:2232-2241.

244. Takemi M, Masakado Y, Liu M, Ushiba J. Sensorimotor event-related desynchronization represents the excitability of human spinal motoneurons. *Neuroscience*. 2015;297:58-67.

245. Niedermeyer E. The normal EEG of the waking adult. In: Niedermeyer E, da Silva F, eds. *Electroencephalography Basic Principles, Clinical Applications and Related Fields*. Lippincott Williams & Wilkins; 2005.

246. Kim T, Kim S, Lee B. Effects of action observational training plus brain-computer interface-based functional electrical stimulation on paretic arm motor recovery in patient with stroke: a randomized controlled trial. *Occup Ther Int*. 2016;23(1):39-47.

247. King CE, Wang PT, McCrimmon CM, Chou CC, Do AH, Nenadic Z. The feasibility of a brain-computer interface functional electrical stimulation system for the restoration of overground walking after paraplegia. *J Neuroeng Rehabil*. 2015;12(1):1-11.

248. Vučković A, Wallace L, Allan DB. *Hybrid Brain-Computer Interface and Functional Electrical Stimulation for Sensorimotor Training in Participants with*

*Tetraplegia*. Vol 39.; 2014.

249. Widerstrom-Noga EG, Felipe-Cuervo E, Yezierski RP. Chronic pain after spinal injury: Interference with sleep and daily activities. *Arch Phys Med Rehabil*. 2001;82(11):1571-1577.

250. Norrbrink Budh C, Hultling C, Lundeberg T. Quality of sleep in individuals with spinal cord injury: a comparison between patients with and without pain. *Spinal Cord*. 2005;43(2):85-95.

251. Mann, R; Schaefer, C, Sadosky, A, Bergstrom, F, Baik, R, Parsons, B, Nalamachu, S, Stacey, B R, Tuchman, M, Anschel, A, Nieshoff EC. Burden of spinal cord injury-related neuropathic pain in the United States: retrospective chart review and cross-sectional survey. *Spinal Cord*. 2013;51(7):564-570.

252. Attal N, Mazaltarine G, Perrouin-Verbe B, Albert T. Chronic neuropathic pain management in spinal cord injury patients. What is the efficacy of pharmacological treatments with a general mode of administration? (oral, transdermal, intravenous). *Ann Phys Rehabil Med*. 2009;52(2):124-141.

253. Siddall PJ. Management of neuropathic pain following spinal cord injury: now and in the future. *Spinal Cord*. 2009;47(5):352-359.

254. Teasell RW, Mehta S, Aubut JL, Wolfe DL, Hsieh JTC, Townson AF. A systematic review of pharmacological treatments of pain following spinal cord injury. *Robert W Teasell, Swati Mehta, Jo-Anne L Aubut, Brianne Foulon, Dalt L Wolfe, Jane TC Hsieh, Andrea F Townson, Christine Short, Spinal Cord Inj Rehabil Res Team*. 2010;91(5):816-831.

255. Plunkett J a, Yu CG, Easton JM, Bethea JR, Yezierski RP. Effects of interleukin-10 (IL-10) on pain behavior and gene expression following excitotoxic spinal cord injury in the rat. *Exp Neurol*. 2001;168(1):144-154.

256. Yu CZ, Liu YP, Liu S, Yan M, Hu SJ, Song XJ. Systematic administration of B vitamins attenuates neuropathichyperalgesia and reduces spinal neuron injury following temporary spinal cord ischaemia in rats. *Eur J Pain*. 2014;18(1):76-85.

257. Jurcak V, Tsuzuki D, Dan I. 10/20, 10/10, and 10/5 systems revisited: Their validity as relative head-surface-based positioning systems. *Neuroimage*. 2007;34(4):1600-1611. doi:10.1016/j.neuroimage.2006.09.024.

258. Vidaurre C, Sander TH, Schlögl A. BioSig: the free and open source software library for biomedical signal processing. *Comput Intell Neurosci*. 2011;2011:935364. doi:10.1155/2011/935364.

259. Benjamini Y, Yekutieli D. The control of the false discovery rate in multiple testing under depencency. *Ann Stat*. 2001;29(4):1165-1188. doi:10.1214/aos/1013699998.

260. Marshall PJ, Meltzoff AN. Neural Mirroring Systems: Exploring the EEG Mu Rhythm in Human Infancy. *Dev Cogn Neurosci*. 2012;1(2):110-123. doi:10.1016/j.dcn.2010.09.001.Neural.

261. Pfurtscheller G, Stancák A, Neuper C. Event-related synchronization (ERS) in the alpha band - An electrophysiological correlate of cortical idling: A review. *Int J Psychophysiol*. 1996;24:39-46. doi:10.1016/S0167-8760(96)00066-9.

262. Partanen J, Soininen H, Kononen M, Kilpelainen R, E-l H. EEG reactivity correlates with neuropsychological test scores in Down's syndrome. *Acta Neurol Scand*. 1996;94:242-246.

263. Tran Y, Boord P, Middleton J, Craig a. Levels of brain wave activity (8-13 Hz) in persons with spinal cord injury. *Spinal Cord*. 2004;42(2):73-79. doi:10.1038/sj.sc.3101543.

264. Cuspineda ER, Machado C, Virues T, et al. Source analysis of alpha rhythm reactivity using LORETA imaging with 64-channel EEG and individual MRI. *Clin EEG Neurosci*. 2009;40(3):150-156. doi:10.1177/155005940904000306.

265. Rowe DL, Robinson PA, Rennie CJ. Estimation of neurophysiological parameters from the waking EEG using a biophysical model of brain dynamics. *J Theor Biol*. 2004;231(3):413-433. doi:10.1016/j.jtbi.2004.07.004.

266. Stern J, Jeanmonod D, Sarnthein J. Persistent EEG overactivation in the cortical pain matrix of neurogenic pain patients. *Neuroimage*. 2006;31(2):721-731. doi:10.1016/j.neuroimage.2005.12.042.

267. Hasan MA, Fraser M, Conway BA, Allan DB, Vučković A. Reversed cortical over-activity during movement imagination following neurofeedback treatment for central neuropathic pain. *Clin Neurophysiol*. 2016;127(9):3118-3127. doi:10.1016/j.clinph.2016.06.012.

268. Duann J-R, Chiou J-C. A Comparison of Independent Event-Related Desynchronization Responses in Motor-Related Brain Areas to Movement Execution, Movement Imagery, and Movement Observation. *PLoS One*. 2016;11:1-16. doi:10.1371/journal.pone.0162546.

269. Gomez-Pilar J, Corralejo R, Nicolas-Alonso LF, Álvarez D, Hornero R. Neurofeedback training with a motor imagery-based BCI: neurocognitive improvements and EEG changes in the elderly. *Med Biol Eng Comput*. 2016;54(11):1-12. doi:10.1007/s11517-016-1454-4.

270. Siddall PJ, McClelland JM, Rutkowski SB, Cousins MJ. A longitudinal study of the prevalence and characteristics of pain in the first 5 years following spinal cord injury. *Pain*. 2003;103(3):249-257.

271. Farrar JT, Farrar JT, Portenoy RK, et al. De®ning the clinically important difference in pain outcome measures. *Pain*. 2000;88:287-294.

272. Martin WJJM, Ashton-James CE, Skorpil NE, Heymans MW, Forouzanfar T. What constitutes a clinically important pain reduction in patients after third molar surgery? *Pain Res Manag*. 2013;18(6):319-322.

273. Cepeda MS, Africano JM, Polo R, Alcala R, Carr DB. What decline in pain intensity is meaningful to patients with acute pain? *Pain*. 2003;105:151-157. doi:10.1016/S0304-3959(03)00176-3.

274. Gruzelier JH. EEG-neurofeedback for optimising performance. I: A review of cognitive and affective outcome in healthy participants. *Neurosci Biobehav Rev*. 2014;44:124-141. doi:10.1016/j.neubiorev.2013.09.015.

275. Jensen MP. A Neuropsychological Model of Pain: Research and Clinical

Implications. *J Pain*. 2010;11(1):2-12.

276. Green JB, Sora E, Bialy Y, Ricamato a, Thatcher RW. Cortical sensorimotor reorganization after spinal cord injury: an electroencephalographic study. *Neurology*. 1998;50(4):1115-1121. doi:10.1212/WNL.50.4.1115.

277. Pfurtscheller G, Linortner P, Winkler R, Korisek G, Müller-Putz G. Discrimination of motor imagery-induced EEG patterns in patients with complete spinal cord injury. *Comput Intell Neurosci*. 2009;2009:1-7. doi:10.1155/2009/104180.

278. Luck SJ. An introduction to event-related potentials and their neural origin. In: *An Introduction to the Event-Related Potential Technique*. Massachusetts Institute of Technology; 2005:1-50. doi:10.1118/1.4736938.

279. Kirshblum SC, Burns SP, Biering-Sorensen F, et al. International standards for neurological classification of spinal cord injury (Revised 2011). *J Spinal Cord Med*. 2011;34(6):535-546. doi:10.1179/107902611X13186000420242.

280. J.Sejnowski AB and T. Information-Maximization Approach to Blind Separation and Blind Deconvolution. *Neural Comput*. 1995;7(1994):1129-1159. file:///C:/MyHome/Recent_paper/bell.blind.pdf.

281. Lee TW, Girolami M, Sejnowski TJ. Independent component analysis using an extended infomax algorithm for mixed subgaussian and supergaussian sources. *Neural Comput*. 1999;11(2):417-441. doi:10.1162/089976699300016719.

282. Acar ZA, Makeig S. Neuroelectromagnetic Forward Head Modeling Toolbox. *Neurosci Methodes*. 2010;190(2):258-270. doi:10.1016/j.drugalcdep.2008.02.002.A.

283. Nunez, P.L., Srininvasan R. *Electric Fields in the Brain: The Neurophysics of EEG*. Oxford University Press; 2006.

284. Darbellay GA, Vajda I. Estimation of the Information by an Adaptive Partitioning of the Observation Space. *IEEE Trans Inf Theory*. 1999;45(4):1315-1321. doi:10.1109/18.746793.

285. Frey BJ, Dueck D. Clustering by passing messages between data points. *Science (80- )*. 2007;315:972-976.

286. Mayberg HS, Liotti M, Brannan SK, et al. Reciprocal limbic-cortical function and negative mood: Converging PET findings in depression and normal sadness. *Am J Psychiatry*. 1999;156(5):675-682.

287. Nielsen FÅ, Balslev D, Hansen LK. Mining the posterior cingulate: Segregation between memory and pain components. *Neuroimage*. 2005;27:520-532. doi:10.1016/j.neuroimage.2005.04.034.

288. Leech R, Braga R, Sharp DJ. Echoes of the brain within the posterior cingulate cortex. *J Neurosci*. 2012;32(1):215-222.

289. Bear, M. F., Connors, B.W., Paradiso MA. *Neuroscience, Exploring the Brain*. Baltimore: Lippincott Williams&Wilkins; 2007.

290. Osuagwu BA, Vuckovic A. Similarities between explicit and implicit motor imagery in mental rotation of hands: An EEG study. *Neuropsychologia*. 2014;65:197-210.

doi:10.1016/j.neuropsychologia.2014.10.029.

291. Maurer K, Riederer P, Heinsen H, Beckmann H. Altered P300 topography due to functional and structural disturbances in the limbic system in dementia and psychoses and to pharmacological conditions. *Psychiatry Res*. 1989;29(3):391-393.

292. Weisenberg M. Cognitive aspects of pain. In: Wall P, Melzack R, eds. *Text Book of Pain*. Edinburg: Churchill-Livingstone; 1994:275-289.

293. Miltner WHR, Krieschel S, Gutberlet I. P300–a signature for threat processing in phobic subjects. *Psychophysiology*. 2000:37-71.